studentská konference

CHEMIE JE ŽIVOT

26–27. 11. 2020

SBORNÍK PŘÍSPĚVKŮ

VYSOKÉ UČENÍ TECHNICKÉ V BRNĚ
FAKULTA CHEMICKÁ

Studentská odborná konference
CHEMIE JE ŽIVOT 2020
Sborník příspěvků

Editor: Ing. Petr Dzik, Ph.D.
Nakladatel: Vysoké učení technické v Brně, Fakulta chemická,
Purkyňova 464/118, 612 00 Brno

Vydání: první
Rok vydání: 2020
ISBN: 978-80-214-5921-2
Tato publikace neprošla redakční ani jazykovou úpravou

OBSAH

POSTEROVÁ STŘEDOŠKOLSKÁ SEKCE

Validace komerčně dostupných T-DNA inzerčních mutantů *Arabidopsis thaliana* 14
Martina Brabcová
Ing. Hana Dufková

Studium reakčních procesů v rámci sanační metody ISCO 15
Tibor Malinský
Ing. Radek Škarohlíd, Mgr. Ing. Marek Martinec, Ph.D.

Vývoj voltametrické metody stanovení léčiva atomoxetinu. 16
Martin Slavík, Renáta Šelešovská

SEKCE BAKALÁŘSKÝCH A MAGISTERSKÝCH STUDENTŮ

Produkcia polyesterov pomocou extrémofilných baktérií 18

Využití metabolomiky pro charakterizaci hlavních změn révy vinné v rámci vegetačního cyklu, a při různých způsobech kultivace 26
Bc. Adam Behner
Doc. Ing. Milena Stránská, Ph.D.

Visible-light photoinitiators for cationic and free-radical photopolymerization studied by indirect EPR techniques. . . 28
Kristína Czikhardtová, Dana Dvoranová

Use of Poly(3-hydroxybutyrate) as Polymer Base for Drug Delivery Systems 30
Nicole Černeková
Adriana Kovalcik

Analýza G-kvadruplexů v genomech lidských parazitických červů 32
Michaela Dobrovolná
Alessio Cantara
Jean-Louis Mergny
Václav Brázda

Neural networks and their use in study of quantum-chemical systems 34
Peter Fraško, Peter Poliak

Efekt povrchové modifikace škrobových plniv pomocí polydimethylsiloxanu na proces plnění tvrdých želatinových tobolek 36
Bc. Petra Havelková
Ing. Pavlína Komínová, prof. Ing. Petr Zámostný, Ph.D.

Manufacturing of personalised medicines by impregnation of mesoporous silica tablets 38
Zuzana Hlavačková
Supervisor: prof. Ing. František Štěpánek Ph.D.
Consultants: Ing. David Zůza

Evolučné inžinierstvo PHA produkujúcich baktérií 40
Halomonas Halophila
Bc. Terézia Ikrényiová
doc. Ing. Stanislav Obruča, Ph.D.

Sledovanie poškodenia miechy potkana pomocou magnetickej rezonancie metódou DTI. 46
Bc. Zuzana Kodadová

Interakcia hormónov a liečiv s pôdnou organickou hmotou . . . 48
Bc. Soňa Krajňáková
Prof. Ing. Martina Klučáková PhD.

Ošetření nápojů pomocí pulzního elektrického pole. 57
Bc. Gabriela Kuncová, Ing. Iveta Horsáková, Ph.D.

Optimalizácia SPME v spojení s GC-MS/MS na stanovenie cypermetrínu v chemických postrekoch 58
Nikola Kurucová
Agneša Szarka, Svetlana Hrouzková,
Francisco Javier Arrebola-Liébanas

Využití smíšených tkáňových kultur ve výzkumu biodistribuce nanočástic 60
Bc. Pavlína Michaláková
vedoucí práce: Ing. Denisa Lizoňová

Príprava a magnetické vlastnosti železnatých komplexov s pyridyl-benzimidazolovými ligandami 67
Bc. Jana Vojčíková
Doc. Ing. Ivan Šalitroš PhD. 2020

SEKCE DOKTORSKÝCH STUDENTŮ

Lipidomic Analysis as a Tool for a Comprehensive Description of Atherosclerotic Plaques 80
Kamila Bechynska
Richard Voldrich, Hynek Macha, Vit Kosek, David Netuka, Vladimir Havlicek, Jana Hajslova

Characterization of selected non-traditional cereals for development of enriched cereal products. 82
Agáta Bendová
Michal Pecháček, Ivana Márová

Development of an analytical method for the determination of phytocannabinoids and their bioavailability in rat blood plasma 84
Zuzana Bínová
Marie Fenclová, František Beneš, Petra Peukertová, Jana Hajšlová

Preparation of Mg-Al-Ti Bulk Materials Via Powder Metallurgy. 86
Ing. Roman Brescher
Ing. Matěj Březina, Ph.D.

Fixation of the Lead in Alkali Activated Materials Based on Different Types of Ashes 88
Ing. Vladislav Cába
Ing. Jan Koplík, PhD.

Bioaccessibility of Metals in Urban Aerosol 89
Hana Cigánková

Aminoclay as Drug Carrier. 91
Jakub Dušek

Preparation and Characterization of Functionalized Wound Dressings 93
Lucia Dzurická
Agáta Bendová, Julie Hoová, Petra Matoušková, Ivana Márová

High Throughput Platform for Identification And Characterization Of Electrogenic Bacteria. 95
Jiri Ehlich
Lukasz Szydlowski Ph.D.

Determination of micro-bioplastics in solid matrix. 96
Jakub Fojt
Ivana Románeková, Bára Komárková
Radek Přikryl, Jiří Kučerík

Study of Cholesterol's Effect on the Properties of Catanionic Vesicular Systems 98
Martina Havlíková, Filip Mravec

Characterization of Hydrogels with Amphiphilic Structures . . 100
Richard Heger
Miloslav Pekař

Study of simple electrolytes for magnesium batteries 102
Jiří Honč

Humid Air Cooling by Shell and Tube Heat Exchangers. 103
Petr Horvát
Jaroslav Vlasák, Josef Kalivoda, Ondřej Krištof, Tomáš Svěrák

Spectroscopic Study of Human Blood Plasma for Early Detection of Hepatocellular Carcinoma Kateřina Hrubešová 105
Lucie Habartová, Petr Hříbek, Petr Urbánek, Vladimír Setnička

The Influence of Alkaline Activator Type on the Carbonatation Process of the Alkali-activated Blast Furnace Slag 113
Petr Hrubý
Vlastimil Bílek, Lukáš Kalina, František Šoukal, Libor Topolář, Richard Dvořák

Characterization of Bacterial Strains Obtained in Evolutionary Engineering. 115
Vendula Chatrná
Stanislav Obruča, Ivana Nováčková

Assessment of potential heavy metal pollution of road dust in arid urban area. 117
Petr Chrást
Jan Chalabala, Václav Pecina, Martin Brtnický, David Juřička, Jindřich Kynický,
Michaela Vašinová Galiová

Surface Treatment of Cementitious Systems by Silicates. 119
Valeriia Iliushchenko
Lukáš Kalina, Petr Hrubý, František Šoukal, Tomáš Opravil

Study of the influence of water coefficient on porosity and mechanical properties of high-performance concrete 121
Martin Janča, Pavel Šiler, Martin Alexa

Microwave-Assisted Preparation of Organo-Lead Halide Perovskite structures for electronics. 129
Jan Jancik, Anna Jancik Prochazkova, Markus Clark Scharber, Alexander Kovalenko, Jiří Másilko, Niyazi Serdar Sariciftci, Martin Weiter, and Jozef Krajcovic

Relaxation Behaviour of Hydrogel Materials Using Classical Rheology Methods. 131
Martin Kadlec
Jiří Smilek, Miloslav Pekař

Simple multi-analyte LC-MS method for the determination of food additives in soft drinks and alcoholic beverages . . . 133
Ing. Aliaksandra Kharoshka
Ing. Aleš Krmela, Ph.D., Dr. Ing. Věra Schulzová

Preparation of metakaolin with high whiteness 135
Jan Kotrla
Jiří Bojanovský, Tomáš Opravil, Petr Hrubý

Thermophilic Bacterium *Schlegelella thermodepolymerans* DSM 15344 as a Producer of Polyhydroxyalkanoates 137
Xenie Kouřilová, Jana Musilová, Karel Sedlář, Kristína Bednárová
Iva Pernicová, Stanislav Obruča

Development of a method for simultaneous determination of various esters of MCPD and glycidol in palm fat by supercritical fluid chromatography 139
Tomáš Kouřimský
Vojtěch Hrbek, Klára Navrátilová, Jana Hajšlová

Tuning Solid State Polymorph Emission of Sterically Hindered Push-Pull Substituted Stilbenes 141
Matouš Kratochvíl
Karel Pauk, Stanislav Luňák Jr., Aneta Marková, Aleš Imramovský, Martin Vala, Martin Weiter

Monitoring of Pharmaceuticals in Scottish Rivers Using Passive Sampling Devices 143
Pavlína Landová
Ludmila Mravcová, Lydia Niemi, Stuart Gibb

Numerical Simulation of Heterogenous Catalytic Reactions . . 145
Martin Mačák
Petr Vyroubal, Jiří Maxa

Wet Pre-treatment Methods in Macroelements Recovery from Fly Ash Combined with Acid Leaching 147
Michal Marko
Tomáš Opravil, František Šoukal, Jaromír Pořízka

OECT as a Device for Material Characterization: The Role of Parasitic Series Resistance 149
Aneta Marková, Stanislav Stříteský, Martin Weiter, Martin Vala
Visualization of a Ge Structure Using Fluorescent Nanoparticles
Kateřina Marková
Filip Mravec, Miloslav Pekař

Plasticized poly(3-hydroxybutyrate)/poly(D,L-lactide) blends filled with tricalcium phosphate for FDM 3D printing and their biological properties 158
Veronika Melčová
Kateřina Chaloupková, Radek Přikryl, Lucy Vojtová and Michala Rampichová

Využití smíšených tkáňových kultur ve výzkumu biodistribuce nanočástic 160
Bc. Pavlína Michaláková
vedoucí práce: Ing. Denisa Lizoňová

Monitoring of Gadolinium Anomaly in Soil, Grapevine and Wine Samples from the Czech Republic. 167
Frederika Mišíková
Anna Krejčová, Jan Patočka

Olive Oil Authenticity: Detection of Soft-Deodorized Oils in Extra-Virgin Olive Oils Using Metabolomic Approach 177
Klára Navrátilová
Vojtěch Hrbek, Kamila Hůrková, Jana Hajšlová
Assessment of air pollution in the Czech Republic by emerging chlorinated contaminants
Ondřej Pařízek
Jakub Tomáško, Jana Pulkrabová

Contamination of Urban Soils by Cd: An Example of a Coal Mining City (Shariin Gol, Mongolia) 181
Václav Pecina
Renata Komendová
David Juřička
Martin Brtnický

Fast Centrifugal Partitioning Chromatography (FCPC) – Innovative Method for Separation of Biologically Active Compounds from *Cannabis* 183
Petra Peukertová, František Beneš, Marie Fenclová, Zuzana Bínová, Matěj Malý,
Jana Hajšlová

The Influence of Non-canonical Structures on the P53 Isoforms Binding to DNA. 185
Otília Porubiaková
Natália Bohálová2,3, Václav Brázda

Novel method for isolation of PHB from bacterial biomass . . 193
Aneta Pospíšilová,
Radek Přikryl, Ivana Nováčková

Effects of microplastics to aquatic environment 195
Ing. Petra Procházková

New possibilities in the analysis of modified trichothecenes type A in oats: immunoaffinity purification and enzymatic hydrolysis 197
Nela Průšová, Zbyněk Džuman, Jana Hajšlová, Milena Stránská-Zachariášová

Study of the Influence of Selected Compounds on Stability of Beer Foam 199
Lenka Punčochářová

Analysis of the Mixing Process Performance in Mixtures for Direct Tablet Compression Using Segregation Test. 201
Simona Römerová
Adam Karaba, Petr Zámostný

The authenticity of Poppy Seeds: How to Detect the Undeclared Hydrothermal Treatment?. 207
Kateřina Šebelová
Monika Benešová, Lucie Chytilová, Vladimír Kocourek, Jana Hajšlová,

Inorganic Thermal insulation material for masonry elements. 209
Martin Sedlačík
Tomáš Opravil

Mixotrophic growth and increased salinity – possible tools for increasing the PHB production in cyanobacteria? 211
Zuzana Šedrlová
Eva Slaninová, Petr Sedláček, Ines Fritz, Stanislav Obruča.

An isolation of a protein from a wheat bran 213
Zuzana Slavíková
Jaromír Pořízka, Pavel Diviš

Utilization of recycled brick waste for growing the agricultural plants 215
Ing. Barbora Šmírová
doc. Ing. Tomáš Opravil, Ph.D.

Characterization of SiO_2 Nanofluid by High Resolution Ultrasonic Spectroscopy 217
Sarka Sovova,
Miloslav Pekar
Determination of biogenic amines in Swiss and Dutch type cheeses
Michal Sýkora
Eva Vítová, Agnieszka Pluta-Kubica

Study of Liposomes Membrane Properties by Fluorescence Spectroscopy 220
Jana Szabová
Filip Mravec

Contamination of Vegetable Oils by Mineral Oils and Polycyclic Aromatic Hydrocarbons: A Czech Market Survey 221
Jakub Tomáško
Veronika Vondrášková, Jana Pulkrabová

The Effect of Freezing Rate on Properties of PVA Hydrogels Prepared by Cyclic Freezing/Thawing 223
Monika Trudičová
Jan Zahrádka, Petr Sedláček, Miloslav Pekař

The Effect of Substitution and Aromatic Ring Condensation on the Optical Properties of Alloxazine: a Theoretical Study 225
Jan Truksa
Denisa Cagardová, Martin Michalík, Jan Richtár, Jozef Krajčovič, Martin Weiter, Vladimír Lukeš

Occurrence of chlorinated paraffins in human blood serum and problems of their quantification 231
Denisa Turnerová
Jakub Tomáško, Jana Pulkrabová

Can high-resolution mass spectrometry (HRMS) –based metabolomics be used for a varietal classification of wines? 233
Leos Uttl
Vaclav Kadlec, Zbynek Dzuman, Mona Ehlers, Carsten Fauhl-Hassek, Jana Hajslova

Utilization of Mica Separated from Washed Kaolin 235
Ing. Josef Vaculík
doc. Ing. Tomáš Opravil, Ph.D.

Antidepressants and Anxiolytics in the Environment 236
Petra Venská, Martina Repková

Use of a pilot scrubber separation device for specific pollutant in the air 238
Jaroslav Vlasák
Tomáš Svěrák, Ondřej Krištof, Josef Kalivoda, Petr Horvát

Police Officer Exposure to Polycyclic Aromatic Hydrocarbons in Three Locations of the Czech Republic. 239
Veronika Vondrášková
Ondřej Pařízek
Kateřina Urbancová
Jana Pulkrabová

Utilization of Grape Seed Lignin in Polyhydroxyalkanoate Blends 241
Pavel Vostrejš
Adriana Kovalcik

Transport Properties of Biopolymeric Hydrogels 243
David Vyroubal, Martina Klučáková

Preparation of Mg-Ti Based Bulk Materials via Powder Metalurgy 254
Martin Žilinský

POSTEROVÁ STŘEDOŠKOLSKÁ SEKCE

VALIDACE KOMERČNĚ DOSTUPNÝCH T-DNA INZERČNÍCH MUTANTŮ *ARABIDOPSIS THALIANA*

Martina Brabcová

Střední průmyslová škola chemická Brno, příspěvková organizace Vranovská 65, 614 00 Brno-Husovice, Česká republika, brabcova.martina17@spschbr.info

ÚVOD

Cílem práce bylo ověření přítomnosti mutace u celkem 10 vybraných genů HSP modelové rostliny huseníčku rolního (*Arabidopsis thaliana*), za účelem sestavení kolekce mutantních linií rostlin využitelné pro následující výzkum role proteinů HSP v regulaci klíčení semen. Semena byla získána prostřednictvím instituce NASC, která produkuje rozsáhlé množství mutantních linií, ale je vždy výrazně doporučováno linie před započetím výzkumného procesu ověřit.

EXPERIMENT

- k extrakci DNA byly využity dva protokoly
- srážení v isopropanolu
- srovnání účinnosti – stanovení koncentrace pomocí Nanodropu
- časově nejméně náročný protokol

***Tab. 1:** Postup extrakce DNA (RT – laboratorní teplota)*

Úkon	Čas/Množství
Homogenizace	-
Extrační pufr	400 µl
Vortex	několik sekund
Centrifugace	5 min, RT
Nová zkumavka	200 µl
isopropanol	200µl
Centrifugace	5 min, RT
Odstranit supernatant	-
70% ethanol	400 µl
Centrifugace	5 min, RT
Odstranit supernatant	-
Vysušit	RT
Přidat vodu	50 µl
Uschovat v lednici	-

- provedení PCR se speciálně navrženými a syntetizovanými primery
- LP primer – ohraničení levé strany bez T-DNA
- LB primer – ohraničení levé strany s T-DNA (mutantní)
- RP – ohraničení pravé strany

***Tab. 2:** Přehled reakčních směsí pro PCR*

Reakční směs			
Genomická DNA		T-DNA	
	V [µl]		V [µl]
H_2O	8	H_2O	8
10× Buffer	1,5	10× Buffer	1,5
LP	1,5	LB	1,5
RP	1,5	RP	1,5
dNTP	1,5	dNTP	1,5
Taq	0,15	Taq	0,15

***Tab. 3:** Program PCR*

Program PCR		
T [°C]	t [min]	Opakování
94	3	
94	0,5	
55	0,66	31 ×
72	1,5	
72	5	
4	30	

- k detekci DNA využití elektroforézy na 1,2% agarosovém gelu při elektrickém napětí 90 V
- k vyzualizaci byla přidána barva Green Safe, detekce DNA pod UV lampou
- určení statusu linie

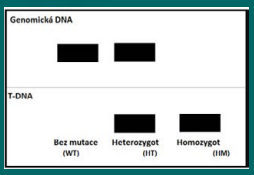

***Obr. 1:** Vyhodnocení agarosové elektroforézy*

VÝSLEDKY A DISKUSE

- Ověření přítomnosti T-DNA u 10 inzerčních linií *A. thaliana* dostupných z NASC.
- Šest genů HSP70 a čtyři geny HSP90.
- Tři typy T-DNA - SALK (7 linií), SAIL (1 linie), GABI (2 linie) .
- Ze sedmi linií SALK mělo být čistě HM pět.
- Potvrzeně byly tři linie.
- Dvě linie segregující s HM vzorkem (znovu namnožit a ověřit).
- Dvě linie byly segregující, ale bohužel neposkytly HM.
- SAIL linie měla být segregující, ale žádnou mutaci nenesla.

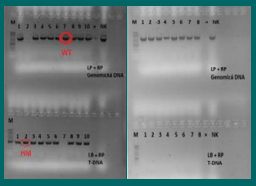

***Obr. 2:** SALK HSP90-2* ***Obr. 3:** SAIL HSP70-11*

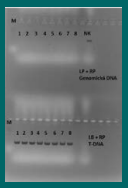

***Obr. 4:** SALK HSP70-1* ***Obr. 5:** SALK HSP70-12*

- GABI linie byly náročnější k odhalení HM rostliny (soubor více zkumavek – cca 20).
- Linie HSP70-13 nesla čistě HM potomstvo.
- U linie HSP70-9 nebyla nalezena čistě HM rostlina.
- Pouze ve zkumavce č. 4 byl nalezen jeden vzorek.

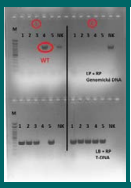

***Obr. 6:** GABI HSP70-13* ***Obr. 7:** GABI HSP70-9-4 (1. a 2. rostlina)*

ZÁVĚR

Pravděpodobnost, že z instituce NASC dojdou rostliny *A. thaliana*, které na daném genu nenesou mutaci v takovém stavu, v jakém je deklarovaná, je velká z důvodu rozsáhlé distribuce semen modelového organismu a kvůli náročnosti přípravy mutantní rostliny. Vyjma GABI linie, které jsou dodávány jako set semenných vzorků, ze kterých je třeba vyselektovat čistě homozygotní linii, ze zbývajících osmi testovaných linií byla správnost ověřena u šesti. Z těchto šesti však byly tři linie segregující, což sice odpovídalo tvrzení NASC, avšak tyto neposkytnuly homozygotní jedince v potomstvu. Z uvedených výsledků vyplývá, že ověření správnosti požadované mutace je vzhledem k poměrně výrazné chybovosti nutné u všech komerčně dostupných T-DNA inzerčních linií *A. thaliana* a musí předcházet všem následným výzkumným experimentům.

Studium reakčních procesů v rámci sanační metody ISCO

Tibor Malinský[1], Ing. Radek Škarohlíd[2], Mgr. Ing. Marek Martinec, Ph.D.[2]

[1]První soukromé jazykové gymnázium v Hradci Králové, s. r. o., Brandlova 875, 500 03, Hradec Králové
[2]Vysoká škola chemicko-technologická v Praze, Fakulta technologie ochrany prostředí, Technická 5, Dejvice, 166 28, Praha 6

Úvod

V současné době se svět potýká s kontaminací podzemních vod. Jedním z nejčastějších kontaminantů jsou relativně perzistentní chlorované etheny. K odstranění těchto látek se používá mnoho sanačních metod, z nichž jedna je in situ chemická oxidace (ISCO) s využitím peroxodisíranu (PDS) aktivovaného pomocí kyselinou citronovou chelatovaného Fe(II).

Cíle práce

- V laboratorním měřítku otestovat účinnost této metody pro odstranění 1,1,2-trichlorethenu (TCE).
- Zjistit vliv počátečního molárního poměru PDS/Fe(II) na účinnost odstranění TCE.
- Zjistit vliv počátečního molárního poměru PDS/Fe(II) na účinnost využití PDS.
- Určit nedostatky experimentálního designu, jenž byl pro danou činnost speciálně navrhnut.

Mechanismus

Fe(II) aktivuje PDS, díky čemuž vznikne síranový radikál, který efektivně oxiduje polutanty (viz rovnice 1). Je-li v systému příliš mnoho Fe(II), tak vzniknuvší radikály zpětně reagují s železnatým kationtem za vzniku síranového aniontu a Fe(III) (viz rovnice 2). Proto je nutné jeho množství regulovat např. kyselinou citronovou (CA), jež kationt chelatuje.

$$S_2O_8^{2-} + Fe^{2+} \rightarrow Fe^{3+} + SO_4^{2-} + SO_4^{\cdot-} \quad (1)$$

$$SO_4^{\cdot-} + Fe^{2+} \rightarrow Fe^{3+} + SO_4^{2-} \quad (2)$$

Obr. 1 PRSOR

Experimentální část

Speciálně pro tento výzkum byl navržen reaktor PRSOR (viz obr. 1), který umožňuje práci s volatilními látkami, neb jej lze uzavřít teflonovým septem. Cílů práce bylo dosáhnuto pomocí šesti systému PDS/CA/Fe(II)/TCE v destilované vodě s odlišným molárním poměrem PDS/Fe(II). Pro svou špatnou rozpustnost ve vodě byl zásobní roztok TCE připravován v methanolu.

Experimenty v PRSORu probíhaly v duplikaci současně s kontrolou (pouze voda a TCE) za laboratorní teploty a bylo z nich v časech 7, 28, 46 a 65 minut od zahájení odebíráno na head-space plynovou chromatografii, aby byl zjištěn pokles TCE, a na kapilární elektroforézu za účelem zjištění úbytku PDS.

Výsledky a diskuze

Na grafu 1 lze vidět změny koncentrace TCE. Systémy s větším množstvím aktivátoru zdegradovaly více TCE za stejný čas – jsou tedy rychlejší. Výjimka je fialový systém, kde vzniknuvší radikály zpětně reagovaly s přebytečnými železnatými kationty během prvních několika chvil, a tak se přeměnily na síranové anionty (SA) bez účinné degradace (viz rovnice 2).

Graf 2, na kterém jsou zaznamenány úbytky PDS, potvrzuje předchozí mínění. Je-li v systému příliš mnoho aktivátoru, přemění se veškeré PDS na SA během prvních několika momentů, tudíž vymizí ze systému a nezdegraduje TCE. Kvůli použití vypočítané počáteční hodnoty namísto té skutečné vznikly drobné nepřesnosti (viz červený a oranžový systém).

Z předchozích výsledků bylo spočítáno RSE (reaction stoichiometry efficiency), které udává kolik molů TCE je 1 mol PDS schopen zdegradovat (viz graf 3). S větším množstvím aktivátoru je sice sanace rychlejší, ale klesá účinné využití PDS. (Kvůli chybám měření není červený a oranžový systém na začátku uveden.)

Kvůli tomu, že TCE bylo připraveno v methanolu, tak byly pozorovány i změny v jeho koncentraci (graf 4). Výsledky naznačují, že mohlo docházet i k jeho oxidaci. Chybové úsečky ale naznačují velkou nejistotu. Chromatograf byl totiž nastaven na chlorované etheny, nikoliv na nižší alkoholy, může se tak jednat o chybu měření.

S úbytkem PDS byl měřen i nárůst SA (viz graf 5) a porovnán s PDS (viz graf 6). Očekávalo by se, že rozdíly koncentrací budou ekvivalentní, ovšem nejsou. Nepřesnosti mohly být způsobeny chybou měření, ale nastal i případ, kdy změna koncentrace PDS byla větší. Jedno z vysvětlení je, že SA reagují s H^+ a vzniká tak SO_3, což je plyn a ze systému tak odchází.

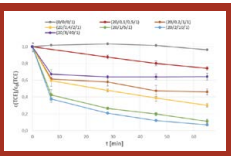

Graf 1 Degradace TCE v jednotlivých systémech

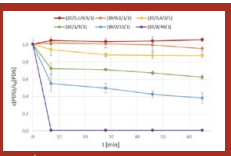

Graf 2 Úbytek PDS v jednotlivých systémech

Graf 3 RSE (reaction stoichiometry efficiency), zobrazení kolik molů TCE je 1 mol PDS schopen zdegradovat

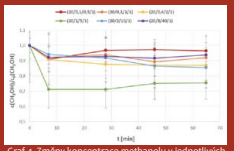

Graf 4 Změny koncentrace methanolu v jednotlivých systémech

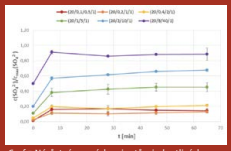

Graf 5 Nárůst síranových aniontů v jednotlivých systémech

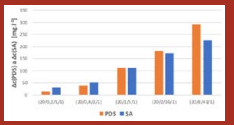

Graf 6 Porovnání úbytku PDS a nárůstu síranových aniontů v jednotlivých systémech

Závěr

Čím větší množství aktivátoru v systému, tím větší množství TCE je zdegradováno, jelikož je vyprodukováno více síranových radikálů, ale příliš mnoho aktivátoru způsobuje přeměnu síranových radikálu na SA, tudíž degradace je neúčinná.

S větším množstvím aktivátoru klesá účinné využití PDS. Je-li potřeba rychlá sanace, je výhodné použít více aktivátoru, pokud ovšem jde o účinné využití PDS, je žádoucí použít méně aktivátoru. Sanace potrvá déle, ale bude ušetřen materiál

V průběhu experimentálních prací byly identifikovány nedostatky experimentálního designu např. potencionální reakce oxidantů s methanolem nebo nepřesnosti způsobené neznalostí skutečné koncentrace PDS v systému.

Přínos

Výsledky této práce by mohly být využity na lokalitách v ČR, které jsou podle webu Ministerstva životního prostředí chlorovanými etheny znečištěny. Jedná se např. o Mariánské hory, Záluží u Litvínova, Neratovice, Březnice a Červený Kostelec.

Navazující studie

Navazující studie by mohly zdokonalit experimentální design tím, že by optimalizovaly metodu na zjištění skutečné počáteční koncentrace PDS v systému namísto použití hodnoty vypočtené. Dále by mohly vyvinout metodu na měření methanolu, či by TCE připravily přímo ve vodě. V neposlední řadě by v navazujících studií mohly být experimenty prováděny za nižších teplot, tedy za teplot podobné těm, které jsou v horninovém prostředí.

Vývoj voltametrické metody stanovení léčiva atomoxetinu

Martin Slavík, Renáta Šelešovská

Střední průmyslová škola chemická Pardubice, sperylit24@gmail.com

ÚVOD

Atomoxetin (ATX) se systematickým názvem (3R)-N-methyl-3-(2-methylphenoxy)-3-phenylpropan-1-amine působí jako účinná látka v léčivech, která se využívají pro tlumení symptomů hyperkinetické poruchy známé jako ADHD, jež postihuje především děti a mladistvé.

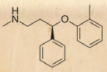

Schéma 1: Strukturní vzorec atomoxetinu

Nejčastější metodou stanovení ATX je vysokotlaká kapalinová chromatografie v kombinaci s různými detektory. V literatuře byla popsána pouze jedna metoda voltametrického stanovení ATX s využitím elektrody ze skelného uhlíku (GCE), která umožnila dosažení detekčního limitu 6,9×10^{-5} mol/l [1]. Cílem této práce bylo studium voltametrického chování ATX a vývoj voltametrické metody jeho stanovení s využitím borem dopované diamantové elektrody (BDDE).

EXPERIMENTÁLNÍ ČÁST

Použité vybavení

- **Polarografický analyzátor**
  - Eco-Tribo Polarographs, software POLAR. PRO 5.1
- **Elektrody**
  - pracovní borem dopovaná diamantová elektroda (BDDE)
  - referentní nasycená argentchloridová elektroda
  - pomocná elektroda platinový drátek
- **Další přístroje** – pH metr, váhy, ultrazvuková lázeň

Obr. 1: Použitý polarografický analyzátor a detail BDDE

Použité chemikálie

- standardní roztok ATX v destilované vodě (1×10^{-3} mol/l)
- roztoky ATX o nižší koncentraci připravovány denně čerstvé ředěním základním elektrolytem
- základní elektrolyty
  - Bristonův-Robinsonův pufr (pH 2 – 12)
  - 0,1 M HNO_3

Metodika

- **Studium voltametrického chování ATX**
  - cyklická voltametrie (CV) – E_s = –1000 mV, E_{switch} = +2200 mV, v = 100 mV
- **Vývoj metody stanovení ATX**
  - diferenční pulzní voltametrie (DPV) – E_s = +500 mV, E_{fin} = +2000 mV, v = 50 mV/s, *výška pulzu* = 50 mV, *šířka pulzu* = 20 ms
- **Předúprava BDDE** – 20 CV, E_s = –1000 mV, E_{switch} = +2200 mV, v = 100 mV
- **Analýza modelových/reálných vzorků** – metoda přídavku standardního roztoku

VÝSLEDKY A DISKUSE

Studium voltametrického chování ATX

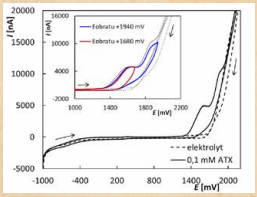

Obr. 2: CV voltamogram ATX (1×10^{-4} mol/l) na BDDE v prostředí BRB o pH 4,5

→ ATX poskytuje 2 ireverzibilní oxidační signály

→ Ireverzibilita elektrodových reakcí byla potvrzena i při změně potenciálů obratu

Závislost na pH

→ ATX poskytuje 2 oxidační píky v celém testovaném rozsahu pH 1–12

→ S rostoucím pH se zhoršuje tvar signálů a jejich vyhodnotitelnost

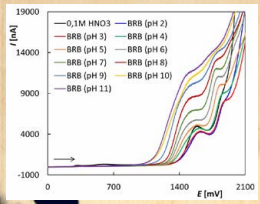

Obr. 3: Anodické části CV voltamogramů ATX (1×10^{-4} mol/l) na BDDE v závislosti na pH

Vývoj metody stanovení ATX

(koncentrace ATX - 1×10^{-5} mol/l)

Volba vhodného základního elektrolytu

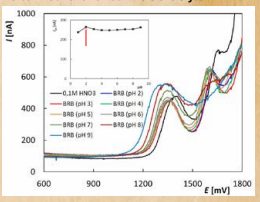

Obr. 4: DPV voltamogramy ATX v závislosti na pH zaznamenané na BDDE, závislost I_p na pH

→ ATX poskytuje 2 oxidační signály v celém testovaném rozsahu pH 2–12, které se příliš nemění

→ Z vložené závislosti vyplývá, že nejvyšší pík byl naměřen v prostředí BRB o pH 2

Optimalizace parametrů DPV

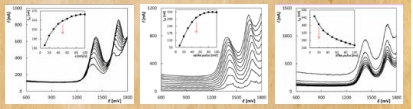

Obr. 5: DPV voltamogramy ATX v závislosti na rychlosti polarizace, výšce a šířce pulzu na BDDE, vložené závislost I_p na jednotlivých parametrech

→ Na základě získaných závislostí byly vybrány následující parametry DPV: rychlost polarizace (v) 50mV/s, šířka pulzu 20 ms a výška pulzu 50mV

Předúprava BDDE

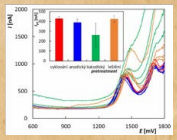

Obr. 6: DP voltamogramy ATX v závislosti na procesu předúpravy pracovní elektrody

- Cyklování
- Anodická předúprava
- Katodický předúprava
- Leštění na alumině

→ Nejvyšší signál po aktivaci cyklováním

Analýza modelových roztoků

Měření koncentračních závislostí ATX

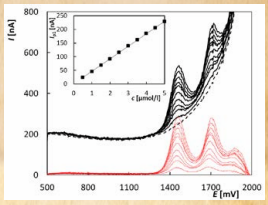

Obr. 7: DP voltamogramy ATX na BDDE v závislosti na koncentraci, c_{ATX} = 5×10^{-7} až 5×10^{-6} mol/l)

→ LOD = 3,9×10^{-8} mol/l

→ LOQ = 1,3×10^{-7} mol/l

→ LDR = 2.5×10^{-7} až 2×10^{-5} mol/l

Stanovení ATX v modelových vzorcích

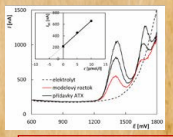

Obr. 7: Příklad analýzy modelového vzorku ATX metodou standardního přídavku

c (mol/l)	stanoveno (mol/l)	RSD (%)
5,0×10^{-6}	(4.990±0,065)x10^{-6}	1,96
1,0×10^{-5}	(1.013±0,024)×10^{-5}	3,58

→ Metoda umožňuje stanovení správných a dobře opakovatelných výsledků

ZÁVĚR

→ ATX poskytuje na BDDE 2 oxidační píky využitelné pro analýzu

→ Byla vyvinuta spolehlivá, rychlá a levná metoda stanovení ATX

→ Získaný detekční limit byl nižší než s využitím GCE

→ Tato metoda byla úspěšně aplikována při analýze modelových vzorků

Další postup

→ Aplikace nové metody při analýze praktických vzorků léčiv s obsahem ATX

Výchozí zdroj: [1] M. Pérez-OrtizC. MunozC. Zapata-Urbanize ÁlvarezLueje: Electrochemical behavior of atomoxetine andits voltammetric determination in capsules. Talanta 82, 398-403 (2010)

Poděkování: Práce byla financována GA ČR projektem č. 20-01589S.

SEKCE BAKALÁŘSKÝCH A MAGISTERSKÝCH STUDENTŮ

Produkcia polyesterov pomocou extrémofilných baktérií

Kristína Bednárová
Xenie Kouřilová, Stanislav Obruča

Vysoké učení technické v Brně, Fakulta chemická, Ústav chemie potravin a biotechnologií
Purkyňova 464/118, 612 00 Brno, Česká republika
xcbednarovak@vutbr.cz

1 Úvod

Polyhydroxyalkanoáty (PHA) sú prirodzene sa vyskytujúce alifatické polyestery tvorené monomérmi R-hydroxyalkánovej kyseliny, ktoré sú spojené esterovou väzbou. Pozostávajú z uhlíka, vodíka a kyslíka. Tieto biopolyméry sú syntetizované grampozitívnymi a gramnegatívnymi baktériami vo forme intracelulárnych iklúzií ako zásoba uhlíka a energie. PHA sa akumulujú v baktériách počas nevyvážených rastových podmienok v dôsledku obmedzeného prísunu nevyhnutných živín, ako je dusík, fosfor alebo horčík, a nadbytku vhodného zdroja uhlíku. Ukladajú sa v cytoplazme buniek vo forme granúl, lipidických inklúzií, čo predstavuje výhodu uskladnenia prebytočného uhlíka. Sú nerozpustné vo vode, vďaka čomu neovplyvňujú fyziologickú kondíciu mikroorganizmov. Povrch granúl je obklopený membránou zloženou z fosfolipidov a proteínov[1,2].

Termofily sú organizmy, ktoré nielen prežívajú, ale aj prosperujú pri teplotách and 45°C. Prvýkrát boli objavené v roku 1888 Miguelom, ktorý charakterizoval termofily, ktoré tvorili aeróbne spóry a boli schopné rásť pri 70 °C. Predpokladá sa, že termofilné baktérie patria medzi jedny z prvých organizmov žijúcich na Zemi. Okrem prírodných prostredí akými sú napríklad gejzíry, horúce pramene a hydrotermálne prieduchy, kde teploty ľahko presahujú 100 °C, sa nachádzajú aj na miestach vytvorených človekom. Medzi tieto prostredia patria čističky odpadových vôd, priemyselné odpadové toky, komposty alebo aktivované kaly[3, 4, 5].

Podľa optimálnej teploty rastu ich možno rozdeliť na:

- Mierne termofily - optimálny rast od 45 do 65 °C
- Extrémne termofily - optimálny rast od 65 do 85 °C
- Hypertermofily - optimálny rast od 85 °C [6].

Štúdie ukazujú, že termofilné procesy môžu byť stabilnejšie, rýchlejšie a lacnejšie. Termofilné baktérie demonštrujú mnoho výhod pre použitie v priemyselnom odvetví. Veľkou výhodou ich využitia v priemysle sú ich vysoké rýchlosti rastu, ktoré môžu dvakrát až trikrát urýchliť fermentačné procesy oproti technológiám používajúcich mezofilné baktérie. Použitím vysokoteplotného spracovania sa znižuje riziko nežiadúcej mikrobiálnej kontaminácie, znižuje sa šanca fágovej infekcie, zvyšuje sa rozpustnosť

substrátov a zároveň sa znižuje ich viskozita. Vďaka týmto výhodám našli uplatnenie pri výrobe chemických surovín a palív, v enzýmovej technológii a pri biokonverzii odpadov. Za zmienku určite stojí uplatnenie v oblasti génového inžinierstva, ktoré využíva termofilné DNA polymerázy pri polymerázovej reťazovej reakcii na amplifikáciu DNA. Dôležitú úlohu v potravinárskom, papierenskom, farmaceutickom a chemickom priemysle hrajú termostabilné enzýmy degradujúce polyméry[7, 8, 9].

2 Experimentální část

2.1 Mikroorganizmy, kultivácia, analýza

Používané mikroorganizmy boli zakúpené z nemeckej zbierky Leibnitz Institut DSMZ-German Collection of Microorganism and Cell Cultures a to bakteriálne kmene *Thermomonas hydrothermalis* DSM 14834 a *Schlegelella thermodepolymerans* DSM 15344 a z belgickej zbierky BCCM-Belgian Coordinated Collections of Microorganisms a to kmeň *Schlegelella aquatica* LMG 23380.

Inokulačné medium obsahovalo pepton (10 g/l), beef extract (10 g/l), NaCl (5 g/l). Inokulum sa kultivovalo 24 hodín pri teplote 50 °C pri 180 rpm v Erlenmeyerových bankách.

Minerálne medium obsahovalo $Na_2HPO_4 \cdot\cdot 12\ H_2O$ (9 g/l), KH_2PO_4 (1,5 g/l), NH_4Cl (1 g/l), $MgSO_4 \cdot 7\ H_2O$ (0,2 g/l), $CaCl_2 \cdot 2\ H_2O$ (0,02 g/l), NH_4Fe^{III}citrát (0,0012 g/l), yeast extract (0,5/3,0 g/l), TES II (1 ml/l) a zdroj uhlíku (2-20 g/l). Pri skúmaní optimálneho zdroja uhlíku boli bunky kultivované pri teplote 50 °C a následne pri optimálnej teplote rastu. Inokulačný pomer bol 10 %. Kultivácia prebiehala 72 hodín v 250 ml Erlenmeyerových bankách na trepačkách za stáleho miešania pri 180 rpm.

Na screening utilizácie vybraných zdrojov uhlíku boli použité: glukóza, fruktóza, galaktóza, manóza, xylóza, sacharóza, laktóza, škrob a glycerol. Koncentrácia uvedených substrátov bola 20 g/l. Bakteriálne kmene boli kultivované pri štyroch rôznych teplotách a to 45, 50, 55, 60 °C na najvhodnejšom zdroji uhlíku.

Ako prekurzory pre produkciu kopolymérov boli použité: propionát sodný (2 g/l), kyselina valérová (2 g/l), 1,4-butandiol (8 g/l) a γ-butyrolaktón (8 g/l). Do media s obsahom propionátu sodného a kyseliny valérovej bol pridaný substrát stanovený ako najvhodnejší.

Kmeň *Schlegelella thermodepolymerans* bol kultivovaný na modelových hydrolyzátoch mäkkého a tvrdého dreva, ryžovej slamy, bagasy z cukrovej trstiny, pšeničnej slamy a otrubov. Presné zloženie modelových hydrolyzátov je uvedené v tabuľke 1.

Tabuľka 1: Zloženie modelových hydrolyzátov

	koncentrácia [g/l]				
	glukóza	xylóza	arabinóza	manóza	galaktóza
mäkké drevo	16,6	1,0	0,1	2,0	0,3
tvrdé drevo	3,2	12,4	1,0	1,8	1,6
ryžová slama	4,2	13,4	2,4	-	-
bagasa z cukrovej trstiny	2,8	15,0	2,2	-	-
pšeničná slama	11,2	7,2	0,9	-	0,7
pšeničné otruby	0,8	12,4	6,8	-	-

Taktiež bol u daného kmeňa sledovaný vplyv kyslíka na množstvo produkovanej biomasy a PHA. Kultivácia prebiehala v 250 ml Erlenmeyerových bankách pričom objem minerálneho média bol 50; 75; 100; 125; 150; 175 ml.

Získané optimálne kultivačné podmienky boli u daného kmeňa aplikované pri kultivácii v mechanicky miešanom sklenenom laboratórnom bioreaktore Biostat B-plus s objemom minerálneho media 3,5 l. Kultivácia prebiehala po dobu 24 hodín, pri teplote 55 °C a pH 7. Obsah rozpusteného kyslíka bol regulovaný na 20 %.

Biomasa bola stanovovaná gravimetricky. Obsah PHA bol analyzovaný pomocou plynovej chromatografie s plameňovo ionizačným detektorom od firmy Thermo Scientific, Trace 1300. Použitá kolóna bola od firmy Thermo Scientific TG-WAXMS, s dĺžkou 30 m, I.D.: 0,32 mm a šírkou filmu 0,5 μm. Ako nosný plyn bol použitý dusík s prietokom 2 ml/min. Biomasa s hmotnosťou 8-11 mg bola rozpustená v 1 ml chloroformu a následne bola pridaná transesterifikačná zmes (15% roztok kyseliny sírovej v methanole s vnútorným štandardom kyselinou benzoovou 5 mg/ml) v objeme 0,8 ml. Uzavreté vialky boli umiestnené v termostate pri teplote 95 °C po dobu 3 hodiny. Po ochladení na laboratórnu teplotu sa do vzoriek pridalo 0,5 ml 0,05 M hydroxidu sodného. Po ustálení fázového rozhrania bolo do čistých vialiek s chloroformom o objeme 900 μl odobraných, 50 μl organickej fázy. Takto pripravené vzorky boli analyzované plynovým chromatografom.

Bunky bakteriálnych kmeňov *Schlegelella thermodepolymerans* a *Schlegelella aquatica* boli pozorované transmisným elektrónovým mikroskopom. Analýza bola uskutočnená v Biologickom centre Akademie věd České republiky v Českých Budějovicích. Sledované bunky boli kultivované 48 hodín na najlepšom uhlíkatom zdroji za optimálnej teploty. Na analýzu boli dodané v podobe bunkovej suspenzie.

3 Výsledky a diskusia

U kmeňa *Schlegelella thermodepolymerans* bola pomocou molekulárno-biologických metód na úrovni genotypu potvrdená prítomnosť *phaC* génu. Primárne bol bakteriálny kmeň podrobený screeningu utilizácie 1 nesacharidového a 8 sacharidových zdrojov uhlíku v mikrotitračnej doštičke. Najlepšie bola utilizovaná fruktóza, glycerol, glukóza a xylóza. Tieto zdroje uhlíku boli vybrané na kultiváciu v Erlenmeyerových bankách. Naopak baktéria neprosperovala v prostredí škrobu, sacharózy a galaktózy. 72 hodinovou kultiváciou v Erlenmeyerových bankách bol sledovaný vplyv vybraných substrátov na produkciu biomasy a PHB. Pozitívne výsledky boli získané kultiváciou s využitím xylózy, kedy koncentrácia získaného PHB dosiahla hodnotu 4,66 g/l pričom polymér bol obsiahnutý až v 75,18 % biomasy (obrázok 1). Kultúra taktiež dobre prosperovala v prostredí glycerolu a glukózy.

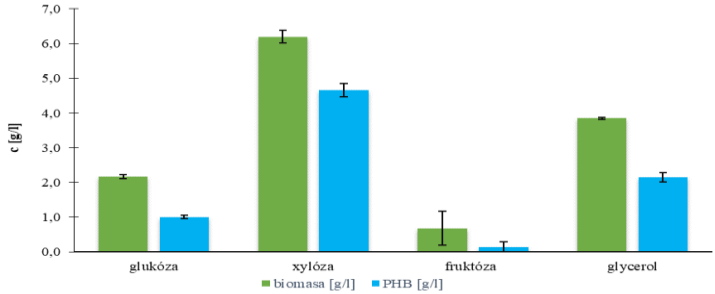

Obrázok 1: Koncentrácie biomasy a PHB po kultivácii kmeňa Schlegelella thermodepolymerans na vybraných substrátoch

Ako najvhodnejšia teplota pre rast a produkciu PHA bola stanovená teplota 55 °C. Na produkciu kopolymérov boli využité prekurzory a to kyselina valérová, propionát sodný, γ-butyrolaktón a 1,4-butándiol. Bakteriálna kultúra utilizovala propionát sodný za tvorby kopolyméru P(3HB-co-3HV). Na rast bakteriálneho kmeňa malo vplyv aj množstvo rozpusteného kyslíka v médiu. Kultivácia prebiehala v 250 ml Erlenmeyerových bankách s rozdielnym objemom minerálneho média. Najväčšia koncentrácia biomasy bola nameraná v najmenšom kultivačnom objeme s obsahom média 50 ml. Najväčšie množstvo polyméru však bolo nasyntetizované v produkčnom médiu s objemom 100 ml (obrázok 2). To potvrdzuje skutočnosť, že parciálna limitácia kyslíkom výrazne podporuje akumuláciu PHA.

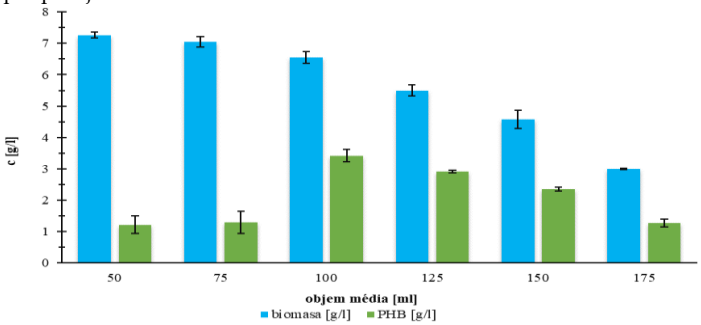

Obrázok 2: Porovnanie vplyvu kyslíka na produkciu biomasy a PHB

Keďže biotechnologickou snahou je znížiť výrobné náklady, bol bakteriálny kmeň podrobený kultivácii na modelových hydrolyzátoch surovín bohatých na lignocelulózu, ktoré vznikajú ako vedľajšie produkty výroby. Najlepšie boli zužitkované modelové hydrolyzáty bagasy z cukrovej trstiny a mäkkého dreva. V porovnaní s kultiváciou na xylóze sa však koncentrácia získaného PHB znížila o viac ako polovicu a zároveň sa znížil aj percentuálny obsah polyméru v biomase.

Vďaka syntéze pomerne vysokých koncentrácií PHA za utilizácie xylózy a vysokému percentuálnemu zastúpeniu v biomase, bol kmeň kultivovaný vo väčšom

produkčnom objeme. Kultiváciou v bioreaktore bola pozorovaná doba trvania lag fázy, exponenciálnej a stacionárnej fázy rastu. Rast buniek však nebol dostatočný, čo malo vplyv aj na množstvo získaného produktu. Percentuálny obsah PHB v biomase sa zhodoval s percentuálnym obsahom získaným kultiváciou v menšom produkčnom objeme. Kultivácia v bioreaktore vyžaduje ďalšiu optimalizáciu podmienok pre dosiahnutie vyšších koncentrácií produktu.

Bakteriálne bunky *Schlegelella thermodepolymerans* kmeňa DSM 15344 boli pozorovné pod transmisným elektrónovým (obr.3). V cytoplazme buniek možno pozorovať rozsiahle množstvo nasyntetizovaných PHA inklúzií. Na mikroskopickom snímku vidieť, že ide o baktériu tyčinkovitého tvaru, pričom dĺžka buniek je 1-2 μm a ich šírka je 0,5-0,6 μm.

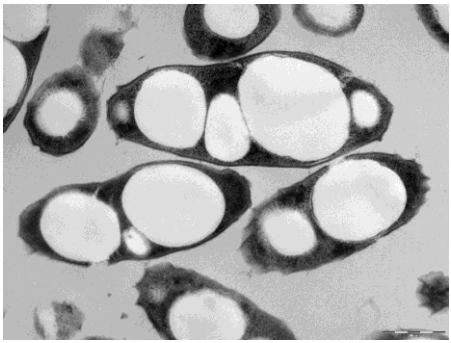

Obrázok 3: Akumulované PHA inklúzií v Schlegelella thermodepolymerans pozorovaná pod transmisným elektrónovým mikroskopom (mierka 500 nm)

Bakteriálny kmeň *Schlegelella aquatica* disponuje génom *phaC*, kódujúci PHA syntázu. Z vybraných 9 uhlíkových zdrojov boli pri kultivácii v mikrotitračnej doštičke najlepšie utilizované glycerol, xylóza a glukóza. Zvyšné testované sacharidy neboli efektívne využité na rast. Za najvhodnejší substrát pre produkciu biomasy a PHB bol na základe stanovení vybraný glycerol. Bakteriálne bunky mali najväčšiu schopnosť rastu a produkcie PHA pri teplote 45 °C. Koncentrácia polyméru v biomase pri danej teplote v prostredí glycerolu dosiahla hodnoty 1,12 g/l s percentuálnym obsahom v biomase 32,53 %. Podobne ako Schlegelella thermodepolymerans tak aj kmeň *Schlegelella aquatica* využíval propionát sodný na produkciu kopolyméru P(3HB-co-3HV). V prípade zvyšných prekurzorov bolo množstvo získanej biomasy veľmi nízke.

Na obrázku 4 možno pozorovať morfológiu bakteriálnej bunky *Schlegelella aquatica* kmeňa LMG 23380. Rovnako ako u kmeňa *Schlegelella thermodepolymerans* ide o baktériu tyčinkovitého tvaru. Polymér je v bunke obsiahnutý len vo veľmi malom objeme. Dĺžka buniek je v rozmedzí 0,8-2,0 μm a jej priemer 0,4 až 0,5 μm.

Obrázok 4: Akumulované PHA inklúzií v Schlegelella aquatica pozorovaná pod transmisným elektrónovým mikroskopom (mierka 500 nm)

Poslednou študovanou baktériou bol termofilný kmeň *Thermomonas hydrothermalis*. Keďže sa nepodarilo izolovať bakteriálnu DNA, bola schopnosť produkcie PHA overená na úrovni fenotypu. Kmeň *Thermomonas hydrothermalis* utilizoval všetky vybrané zdroje uhlíku použité pri screeningu v mikrotitračnej doštičke. Najlepšie boli zužitkované glukóza, xylóza a laktóza. Ako jediný spomedzi študovaných baktérií bol schopný rásť v prostredí škrobu. Najvyššia produkcia PHB bola dosiahnutá utilizáciou glukózy. Bakteriálny kmeň však nevedel efektívne využiť xylózu a laktózu na produkciu polyhydroxyalkanoátov. Teplotné optimum pre rast je 55 °C. Kultiváciou v prostredí prekurzorov bola dosiahnutá produkcia kopolyméru P(3HB-co-4HB), ale aj P(3HB-co-3HV). 1,4-butándiol podporil tvorbu kopolyméru P(3HB-co-4HB) a koncentrácia PHA v bunkách sa zvýšila takmer o polovicu na hodnotu 1,01 g/l (tabuľka 2), v porovnaní s kultiváciou v prostredí glukózy. Zvýšil sa aj percentuálny obsah PHA v biomase na 55,05 %. Vzniknutý kopolymér bol unikátny extrémne vysokou molárnou frakciou 4HB a to až 96,91 mol.%. Využitím propionátu sodného baktéria síce dokázala produkovať P(3HB-co-3HV), no získané koncentrácie boli veľmi nízke.

Tabuľka 2: Výsledky vplyvu prekurzorov na produkciu kopolymérov použitím kmeňa Thermomonas hydrothermalis

prekurzor	biomasa [g/l]	PHA		4HB [mol.%]	3HV [mol.%]	3HB [mol.%]
		[g/l]	[% hm.]			
γ-butyrolaktón	0,06 ± 0,03	-	-	-	-	-
1,4-butándiol	1,84 ± 0,04	1,01 ± 0,07	55,05	96,91	-	3,09
k.valérová	0,05 ± 0,03	-	-	-	-	-
propionát sodný	0,77 ± 0,51	0,16 ± 0,00	14,00	-	14,14	85,86

4 Závery

Bakteriálny kmeň *Schlegelella thermodepolymerans* má unikátnu schopnosť efektívne využívať xylózu na produkciu vysokých koncentrácií PHA. Rast buniek je optimálny pri teplote 55 °C. Baktéria je schopná syntézy kopolyméru P(3HB-co-3HV). Bunky sú senzibilné na množstvo rozpusteného kyslíka a ako sľubné substráty pre produkciu PHA sa javia lignocelulózové hydrolyzáty bohaté na xylózu a glukózu.

Bakteriálne kmene *Thermomonas hydrothermalis* a *Schlegelella aquatica* síce za sledovaných podmienok dokážu produkovať polyhydroxyalkanoáty, no nie v koncentráciách, ktoré by boli pre priemysel zaujímavé. Kmeň *Thermomonas hydrothermalis* je však unikátny produkciou kopolyméru P(3HB-co-4HB) s extrémne vysokou molárnou frakciou 4HB za využitia 1,4-butándiolu. Kopolymér s takto vysokou molárnou frakciou 4HB by mohol mať využitie v medicínskych aplikáciách.

5 Literatúra

1. ALTUN, Müslüm. Polyhydroxyalkanoate production using waste vegetable oil and filtered digestate liquor of chicken manure. Preparative Biochemistry and Biotechnology. 2019, 49(5), 493-500. DOI: 10.1080/10826068.2019.1587626. ISSN 1082-6068. Dostupné z: https://www.tandfonline.com/doi/full/10.1080/10826068.2019.1587626
2. KESHAVARZ, Tajalli a Ipsita ROY. Polyhydroxyalkanoates: bioplastics with a green agenda. Current Opinion in Microbiology [online]. 2010, 13(3), 321-326 [cit. 2019- 11-10]. DOI: 10.1016/j.mib.2010.02.006. ISSN 13695274. Dostupné z: https://linkinghub.elsevier.com/retrieve/pii/S1369527410000275
3. SARMIENTO, Felipe, Rocío PERALTA a Jenny M. BLAMEY. Cold and Hot Extremozymes: Industrial Relevance and Current Trends. Frontiers in Bioengineering and Biotechnology [online]. 2015, 3 [cit. 2019-11-30]. DOI: 10.3389/fbioe.2015.00148. ISSN 2296-4185. Dostupné z: http://journal.frontiersin.org/Article/10.3389/fbioe.2015.00148/abstract
4. ADIGUZEL, Ahmet, Hakan OZKAN, Ozlem BARIS, Kadriye INAN, Medine GULLUCE a Fikrettin SAHIN. Identification and characterization of thermophilic bacteria isolated from hot springs in Turkey. Journal of Microbiological Methods [online]. 2009, 79(3), 321-328 [cit. 2019-11-30]. DOI: 10.1016/j.mimet.2009.09.026. ISSN 01677012. Dostupné z: https://linkinghub.elsevier.com/retrieve/pii/S0167701209003121
5. SATYANARAYANA, Tulasi, Jennifer LITTLECHILD a Yutaka KAWARABAYASI, ed. Thermophilic Microbes in Environmental and Industrial Biotechnology [online]. Dordrecht: Springer Netherlands, 2013 [cit. 2020-04-11]. DOI: 10.1007/978-94-007-5899-5. ISBN 978-94-007-5898-8.
6. GONZÁLEZ-GONZÁLEZ, Roberto, Pablo FUCIÑOS a María Luisa RÚA. An Overview on Extremophilic Esterases. SANI, Rajesh K. a R. Navanietha KRISHNARAJ, ed. Extremophilic Enzymatic Processing of Lignocellulosic Feedstocks to Bioenergy [online]. Cham: Springer International Publishing, 2017,

2017-06-24, s. 181-204 [cit. 2020-04-08]. DOI: 10.1007/978-3-319-54684-1_10. ISBN 978-3-319-54683-4. Dostupné z: http://link.springer.com/10.1007/978-3-319- 54684-1_10

7. CANGANELLA, Francesco a Juergen WIEGEL. Extremophiles: from abyssal to terrestrial ecosystems and possibly beyond. Naturwissenschaften [online]. 2011, 98(4), 253-279 [cit. 2019-11-29]. DOI: 10.1007/s00114-011-0775-2. ISSN 0028-1042. Dostupné z: http://link.springer.com/10.1007/s00114-011-0775-2
8. ZEIKUS, J.G. Thermophilic bacteria: Ecology, physiology and technology. Enzyme and Microbial Technology [online]. 1979, 1(4), 243-252 [cit. 2019-11-30]. DOI: 10.1016/0141-0229(79)90043-7. ISSN 01410229. Dostupné z: https://linkinghub.elsevier.com/retrieve/pii/0141022979900437
9. KAMBOUROVA, Margarita. Thermostable enzymes and polysaccharides produced by thermophilic bacteria isolated from Bulgarian hot springs. Engineering in Life Sciences [online]. 2018, 18(11), 758-767 [cit. 2020-04-15]. DOI: 10.1002/elsc.201800022. ISSN 16180240. Dostupné z: http://doi.wiley.com/10.1002/elsc.201800022

Využití metabolomiky pro charakterizaci hlavních změn révy vinné v rámci vegetačního cyklu, a při různých způsobech kultivace

Bc. Adam Behner
Doc. Ing. Milena Stránská, Ph.D.

Vysoká škola chemicko-technologická v Praze,
Fakulta potravinářské a biochemické technologie,
Ústav analýzy potravin a výživy

Technická 3, 16628, Praha 6, Česká republika
behnera@vscht.cz

Vinná réva (*Vitis vinifera*) je historicky jednou z nejdéle kultivovaných rostlin. Díky produkci hroznů patří mezi celosvětově ekonomicky významné plodiny. V kulinářství nebo v tradiční medicíně se však také využívají i ostatní části této rostliny, například listy (balkánská kuchyně). Chemické složení vinné biomasy je silně ovlivňováno vnějšími faktory, jako je lokalita pěstování, zemědělské agropraktiky, odrůda, vegetační období nebo přírodní podmínky. Rozdíly v chemickém složení lze také pozorovat v jednotlivých částech rostliny (stonek/list). Tato práce se zabývá studiem metabolomu rostliny révy vinné za využití pokročilých nástrojů moderní analytické chemie – ultra-vysokoúčinné kapalinové chromatografie ve spojení s vysokorozlišovací hmotnostní spektrometrií (U-HPLC-HRMS/MS). Metabolomickému fingerprintingu byl podroben biomateriál z rostliny vinné révy (listy a stonky). Celkem bylo analyzováno cca 520 vzorků reprezentujících čtyři různé odrůdy odebrané ze dvou českých vinic. Odběr vzorků probíhal ve všech čtyřech ročních ob-

dobích, díky čemuž mohl být prozkoumán celý vegetační cyklus rostliny. Cílem této studie bylo demonstrovat potenciál metody metabolomického fingerprintingu pomocí U-HPLC-HRMS/MS, která by sloužila jako nástroj pro autentizaci listů/stonků révy vinné.

Klíčová slova: *Vitis vinifera, listy, stonky, autenticita, ultra-vysokoúčinná kapalinová chromatografie ve spojení s vysokorozlišovací hmotnostní spektrometrií*

Visible-light photoinitiators for cationic and free-radical photopolymerization studied by indirect EPR techniques

Kristína Czikhardtová, Dana Dvoranová

Institute of Physical Chemistry and Chemical Physics,
Faculty of Chemical and Food Technology, Slovak University of Technology in Bratislava

Radlinského 9, SK-812 37 Bratislava, Slovak Republic
xczikhardtova@stuba.sk

Recently, the development and use of photopolymerization processes, both cationic (CP) and free-radical photopolymerization (FRP), has greatly increased due to the advantages afforded by light-induced polymerization compared to traditional thermal polymerization methods. However, the oxygen inhibition in the free radical polymerization (FRP) and frequent utilization of harmful UV light signify major limitations. Therefore, it is necessary to establish new photoinitiating systems (PIS) or photoinitiators (PI), which will match to the near UV or visible light emission. In this contribution, we focused on detailed study of visible-light active two component photoinitiating systems, consisting of various photoinitiators and photosensitizers (PS), by indirect EPR techniques (spin-trapping or spin-scavenging) [1-4]. We successfully identify reactive paramagnetic species generated upon visible-light irradiation and we confirmed the effective generation of reactive oxygen species (e.g. superoxide radical anion) in the visible-light exposed systems containing photosensitizers and molecular oxygen. the mechanism of FRP was also affirmed by generated

reactive carbon-centered radicals, as corresponding spin-adduct, upon visible-light exposure of photosensitizers in combination with iodonium salts (electron acceptor) or amines (electron donor) under inert atmosphere. Furthermore, photosensitizers (e.g. *chlorophyllin* or *pyropheophorbide-a*) have a promising utilization in photodynamic therapy (PDT) in the destruction of tumors (in summary oncological and also multiple non-oncological diseases) by produced reactive oxygen species (ROS).

Acknowledgement: This work was supported by the Scientific Grant Agency of the Slovak Republic (VEGA Project 1/0026/18).

References

[1] Mokbel, H.; Anderson, D.; Plenderleith, R.; Dietlin, C.; Morlet-Savary, F.; Dumur, F.; Gigmes D.; Fouassier, J.-P., Lalevée, J. Polym. Chem. **2017**, 8(36), 5580 – 5592.

[2] Yagci, Y.; Jockusch, S.; Turro, N. J. Macromolecules **2010**, 43(15), 6245 – 6260.

[3] Breloy, L.; Ouarabi, C.A.; Brosseau, A.; Dubot, P.; Brezova, V.; Abbad Andaloussi, S.; Malval, J.-P., Versace, D.-L. ACS Sust. Chem. Engin. **2019**, 7(24), 19591–19604.

[4] Adriouach, S.; Vorobiev, V.; Trefalt, G.; Allémann, E.; Lange, N.; Babič, A. Nanomedicine: Nanotechnology, Biology and Medicine **2018**

Use of Poly(3-hydroxybutyrate) as Polymer Base for Drug Delivery Systems

Nicole Černeková[1]
Adriana Kovalcik[2]

[1]Brno University of Technology, Faculty of Chemistry, Institute of Physical and Applied Chemistry

Purkyňova 118, 612 00 Brno, Czech Republic
xccernekova@vutbr.cz

[2]Brno University of Technology, Faculty of Chemistry, Institute of Food Chemistry and Biotechnology

Purkyňova 118, 612 00 Brno, Czech Republic

One of the most discussed applications of polyhydroxyalkanoates (PHA) is their use in medicine as scaffolds, drug carrier systems, and wound dressings, made by solution casting, electrospinning, or thermoplastic extrusion. Often, the porosity was found as an essential attribute of specimens used for pharmaceutical and medical applications. the PHA porous materials offer unique properties such as biocompatibility, bioactivity, non-cytotoxicity, and biodegradability. This contribution is focused on the study of the release of active substances from porous structures based on poly(3-hydroxybutyrate) (PHB) films. PHB is a semicrystalline biopolyester with the ability to degrade in vivo and in vitro without toxic substances.

The porous scaffolds were formed from PHB by electrospinning. This work confirmed that the morphology of PHB scaffold

is possible to varied by the PHB concentration and solvents used for electrospinning. Scanning electron microscopy revealed the formation of different morphologies, including porous, filamentous/beaded, and fibre structure films. As the model drug for incorporation into PHB meshes was used Levofloxacin, which possess with a high antibacterial efficiency against gram-positive and gram-negative bacteria. Its entrapment efficiency was found to be dependent on the viscosity of the PHB solution used for electrospinning, its incorporation in meshes was confirmed by Fourier-transform infrared spectroscopy and UV-VIS spectroscopy. the effect of the morphology of the films on the Levofloxacin release profile was screened in vitro in phosphate-buffered saline solution. the antimicrobial efficiency of all tested samples was confirmed by agar diffusion testing.

Acknowledgement: This work was funded through the Internal Brno University of Technology project FCH-S-20-6316.

Keywords: *polyhydroxyalkanoates, scaffolds, electrospinning, antimicrobial activity, morphology*

Analýza G-kvadruplexů v genomech lidských parazitických červů

Michaela Dobrovolná [1, 2]

Alessio Cantara [2]

Jean-Louis Mergny [2]

Václav Brázda [1, 2]

[1]Faculty of Chemistry, Brno University of Technology, Institute of Physical and Applied Chemistry, Brno, Czechia

[2]Department of Biophysical Chemistry and Molecular Oncology, Institute of Biophysics, Academy of Sciences of the Czech Republic, Brno, Czechia.

[3]Department of Experimental Biology, Faculty of Science

Masaryk University, Brno, Czechia.
212674@vutbrno.cz

Onemocnění způsobená parazitickými červy jsou velmi rozšířená u lidí v rozvojových zemích. Podle WHO je parazity celosvětově infikováno přibližně 2 miliardy lidí. Etiologickými činiteli parazitických infekcí jsou zejména parazité kmene *Nematoda* (hlístice) a *Platyhelminthes* (ploštěnci) vyvolávající reakce imunitního systému, podvýživu a chudokrevnost, které jsou primární příčinou onemocnění. Vzrůstající rezistence parazitů na lidská anthelmintika je urychlována jejich nadužíváním, špatnou prevencí a kontrolou infekce. Terapeutický potenciál malých molekulových ligandů vá-

zajících G-kvadruplexy (G4s) byl demonstrován například při stabilizaci G4 struktur, anebo eliminaci patogenů rezistentních na léky. G4s jsou typem sekundární struktury nukleových kyselin tvořené v oblastech bohatých na guanin se schopností regulovat proces genové exprese, opravy poškozené DNA, nebo transkripce a translace v onkogenech. K identifikaci a porovnání potenciálních sekvencí tvořících G-kvadruplex (PQS) v jaderných a mitochondriálních genomech šesti zástupců kmene *Platyhelminthes* a čtyř zástupců kmene *Nematoda* (které by mohly ukázat vhodná cílová místa pro navázání G4 ligandů sloužící k predikci nových míst účinků léčiv a pomoci při vývoji efektivnějších léčiv) byl požit webový nástroj G4Hunter. Byla potvrzena nenáhodná distribuce PQS v genomu a mtDNA analyzovaných organismů. Nejvíce G4 bylo lokalizováno v těsné blízkosti genů, což naznačuje jejich roli v genové regulaci. Zajímavé je, že v méně infekčních zástupcích, jak z kmene *Platyhelminthes*, tak z kmene *Nematoda* bylo nalezeno více PQS, naproti tomu více infekční zástupci vykazovali nižší frekvenci PQS a nižší celkový obsah guaninu a cytosinu.

Neural networks and their use in study of quantum-chemical systems

Peter Fraško, Peter Poliak

Institute of Physical Chemistry and Chemical Physics,
Faculty of Chemical and Food Technology, Slovak University
of Technology in Bratislava

Radlinského 9, SK-812 37 Bratislava, Slovak Republic
peter.frasko@gmail.com

Computational chemistry has become an integral part of many workplaces in recent years, offering the opportunity to obtain information about systems without the use of expensive measuring techniques. Despite advances in computational technology, quantum-chemical methods are still time-consuming or, in the case of faster methods, inaccurate. Neural networks are a potentially effective tool for solving this issue. Assuming we have a sufficient number of molecular geometries and their corresponding energies, the neural network should be able to learn these relationships between the molecular geometry and its energy. Therefore, such a network can be used for fast and accurate energy prediction, which can then be advantageously used, e.g. in molecular dynamics including chemical reactions.

In this contribution we selected 20 basic proteinogenic amino acids as a dataset. the database for the amino acid model was created by molecular dynamics in XTB 6.2.2 [1]. All conformations from the simulation trajectory were used in the database. From the obtained molecular-dynamic trajectories, we created 4 databases, three of which contained selected separate amino acids (alanine, histidine and aspartic acid) and the fourth includes all 20 amino

acids. for training models we used SchNet software package [2]. Models trained on individual molecules have achieved high accuracy exceeding the level of chemical accuracy. It can be assumed that these models could be successfully used together with molecular dynamics to rapidly obtain relatively accurate quantum-chemical information and monitor their evolution over time. The optimal strategy is represented by models learned on the database of 20 amino acids. These should describe the dynamics of the individual amino acids with sufficient accuracy. However, such a model is likely to insufficiently map the interaction between amino acids. Therefore, for use in proteins, it would be necessary to expand the database to include amino acid dimers. However, they already consist of more than 20 atoms, which requires significantly higher learning time.

Keywords: *neural network, machine learning, SchNet, aminoacids*

References:

[1] BANNWARTH,C., EHLERT, S., GRIMME, S., GFN2-xTB-An Accurate and Broadly Parametrized Self-Consistent Tight-Binding Quantum Chemical Method with MultipoleElectrostatics and Density-Dependent Dispersion Contributions, J. Chem. Theory Comput. 2019, 15, 3, 1652 – 1671.

[2] SCHÜTT,K.,T., KINDERMANS,P.,J., SAUCEDA,H.,E., CHMIELA,S., TKATCHENKO,A., MÜLLER,K.,R., SchNet: A continuous-filter convolutional neural network for modeling quantum interactions, 31st Conference on Neural Information Processing Systems (NIPS 2017), Long Beach, CA, USA.

Efekt povrchové modifikace škrobových plniv pomocí polydimethylsiloxanu na proces plnění tvrdých želatinových tobolek

Bc. Petra Havelková
Ing. Pavlína Komínová, prof. Ing. Petr Zámostný, Ph.D.

VŠCHT Praha, Fakulta chemické technologie, Ústav organické technologie

Technická 5, 166 28 Praha 6 – Dejvice, Česká republika
havelkoc@vscht.cz

Jedním z klíčových faktorů, které ovlivňují proces plnění tvrdých želatinových tobolek, jsou sypné vlastnosti plněného prášku. Ty se odráží nejen v požadovaných atributech kvality finálního produktu, jako je např. plněná hmotnost nebo hmotnostní proměnlivost, ale také v efektivnosti a bezproblémovém provedení samotné jednotkové operace. Jelikož jsou sypné vlastnosti ovlivněny charakterem použitého materiálu i procesními podmínkami, je nutné věnovat studiu sypných vlastností značnou pozornost a při jejich optimalizaci brát v úvahu oba tyto aspekty.

Cílem práce bylo studium a optimalizace třísložkové směsi (kukuřičný škrob, aktivní farmaceutická substance (API), dimetikon), která je průmyslovým partnerem používána pro plnění tvrdých želatinových tobolek pomocí plnícího disku. Na základě provedených měření byla stanovena závislost tokových vlastností směsí na zvolené formulační strategii (postupu přípravy) a charakteru použitého škrobu. Za tímto účelem byly v rámci provedené studie hodnoceny dva nativní (Merizet 141, Uni-Pure FL) a dva předželované škroby

(Lycatab C, Starcap 3001), které se lišily svými fyzikálně-chemickými vlastnostmi.

Při studiu tokových vlastností se nejprve stanovily hodnoty Carrova kompresibilitního indexu (CI). Dále byl pro analýzu využit práškový reometr Freeman FT4. Vybrané směsi byly následně charakterizovány i pomocí skenovacího elektronového mikroskopu (SEM) s využitím detektoru sekundárně odražených elektronů (SE).

Z výsledků provedených testů bylo zjištěno, že na sypné vlastnosti směsí má největší vliv charakter použitého škrobu. Směsi připravené z částečně předželovaných škrobů vykazovaly obecně lepší tokovost než směsi připravené ze škrobů nativních. Nativní škroby jsou dle provedených měření na rozdíl od předželovaných škrobů klasifikovány jako kohezní a mají tedy tendenci k soudržnosti vlivem přítomnosti nevazebných interakcí mezi částicemi. To má obecně za následek jejich horší sypné vlastnosti.

Dále bylo patrné, že jednotlivé typy škrobů reagují na modifikace odlišným způsobem. To je především způsobeno charakterem částic škrobu. Částice použitých předželovaných škrobů jsou velké, členité a mají nerovnoměrný povrch. Dimetikon tak není distribuován na povrchu, nýbrž se dostává do nerovností. V důsledku toho nevykazovaly modifikace originálního postupu přípravy v případě předželovaných škrobů výrazný efekt. Naopak v případě nativních škrobů, kdy jsou částice méně členité a mají hladký povrch, zůstává dimetikon přítomen na jejich povrchu a vytváří kapalinové můstky mezi částicemi škrobu. Dochází tak ke vzniku aglomerátů. Použitý způsob modifikace má následně dopad na distribuci dimetikonu a charakter vzniklých aglomerátů odrážející se ve výsledné sypné vlastnosti finální směsi. Ke vzniku aglomerátů pravděpodobně přispívá i vlhkost ve vzorcích jednotlivých škrobů.

Manufacturing of personalised medicines by impregnation of mesoporous silica tablets

Zuzana Hlavačková
Supervisor: prof. Ing. František Štěpánek Ph.D.
Consultants: Ing. David Zůza

University of Chemistry and Technology, Prague,
Faculty of Chemical Engineering
Department of Chemical Engineering

Technická 3, Praha 6, 16000,
hlavacku@vscht.cz

Current drug manufacture methods are based on large scale production with few dosage strength variations. A new manufacturing method is needed to reach the patient-specific requirements for personalized medicine. the main idea of personalized medicine is that drugs are tailored to the individual patient using patient-specific information. Different ways of producing personalized medication are currently investigated, for example 3D print or drop-on-demand (DoD) technique.

This work aimed to explore the effect and possible use of placebo tablets with silica particles to meet the patient-specific requirements for personalized medicine. the placebo tablets containing mesoporous silica were prepared to meet the manufacturing criteria such as hardness and friability. the tablets were filled layer-by-layer with a precise dose of API by drop-on-demand (DoD) technique, which is a liquid dosing system with validated precision. It was found that the number of layers affects the dissolu-

tion profile of the tablet. Thus, different dissolution profiles can be achieved. Overall, this method shows the potential to be used in personalized medicine, where various doses and specific dissolution profiles are needed to fit the patient's requirements.

Evolučné inžinierstvo PHA produkujúcich baktérií *Halomonas Halophila*

Bc. Terézia Ikrényiová
doc. Ing. Stanislav Obruča, Ph.D.

Vysoké učení technické v Brně, Fakulta chemická, Ústav chemie potravin a biotechnologií, Purkyňova 464/118, Královo Pole, 61200, Brno, Česká republika
Agátová 9, Malacky, 901 01, Slovenská republika
teres.ikrenyiova@gmail.com

1 Úvod

Plasty boli donedávna známe len ako výrobky z ropy a jej derivátov. Postupne sa stali náhradou tradičných materiálov a využívame ich dodnes [1]. Dopyt po nich neustále narastá, keďže sú všestranne využiteľné. Dôsledkom toho, že sa len veľmi pomaly rozkladajú, nastávajú ekologické problémy pri ich skládkovaní alebo po ich spaľovaní.

Riešením je nahradenie konvenčných plastov biodegradovateľnými. Biodegradovateľné polyméry vznikajú často dôsledkom deficitu rastových prvkov pri dostatočnej koncentrácii uhlíka v bunkách mikroorganizmov. Zabezpečujú úschovu uhlíka a energie, a tak sa mikroorganizmy chránia pred prípadnou zmenou podmienok prostredia. Medzi biodegradovateľné polyméry patria aj polyhydroxyalkanoáty [2]. Baktéria *Halomonas halophila* je schopná syntetizovať tento prírodný polyester vo forme poly-3-hydroxybutyrátu. Vznik kopolyméru poly(3HB-*co*-3HV) je možné docieliť s použitím vhodnej koncentrácie kyseliny valérovej pri kultivácii. Metódami evolučného inžinierstva sa dosiahne menší inhibičný účinok a prípadne vyššie zastúpenie 3-hydroxyvalerátu (3HV) v kopolymére. Aplikáciou stresového faktoru v laboratórnych podmienkach je možné docieliť, že adaptované organizmy budú odolnejšie voči stresu, a teda vhodnejšie pre priemyselné využitie [3].

Podľa pomeru 3HB a 3HV má výsledný polymér rozdielne vlastnosti. PHB je neohybný a krehký materiál, ktorý je ťažké previesť do kryštalickej podoby. 3HV dodáva vzniknutému kopolyméru P(3HB-*co*-3HV) väčšiu ohybnosť, tuhosť a vzrast predĺženia (materiálu) [4].

2 Experimentálna časť

Aby bol dosiahnutý vyšší obsah 3HV v kopolymére poly(3HB-*co*-3HV), boli v experimentálnej časti uskutočňované kultivácie s cieľom adaptovať baktérie *Halomonas halophila* na substrát kyselinu valérovú (schéma kultivácie viď. Obrázok 1). Pred samotným evolučným experimentom boli najskôr realizované viaceré kultivácie v dôsledku nájdenia vhodného substrátu (a jeho koncentrácie) pre baktérie *Halomonas halophila*. Využívaná bola samostatne kyselina valérová ako prekurzor 3HV pre bakteriálne bunky, ale aj v spojení s glukózou, pyruvátom sodným, propionátom sodným a glycerolom. Kultivačné podmienky boli optimalizované, pretože kyselina valérová má zároveň inhibičný efekt na rast buniek. Kyselina valérová bola v prvej kultivácii pridávaná ihneď do minerálneho produkčného média, v ďalších kultiváciách až po uplynutí 24 hodín od začatia kultivácie. Taktiež bola pozmenená pri jednotlivých kultiváciách jej koncentrácia. Adaptované bakteriálne bunky po kultivácii v porovnaní s neadaptovanými bunkami možno vidieť na fotografii s názvom Obrázok 2.

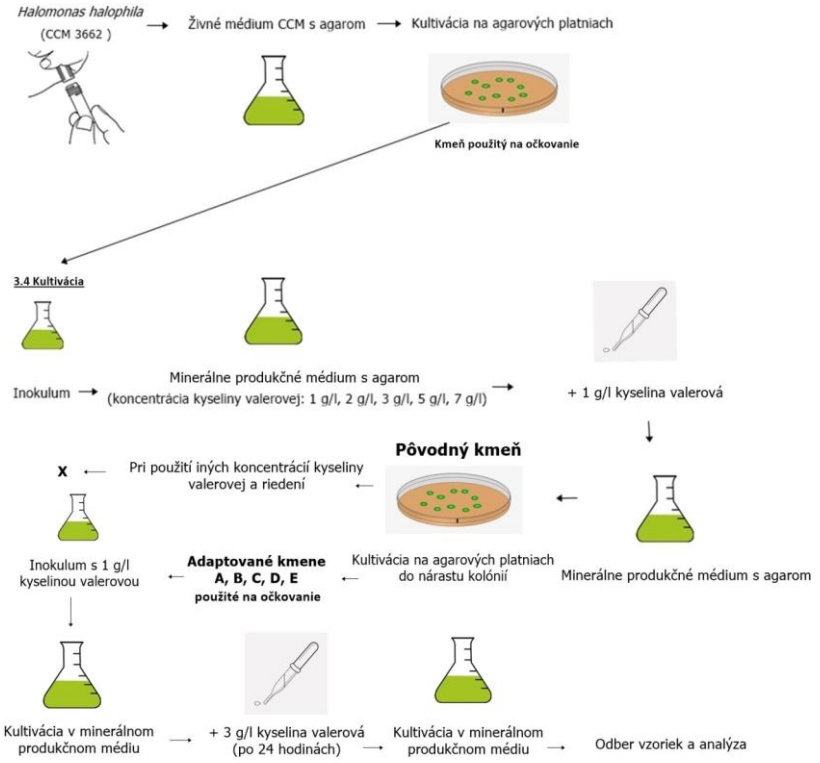

Obrázok 1: Schéma kultivácií vedúcich k zisku adaptovaných kmeňov baktérií Halomonas halophila

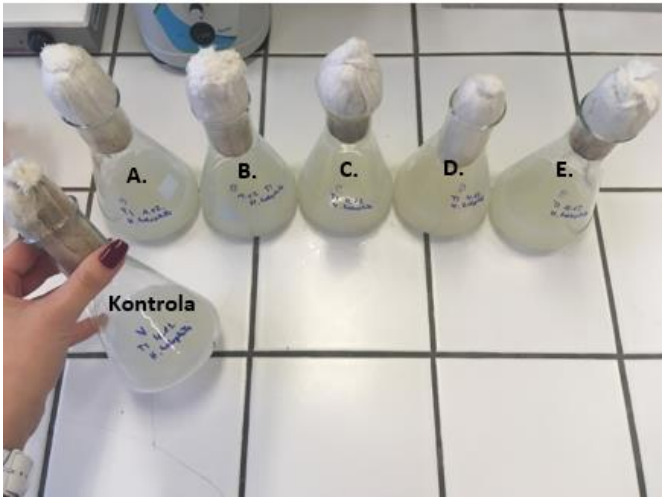

Obrázok 2: Adaptované bakteriálne bunky po kultivácii v minerálnom produkčnom médiu v porovnaní s neadaptovanými bunkami[1]

Tabuľka 1: Adaptované kmene použité ku kultivácii s cieľom produkcie PHA

Označenie kultivačných baniek	Koncentrácia kyseliny valérovej [g/l]
A	3
B	3 (riedenie 10^{-1})
C	2
D	1
E	1 (riedenie 10^{-1})

3 Závery

Bolo zistené, že využitie kyseliny valérovej ako zdroj uhlíka pre bakteriálne bunky bude postačujúce. Ďalšie vyššie spomínané substráty nebolo potrebné počas evolučných experimentov pridávať navyše do produkčného média.

Po kultivácii s kyselinou valérovou ako substrátom pre baktérie bolo zistené, že jej vyššie koncentrácie ako 3 g/l nevedú k produkcii dostatočnej koncentrácie PHA. Pri veľmi nízkych koncentráciách kyseliny valérovej 0,1 g/l a 0,5 g/l bol obsah 3HV v PHA nízky. Vyhovujúca koncentrácia tohto prekurzoru, pri ktorej bunky vykazujú dostatočnú produkciu PHA, je 3 g/l. Taktiež bolo zistené, že kyselina by mala byť pridaná až po 24 hodinách kultivácie v minerálnom produkčnom médiu. Bunky sú už takmer v

[1] Označenie kultivačných baniek podľa použitej koncentácie kyseliny valerovej viď. Tabuľka 1

stacionárnej fáze a inhibičný efekt kyseliny má na nich menší vplyv, čo navýši množstvo utilizovaných PHA.

V práci sú aj porovnávané pôvodné kmene baktérie *Halomonas halophila* s kmeňmi, ktoré boli adaptované na kyselinu valérovú. Nárast kolónií bol pozorovaný pri nižších koncentráciách kyseliny 1 g/l, 2 g/l (okrem riedenia kultúry 10^{-1}) a 3 g/l. Koncentrácie kyseliny 5 g/l a 7 g/l boli pre baktérie inhibujúce. Bol potvrdený predpoklad, že u adaptovaných kmeňov baktérií dochádza k lepšej utilizácii kyseliny valérovej a jej väčšej inkorporácie do kopolyméru, ako u pôvodných kmeňov (bolo zistené, že vyšší obsah 3HV v kopolymére bol dosiahnutý u adaptovaných kmeňov).

Z výsledkov práce vyplýva, že najvyššie množstvo biomasy, PHA a množstvo 3HV v kopolymére bolo dosiahnuté u adaptovaného kmeňa označeného ako B (viď. Obrázok 3) a Obrázok 4). Baktérie *Halomonas halophila* boli adaptované na kyselinu valerovú o koncentrácii 3 g/l (riedenie kultúry 10^{-1}). Obsah 3HV v kopolymére 20,24 mol. %. U pôvodných kmeňov bol pri použití rovnakej koncentrácie kyseliny zistený obsah 3HV v kopolymére len 6,74 mol. %.

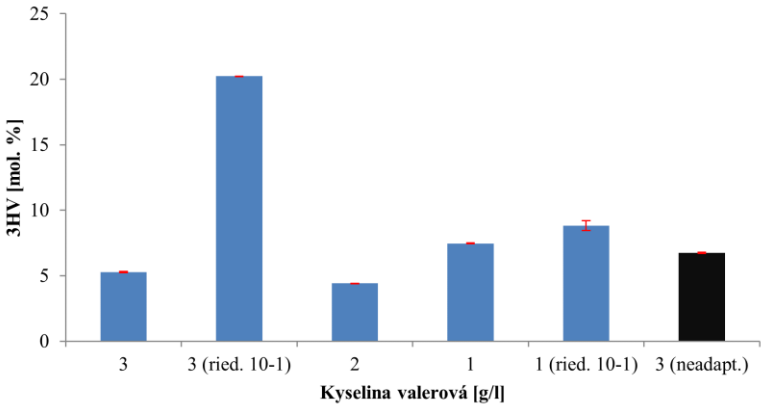

Obrázok 3: Množstvo 3HV v kopolymére u baktérií adaptovaných na rôzne koncentrácie kyseliny valérovej v porovnaní s neadaptovaným kmeňom

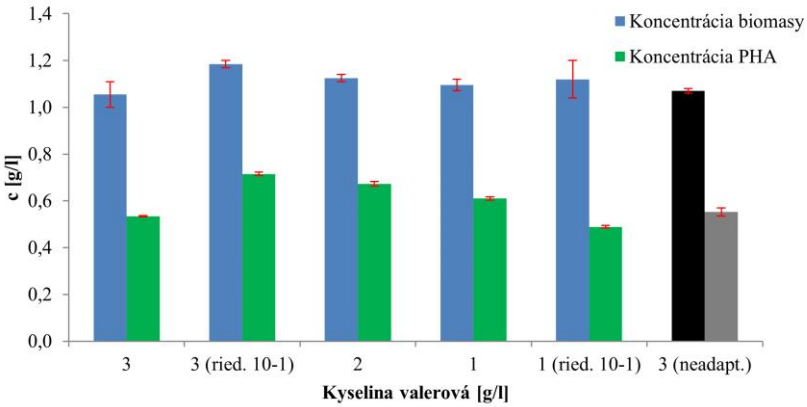

Obrázok 4: Množstvo biomasy a PHA u baktérií adaptovaných na rôzne koncentrácie kyseliny valérovej v porovnaní s neadaptovaným kmeňom

Práca dokazuje, že evolučné inžinierstvo je nástroj, ktorý má potenciál pre zlepšenie produkčných vlastností *Halomonas halophila*, a to nielen v zmysle navýšenia výťažku, ale tiež vylepšenia materiálových vlastností pripravených materiálov. Vyšší obsah 3HV v kopolymére by zmenil jeho výsledné vlastnosti a zabezpečil tak lepšie využitie v niektorých priemyselných procesoch a odvetviach. PHA ako prírodné polyestery by mohli nahradiť konvenčné plasty. Nepredstavovali by tak hrozbu pre životné prostredie a boli by rozkladané neenzymaticky alebo enzymaticky pomocou extracelulárnych enzýmov mikroorganizmov.

4 Literatúra

[1] MÚDRY, Michal. *Ecoplast from Slovakia*. Strojárstvo/Strojírenství. Žilina: MEDIA/ST, 2013, 17(4), 110-111 [cit. 2020-10-19]. ISSN 1335-2938. Dostupné tiež z: http://www.floowie.com/sk/citaj/1378047803515ad8c7e031c/#/strana/113/zvacsenie/100

[2] SIMON-COLIN, Christelle, Gérard RAGUÉNÈS, Joelle COZIEN a Jean G. GUEZENNEC. *Halomonas profundus sp. nov., a new PHA-producing bacterium isolated from a deep-sea hydrothermal vent shrimp*. Journal of Applied Microbiology. 2008, 104(5), 1425-1432 [cit. 2020-10-19]. DOI: 10.1111/j.1365-2672.2007.03667.x. ISSN 1364-5072. Dostupné tiež z: http://doi.wiley.com/10.1111/j.1365-2672.2007.03667.x

[3] PAGE, Wiliam J., Janet MANCHAK a Brent RUDY. *Formation of Poly(Hydroxybutyrate-Co-Hydroxyvalerate) by Azotobacter vinelandii UWD*. Applied and enviromental mikrobiology. Department of Microbiology, University of Alberta, Canada: American Society for Microbiology, 1992, 9(58), 2866-2873 [cit. 2020-10-19]. ISSN 00992240. Dostupné tiež z: https://aem.asm.org/content/aem/58/9/2866.full.pdf

[4] KOURMENTZA, Constantina, Jersson PLÁCIDO, Nikolaos VENETSANEAS, Anna BURNIOL-FIGOLS, Cristiano VARRONE, Hariklia N. GAVALA a Maria A. M. REIS. *Recent Advances and Challenges towards Sustainable Polyhydroxyalkanoate (PHA) Production.* Bioengineering. 2017, 4(4) [cit. 2020-10-19].. DOI:

10.3390/bioengineering4020055. ISSN 2306-5354. Dostupné tiež z: http://www.mdpi.com/2306-5354/4/2/55

Chcela by som poďakovať vedúcemu mojej bakalárskej práce doc. Ing. Stanislavovi Obručovi, Ph.D. za všetky rady a pripomienky k písaniu nielen teoretickej časti práce, ale najmä za vedenie celej experimentálnej časti. Veľká vďaka patrí taktiež Ing. Ivane Nováčkovej za koordináciu mojej práce v laboratóriu a pomoc pri spracovaní výsledkov experimentov. Ďakujem aj všetkým ostatným, ktorí ma počas tohto obdobia podporovali.

Sledovanie poškodenia miechy potkana pomocou magnetickej rezonancie metódou DTI

Bc. Zuzana Kodadová

Slovenská technická univerzita, Fakulta chemickej a potravinárskej technológie, Centrálne laboratória

Radlinského 2102/9, 812 37 Bratislava, Slovensko
kodadova.zuzka@gmail.com

Poranenie miechy môže spôsobiť vážne poruchy pohybového aparátu ako dočasné alebo permanentné ochrnutie. Je preto dôležité čo najpresnejšie charakterizovať rozsah vzniknutého poškodenia a zvoliť adekvátnu terapiu. Zobrazovanie tenzora difúzie pomocou magnetickej rezonancie (DTI) je metóda, ktorá umožňuje skúmať vláknité štruktúry ateda je často využívaná pri charakterizácii poškodenia bielej hmoty v centrálnej nervovej sústave. Cieľom tejto štúdie bolo zhodnotiť vplyv aplikovanej terapie na báze aktívneho alginátu na modely kontúzneho poškodenia miechy ex vivo.

Na DTI analýzu boli použité izolované miechy z dvoch skupín zvierat po kontúznom poškodení a následnou aplikovanou liečbou (N=7), alebo aplikáciou fyziologického roztoku (N=6) a izolované miechy zo skupiny sham operovaných zvierat (N=6). MR dáta z difúzne vážených obrazov boli spracované v programe DSI Studio, kde bol vypočítaný tenzor difúzie a na zobrazenie traktov bol použitý deterministický fiber tracking algoritmus.

Poškodenie miechy sme kvantifikovali pomocou štyroch základných parametrov difúzie: frakčná anizotropia (FA), axiálna difúzivita (AD), radiálna difúzivita (RD) a priemerná difúzivita (MD). Pa-

rametre sme vyhodnocovali na úrovni celej miechy, na úrovni rezu a na úrovni regiónu v oblasti dorzálneho traktu.
Rozdiel medzi liečenou a neliečenou skupinou bol pri vyhodnocovaní na úrovni celej miechy aj v jej jednotlivých rezoch výrazný pri hodnotách FA. Pri parametroch AD a MD sme pozorovali vplyv aplikovanej terapie taktiež na úrovni rezu. Výsledky z oblasti dorzálneho miechového traktu korelovali s kvantifikáciou na úrovni rezu. Metódu DTI sme použili pri štúdii kontúzneho poškodenia miechy potkana. Sledovali sme vplyv aplikovaného liečiva na stav poškodenia, pričom sme použili 3 prístupy kvantifikácie. Konkrétne kvantifikáciu na úrovni celej miechy, na úrovni rezu a kvantifikáciu v rezoch z oblasti dorzálneho traktu. Vo všetkých 3 prípadoch bol signifikantný rozdiel medzi zdravou a poškodenou miechou vo všetkých sledovaných parametroch. Rozdiel medzi liečenou a neliečenou skupinou bol významný najmä pri parametri FA.
Metóda DTI poskytuje cenné informácie o samotnom poškodení a je užitočná aj pri sledovaní progresu počas medikamentóznej terapie. Pomocou takýchto meraní môžeme vyhodnotiť účinnosť zvolenej terapie.

Interakcia hormónov a liečiv s pôdnou organickou hmotou

Bc. Soňa Krajňáková
Prof. Ing. Martina Klučáková PhD.

Vysoké učení technické v Brne, Fakulta chemická, Ústav fyzikálnej chemie
Purkyňova 464, 612 00, Brno
xckrajnakova@vutbr.cz

1 Úvod

Do životného prostredia sa neustále dostávajú viaceré chemické látky, medzi ktoré sa zaradzujú aj liečivá a hormóny.

Lieky sú chemické látky konzumované za účelom miernenia bolesti, liečby a prevencie chorôb. Po konzumácii sú absorbované tkanivom a spracované mikroorganizmami a enzýmami vrámci metabolických dráh[1]. Takto spracované lieky opúšťajú organizmus v podobe metabolitov, konjugátov alebo dokonca v podobe nezmenenej aktívnej formy. Len v prípade antibiotík je množstvo aktívnej látky vylúčenej ľudským organizmom približne 90 % z pôvodnej dávky[2].

Čistiarne odpadových vôd nie sú dostatočne účinné pri eliminácii týchto produktov, čoho dôsledkom sa dostavajú do životného prostredia[3]. Riziko pre životné prostredie predstavujú najmä kvôli svojej perzistencii a odolnosti voči rozkladu. Pravdaže tieto procesy sú ovplyvnené najmä štruktúrou týchto liečiv[2].

Hormóny sú produkty endokrinného systému organizmu a zároveň sa môžu do organizmu dostať v liekovej forme. Najväčšie riziko pre životné prostredie predstavujú steroidné estrogénne hormóny a to najmä percento hormónov vylúčených dobytkom. Celková ľudská populácia vylúči ročne priemerne 30 000 kg prirodzených steroidných estrogénov do životného prostredia. V prípade dobytku, len v Európe a USA je toto množstvo ročne 83 000 kg[4].

Rovnako ako v prípade liečiv je problémom vstupu týchto látok do životného prostredia nedostatočná účinnosť čistiarní odpadových vôd[4]. O kompletnej eliminácii týchto látok z odpadovej vody rozhoduje najmä koncentrácia zastúpených hormónov, ich komplexnosť, odlišnosť v štruktúre a prítomnosť v aktívnej a konjugovanej forme. Spracovaná odpadová voda sa môže v určitých krajinách použiť na zavlažovanie alebo úpravu pôdy. Nadzemný tok prispieva ku kontaminácii horných častí pôd, kde môže dôjsť ku transportu k podzemným vodám a postupne až k povrchovým vodám[5].

Alternatívou, ktorou sa hlavne nespotrebované liečivá dostávajú do životného prostredia sú skládky alebo splachovanie týchto liekov v domácnostiach[6].

Prítomnosť týchto látok je závislá na ich fyzikálno-chemických vlastnostiach a tiež na okolitých podmienkach prostredia. Kľúčovými faktormi sú najmä obsah organickej hmoty (OM) a pH[7].

Výsledky doposiaľ vykonaných štúdii poukazujú na to, že čím vyšší je obsah zastúpenej OM v pôde tým vyššia je tendencia hormónov a liečiv sa na pôdu nasorbovať[8]. Takýto proces bol pozorovaný *Zhang a kol.*, ktorí pozorovali sorpciu trimetoprímu, sulfapyridinu, sulfamtru a sulfadimetoxínu na sediment získaný z čistiarne odpadových vôd[9]. Obsah OM poskytuje možnosť špecifickej sorpcie najmä pre látky, ktoré nie sú závislé na vlastnej polarite[4].

V prípade polárnych látok je vplyvným faktorom sorpcie pH. Dôsledkom zmeny hodnoty pH môže dôjsť k zmene náboja v štruktúre danej látky. *Šebesta a kol.* takýto priebeh pozorovali pri sorpcii ibuprofénu. Pozorovaná bola znížená sorpcia pri narastajúcej hodnote pH. Dôvodom bola prítomnosť elektrostatického odpudzovania medzi záporne nabitým ibuprofénom a povrchom pôdy[10].

Cieľom tejto práce bolo preštudovať interakciu hormónov a liečiv s pôdnou organickou hmotou. V praktickej časti bol na toto preskúmanie interakcie s pôdou použitý ibuprofén.

2 Experimentálna časť

Pre vykonanie jednotlivých experimentov bolo ako skúmané liečivo zvolený Ibuprofen zakúpený od Sigma Aldrich. Ako matrica boli použité lužné pôdy zo sedimentu rieky Bečva z oblasti Jablůnka. Vzorky boli odoberané 45 km od prameňa. Konkrétne vlastnosti použitej matrice sú nasledovné:

- pH (KCl): 6,43
- pH (H2O): 7,38
- Celkový obsah organického uhlíka: 2,23 %
- Pomer huminovej kyseliny ku fulvovej kyseline: 1,22 %
- Obsah uhlíka humusových látok: 0,51 %
- Obsah uhlíka rozpustného vo vode: 240
- Obsah uhlíka rozpustného v horúcej vode: 624
- Katiónový výmenná kapacita: 13,4 meq/100 g
- Obsah humusu: 3,84 %
- Stupeň humifikácie: 12,6 %

2.1 Prvý experiment

V prvom experimente bol pripravený zásobný roztok ibuprofénu o koncentrácii 8,25 mg dm^{-3}. Nasledovala príprava piatich roztokov s koncentráciami 0,0825, $8{,}25 \cdot 10^{-3}$, $8{,}25 \cdot 10^{-4}$, $4{,}125 \cdot 10^{-4}$ a $8{,}25 \cdot 10^{-5}$ mg dm^{-3}.

Do 12 plastových skúmaviek bola navážená na analytických váhach 0,5 g pôdy.

Experiment bol vykonaný v dvoch cykloch. V prvom cykle bola vykonaná sorpcia, kde na naváženú pôdu bolo aplikovaných 25 ml jednotlivých roztokov. Tieto roztoky sa nechali miešať presne 48 hodín na miešačke. Následne bol centrifugáciou jednotlivých vzoriek získaný supernatant a sediment.

Sediment sa nechal sušiť na Petriho miskách a bol použitý v druhom cykle, desorpcii. Pri desorpcii bolo na vysušený sediment aplikovaných 25 ml Mili-Q vody. Nasledoval rovnaký postup ako pri sorpcii.

Supernatanty získané po centrifugácii boli prefiltrované pomocou striekačkových filtrov o veľkosti pórov 0,45 μm. Nasledovalo premeranie pH a vodivosti pomocou pH metru METTLER TOLEDO, SevenMulti a konduktometru METTLER TOLEDO, Seven Easy. Zanalyzovaná bola tiež absorbancia jednotlivých vzoriek UV-VIS spektrofotometrom Hitachi v rozmedzí vlnových dĺžok 200 až 600 nm.

Pred konečnou analýzou kvapalinovou chromatografiou s hmotnostne spektrometrickou detekciou (HPLC/MS) bolo potrebné vzorky ešte dodatočne zakoncentrovať.

Použitá bola extrakcia tuhou fázou (SPE). Vzorky boli nariedené na objem 200 ml. Použité boli 3 ml kolonky Supel™, ktoré boli kondiciované 2 ml 10% roztokom metanolu, nasledovala ekvilibrácia 2 ml Mili-Q vody. Po odkvapkaní celého objemu vzorky boli kolónky premyté 2 ml 10% metanolu a následne 2 ml Mili-Q vody. Nasledovalo sušenie sorbentu po dobu 20 až 30 minút. Po vysušení bola vykonaná elúcia analytu pomocou 2 ml zmesi acetónu a etylacetátu zmiešaných v pomere 50:50. Rýchlosť extrakcie bola nastavená tak, aby do odpadu okvapkával extrakt rýchlosťou 1 kvapka za sekundu. Eluát bol pri odkvapkávaní zachytávaný do vysokých vialok. Nasledovalo odparovanie eluátu vo vialkách pod dusíkom a rozpúšťanie odparku v 500 μl zmesi metanolu a Mili-Q vody zmiešaných v pomere 50:50. Zakoncentrovaný extrakt bol následne prefiltrovaný cez striekačkové filtre o veľkosti pórov 0,22 μm.

Finálna analýza bola vykonaná na kvapalinovom chromatografe Agilent 1 100 Series a hmotnostnom spektrometre Agilent 6 320 Series. Konkrétne parametre analýzy sú zobrazené v *Tabuľka č.1.*

Tabuľka č.1: Parametre HPLC/MS

Kvapalinová chromatografia	
Kolóna	KINETEX C18
Rozmery kolóny	150x3 mm
Veľkosť častíc	2,6 μm
Nástrek	20 μl
Teplota kolóny	40 °C
Mobilná fáza	MeOH a 0,001 M HCOOH
Rt[1] Ibuprofénu	11,6 min
Hmotnostná spektrometria	
Tlak zmlžovača	30 psi
Prietok sušiaceho plynu	10 l min
Teplpota sušiaceho plynu	350 °C
Sken	110-290 m/z, priemerné
Mód	Negatívny
Cielená hmota	205 m/z

[1] Rt – retenčný čas

2.2 Druhý experiment

Výsledky prvého experimentu poukázali na potrebu optimalizácie metódy HPLC/MS. Zároveň bolo potrebné zmeniť koncentráciu analyzovaného ibuprofénu, keďže táto metóda nedokázala zaznamenať množstvo liečiva po sorpcii a desorpcii. Pripravený bol preto zásobný roztok 20 mg dm^{-3} a z neho roztoky o koncentrácii 1, 2, 3, 4 a 5 mg dm^{-3}. Nasledovali kroky, ktoré sa zhodovali s predošlým experimentom. Pôda po desorpcii bola dodatočne analyzovaná pomocou infračervenej spektrometrie s Fourrierovou transformáciou (FT-IR) metódou DRIFT. Použitý bol FTI-IR spektrometer Nicolet iS50.

Pred analýzou HPLC/MS boli supernatanty prefiltrované striekačkovými filtrami o veľkosti pórov 0,20 μm do 1 ml vialok. Pri analýze bol namiesto negatívneho módu použitý pozitívny a sledovaná hmota bola pozmenená na hodnotu 161 m/z.

3 Výsledky

Výsledky prvého experiment poukázali na nutnosť optimalizácie metódy, keďže nebolo možné získať konkrétne hodnoty koncentrácii ibuprofénu vo vzorkách.

Jednotlivé vzorky boli premerané pomocou UV-VIS spektrometra pri vlnovej dĺžke 200 až 600 nm. Tieto dáta boli použité na simuláciu priebehu sorpcie a desorpcie. Väčší význam sa prikladá hodnotám získaným HPLC/MS.

Výsledky HPLC/MS zobrazené na *Obrázok č.1* a *Obrázok č.3* poukázali na nárast nasorbovaného množstva ibuprofénu s narastajúcou koncentráciou. Vyššie koncentrácie ibuprofénu poskytli väčšie množstvo látky, ktorá sa dokázala na pôdnu organickú hmotu naviazať. Tomuto priebehu odpovedajú aj hodnoty účinnosti sorpcie, ktorých priemerna hodnota bola 52,7 %.

V prípade desorbovaného množstva získaného HPLC/MS bol podobne pozorovaný nárast. Tento nárast nebol až tak výrazný v porovnaní so sorpciou, hodnoty sa pohybovali v rozmedzí 3,15 až 11,2 μg g^{-1}. V prípade účinnosti desorpcie bol zaznamenaný podobný nárast, kde priemerná hodnota účinnosti činila 4,1 %. Väčšina ibuprofénu teda zostala v naviazanej podobe.

Prostredníctvom FT-IT spektrometrie bolo možné potvrdiť prítomnosť naviazaného Ibuprofénu na pôde. Na *Obrázok č.5* je možné vidieť v spektre naviazaného Ibuprofénu v oblasti 3000 cm^{-1} až 2800 cm^{-1} výrazne vibrácie väzieb C-H, $C\text{-}H_2$ a $C\text{-}H_3$. Tieto vibrácie mohli byť spôsobene Ibuprofénom alebo pôdou.

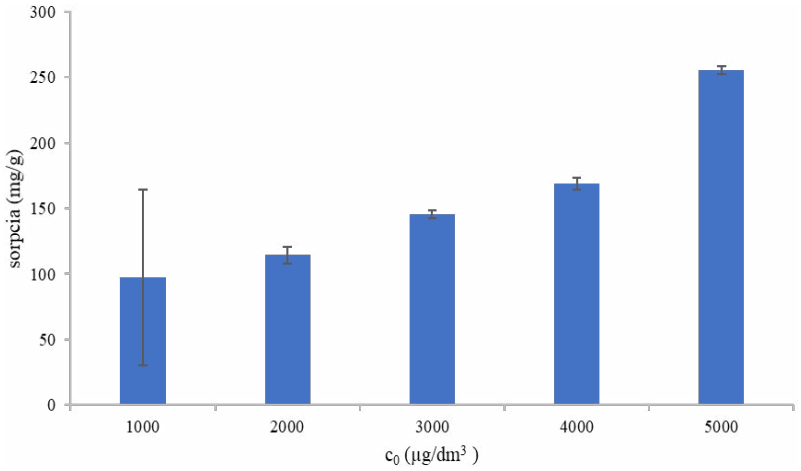

Obrázok č.1: Nasorbované množstvo Ibuprofenu

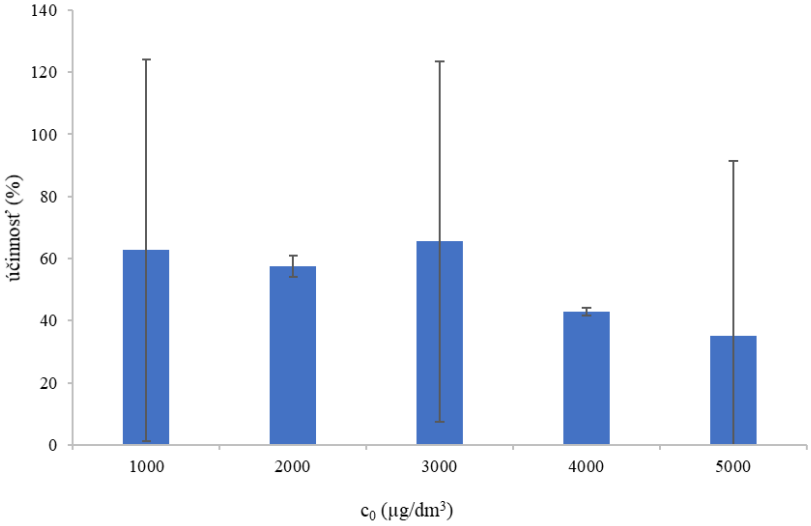

Obrázok č.2:Účinnosť sorpcie Ibuprofénu

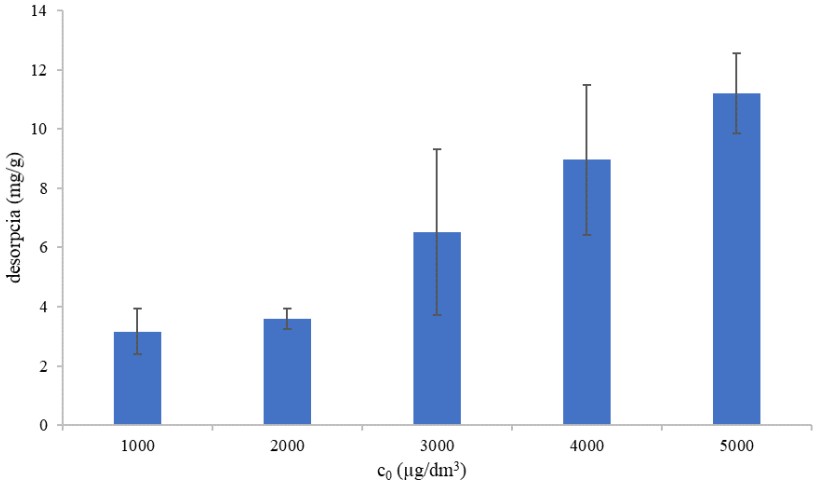

Obrázok č.3: Množstvo desorbovaného Ibuprofénu

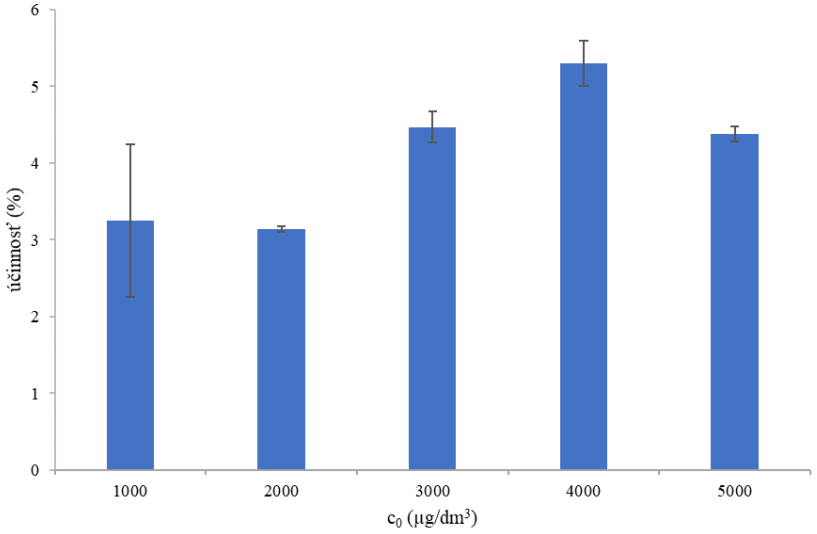

Obrázok č.4: Účinnosť desorpcie Ibuprofénu

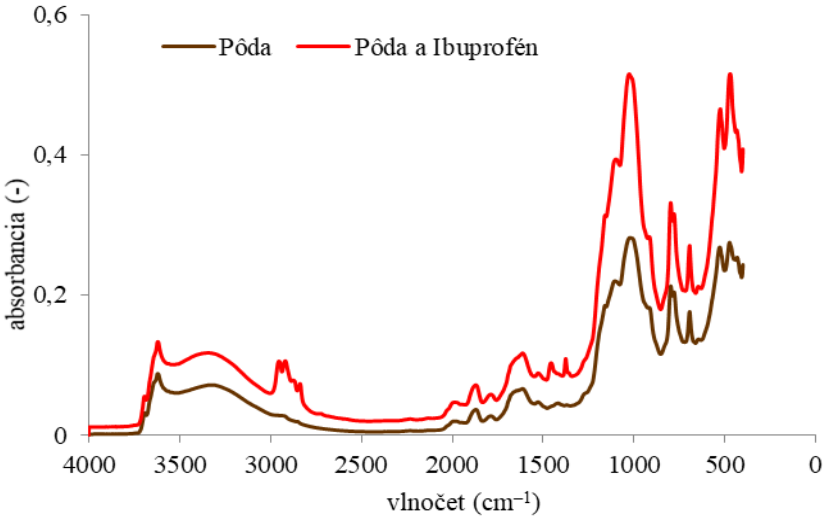

Obrázok č.5: FT-IR spektrum Ibuprofénu s pôdou

4 Záver

V tejto práci bola preskúmaná problematika výskytu liečiv a hormónov v životnom prostredí, konkrétne v pôde. Popísaný bol tiež vplyv určitých faktorov na priebeh sorpcie a desorpcie.

Experimentálne bol tento proces interakcie s pôdou preskúmaný prostredníctvom protizápalového liečiva Ibuprofénu. Z výsledných dát bolo možné získať informácie o procesoch sorpcie a desorpcie. Pozorovaný bol nárast v nasorbovanom množstve a teda v množstve naviazaného ibuprofénu. Získané boli tiež dáta o účinnosti týchto procesov, kde v prípade sorpcie bol zaznamenaný nárast s maximálnou hodnotou účinnosti 62,68 %. V prípade desorpcie bol nevýrazný nárast s maximálnou hodnotou účinnosti 5,3 %. Celkovo výsledky poukazujú na malú tendenciu Ibuprofénu prechádzať do mobilnej fázy. V prirodzenom prostredí by tento priebeh znamenal nižší obsah ibuprofénu v mobilnej fáze. Vo väčšine prípadov je ibuprofen zastúpený v prírode v nižších koncentráciách, čím sa zvyšuje riziko jeho transportu do podzemných vôd.

5 Literatura

1. AL-FARSI, Rayal. a kol. Assessing the Presence of Pharmaceuticals in Soil and Plants Irrigated with Treated Wastewater in Oman. *Int J Recycl Org Waste Agricult* [online]. 2018, **7**(4), 1-12 [cit. 2019-05-19]. DOI: 10.1007/s40093-018-0202-1. ISSN 2251-7715. Dostupné z: https://link.springer.com/article/10.1007/s40093-018-0202-1Citace 2
2. KUMAR, Kuidip, Yogesh CHANDER, Satish C. GUPTA a Ashok SINGH. Antibiotic Use in Agriculture and Its Impact on the Terrestrial Environment. *Advances in Agronom*. 2005, **87**(1), 1-54. DOI: 10.1016/S0065-2113(05)87001-4. ISSN 0065-2113 Dostupné z: https://www.sciencedirect.com/science/article/pii/S0065211305870014
3. KUSTER, Marina, Maria JOSÉ LÓPEZ DE ALDA a Damiá BARCELÓ. Analysis and distribution of estrogens and progestogens in sewage sludge, soils and sediments. *TrAC Trends in Analytical Chemistry*. 2004, **23**(10-11), 790-798. DOI: 10.1021/ac015717z Dostupné z: https://www.sciencedirect.com/science/article/pii/S0165993604030390
4. ADEEL, Muhammad, Dennis FRANCIS a Xiaoming SONG. Environmental impact of estrogens on human, animal and plant life: A critical review. *Environment International*. 2017, **2017**(99), 107-119. DOI: 10.1016/j.envint.2016.12.010 Dostupné z: https://www.sciencedirect.com/science/article/pii/S0160412016304494
5. GEOPPERT, Nadine, Ishai DROR a Brian BERKOWITZ. Detection, fate and transport of estrogen family hormones in soil. *Chemosphere*. 2014, **95**(1), 336-345. DOI: 10.1016/j.chemosphere.2013.09.039 Dostupné z: https://www.sciencedirect.com/science/article/pii/S0045653513012794?via%3Dihub
6. ROSA, Ján. *Nakládání s odpady v lékárně se zaměřením na zpětný odběr a likvidaci léčiv*. Čelákovice, 2015. Diplomová práca. Vyšší odborná škola, střední škola, jazyková škola správem státní jazykové zkoušky a základní škola MILLS, s.r.o.
7. SHERR, Frank. *Sorption, degradation and transport of estrogens and estrogen sulphates in agricultural soils*. Lincoln University Faculty of Agricultural and Life Science Soil and Physical Science Group, 2009. Dizertačná práca. University of Bayreuth
8. YING, Guang-Guo a Rai S KOOKANA. Occurrence and fate of hormone steroids in the environment. *Environment International*. 2002, **28**(6), 545-551. DOI: 10.1016/S0160-4120(02)00075-2 Dsotupné z: https://www.sciencedirect.com/science/article/pii/S0160412002000752
9. ZHANG, Ya-Lei. Sorption-desorption and transport of trimethoprim and sulfonamide antibiotics in agricultural soil: Effect of soil type, dissolved organic matter, and pH. *Environmental Science and Pollution Research*. 2014, **21**(9). DOI: 10.1007/s11356-014-2493-8. Dostupné z: https://link.springer.com/article/10.1007/s11356-014-2493-8
10. HILLER, Edgar a Martin ŠEBESTA. Effect of temperature and Soil pH on the sorption of ibuprofen in agricultural soil. *Soil and Water Research*. 2017, **12**(2). DOI: 10.17221/6/2016-SWR. Dostupné z: https://www.agriculturejournals.cz/web/swr.htm?type=article&id=6_2016-SWR

Poďakovanie

Rada by som týmto poďakovala pani prof. Ing. Martine Klučákovej, Ph.D., za odborné rady a čas, ktorý mi venovala počas vypracovávania bakalárskej práce. Ďalej by som chcela poďakovať Ing. Jánovi Rybárikovi a Ing. Petre Sukovej za ich rady, čas a pomoc pri riešení bakalárskej práce. Nakoniec by som chcela poďakovať svojej rodine a priateľom za podporu, ktorú mi počas štúdia poskytli.

Ošetření nápojů pomocí pulzního elektrického pole

Bc. Gabriela Kuncová, Ing. Iveta Horsáková, Ph.D.

Vysoká škola chemicko-technologická v Praze,
Fakulta potravinářské a biochemické technologie,
Ústav konzervace potravin

Technická 3, 16628, Praha 6
kuncovag@vscht.cz

Tato práce si klade za cíl představit novou perspektivní non-termální metodu ošetření potravin – pulzní elektrické pole. Je věnována stručnému vysvětlení základních principů, na kterých je tato metoda a její účinnost založena. Popisuje jednotlivé konstrukční komponenty systému PEF pro ošetření potravin. Dále je zaměřena na možné aplikace pulzního elektrického pole v oblasti potravinářství a blíže popisuje dosažených výsledků použití této metody při pasteraci, extrakci, sušení a zmrazování. V práci jsou rovněž shrnuty účinky této metody na nutričně hodnotné a biologicky aktivní látky, stejně jako na procesní kontaminanty a mikroorganismy. Vzhledem k zaměření na ošetření nápojů, je v ní rozebrána i aplikace v nápojovém průmyslu.

V experimentální části práce je studován účinek ošetření pulzním elektrickým polem na suspenzi *Saccharomyces cerevisiae*. Je posuzován vliv nastavení hlavních parametrů ošetření (intenzita elektrického pole a frekvence pulzů) na redukci počtu mikroorganismů. Dosavadní výsledky prokazují, že vyšší účinnosti je dosaženo při nastavení vyšší frekvence pulzů a rovněž i vyšší intenzity elektrického pole.

Optimalizácia SPME v spojení s GC-MS/MS na stanovenie cypermetrínu v chemických postrekoch

Nikola Kurucová
Agneša Szarka, Svetlana Hrouzková, Francisco Javier Arrebola-Liébanas

Slovenská technická univerzita v Bratislave,
Fakulta chemickej a potravinárskej technológie,
Ústav analytickej chémie

Radlinského 9, 812 37, Bratislava, Slovensko
nik.kurucova@gmail.com

Cypermetrín je insekticíd nachádzajúci sa v produktoch určených na plošné poľnohospodárske, ale aj domáce účely. Kontrola kvality týchto produktov je veľmi dôležitá v krajinách s rozvinutým poľnohospodárskym priemyslom, nakoľko v posledných rokoch neustále rastie obchod s nelegálnymi a falošnými prípravkami, ktoré neobsahujú danú aktívnu látku alebo jej požadovanú koncentráciu. Tento nelegálny obchod môže predstavovať aj možné riziko pre ľudské zdravie a životné prostredie, keďže nie je známe reálne zloženie výrobkov. Problémom ich analýzy je však vysoká koncetrácia pesticídu (cypermetrínu), ktorá sa v týchto produktoch nachádza. To spôsobuje komplikácie pri ich analýze pomocou plynovej chromatografie v spojení s tandemovou hmotnostnou spektroskopiou (GC- MS/MS). Pred analýzou chemických postrekov je potrebné zriedenie vzoriek, čo spôsobuje značné chyby meraní.
Cieľom práce je vývoj jednoduchej, rýchlej a šetrnej metódy na stanovenie vysokej koncentrácie cypermetrínu v chemických po-

strekoch. Bola optimalizovaná automatizovaná metóda, pri ktorej chyba analýzy bola minimalizovaná vďaka odstráneniu opakovaného kroku zrieďovania. Na extrakciu cypermetrínu z chemických postrekov sa využila mikroextrakcia na tuhej fáze (SPME) v headspace (HS) móde a na následnú analýzu GC-MS/MS metóda. Bolo zistené, že optimálne parametre analýzy sú: teplota pece 250 oC a teplota dávkovača 200 oC. Pri optimalizácií SPME sa študovali rôzne parametre, ako typ vlákna, teplota a čas extrakcie. Vhodné vlákno pre izoláciu cypermetrínu pomocou SPME je polydimetylsiloxán, použité pri extrakčnej teplote 30 oC po dobu extrakcie 30 min. Zistilo sa, že optimálny čas desorpcie je 5 min. Vyvinutá metóda GC-MS/MS v spojení s HS-SPME bola následne aplikovaná na analýzu reálnej vzorky chemického postreku sobsahom cypermetrínu 4 900 mg L-1. Výsledky ukázali, že daná metóda je vhodná na stanovenie cypermetrínu v týchto produktoch.

Kľúčové slová: *cypermetrín, chemické postreky, SPME, GC-MS/MS*

Využití smíšených tkáňových kultur ve výzkumu biodistribuce nanočástic

Bc. Pavlína Michaláková
vedoucí práce: Ing. Denisa Lizoňová

Vysoká škola chemicko-technologická v Praze, Fakulta chemicko-inženýrská, Ústav chemického inženýrství.
Technická 5, Dejvice, 166 28 Praha 6, Česká republika
michalap@vscht.cz

1 Úvod

I přes značný pokrok na poli onkologické léčby zde přetrvává velké riziko mnoha nežádoucích účinků a zhoršení kvality života pacientů. To je z velké míry zapříčiněno současně užívanými cytostatiky. Signifikantní procento z nich totiž není schopno léčivo doručit pouze k nádorovým buňkám[1]. Tím dochází také k omezení terapeutické použitelnosti této léčby. Jelikož dochází k nadměrné expozici zdravých tkání, nejsou mnohdy intravenózně podaná cytostatika dopravena k nádorovým buňkám v efektivních koncentracích. K maximalizaci účinnosti léčby a minimalizaci nežádoucích účinků by mohlo dojít užitím transportních nosičů – nanočástic – které by léčivo doručily pouze na cílené místo (nádor)[2, 3]. Jejich užití sebou přináší mnoho výhod, přičemž největší z nich je možnost použití velkého množství léčiva, či případně proléčiva, které se uvolní až v nádoru. Problémem této léčby ovšem zatím zůstává, že jsou nanočástice ve velké míře vychytávány buňkami imunitního systému – makrofágy – v procesu zvaném fagocytóza (*Obrázek 1*). Při něm dochází k rozpoznání nanočástic a jiných cizorodých látek imunitními buňkami, jejich pohlcení a následné akumulaci v játrech a slezině[4]. To vede ke snížení doby cirkulace v krevním řečišti a tím pádem také ke snížení pravděpodobnosti úspěšného dopravení nanočástic do nádoru.

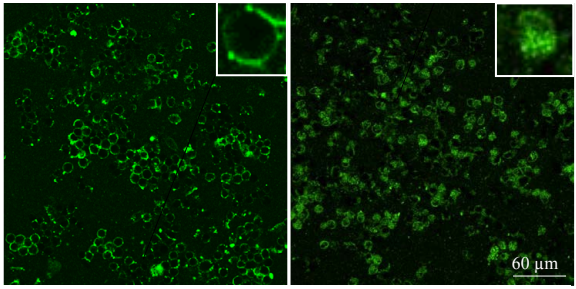

Obrázek 1: Proces fagocytózy fluorescenčně značených nanočástic makrofágy v čase. Vlevo: začátek procesu, kdy je lokalizace nanočástic na povrchu buněk versus vpravo: pokročilé stadium fagocytózy, kdy jsou nanočástice lokalizovány uvnitř buněk.

Tento nežádoucí proces může být minimalizován například modifikací nanočástic polymerem poly(*N*-(2-hydroxypropyl) methakrylamidem) (pHPMA)[5], který snižuje adsorpci krevních proteinů na nanočástice (opsonizace) a tím zabraňuje jejich rozpoznání imunitními buňkami.

V této práci byly studovány interakce nanočástic s nádorovými a imunitními buňkami pomocí průtokové cytometrie a fluorescenční mikroskopie. Kolorektální karcinom je dlouhodobě jednou z nejčastějších diagnóz rakoviny a to nejen v České republice[6]. V této práci byly jako zástupce nádorových buněk použity právě buňky kolorektálního karcinomu.

Nejprve byly připraveny křemičité nanočástice, které byly následně modifikovány polymerem pHPMA. Rozeznání nádorových buněk bylo v případě této práce dosaženo na základě interakce protilátka-antigen (*Obrázek 2*), kdy byly nanočástice modifikovány monoklonální protilátkou IgG M75 [7]. Tato protilátka je specifická pro karbonickou anhydrázu IX (CA IX), jež je preexprimována na pevných hypoxických nádorech (například na nádorech kolorektálního karcinomu) a ve zdravých tkáních se vyskytuje velmi vzácně[8]. V experimentech s fluorescenčním mikroskopem byly použity smíšené buněčné kultury, aby mohlo být ověřeno, zda je možné specifickou adhezi na nádorové buňky a fagocytózu makrofágů detekovat také simultánně, tedy v kompetitivním prostředí a případně posoudit, zda některý z těchto procesů převažuje.

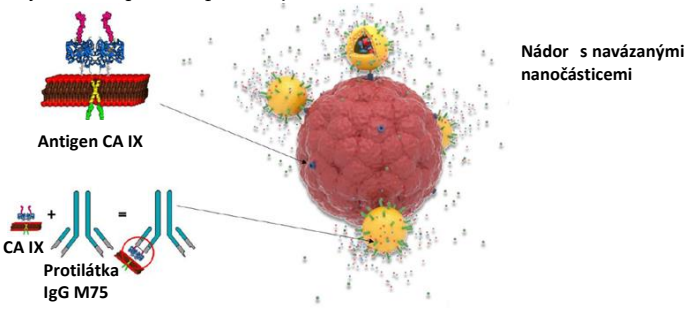

Obrázek 2: Ilustrace aktivního cílení nanočástic na základě vazby protilátka-antigen.

2 Experimentální část

2.1 Příprava a charakterizace nanočástic

Fluorescenčně značené křemičité nanočástice, byly syntetizovány a modifikovány způsobem popsaným dříve[5]. Nanočástice byly nejprve modifikovány polymerem pHPMA (SiO_2-pHPMA) a dále protilátkou IgG M75 (SiO_2-pHPMA-M75). K ověření, zda protilátka IgG M75 váže antigen, byl proveden imunotest. Tento experiment byl proveden na polystyrénové 96-jamkové destičce se speciálně upravenými jamkami s antigenem (PG-MBP, epitop=část antigenu rozeznávaná IgG M75) a kontrolou (MBP). Do prvního řádku byly přidány suspenze nanočástic a v následujících řádcích byla koncentrace částic vždy dvakrát snížena. Po 1h inkubace byly jamky promyty fosfátovým pufrem (PBS).

Nanočástice modifikované monoklonální protilátkou IgG M75 měly zůstat přichyceny k povrchu destičky, zatímco nanočástice modifikované pouze polymerem pHPMA měly být odmyty PBS (*Obrázek 3*). Fluorescence byla analyzována pomocí fluorescenční čtečky Tecan Infinite M200.

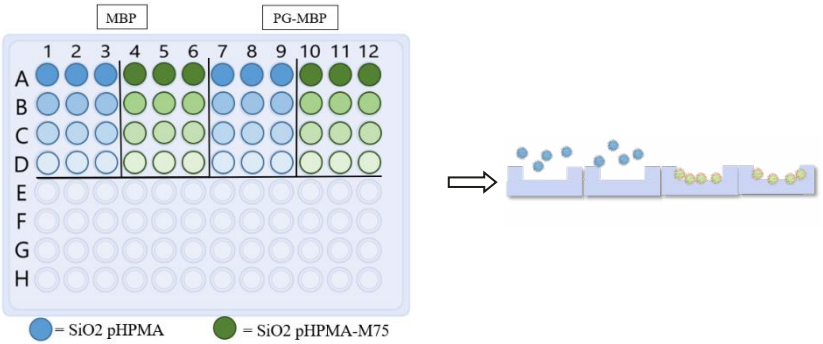

Obrázek 3: Schéma 96-jamkové destičky při provádění imunotestu. Částice bez protilátky (modře) jsou odmyty, zatímco částice s protilátkou (zeleně) jsou naadherovány k povrchu destičky.

2.2 Průtoková cytometrie

Pro experimenty s buňkami byly použity 2 typy buněčných linií – nádorové buňky HT-29, které exprimují CA IX a imunitní buňky J774A.1 (=makrofágy, neexprimují CA IX). Buňky byly sklizeny, spočítány pomocí hemocytometru a v množství 220 000 buněk napipetovány do zkumavek. Po zcentrifugování buněk a jejich promytí 0,5 ml PBS k nim byly přidáno 0,8 mg nanočástic. Po určité době inkubace byly vzorky promyty PBS a přefiltrovány do zkumavek pro průtokovou cytometrii. Experimenty byly prováděny s konstantním množstvím nanočástic a studovaly závislost procesů fagocytózy a specifické adheze v čase. Při měření pomocí průtokové cytometrie byla měřena fluorescence jednotlivých buněk (nanočástice byly značeny fluoresceinem, λ_{ex}=488 nm, λ_{em}=516 nm).

2.3 Fluorescenční mikroskopie

Ke studování, jak se budou vázat částice na imunitní a nádorové buňky v kompetitivním prostředí bylo využito fluorescenční mikroskopie. Pro tyto experimenty byly připraveny smíšené buněčné kultury imunitních buněk J774A.1 a nádorových buněk HT-29. Oba typy buněčných linií byly společně zaočkovány do 24-jamkové destičky v celkovém množství 50 000 buněk na jamku (do jedné jamky bylo tedy zaočkováno 25 000 HT-29 a 25 000 J774A.1 buněk). Po 48 hodinách inkubace, kdy se množství buněk v jamkách mělo zvýšit na 200 000 (doba dělení buněk je zhruba 24 hodin), byly přidány nanočástice. Pro označení imunitních buněk ve smíšených kulturách HT-29 a J774A.1 byly použity mikročástice pHrodo™ Red Zymosan Bioparticles™ (pHrodo™), které jsou fluorescenční jen po pohlcení imunitními buňkami.

3 Výsledky a diskuse

3.1 Příprava a charakterizace nanočástic

Částice byly charakterizovány pomocí dynamického rozptylu světla (DLS) a transmisního elektronového mikroskopu (TEM). Měření pomocí DLS bylo provedeno v kyvetách s PBS bezprostředně po přípravě a modifikaci nanočástic. Jejich velikost byla 160 nm. *Obrázek 4* ukazuje distribuci velikosti připravených nanočástic podle objemu a jejich TEM snímek.

Schopnost protilátky IgG M75 vázat antigen byla ověřena imunotestem. Δ Fluorescence je rozdíl mezi signálem získaným z jamek modifikovaných antigenem PG-MBP a signálem z jamek pouze s kontrolním proteinem MBP. V případě nanočástic SiO_2-pHPMA je výsledný signál negativní, což může být důsledkem nepřesného pipetování, či vyšší afinity těchto nanočástic ke kontrolnímu proteinu než k antigenu.

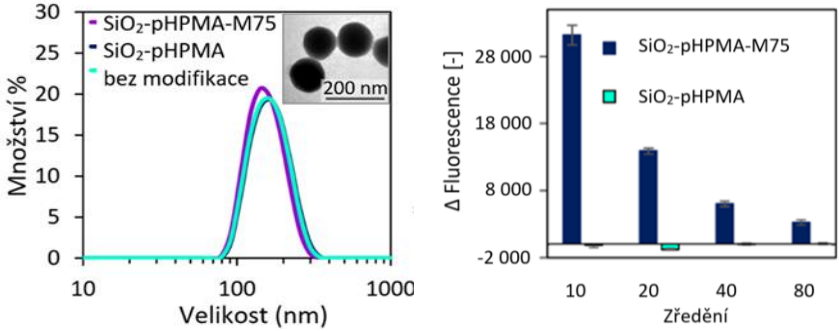

Obrázek 4: Vlevo: distribuce velikosti nanočástic a jejich TEM snímek. Vpravo: Výsledky imunotestu. Protilátka IgG M75 je schopna vázat antigen.

3.2 Průtoková cytometrie

Experiment ke zjištění časové závislosti procesů fagocytózy nanočástic makrofágy a interakcí protilátka-antigen byl proveden s nanočásticemi o koncentraci 40 μg/ml a s 220 000 buňkami. Výsledky z průtokového cytometru jsou vyobrazeny na *Obrázek 5*. Pro účely farmakokinetického modelu bude využita rychlost těchto procesů. Na vodorovné ose je znázorněno množství fluorescence jednotlivých buněk. Na svislé ose je četnostní hustota, která udává, jak velké množství buněk se s danou fluorescencí nachází ve vzorku. S rostoucím časem se na grafech fluorescence buněk zvyšuje, protože je na ně navázáno větší množství fluorescenčních nanočástic.

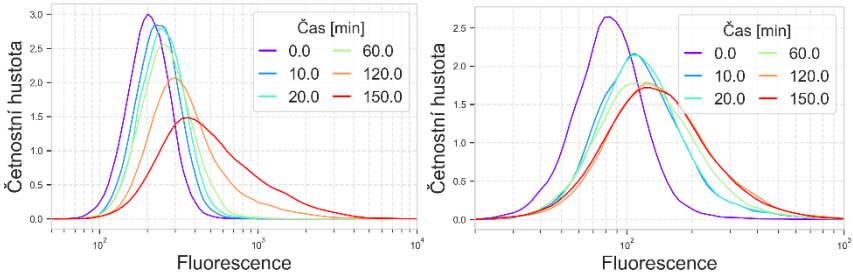

Obrázek 5: Výsledky z průtokové cytometrie s nanočásticemi s protilátkou a imunitními buňkami J774A.1 (vlevo) či nádorovými buňkami HT-29 (vpravo).

3.3 Fluorescenční mikroskopie

Pomocí fluorescenční mikroskopie byly získány snímky smíšených buněčných kultur imunitních a nádorových buněk. Imunitní buňky J774A.1 byly nejprve označeny mikročásticemi pHrodo™, které jsou fluorescenční jen po pohlcení imunitními buňkami (*Obrázek* ***6***). Díky lokalizaci fluorescence bylo určeno, že imunitní buňky rostou jednotlivě (červená), zatímco nádorové buňky HT-29 (nejsou fluorescenční) rostou při sobě a tvoří ostrůvky.

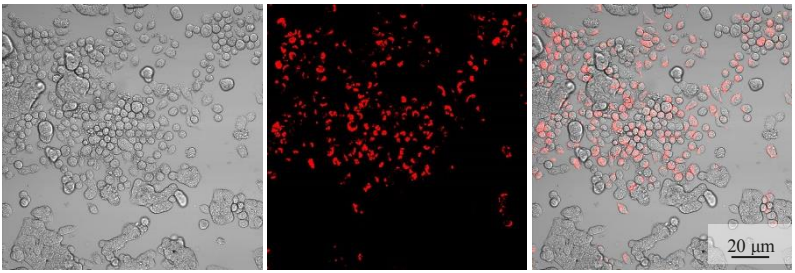

Obrázek 6: Smíšená buněčná kultura po označení mikročásticemi pHrodo™ po 2 hodinách inkubace. Vlevo: transmisní snímek, uprostřed: fluorescenční snímek, vpravo: proložený snímek.

Poté byly se smíšenými kulturami provedeny také experimenty se syntetizovanými nanočásticemi bez protilátky (SiO_2-pHPMA) a s protilátkou (SiO_2-pHPMA-M75). Na snímku *Obrázek* **7** můžeme vidět, že nanočástice bez protilátky (SiO_2-pHPMA) se na nádorové buňky HT-29 nevážou. Na snímku *Obrázek 8* můžeme naopak pozorovat jak se částice s protilátkou (SiO_2-pHPMA-M75) zachytávají na membráně nádorových buněk HT-29 (díky výskytu CA IX), zatímco v případě imunitních buněk J774A.1 jsou nanočástice díky fagocytóze lokalizovány uvnitř buněk. Nanočástice SiO_2-pHPMA-M75 se za experimentálních podmínek vážou více na nádorové buňky HT-29 (*Obrázek 8*, vpravo). Na

snímku *Obrázek 8* vlevo je interakce nanočástic s imunitními buňkami o něco menší než na snímku vpravo, což může být zapříčiněno nasycením těchto buněk mikročásticemi pHrodo™.

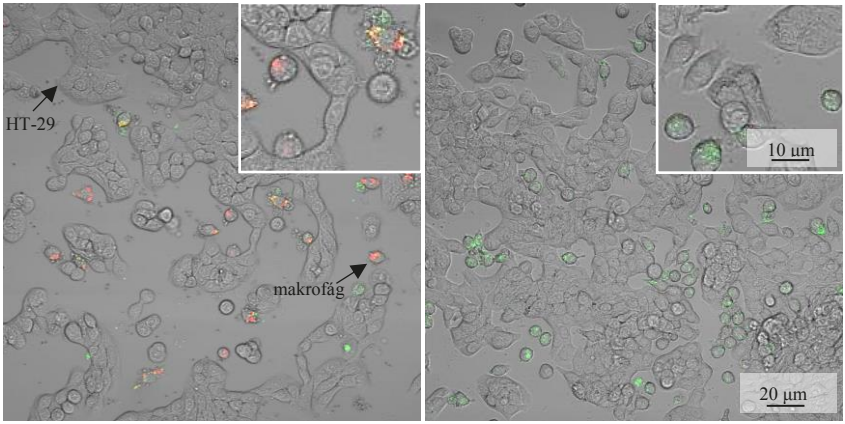

Obrázek 7: Snímky smíšených buněčných kultur z fluorescenční mikroskopie s nanočásticemi bez protilátky (SiO_2-pHPMA) (zelená, nanočástice se nevážou na nádorové buňky HT-29). Vlevo: s mikročásticemi pHrodo™ uvnitř imunitních buněk (červená). Vpravo: bez mikročástic pHrodo™.

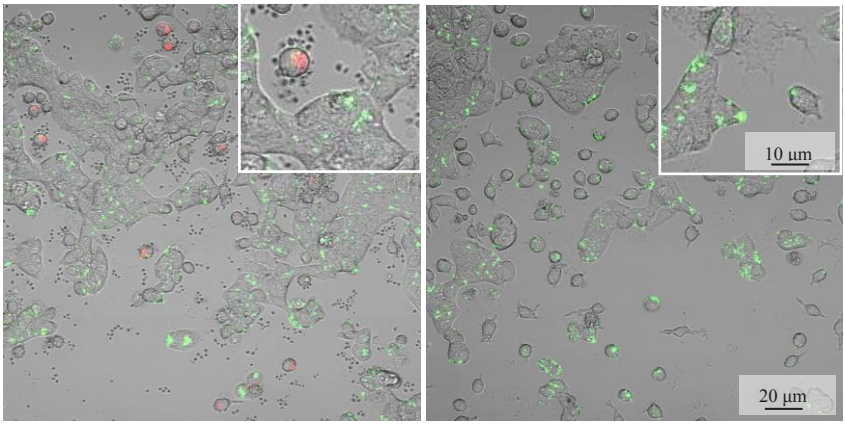

Obrázek 8: Snímky smíšených buněčných kultur z fluorescenční mikroskopie s nanočásticemi s protilátkou (SiO_2-pHPMA-M75). Vlevo: s mikročásticemi pHrodo™ uvnitř imunitních buněk (červená). Vpravo: bez mikročástic pHrodo™. Nanočástice s protilátkou se ve větší míře vážou na nádorové buňky a jsou navázány na jejich membráně. Na snímku vlevo je interakce nanočástic s imunitními buňkami o něco menší než na snímku vpravo, což může být zapříčiněno přesycením těchto buněk mikročásticemi pHrodo™.

4 Závěr

Křemičité nanočástice byly modifikovány polymerem pHPMA a monoklonální protilátkou IgG M75 a následně charakterizovány. Schopnost protilátky IgG M75 vázat antigen byla potvrzena imunotestem a velikost nanočástic byla změřena dynamickým rozptylem světla (d=160 nm). Fluorescenční mikroskopie v kombinaci s průtokovou cytometrií byla použita za účelem pochopení procesů fagocytózy nanočástic makrofágy (buněčná linie imunitních buněk J774A.1) a specifických interakcí protilátka-antigen (buněčná linie kolorektálního karcinomu – HT-29). Pomocí průtokové cytometrie byl zkoumán vliv různých inkubačních časů nanočástic s buňkami a byly získány kvantitativní data pro sestavení farmakokinetického modelu (není v této práci zobrazen). K ověření, zda je možné výše zmíněné procesy detekovat také simultánně, byly provedeny experimenty se smíšenými buněčnými kulturami linií buněk J774A.1 a HT-29, kdy byly imunitní buňky J774A.1 označeny mikročásticemi pHrodo™. Tyto experimenty byly vyhodnoceny pomocí fluorescenční mikroskopie. Potvrdilo se, že se nanočástice s protilátkou IgG M75 vážou na nádorové buňky HT-29 i ve smíšené kultuře a jsou na těchto buňkách detekovány ve větším množství, v porovnání s buňkami imunitními. Toho je dosaženo díky použití polymeru pHPMA („zneviditelnění" částic) a protilátek IgG M75 (aktivní cílení).

Poděkování
Mé poděkování patří zejména Ing. Denise Lizoňové za její odbornou pomoc a vedení práce. Dále Ing. Ivaně Křížové a Ing. Jiřímu Kolářovi za vyhodnocení experimentů pomocí průtokové cytometrie. Ráda bych poděkovala také prof. Františkovi Štěpánkovi, Ph.D.za jeho cenné poznatky.

5 Literatura

1. Vasir, J. K.; Labhasetwar, V., Targeted Drug Delivery in Cancer Therapy. *Technology in Cancer Research & Treatment* **2005,** *4* (4), 363-374.
2. Kumari, P.; Ghosh, B.; Biswas, S., Nanocarriers for cancer-targeted drug delivery. *J Drug Target* **2016,** *24* (3), 179-91.
3. Malam, Y.; Loizidou, M.; Seifalian, A. M., Liposomes and nanoparticles: nanosized vehicles for drug delivery in cancer. *Trends Pharmacol Sci* **2009,** *30* (11), 592-9.
4. Owens, D. E., 3rd; Peppas, N. A., Opsonization, biodistribution, and pharmacokinetics of polymeric nanoparticles. *Int J Pharm* **2006,** *307* (1), 93-102.
5. Lizoňová, D.; Majerská, M.; Král, V.; Pechar, M.; Pola, R.; Kovář, M.; Štěpánek, F., Antibody-pHPMA functionalised fluorescent silica nanoparticles for colorectal carcinoma targeting. *RSC Advances* **2018,** *8* (39), 21679-21689.
6. Douaiher, J.; Ravipati, A.; Grams, B.; Chowdhury, S.; Alatise, O.; Are, C., Colorectal cancer-global burden, trends, and geographical variations. *J Surg Oncol* **2017,** *115* (5), 619-630.
7. Závada, J.; Závadová, Z.; Pastorek, J.; Biesová, Z.; Ježek, J.; Velek, J., Human tumour-associated cell adhesion protein MN/CA IX: identification of M75 epitope and of the region mediating cell adhesion. *British Journal of Cancer* **2000,** *82* (11), 1808-1813.
8. Král, V.; Mader, P.; Collard, R.; Fábry, M.; Horejsí, M.; Rezácová, P.; Kozísek, M.; Závada, J.; Sedlácek, J.; Rulísek, L.; Brynda, J., Stabilization of antibody structure upon association to a human carbonic anhydrase IX epitope studied by X-ray crystallography, microcalorimetry, and molecular dynamics simulations. *Proteins* **2008,** *71* (3), 1275-87.

STU FCHPT
SLOVENSKÁ TECHNICKÁ UNIVERZITA V BRATISLAVE
FAKULTA CHEMICKEJ A POTRAVINÁRSKEJ TECHNOLÓGIE
ODDELENIE ANORGANICKEJ CHÉMIE

PRÍPRAVA A MAGNETICKÉ VLASTNOSTI ŽELEZNATÝCH KOMPLEXOV S PYRIDYL-BENZIMIDAZOLOVÝMI LIGANDAMI

Študentská vedecká konferencia

Bc. Jana Vojčíková
Doc. Ing. Ivan Šalitroš PhD.

2020

Úvod

Všeobecne známe vlastnosti magnetických materiálov pozorujeme a využívame v rôznych spotrebičoch. Najviac známe permanentné magnety, využívané napríklad na ovládanie zapaľovania v automobiloch alebo v elektrických motoroch, tvoria len malú skupinu magnetov. Pevné disky počítačov, mikrovlné rúry, platobné katy – to je len pár príkladov, ktorých funkčnosť by bez prítomnosti magnetov nebola možná. Prirodzene sa vyskytujúci oxid železnato-železitý Fe_3O_4, nachádzajúci sa napríklad v mozgoch mnohých zvierat, slúži ako „biologický kompas“ na navigáciu v geomagnetickom poli Zeme.

V súčasnosti je hlavným cieľom koordinačnej chémie štúdium magnetických vlastností koordinačných zlúčenín. Dôvodom je potenciálne široké spektrum využitia týchto látok v technológiách a taktiež štúdium závislosti magnetických vlastností od ich zloženia a štruktúry. Samostatnú kapitolu v magnetochémii tvorí výskum spin crossover javu. Jedná sa o situáciu, kedy jedna látka má rozdielne fyzikálne, optické a štrukturálne vlastnosti, v závislosti od počtu nespárených elektrónov. Najväčší význam majú materiály, ktoré vykazujú spinový prechod pri izbovej teplote a taktiež termálnu hysteréziu. Prechod medzi jednotlivými stavmi je vratný a ovplyvniteľný vonkajšími podmienkami. S využitím poznatku, že spinový stav látky vieme korigovať, sa táto oblasť začala rýchlo rozvíjať a využívať v priemysle.

Teoretické poznatky z oblasti magnetochémie sa využijú pri interpretácii a štrukturálnej charakterizácii pripravených látok. Experimentálna časť práce sa venuje príprave koordinačných zlúčenín, pri ktorých je energia párovania spinov a vplyv poľa na štiepenie energetických hladín takmer rovnaká, teda prítomnosť spin crossover prechodu, je ovplyvnená predovšetkým zmenou vonkajších podmienok.

Cieľom bolo pripraviť a pomocou rôznych techník popísať zloženie, štruktúru a magnetické vlastnosti koordinačných zlúčenín, ktoré vykazujú teplotne a svetlom indukovaný spin crossover efekt.

Teoretické minimum

Koordinačné zlúčeniny iónov prechodných kovov s valenčnou konfiguráciou $3d^4$-$3d^7$ môžu za určitých okolností vykazovať spinový prechod (ďalej už len SCO, z angl. „**S**pin **Cro**ssover), pri ktorom ión kovu mení spin ako reakciu na zmenu teploty, pôsobenie tlaku, žiarenia alebo pod vplyvom magnetického poľa. SCO je riadený silou pôsobenia kryštálového poľa ligandov (Δ) a párovacou energiou spinov (*P*). Keď je ión kovu v oktaédrickom alebo pseudooktaédrickom usporiadaní vystavený pôsobeniu kryštálového poľa ligandov, dochádza k štiepeniu degenerovyných orbitálov na nižšiu, trojnásobne degenerovanú hladinu (t_{2g}) a vyššiu, dvojnásobne degenerovanú hladinu (e_g). Oktaédrické komplexy s elektrónovou konfiguráciou valenčnej vrstvy $3d^4$-$3d^7$ môžu byť vysokospinové (ďalej už len **HS,** z angl. „**H**igh **S**pin“) alebo nízkospinové (ďalej už len **LS**, z angl. „**L**ow **S**pin“), vzhľadom na to, či je intenzita poľa ligandu silnejšia alebo slabšia ako energia párovania spinov. Sila kryštálového poľa ligandov rastie v poradí, ktoré sa nazýva aj spektrochemický rad ligandov: $I^- < Br^- < Cl^- < SCN^- < F^- < OH^- < H_2O < NCS^- < py < en < NO_2^- < CN^-. < CO$.

V prípade, že energia kryštálového poľa ligandov Δ je väčšia ako energia spárovania spinov *P*, dochádza k obsadzovaniu orbitálov elektrónmi v súlade s výstavbovým princípom, ktorý hovorí o tom, že najprv sa obsadí energeticky dostupnejší orbitál (t_{2g}), a až potom dôjde k obsadzovaniu orbitálu e_g [1]. Centrálny atóm je teda v LS stave. Situácia kedy energia spárovania elektrónov *P* je porovnateľne väčšia ako Δ, centrálny atóm má maximálny počet nespárených elektrónov a je v HS stave. V poslednom prípade, kedy sú tieto energie *P* a Δ porovnateľné, závisí spinový stav centrálneho atómu len od vonkajších podmienok a látka môže meniť svoj stav z HS na LS a naopak. Rovnováha medzi spinovým prechodom sa mení vplyvom teploty, magnetického poľa, tlaku a elektromagnetického žiarenia. Rovnováha medzi spinovým prechodom sa mení vplyvom teploty, magnetického poľa, tlaku a elektromagnetického žiarenia. SCO môžeme definovať ako závislosť mólového zlomku HS frakcie od termodynamickej teploty, čo nazývame konverznou krivkou.

Tvar konverznej krivky môže byť rôzny v závislosti od toho, ako dochádzalo k zmene spinu danej frakcie. Prechod môže byť prudký, graduálny, nekompletný, s hysteréziou alebo viackrokový.

Konverzia medzi HS a LS stavom je sprevádzaná zmenou fyzikálnych vlastností. Dochádza k zmene dĺžky väzieb medzi centrálnym atómom a ligandom, k zmene objemu molekuly a deformácii koordinačného polyédra. S týmito zmenami u niektorých koordinačných zlúčenín dochádza k zmene farby v dôsledku rôznej optickej absorpcie jednotlivých stavov. To umožňuje detekovať výskyt teplotne indukovaného SCO a teplotnú závislosť použitím rôznych fyzikálnych metód. Pri teplotne indukovanom SCO je HS stav uprednostňovaný pri zvýšení teploty a LS pri jej znížení. Rýchlosť zmeny spinového stavu závisí od prítomnosti medzimolekulových väzieb ako sú vodíkové väzby, alebo interakcie jadier s elektrónmi v konjugácii.

Veľká pozornosť sa venuje zlúčeninám, ktoré vykazujú tzv. LIESST efekt (z ang. **L**ight **I**nduced **E**xcited **S**pin **S**tate **T**rapping). Podmienkou fotoindukovaného spinového prechodu je teplotne indukovaný prechod, ale nie všetky zlúčeniny s tepelným SCO musia vykazovať LIESST efekt. Princípom je ožiarenie vzorky elektromagnetickým žiarením vhodnej vlnovej dĺžky v LS stave pri nízkej teplote, čo indukuje čiastočnú alebo úplnú konverziu z LS na HS. LIESST efekt sa vyskytuje vždy pri teplote nižšej ako $T_{1/2}$. T_{LIESST} parameter predstavuje kritickú teplotu, nad ktorou už nemožno fotoindukovať látku v LS do HS stavu svetelným ožiarením. T_{LIESST} sa vypočíta zo vzťahu

$$T_{LIESST} = \min \frac{\partial(\chi T)}{\partial T} \quad (1)$$

Súvis medzi týmito teplotami je zatiaľ predmetom ďalšieho výskumu, rovnako ako aj vzťah medzi T_{LIESST} a štrukturálnymi vlastnosťami tepelne indukovaného SCO. Po ožiarení sa látka dostane do metastabilného stavu, pričom postupne relaxuje a nadobúda opäť termodynamicky výhodnejšiu konformáciu. Ak dôjde k ožiareniu látky, ktorá sa nachádza v HS s väčšou vlnovou dĺžkou ako bola použitá pri LIESST tak pozorujeme tzv. reverse-LIESST efekt.

Ciele práce:

1. Príprava a štruktúrna charakterizácia nových tetradentátnych aromatických ligandov s N-donorovými atómami. (NMR, IČ, RTG difrakčná analýza)
2. Príprava a analýza koordinačných zlúčenín železa pomocou IR, UV – VIS, NMR a elementárnej analýzy.
3. Meranie magnetických vlastností pripravených koordinačných zlúčenín železa pomocou MPMS SQUID magnetometra.
4. V prípade preukázania SCO pripravených koordinačných zlúčenín, skúmanie LIESST efektu.

Výsledky práce a diskusia

1. Príprava a štruktúrna charakterizácia ligandov

Pri príprave tetradentátnych ligandov sa v obidvoch prípadoch vychádzalo z prekurzora **pybzim**, (2-(pyridín-2-yl)-1H-benzimidazol) ktorý bol pripravený kondenzačnou reakciou 1,2-diamínbenzénu a kyseliny pyridín-2-karboxylovej podľa už publikovaného postupu [3]. Ďalší krok spočíval v deprotonizácii benzimidazolového kruhu pomocou zásady a jeho následná alkylácia.

Reakcia **pybzimu** a 1,5-dibrómpentánu v prípade ligandu $\mathbf{L_3}$ a 1,6-dibrómhexánu v prípade $\mathbf{L_4}$ sa uskutočnila v roztoku dimetylformamidu pri teplote 120 ℃. Po odparení dimetylformamidu na vákuovej odparke sa zmes olejovo žltej farby extrahovala v systéme dichlórmetán a voda. Po odstránení nečistôt a anorganických zvyškov sa organické frakcie spojili a opäť sa odparilo prebytočné rozpúšťadlo pomocou rotačnej odparky. Takto získaná zmes produktu a nezreagovaného pybzimu sa separovala kolónovou chromatografiou, pričom prítomnosť produktu sa ešte pred tým potvrdila pomocou TLC chromatografie. Ligand $\mathbf{L_3}$ bol pripravený s výťažkom 51% a $\mathbf{L_4}$ s výťažkom 85%. Porovnateľne vyšší výťažok v druhom prípade mohol byť dôsledok použitia silnejšej zásady (KOH) vo výraznom nadbytku, vďaka ktorému došlo k deprotonizácii benzimidazolového kruhu vo väčšej miere, a teda alkylácia na atóme dusíka bola dostupnejšia. Štruktúra ligandu $\mathbf{L_3}$ ($R_f = 0,16$) s výťažkom 51% (1,1g; 2,4 mmol), bola potvrdená ^1H a ^{13}C NMR analýzou. Monokryštály vhodné na RTG difrakčnú analýzu boli získané pomalým odparovaním deuterovaného rozpúšťadla d6-DMSO z NMR kyvety. ^{1}H NMR (300 MHz, CDCl3, 25

°C, δ / ppm): 8,57-845 (m, 1H); 8,19 (d, J = 8,0 Hz, 1H); 7,86 (td, J = 7,8; 1,8 Hz, 1H); 7,69-7,55 (m, 1H); 7,48 (dd, J = 6,0; 2,9 Hz, 1H); 7,36 (ddd, J = 7,5; 4,9; 1,1 Hz, 1H); 7,25-7,08 (m, 2H); 4,66 (t, J = 7,2 Hz, 2H); 1,84-1,51 (m, 2H); 1,31-1,01 (m, 1H) ^{13}C NMR (75 MHz, CDCl3, 25 °C, δ / ppm): 150,02; 149,18; 142,04; 136,36; 44,53; 40,05; 39,77; 39,49; 39,22; 38,93; 38,66; 29,32; 23,29.

V prípade ligandu **L4** bol produktom opäť prášok svetlobéžovej farby. Štruktúru pripraveného ligandu potvrdila aj analýza ^{1}H NMR spektra. Aj v tomto prípade boli získané vhodné monokryštály na RTG difrakčnú analýzu metódou pomalého odparovania deuterovaného rozpúšťadla d6-DMSO z NMR kyvety. ^{1}H NMR (300 MHz, d6-DMSO, 25 °C, δ / ppm): 8,61-8,50 (m, 1H); 8,24 (dd, J = 8,0; 0,8 Hz, 1H); 7,91 (td, J = 7,8; 1,7 Hz, 1H); 7,72-7,61 (m, 1H); 7,54 (dd, J = 6,6; 2,2 Hz, 1H); 7,41 (ddd, J = 7,6; 4,9; 1,1 Hz, 1H); 7,29-7,16 (m, 2H); 4,7 (t, J = 7,3 Hz, 2H); 1,63 (s, 2H); 1,18 (s, 2H) ^{13}C NMR (75 MHz, CDCl3, 25 °C, δ / ppm): 165,47; 150,52; 149,83-149,58; 142,51; 136,98-136,71; 134,17; 67,57; 60,98; 45,17-44,92; 44,92-44,78; 40,54-40,21; 40,08; 39,94; 39,80; 39,66; 39,52; 32,76; 30,34; 30,09; 29,92; 28,80; 26,38; 25,95; 25,39; 23,83; 22,81.

^{1}H NMR spektrá obidvoch ligandov pre aromatickú aj alifatickú oblasť sú veľmi podobné (Obrázok 2).

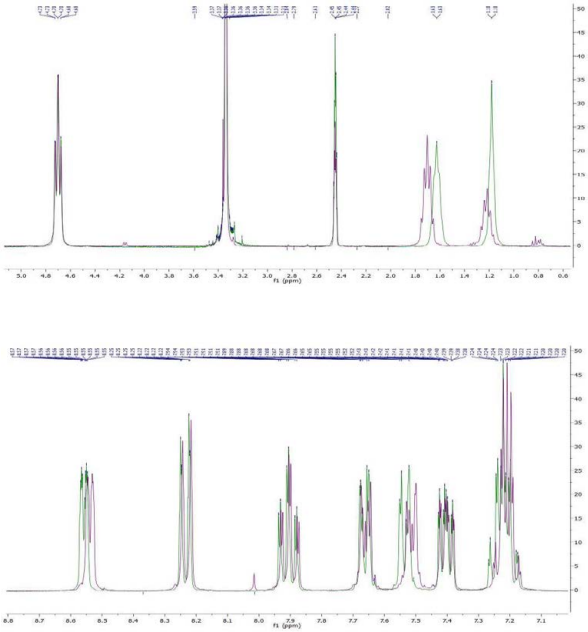

Obrázok 2 1H NMR: Porovnanie alifatickej oblasti ligandov L3 a L4 (hore)a 1H NMR: Porovnanie aromatickej oblasti ligandov L3 a L4 (dole) (L3 - ružová farba L4 - zelená farba)

Kryštálová štruktúra oboch organických ligandov sa určila pomocou difrakčnej RTG analýzy pri teplote 100 K. Ligandy pozostávajú z dvoch benzimidazol-pyridínových častí prepojených cez dusík benzimidazolového kruhu alifatickým pentán-1,5-diylovým reťazcom v prípade ligandu **L3** (Obrázok), a hexán-1,6-diylovým reťazcom v prípade **L4** (Obrázok). Meranie jednotlivých parametrov ukázalo, že ligand **L3** kryštalizuje v ortorombickej kryštálovej sústave s priestorovou grupou Pbca a parametrami: a = 9,5007(3) Å, b = 17.4024(5) Å, c = 29.1339(11) Å, α = 90°, β = 90°, γ = 90° a V = 4816,9(3) Å^3, Z = 8. Ligandy sú orientované paralelne a najsilnejšia nekovalentná interakcia je medzi uhlíkom C13 benzimidazolového kruhu a C22 pyridínového kruhu (π-π interakcia). V kryštálovej štruktúre sa nenachádzajú molekuly rozpúšťadla.

Ligand **L4** kryštalizuje v monoklinickej kryštálovej štruktúre s priestorovou grupou $P2_1/n$. Mriežkové konštanty, uhly, objem bunky a počet molekúl v základnej bunke boli stanovené: a = 10,7477(7) Å, b = 5,8476(3) Å, c = 19.0376(12) Å, α = 90°, β = 92,091(5)°, γ = 90° a V = 1195,68(12) Å^3 Z = 2. Pri paralelnej orientácii ligandov sú prítomné dva druhy interakcií. Nekovalentná väzba medzi C6 benzimidazolového kruhu a C10 pyridínového kruhu so vzdialenosťou 3,391 Å, a interakcia medzi C1 benzimidazolového kruhu a C10 pyridínového kruhu so vzdialenosťou 3,364 Å. Vodíkové väzby nie sú prítomné ani v jednom prípade.

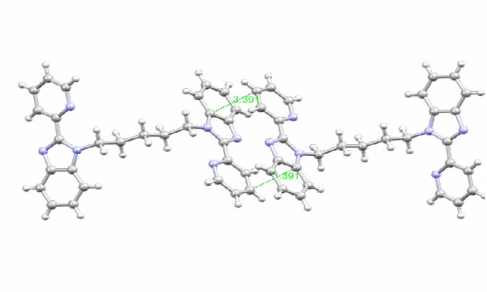

Obrázok 2 Štruktúra ligandu **L3**, medzimolekulové interakcie sú znázornené zelenou prerušovanou čiarou so vzdialenosťou 3,391 Å (C13-C22), M($C_{29}H_{26}N_6$) = 458,56 g/mol, parametre základnej bunky: a = 9,5007(3) Å, b = 17.4024(5) Å, c = 29.1339(11) Å, α = 90°, β = 90°, γ = 90° a V = 4816,9(3) Å^3, Z = 8. C-sivá farba, N-svetlomodrá farba, H-biela farba.

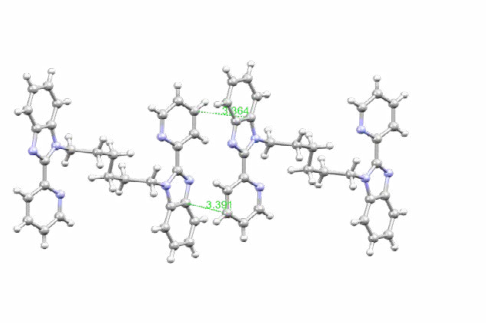

Obrázok 2 Štruktúra ligandu **L4**, intermolekulárne interakcie sú znázornené zelenou prerušovanou čiarou s hodnotami 3,391 Å (C6-C10) a 3,364 Å (C1-C10), M($C_{30}H_{28}N_6$) = 474,613 g/mol, parametre základnej bunky: a = 10,7477(7) Å, b = 5,8476(3) Å, c = 19.0376(12) Å, α = 90°, β = 92,091(5)°, γ = 90°a V = 1195,68(12) Å^3 Z = 2. C-sivá farba, N-svetlomodrá farba, H-biela farba.

2. Železnaté komplexy a ich magnetické vlastnosti

V rámci tohto projektu sa pripravili dve koordinačné zlúčeniny reakciou ligandu **L4** s tetrafluoroboritanom (komplex **1**) alebo chloristanom železnatým (komplex **2**) v acetonitrilovom roztoku. Presná štruktúra pripravených železnatých komplexov s ligandom **L4** nie je známa, pretože sa nepodarilo pripraviť monokryštály vhodné na RTG difrakčnú analýzu. Vzhľadom na to, že produkty sú dobre rozpustné, prvou použitou kryštalizačnou technikou bola nerušená kryštalizácia. Časť prefiltrovaného roztoku komplexu sa nechala sa na tmavom mieste pri laboratórnej teplote a časť pri teplote okolo 4° C. Rýchlemu odparovaniu rozpúšťadla sa zamedzilo použitím vzduchotesnej parafínovej fólie, ktorá sa perforovala. Počtom a veľkosťou dier sa regulovala rýchlosť odparovania, teda časový faktor, ktorý je pri tomto type kryštalizácie podstatný. Ani po uplynutí dostatočne dlhého času v nasýtenom roztoku nevznikli kryštály. Vylúčenie kryštálov sa nedosiahlo ani zmenšením rozpustnosti pridaním metanolu, v ktorom sa produkt nerozpúšťal ani pri zvýšenej teplote. Poslednou použitou technikou bola difúzia pár rozpúšťadla (dietyléter alebo diizopropyléter) do matičného lúhu pri nízkej teplote. Žiadna z použitých techník neumožnila vznik kryštálov vhodných na analýzu.

Keďže sa produkt izoloval vo forme prášku z rozpúšťadla v ktorom je znova úplne rozpustný, môžeme tvrdiť že sa nejedná o koordinačný polymér a pravdepodobnejšie sú niektoré zo znázornených štruktúr (Obrázok 3). Jednou z možností je jednojadrový komplex $[Fe(\mathbf{L_4})_2](A)_2$ (kde A^- je ClO_4^- alebo BF_4^- anión, Obrázok 3a), kde jeden ligand vystupuje ako tetradentátny a druhý ako bidendátny. Aj v druhom prípade možno uvažovať o jednojadrovom komplexe so zložením $[Fe(\mathbf{L_4})_3](A)_2$ (Obrázok 3b), pričom všetky tri ligandy **L4** sú bidendátne. V poslednom prípade ide o dvojjadrový komplex $[Fe_2(\mathbf{L_4})_3](A)_4$, pričom všetky tri ligandy sú tetradentátne. Dva ligandy sú chelátujúce a jeden je mostíkový (Obrázok 3c). Vzhľadom na to, že obidva komplexy boli pripravované v stechiometrickom pomere 1:1, (ligand a železnatá soľ) zrejme pôjde o dvojjadrové komplexy so vzorcom $[Fe_2(\mathbf{L_4})_3](A)_4$. Železnatý katión je hexakoordinovaný tromi atómami dusíka z benzimidazolového kruhu a tromi dusíkmi pochádzajúcich z pyridínového kruhu. Na koordinácii jedného Fe^{2+} sa teda pravdepodobne podieľajú tri benzimidazol-pyridínové fragmenty pochádzajúce z dvoch molekúl ligandov **L4**.

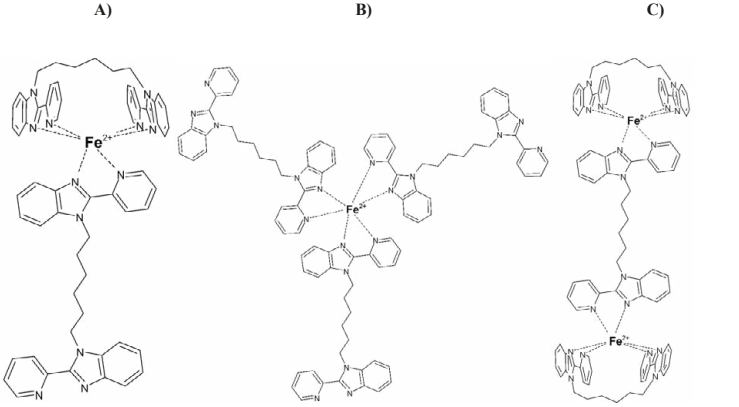

Obrázok 3 Schematické nákresy predpokladaných štruktúr komplexov a) jednojadrový komplex $[Fe(\mathbf{L_4})_2](A)_2$ b) jednojadrový komplex $[Fe(\mathbf{L_4})_3](A)_2$ c) dvojjadrový komplex $[Fe_2(\mathbf{L_4})_3](A)_4$.

Meranie magnetických vlastností komplexov **1** a **2** sa uskutočnilo na vzorkách, ktoré bola dostatočne čisté a pripravené v postačujúcom množstve. Závislosť produktovej funkcie χT (pre jedno Fe^{II} centrum) bola skúmaná v rozsahu teplôt od 5 do 400 K pri aplikovanom poli 0,1 T (Obrázok 4). χT = f(T) je výsledkom prepočtu nameraného magnetického momentu vzorky v závislosti od teploty. Pri výpočte funkcie χT sa uvažovala molová hmotnosť pre dvojjadrové komplexy.

Komplex **1** vykazuje graduálny a neúplný SCO prechod, pri teplote vyššej ako je laboratórna teplota. Pri nízkej teplote 25 – 150 K očakávame, že centrálny atóm, bude nadobúdať hodnotu 0, príznačnú pre diamagnetické materiály, akými sú aj železnaté komplexy v LS stave. V skutočnosti je hodnota v rozmedzí 1,2-1,4 cm^3 K mol^{-1}, čo nie je typické. Možnou príčinou vysokej hodnoty je prítomnosť paramagnetickej nečistoty (napr. Fe^{III}), ktorá vznikla čiastočnou oxidáciou vzorky napríklad pri sušení požadovaného produktu. Druhou možnou príčinou je fakt, že menšia časť centrálnych atómov je permanentne v HS stave pri akejkoľvek teplote (tzv. zamrznutá HS frakcia) a zvyšná časť železnatých centrálnych atómov Fe^{II} vykazuje SCO. Pri ďalšom ohreve nad teplotu 300 K pozorujeme nárast hodnoty χT. Toto zvýšenie znamená, že nezamrznuté centrálne atómy Fe^{II} menia svoj spinový stav. Teplota spinového prechodu je $T_{1/2}$ = 370 K. Saturačná HS hodnota nebola stanovená, vzhľadom k tomu, že meranie sa uskutočnilo len po teplotu 390 K (χT = *3,03* cm^3 K mol^{-1}).

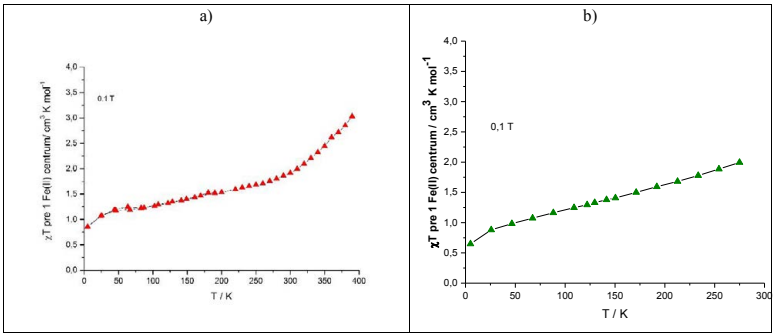

Obrázok 4 Grafy závislosti produktovej funkcie od termodynamickej teploty pre komplex **1** ($[Fe_2(\mathbf{L_4})_3](BF_4)_4$) (a) a pre komplex **2** ($[Fe_2(\mathbf{L_4})_3](ClO_4)_4$) (b)

Závislosť produktovej funkcie od teploty pre komplex **2** nepreukázala prítomnosť SCO (Obrázok 4b). Meranie sa uskutočnilo v rozmedzí 5 – 280 K, aplikované pole bolo rovnaké ako v prípade komplexu **1**. V celom priebehu funkcie je zrejmý postupný nárast hodnôt χT produktu, avšak nič nenasvedčuje tomu, že by mohlo dôjsť k SCO prechodu, keďže na teplotnej krivke chýba náznak plató oblasti pre LS alebo HS stav. Hodnoty χT pri nízkej teplote sa opäť líšia od hodnôt, ktoré sú príznačné pre diamagnetické Fe^{II} komplexy v LS stave. Vzhľadom na to, že presná štruktúra komplexu nie je známa, mohlo dôjsť k zlému určeniu mólovej hmotnosti, čo malo za následok nesprávny prepočet hodnôt χT z nameraných hodnôt efektívneho magnetického momentu.

Záver

Táto práca sa venuje príprave a charakterizácii nových N-donorových ligandov a taktiež problematike magnetických a optických vlastností koordinačných zlúčenín. Údaje obsahujú podrobné informácie o kryštálovej štruktúre, spôsobe prípravy, a magnetické záznamy.

Experimentálna časť sa zaoberá syntézou ligandov, konkrétne **L3** (1,5-bis(2-(pyridín-2-yl)-1H-benzimidazol-1-yl)pentán) a **L4** (1,5-bis(2-(pyridín-2-yl)-1H- -benzimidazol-1-yl)hexán). Príprava spočívala z alkylácie **pybzimu** (2-(pyridín-2-yl)-1H-benzimidazol, 1,5-dibrómpentánom resp. 1,6 dibrómhexánom. Po opakovaných syntézach sa ukázalo, že vhodnejšou zásadou na deprotonizáciu **pybzimu** je hydroxid draselný použitý vo výraznom nadbytku. Náhrada uhličitanu draselného hydroxidom, zvýšila výťažok reakcie o takmer 35%. ^{1}H a ^{13}C NMR analýza potvrdila molekulovú štruktúru v obidvoch prípadoch. Po príprave ligandov nasledovala syntéza koordinačných zlúčenín. Železnaté soli (tetrafluoroboritan a chloristan) boli použité v stechiometrickom pomere 1:1 k ligandom. Ani po použití rôznych kryštalizačných techník, sa nepodarilo získať monokryštály vhodné na RTG difrakčnú analýzu. V obidvoch prípadoch išlo o polykryštalické prášky svetlofialovej farby. Nepriaznivá situácia neumožnila IR spektroskopiu, elementárnu analýzu ani iné techniky, ktoré by pomohli stanoviť presnú štruktúru látok. Na základe použitého pomeru reaktantov, najpravdepodobnejšou štruktúrou bude dvojjadrový železnatý komplex v prípade $[Fe_2(\mathbf{L4})_3](BF_4)_4$.

Molová hmotnosť uvedeného komplexu sa použila na prepočet závislosti magnetického momentu (pre jedno Fe^{II} centrum) od termodynamickej teploty, na závislosť χT vs. T. Priebeh krivky vykazuje neúplný graduálny spin crossover nad izbovou teplotou. Hodnota pre S = 0, sa líši od očakávanej hodnoty. Odchýlka bola spôsobená paramagnetickou nečistotou, alebo frakciou permanentne sa vyskytujúcou v HS stave. Priebeh merania pre komplex $[Fe_2(\mathbf{L4})_3](ClO_4)_4$ nenaznačuje, že by sa jednalo o látku vykazujúcu spin crossover. V tomto prípade mohlo dôjsť k omylu, pri určení mólovej hmotnosti látky.

Ďalší výskum v odvetví koordinačnej chémie sa orientuje jednak na syntézu vhodných chelátujúcich ligandov, ktoré majú vysokú afinitu ku katiónom kovov, a taktiež ich využitiu v príprave koordinačných zlúčenín. Ovplyvňovanie magnetických vlastností pri izbovej teplote, je základným predpokladom pre aplikáciu týchto materiálov v rôznych odvetviach priemyslu.

Zoznam použitej literatúry

1. DEBNÁROVÁ, K. Fotoindukovaný spin crossover v komplexoch železa s bis(benzimidazolyl)pyridínovými ligandami: Bakalárska práca. Bratislava: FCHPT STU, 2019.
2. SEREDYUK, M. – ZNOVJYAK, K.O. – KUSZ, J. – NOWAK, M. – MUÑOZ, C.M. – REAL, CH.A. Control of the spin state by charge and ligand substitution: two-step spin crossover behaviour on a novel neutral iron(II) complex. Dalton Trans., 2014, 43, 16387.

SEKCE DOKTORSKÝCH STUDENTŮ

Lipidomic Analysis as a Tool for a Comprehensive Description of Atherosclerotic Plaques

Kamila Bechynska
Richard Voldrich, Hynek Macha, Vit Kosek, David Netuka, Vladimir Havlicek, Jana Hajslova

University of Chemistry and Technology, Faculty of Food and Biochemical Technology, Department of Food Analysis and Nutrition

Technicka 5, 166 28 Prague 6, Czech Republic
bechynsk@vscht.cz

Atherosclerosis is a chronic inflammatory disease that causes lipids accumulation and the formation of fibrotic plaques in the walls of medium and large arteries. In this way, lipids are involved in the development of coronary heart disease and ischemic stroke, which belong among dominating causes of death in Western civilization. Considering the composition of the atherosclerotic plaque, lipidomic analysis was selected as a suitable tool for its study.
To characterize lipid profile in an atherosclerotic plaque in a longitudinal direction, relevant strategy had to be implemented. In the first phase, the sample preparation of the atherosclerotic plaques (obtained in cooperation with Military University Hospital, Prague) was optimized. Then, a pilot experiment confirmed the different lipids composition in different parts of the plaque. the key experiment was a lipidomic analysis of the atherosclerotic plaque cuts, which revealed different distribution of lipids depending on the progression of stenosis and also between proximal and distal

parts. Increased levels of oxidized free fatty acids and, conversely, a reduced content of plasmalogens were observed in the most affected parts of the plaque. In addition, a targeted screening of oxidized lipids was performed, and 46 oxidized lipids in total were detected in samples. MALDI-MS imaging was also used to describe the atherosclerotic plaque's composition (in collaboration with Laboratory of Molecular Structure Characterization, Academy of Sciences of the Czech Republic). This challenging technique enabled to visualize the spatial distribution of compounds in a sample thus complemented information needed for atherosclerosis pathology study.

Keywords: *atherosclerosis, lipidomics, mass spectrometry*

Acknowledgement: This study was supported by the Ministry of Health of the Czech Republic, grant no. NV18-08-00149

Characterization of selected non-traditional cereals for development of enriched cereal products

Agáta Bendová
Michal Pecháček, Ivana Márová

Brno University of Technology, Faculty of Chemistry, Institute of Food Chemistry and Biotechnology

Purkyňova 118, 612 00 Brno, Czech Republic
xcbendova@fch.vut.cz

Cereals are one of the major food sources in human diet and the beginning of their cultivation is dated thousand years ago. Currently, the interest of the human population in a healthy nutrition and lifestyle is growing. This trend leads to increased interest in traditional cereals and also in less traditional pseudo-cereals, such as quinoa, which is also classified as a so-called superfood. for these reasons, this study was focused on the characterization of active substances and biological effects of selected non-traditional cereals.

In the study, 8 samples of non-traditional cereals were selected, namely amaranth, sorghum, millet, kamut, buckwheat, quinoa, Job's tears and teff. Amaranth, millet and buckwheat were also analysed in the form of flakes. Teff was analysed only in the form of flakes. Sorghum and quinoa were analysed also in their coloured variations. Basic substances of selected cereals such as proteins, lipids or carbohydrates were characterized. Active compounds such as antioxidants, phenolic compounds, gluten or β-glucans were also determined. These substances were mainly

analysed by spectrophotometric methods. for the determination of gluten content RIDASCREEN® Gliadin competitive assay kit was used. Mixed-linkage β-glucan assay kit was used for determination of β-glucans content. for potential application, selected cereals were tested for cytotoxicity on human cells. Determination of cytotoxicity was performed by MTT assay using human keratinocytes HaCaT and human Caucasian colon adenocarcinoma $CaCO^{-2}$.

The results show that some of these non-traditional cereals could gain more attention in the future through their health benefits compared to traditional cereals. It would be interesting to combine them with other active substances that could support immunity or digestion. the best results were obtained for quinoa, amaranth and buckwheat.

Keywords: *cereals, pseudo-cereals, active substances, antioxidants, gluten, β-glucans*

Development of an analytical method for the determination of phytocannabinoids and their bioavailability in rat blood plasma

Zuzana Bínová
Marie Fenclová, František Beneš, Petra Peukertová, Jana Hajšlová

University of Chemistry and Technology, Prague

Technická 5, 166 28 Praha 6, Czech Republic
bobkovaz @vscht.cz

Phytocannabinoids are bioactive compounds occurring in Cannabis sativa L. Currently,non-psychotropic cannabidiol (CBD) has been intensively studied due to its presumed beneficial effects on the human organism (e.g. antioxidant, analgesic, and anti-inflammatory effects, etc.). CBD is sold mainly as a component of various food supplements, the most common are 'CBD oils'. However, under certain conditions, the consumption of CBD-based products carries some risks, which might be associated with the purity of the CBD (which strongly depends on the way of its isolation). To our experience, in many cases, a number of other naturally occurring phytocannabinoids are found in CBD oils, including psychotropic Δ^9-tetrahydrocannabinol (Δ^9-THC). In addition to the need to perform a purity check, the question arises regarding the bioavailability of CBD as it is an important aspect for the evaluation of its effect. for this purpose not only the parent compound but also its metabolites.

The aim of the work was to develop, optimize and validate an

analytical animal method for the determination of phytocannabinoids and their biotransformation products (metabolites) in blood plasma of experimental that were administered in oil and CBD formulations differing in respective carriers. Using this method, the bioavailability of CBD as a function of time was subsequently investigated. At intervals of 2, 4, and 6 hours after intake of the preparations, blood plasma was collected for analysis by ultra-high performance liquid chromatography coupled with tandem mass spectrometry (UHPLC-MS/MS). Only CBD was detected in the samples at the level of quantification. In most cases, CBD concentration reached the apex after two hours, however, when using the oil carrier. CBD (reference) maximum concentration was reached after the four hours after administration. It should be noted that significant variability was observed within the animals' cohort.

Keywords: *phytocannabinoids, UHPLC-MS / MS, plasma*

Preparation of Mg-Al-Ti Bulk Materials Via Powder Metallurgy

Ing. Roman Brescher
Ing. Matěj Březina, Ph.D.

Brno University of Technology, Faculty of Chemistry,
Institute of Materials Chemistry

Purkyňova 464, 612 00 Brno Medlánky, Czech republic
xcbrescher@vutbr.cz

Bulk materials based on the Mg–Al–Ti system were prepared using traditional methods of powder metallurgy, as well as using the sprak plasma sintering (SPS) method. the microstructure of the material, elemental and phase composition was examined. Subsequently, Vickers hardness and flexural strength were measured, and fractographic observation of the fracture surface was performed. It was found that the aluminum was completely dissolved during sintering and subsequent heat treatment, but the titanium particles remained almost intact in the material and worked as a particulate reinforcement. X–ray diffraction spectroscopy detected multiple phases, such as magnesium phase β, magnesium–aluminum solid solution, pure titanium, and titanium nitride. Titanium nitride could be formed because of the reaction of titanium and the nitrogen atmosphere used during sintering. Materials prepared by methods of conventional powder metallurgy showed increased porosity compared to materials prepared by the SPS, resulting in lower hardness and flexural strength. This phenomenon could be caused by Kirkendall effect, where aluminum diffused into magnesium faster than magnesium into aluminum. the hardness increased with increasing the amount of aluminum and titanium

and with the amount of magnesium phase β. Fractographic observation of the fracture surface showed, that titanium particles held firmly in the matrix even after formation of crack, which in some cases passed through the titanium particle itself. This fact might suggest that a diffuse connection between the reinforcement and the matrix may have occurred after the sintering process.

Keywords: *magnesium alloys, aluminium, titanium, spark plasma sintering, hardness, flexural strength*

Fixation of the Lead in Alkali Activated Materials Based on Different Types of Ashes

Ing. Vladislav Cába
Ing. Jan Koplík, PhD.

Brno University of Technology Faculty of Chemistry

Purkyňova 464/118, 612 00 Brno
vladislav.caba@vutbr.cz

The aim of this work was to prepare alkali-activated matrices of sufficient strength based mainly on ash, to reveal the method of fixation of lead in these matrices and to determine the impact of added lead on mechanical properties. the matrices consisted mainly of ash with a mixture of blast furnace slag and sodium water glass as an activator. Five different ashes were used – four of them were from fluidized bed coal combustion and one from pulverized coal combustion. After 28 days, the strengths of the samples were measured to reveal an impact of lead doping. To determine the structure, images, element maps and elemental spectra were taken using a scanning electron microscope with energy dispersive spectroscopy, the samples were analysed on an infrared spectrometer with Fourier transform, X-ray diffraction analysis and electron spectroscopy for chemical analysis were also used. Individual measurements show that lead is accumulated in the form of hydroxide. the impact of lead doping on strength of the matrix was different for individual samples.

Keywords: *alkali activated materials, inhibition, lead, fly ashes*

Bioaccessibility of Metals in Urban Aerosol

Hana Cigánková

Brno University of Technology, Faculty of Chemistry, Chemistry and Technology of Environmental protection

Purkyňova 464/118, 612 00 Brno, Czech Republic
xcbarborikovah@fch.vut.cz

Atmospheric pollution is an increasing cause of concern for human health. Atmospheric particulate matter (PM) is known as the source of several health effects (cardiovascular and respiratory diseases including lung cancer, neurodevelopmental and neurodegenerative diseases). Metals are of particulate interest for the assessment of PM toxicity because of the fact that they are capable generation reactive oxygen species (ROS). ROS induce oxidative stress leading to inflammatory responses and DNA damage.

Large attention should be paid the particle size. Particles in the range of 2.5-10 μm are in most cases deposited in the pharyngeal and tracheal region. In the adoral area, they can be swallowed, thus reacting also in the gastrointestinal tract. Particles less than 1 μm can reach the alveolar lung regions and interact with lung fluids.

Bioaccessibility testing is becoming an increasingly popular exposure assessment method, due to its simplicity and cost effectiveness. In this contribution, the soluble metal fraction extracted with simulated lung fluids (SLFs) is used as an estimation of metal bioaccessible fraction. Metal bioaccessibility is defined as the total metal fraction that is soluble in the target organ (lungs

for respiratory bioaccessibility). the most commonly used SLFs are water and Gamble solution. Gamble solution is representative of the interstitial fluid in the deep lung. As addition of this fluid was on Institute of Analytical Chemistry, Czech Academy of Science developed new SLF called Simulated Alveoli Fluid (SAF), which attempts to simulate extraction in alveoli.
The aim of this contribution is to assess the bioaccessibility of potentially toxic metals (i. e. Fe, Mn, Zn, Ni, Cu, Cd, Co, Pb, V, Cr) associated with urban aerosol collected on nitrocellulose filters in Brno (Veveří street). To measure the total concentration of metals, a portion of the filters were decomposed in concentrated nitric acid using microwave decomposition. Total metal concentrations were measured using ICP-MS. the bioaccessibility was determined after the incubation of samples in three solutions that mimic chemical conditions in the lungs (deionized water, Gamble solution and SAF) for 24 hours at 37 °C. the differences in metal bioaccessibility in different aerosol size fraction were evaluated by sampling two different PM size fraction: $PM_{2.5}$ and PM_1.

Keywords: *metals, bioaccessibility, aerosol, simulated lung fluid*

Aminoclay as Drug Carrier

Jakub Dušek

Brno University of Technology,
Faculty of Chemistry,
Institute of Physical and Applied Chemistry

Purkyňova 464/118, Královo Pole, 61200 Brno 12, Czech Republic
Jakub.Dusek@vut.cz

This study aimed to prepare new drug delivery system with use of aminoclay complexes to enhance the drug release and improve bioavailability of selected drugs. Aminoclay is a relatively new material that belongs to organically modified clays. It is a magnesium phylosilicate that contains 3-aminopropyl groups. the clay material thus modified is characterised by relatively good chemical and mechanical stability, showing no signs of toxicity even at higher concentration. Thanks to easy preparation, and thermal and mechanical stability of inorganic matrix and external amino groups is aminoclay a material with great potential for many applications. By binding the drug to the aminoclay matrix it is expected to improve properties such as solubility, stability, release, bioavailability, biodegradation, etc.

For model samples was used a selection of the bioactive substances: curcumin, diclofenac, ibuprofen, merocyanin and tocopherol. for verification of binding drugs were used methods of FTIR (Fourier Transformation Infrared Spectroscopy) and EA (Elemental Analysis). Furthermore, the content of the bound bioactive substances to the aminoclay matrix was investigated using UPLC (Ultra Performance Liquid Chromatography). What is essential for therapeutic use of bioactive substances is their value of cytotoxicity. for this

study MTT test for evaluation of cytotoxicity was used.
The main motivation of this study was to create new complexes with improved characteristics that would replace existing forms of substances used in pharmaceutical and biomedical applications.

Keywords: *aminoclay, carrier, drug*

Preparation and Characterization of Functionalized Wound Dressings

Lucia Dzurická
Agáta Bendová, Julie Hoová, Petra Matoušková, Ivana Márová

Brno University of Technology, Faculty of Chemistry, Institute of Food Science and Biotechnology

Purkyňova 464/118, 612 00 Brno, Czech Republic
Lucia.Dzuricka@vutbr.cz

This work is focused on preparation and characterization of bioactive hydrogels and nanofiber wound dressings functionalized by active compound in the form of antibiotic drug: ampicillin. Nanofiber dressings were constituted from poly(3-hydroxybutyrate) and hydrogel dressings were created using alginate and chitosan. Prepared wound dressings were tested for possible cytotoxic effects on human cells, antimicrobial activity and the rate of gradual releasing of the incorporated substance into model environments. Nanofibers were assembled by electrospinning and force spinning techniques. Morphology of the prepared nanofibers was confirmed by SEM. Dressings were characterized for gradual release using spectrophotometric methods. Antimicrobial activity against gram-positive and gram-negative strains of microorganisms was also evaluated. the results showed good antimicrobial efficacy of functionalized materials.

Because of the potential application for local skin treatments the cytotoxicity of the prepared materials was tested. Safety of the dressings was determined by MTT assay using human keratinocytes (HaCaT). the majority of the prepared materials has been

proved to be non-cytotoxic, and, thus, safe for topical applications in human subjects. Prepared nanofiber and hydrogel dressings with antimicrobial effect showed promising results for the local treatment of open wounds, such as skin ulcers.

Keywords: *wound dressings, ampicillin, poly(3-hydroxybutyrate), chitosan, alginate, antimicrobial activity, cytotoxicity*

Acknowledgments
This work was supported by the project Nr. FCH-S-20-6316 of the Faculty of Chemistry, Brno University of Technology

High Throughput Platform for Identification And Characterization Of Electrogenic Bacteria.

Jiri Ehlich
Lukasz Szydlowski Ph.D.

Brno University of Technology, Faculty of chemistry, Institute of Materials Chemistry

Purkyňova 464/118, 612 00, Brno, Czech Republic
Jiri.Ehlich@vut.cz

Electrogenic and electron accepting capability of some bacteria strains, are important phenomena which promises advances in the fields of electronically stimulated biotechnological production of valuable chemicals, wastewater treatment, bioremediation, desalination, energy production, novel materials discovery and whole-cell biosensing. Significant boost towards this direction can be achieved with application of high throughput methods known from other biological disciplines. However there is currently a lack of standard and reliable hardware which would enable the same approach in the field of electrogenic bacteria.

Thus we present a platform based on standard Microplate set-up with 24 or 96 single chamber air-cathode Microbial Fuel Cells (MFCs) with integrated reference electrode inside each chamber. All electrodes are individually addressable. the device enables the direct and parallel comparative analysis of microbes from different sources or under different conditions such as electrode potential, pH and growth medium.

Determination of micro-bioplastics in solid matrix

Jakub Fojt[1]
Ivana Románeková[1], Bára Komárková[3, 4]
Radek Přikryl[2], Jiří Kučerík[1]

[1]Brno University of Technology, Faculty of Chemistry, Chemistry and Technology of Environmental Protection

Purkyňova 464/118 612 00 Brno Czech Republic

[2]Brno University of Technology, Faculty of Chemistry, Institute of material science

Purkyňova 464/118 612 00 Brno Czech Republic

[3]Czech Academy of Sciences, Institute of Inorganic Chemistry

Husinec-Řež 1001, Řež 258 00

[4]University of Ostrava, Faculty of Science

30. dubna 22, Ostrava 701 03
xcfojt@fch.vut.cz

Mankind try to replace oil-based plastics by so-called biodegradable bioplastics to minimize plastic pollution. These bioplastics requires specific conditions for biodegradation, which are usually not met in nature. This could lead to formation of microplastic debris „Micro-bioplastics“. There are plenty of analytical methods for determination of conventional microplastic presence or concentration in aquatic systems, the less of studies focus on analysis in soils due complexity of this matrix and there is lack of methods for determination of micro-bioplastics. the most difficult, time

consuming and dangerous for analyte are soil sample pre-treatment and preconcentration or extraction of bioplastics. That's why we have developed direct analytical method using evolved gas analysis (EGA, combination of thermal degradation and mass spectrometry) for determination of micro-bioplastics, which does not require any of these sample preparation techniques. We present data on use this method for determination of micro-bioplastics in Siberian and Czech soils, the standard Lufa soil and in sewage sludge. Application of this method was already successfully demonstrated for determination oil-based microplastics. In this work, as a model bioplastic was used polyhydroxybutyrate (PHB) and polylactic acid (PLA). We demonstrate a fast, robust, and easy EGA method for determination of PHB and PLA micro-bioplastics in soil and other solid matrix with possible differentiation of anthropogenic PHB from natural PHB. In addition, this method could be helpful for verification and precising of biodegradation tests and contamination evaluation of soil after applying micro-bioplastic polluted compost.

Acknowledgement
The financial support of projects FCH-S-20-6446 of Ministry of Education, Youth and Sports are acknowledged.

Keywords: *Micro-bioplastics, microplastics, evolved gas analysis, soil, sewage sludge*

Study of Cholesterol's Effect on the Properties of Catanionic Vesicular Systems

Martina Havlíková, Filip Mravec

Brno University of Technology, Faculty of Chemistry,
Institute of Physical and Applied Chemistry

Purkyňova 464/118, 612 00 Brno, Czech Republic
Martina.Havlikova@vut.cz

This work is focused on the study of properties associated with the effect of cholesterol levels on the stability of vesicular systems based on the ion pair amphiphile hexadecyltrimethylammonium-dodecylsulphate (HTMA-DS) at laboratory temperature. the HTMA-DS catanionic system was doped with dioctadecyldimethylammonium chloride in a 9:1 M ratio and cholesterol in the amount of 0, 3, 13, 23, 33, 43, 53, 63 and 73 mol.% was added. In this system, the size distributions were studied using the dynamic light-scattering technique and the zeta potential was determined. These standard techniques were supplemented by fluorescence spectroscopy technique. Specifically, generalized polarization (GP) was measured using a Laurdan probe. This probe is sensitive to fluidity and membrane hydration at a particular temperature. Due to low stability and high opalescence of samples, spectral techniques were used only for the samples with cholesterol content above 23 mol.%. the results from fluorescence spectroscopy point to a change in the amount of hydration water in the membrane, the largest amount of which is present in the samples with 43 and 53 mol.% cholesterol. Using the light-scattering

technique, the short-term stability of prepared vesicular systems was also observed over the first 36 days. Obtained results confirmed that the most stable systems are those containing 43 or 53 mol.% of cholesterol. This work was supported by the Czech Science Foundation, project No. 19-14024J (GACR), and Ministry of Science and Technology, Taiwan, project No. MOST108-2923-E006-MY3.

Keywords: *Catanionic vesicles, Ion pair amphiphile, Dynamic Light Scattering, Zeta potential, Generalized Polarization, Laurdan, Hydration water.*

Characterization of Hydrogels with Amphiphilic Structures

Richard Heger
Miloslav Pekař

Brno University of Technology, Faculty of Chemistry, Institute of Physical and Applied Chemistry

Purkyňova 464/118, 612 00 Brno, Czech Republic
xchegerr@fch.vut.cz

Nowadays there is an increasing demand for hydrogels with modifiable properties, which would find application especially in health care, pharmacy, or common consumer industry. Inspiration for hydrogel structures can be found in extracellular matrix, which has the character of a hydrocolloid and which is often simulated by hydrogels. It also has a relatively complex composition and some components „only" regulate biochemical processes, while others co-create or influence its properties. Understanding the physicochemical properties of the extracellular matrix is very complex and yet not well described. Hydrogels in this work are trying to use the knowledge gained from the proper functioning of a living organism and then transfer it to the developed hydrogels.
This work deals with the study of preparation and properties, especially rheology, of hydrogels, whose internal structure is modified and controlled by addition of suitable amphiphiles. the specific material solution of this work is based on simple hydrogel matrices, which were prepared from agarose and gelatin. In the frame of this contribution the formation of internal structures was caused by the addition of lecithin. the addition of amphiphilic

substance affects the viscoelastic moduli, the values at the cross over point as well as the relaxation properties.

Keywords: *amphiphile, hydrogel, rheology*

Study of simple electrolytes for magnesium batteries

Jiří Honč

Brno University of Technology, Faculty of Chemistry,
Institute of Materials Chemistry

Purkyňova 464/118, 612 00, Brno
jiri.honc@vut.cz

The study is focused on electrolytes for magnesium batteries. In contrast to electrolytes published in recent scientific articles, which were mostly prepared from either hazardous or expensive substances, the electrolytes in this work were composed of affordable solvents and chemicals, which can be handled at normal laboratory conditions. Specifically, solutions of dimethylsulfoxide and tetrahydrofurane with magnesium chloride, nitrilotriacetic acid, aluminium chloride, and disodium ethylenediaminetetraacetic acid, were examined. the ability of electrolyte to oxidize and deposit magnesium was characterized using cyclic voltammetry. More information about the kinetics of electrochemical reactions in terms of polarization resistance was obtained by electrochemical impedance spectroscopy. EIS was also used to reveal formation of oxide layer on electrode and its homogeneity. Magnesium electrodes from electrochemical measurements were finally examined by scanning electron microscopy with energy-dispersive X-ray spectroscopy. Based on the SEM pictures and EDS data, the effect of humidity and atmospheric oxygen on magnesium electrode corrosion during electrochemical cycling was discussed.

Keywords: *magnesium batteries, electrolyte, cyclic voltammetry, electrochemical impedance spectroscopy (EIS).*

Humid Air Cooling by Shell and Tube Heat Exchangers

Petr Horvát
Jaroslav Vlasák, Josef Kalivoda, Ondřej Krištof, Tomáš Svěrák

Brno University of Technology, Faculty of Chemistry, Institute of Materials Chemistry

Purkyňova 464/118, 612 00 Brno, Czech Republic
Petr.Horvat@vut.cz

The processes of cooling by shell and tube heat exchangers for subsequent application in processes of removal of gaseous air contaminants via liquid absorber is the major topic of this work. the aim of the work is to verify both the theoretical computational relations and the theoretical convenience of silicon carbide as a better heat transfer surface material compared with traditional borosilicate glass material characterized by two orders of magnitude worse thermal conductivity. Heat transfer on semi-operating shell and tube heat exchangers with baffles and glass or silicon carbide heat exchange surface is examined by cooling the humid air by 50% propylene glycol in tubes having an inlet temperature just above 0 °C.

Coolant flow can be regulated in many steps, but only laminar flow rates are available. Unfortunately, the coolant inlet temperature cannot be precisely regulated, just only precisely measured (as outlet temperature). Three-way flow of coolant is used, so speed of coolant is three-times higher in tubes. Relative air humidity, temperature and flow of air is measured.

Local air heat transfer coefficient is low due to low ventilator pow-

er, low temperature, and low humidity. the effect of coolant and heat transfer surface on transferred heat is almost negligible. the efficiency of exchangers is very high (91–94 % with carbide and 88–89 % with glass). the trend of a slight increase in efficiency is observed with increasing flow of both fluids. Flow turbulization is the reason. the three-way flow of coolant may also negatively affect the efficiency, it will be verified with a higher heat transfer coefficient condition.

The theoretical model using the *j* factor, the correction factors for the baffles, and the correction for air humidity condensation have proven to be appropriate under the examined conditions. the trend of overestimating the model at higher flow rates, especially air, was shown. This trend will be examined with a higher heat transfer coefficient condition. the result is also affected by the inaccuracy of the calculation of the mean temperature difference, especially for carbide heat exchanger, caused by failure to use most of the heat exchanger potential. the results also evaluate the heat loss through the shell and the heat exchanged in addition by air humidity condensation.

After the experiments with an increased local air heat transfer coefficient, the experiments with coolant temperature below 0 °C will probably follow and heat exchange affected by icing would be observed. the air temperature profile will be computer modeled and verified by measuring the temperature close to the middle of the carbide exchanger. Then, cooling of air will be situated in front of the separation of gaseous impurities from gas into liquid using a scrubber, more effective at lower temperatures. Separation of some pollutants could also take place by condensation in the exchanger at very low temperatures, or high pressures.

Keywords: *shell and tube heat exchanger, heat transfer, cooling, humidity condensation*

Spectroscopic Study of Human Blood Plasma for Early Detection of Hepatocellular Carcinoma

Kateřina Hrubešová
Lucie Habartová, Petr Hříbek, Petr Urbánek, Vladimír Setnička

University of Chemistry and Technology Prague, Faculty of Chemical Engineering,
Department of Analytical Chemistry
Technická 5, 166 28 Prague 6, Czech Republic
Katerina.Hrubesova@vscht.cz

1 Introduction

Hepatocellular carcinoma (HCC) is the seventh most frequent type of cancer, and its global incidence is constantly rising[1]. In addition, it exhibits one of the highest mortality rates of all cancer types, with the chance of a 5-year survival being below 10%. The high mortality of HCC is associated with suboptimal performance of the currently employed methods, especially for early stages of the disease. This often results in a late diagnosis making the treatment by surgical resection, transplantation, or ablation no longer effective or even inapplicable[2].

Over 85% of HCC cases develop from cirrhosis[3], which is an irreversible damage to the liver structure leading to a decrease in their functionality. This chronic condition may be a consequence of several health issues: infection with chronic hepatitis (type B and C), excessive consumption of alcohol, and non-alcoholic fatty liver disease, which is tied to obesity[4-6]. A precautionary screening of the high-risk group of cirrhosis patients is; therefore, crucial for the early diagnosis of HCC and for the reduction of its high mortality. However, the current screening procedure depends mainly on regular ultrasound examinations, with approximately 60% sensitivity to early stages of HCC[7]. Not even the only clinically used biomarker, alpha-fetoprotein, shows sufficient sensitivity and specificity[8].

In our research, we focus on the application of vibrational and chiroptical spectroscopic techniques for the analysis of blood plasma of HCC patients and patients with liver cirrhosis. There are several advantages to this approach. First, the collection of blood plasma is a routine medical procedure, which is almost non-invasive. Blood is in direct contact with organs and contains a high number of proteins and metabolites, whose structure and concentrations may be altered by the tumorous growth even before the clinical manifestation of the disease. Second, vibrational spectroscopic techniques collect data about the whole blood plasma sample allowing for the simultaneous analysis of all present molecules. They are sensitive to molecular composition of the sample,

concentration of the molecules present and are even capable of detecting changes in their spatial structure[9, 10]. Moreover, the analysis is fast, low-cost and requires only a small amount of sample with no or minimal preparation. In our research, we use both Fourier-transform infrared (FT-IR) spectroscopy and Raman spectroscopy, which provide complementary information to a certain extent and; thus, their combination offers a more detailed insight into the composition of the sample. Further, our study includes one technique of chiroptical spectroscopy – electronic circular dichroism (ECD), which is based on the detection of a difference in absorption of left and right circularly polarized radiation by the sample and reflects the overall conformation of chiral molecules[11]. We believe that this approach may help to identify novel biomarkers, which would allow for the early detection of HCC and; thus, improve the effectiveness of the currently employed screening methods.

2 Experimental

2.1 Blood plasma samples

The enrolment of 22 patients with hepatocellular carcinoma (diagnosed according to standard diagnostic criteria published by The European Association for the Study of the Liver[3]) and 11 patients suffering from liver cirrhosis was conducted at the Department of Gastroenterology, Hepatology and Metabolism, First Faculty of Medicine, Charles University and Military University Hospital in Prague. The group of HCC patients comprised of 2 patients in stage A, 10 patients in stage B and 8 patients in stage C (according to Barcelona-Clinic Liver Cancer staging system[12]).

Whole blood was collected into a K3EDTA tube, centrifuged at 1 500 × g for 10 minutes and the resulting blood plasma fractions were stored at −80 °C. Prior to the spectroscopic analysis, the samples were thawed at room temperature and centrifuged through a 0.45 μm polyvinylidene difluoride membrane at 13 000 × g for 10 minutes.

2.2 Spectroscopic measurements

Infrared spectra were collected on the Nicolet 6700 FT-IR spectrometer (Thermo Fisher Scientific, USA) using the technique of attenuated total reflection with a zinc selenide crystal. Filtered plasma was measured in the spectral range of 4000–400 cm^{-1} with 512 accumulations and a resolution of 4 cm^{-1}. To remove the dominant bands of water, the spectrum of distilled water acquired under the same experimental conditions was subtracted from the sample spectra. Additionally, water vapour lines, which may overlap important spectral details, were removed by subtracting a spectrum of pure water vapour. The distortion and offset of the spectral baseline were corrected using the linear baseline correction function in the Unscrambler X software (Camo, Norway).

Raman spectra were collected using the ChiralRAMAN-2X spectrometer (BioTools, Inc., USA) equipped with an Opus 2W/MPC6000 laser system (Laser Quantum, UK) with a visible excitation of 532 nm. The spectra were measured in a quartz cell with an optical path length of 4 mm with a resolution of about 7 cm^{-1} in the spectral range of 200–2500 cm^{-1} with 12-hour acquisition period and laser power set to 150 mW. To reduce the undesired fluorescence background present in the measured spectra, we employed

an approach previously developed in our laboratory[13], which consists of a combination of kinetic quenching and photobleaching. The amount of 10 mg of NaI, acting as a fluorescence quencher, was added to 100 μl of filtered plasma, which was then photobleached at 280 mW of laser power for 12 h prior to the analysis. The distortion of the baseline caused by residual fluorescence was corrected by subtraction of the background, which was generated by highly smoothing the original spectra using FFT filtering. The resulting spectra were normalized on the intensity of the amide I band (1658 cm^{-1}).

Measurements of the ECD spectra of blood plasma were performed using the J-815 CD spectrometer (Jasco, Japan). The spectra were measured in a quartz cell with an optical path length of 0.1 mm with the following experimental parameters: a spectral range of 185–280 nm, 6 accumulations, a scanning speed of 50 nm min^{-1}, a response time of 2 s, a data pitch of 0.1 nm and a sensitivity of 100 mdeg. Prior to the analysis, blood plasma was diluted in a 1:3 volume ratio with sterile phosphate buffer (pH 7.4) to avoid saturation of the detector. No additional processing of the spectra was carried out.

2.3 Statistical analysis

The spectroscopic data were evaluated using principal component analysis followed by linear discriminant analysis (PCA-LDA) utilizing the Unscrambler X (Camo, Norway, www.camo.com) and the XLstat software (Addinsoft, USA, www.xlstat.com). PCA is an unsupervised multivariate method that reduces the high number of variables of the spectral data to only a few principal components (PCs) describing most of the variation. For PCA, the data were mean-centred and a singular value decomposition algorithm with a 20-fold cross-validation was used. The resulting PCs then served as an input for LDA, which is a supervised method used for the classification of the samples. LDA included leave-one-out cross-validation.

3 Results and discussion

3.1 Fourier-transform infrared spectroscopy

Average FT-IR spectra of the blood plasma of both studied groups (Figure 1, left) show two intense bands at 1637 and 1546 cm^{-1}, which are assigned to amide I (C=O stretching) and amide II (a combination of N—H bending and C_α—N stretching) vibrations of peptide bonds in proteins. Additional bands may be observed at 1454 (CH_2 and CH_3 bending of phospholipids and proteins) and 1400–1240 cm^{-1} (COO^- stretching of proteins and cholesterol)[10]. The average spectra show no apparent differences between the studied groups and; thus, the PCA was applied on the data set (spectral region 1680–800 cm^{-1}) to detect possible sources of variability between the spectra, which were visualized by the loadings plots of the generated PCs. For example, the first PC (Figure 1, right), describing 68% of variability, suggests that the most significant changes occur between the relative intensities of the amide I and amide II bands. Further, the PC-1 loading exhibits a noteworthy feature in the region of the amide I band, as its maximum is in comparison with the average spectra shifted to 1654 cm^{-1}, which indicates changes

in the band profile suggesting variations in the secondary structure of proteins between the studied samples[10, 14].

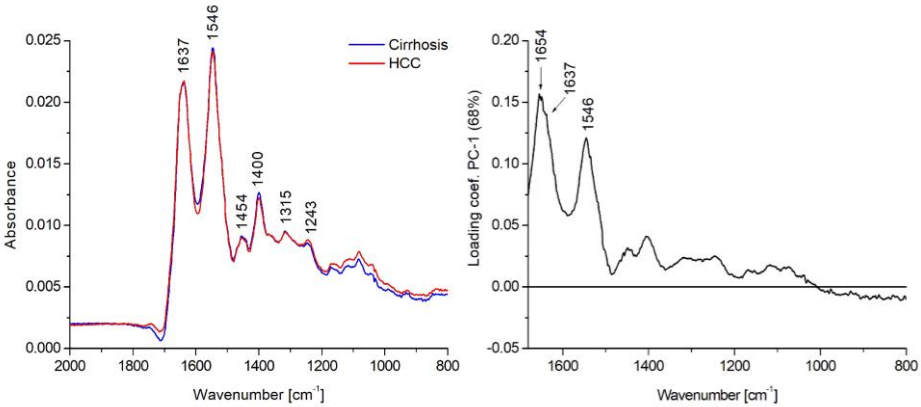

Figure 1: Average FT-IR spectra of the blood plasma of patients with hepatocellular carcinoma (red, n = 20) and liver cirrhosis (blue, n = 11) (left). Loadings plot for PC-1 for the spectral region of 1680–800 cm^{-1} (right).

3.2 Raman spectroscopy

The most intense bands in the Raman spectra (Figure 2, left) at 1006, 1158 and 1519 cm^{-1} are assigned to C—C and C=C vibrations of carotenoids. Their high intensity originates from the resonance enhancement occurring due to the overlap of their electronic absorption bands with the excitation wavelength of 532 nm[15]. The regions of amide I (1656 cm^{-1}, C=O stretching) and amide III (1230–1350 cm^{-1}, a combination of N—H and C—H bending) again reflect the conformation of proteins[9, 16]. Other observable features are bands of the bending vibration of CH_2 and CH_3 groups of phospholipids and protein sidechains at 1450 cm^{-1}, the vibration of aromatic amino acid sidechains at 1192 and 1006 cm^{-1} (overlap with carotenoids) and the skeletal vibration of C—C and C—N bonds in the peptide backbone of proteins at 960 cm^{-1}. The average spectra show that the biggest differences between the studied groups are in the intensities of the carotenoid bands. Carotenoids are natural antioxidants and play an important role in the ability of the organism to deal with oxidative stress, which is a secondary feature of many diseases, including cancer. We have previously detected similar trends also for other diseases, e.g. pancreatic cancer[17], which suggests that the decrease in the intensities of carotenoid bands is not specific for HCC. Therefore, the carotenoid regions were excluded from the PCA-LDA evaluation. Besides the aforementioned carotenoids, PC-1, describing 91% of the total variability, showed several other regions exhibiting increased variability (Figure 2, right). For example, the amide III region points to a shift in the relative intensities of bands at 1270 and 1285 cm^{-1}. This shift is also visible between the average spectra of HCC and cirrhosis samples, indicating changes in the secondary structure of proteins[16]. Based on the PC loadings together with the differences observed between the average Raman spectra of the two studied groups,

the following spectral regions were selected for the PCA-LDA: 930–1040, 1180–1220, 1250–1350 cm^{-1}.

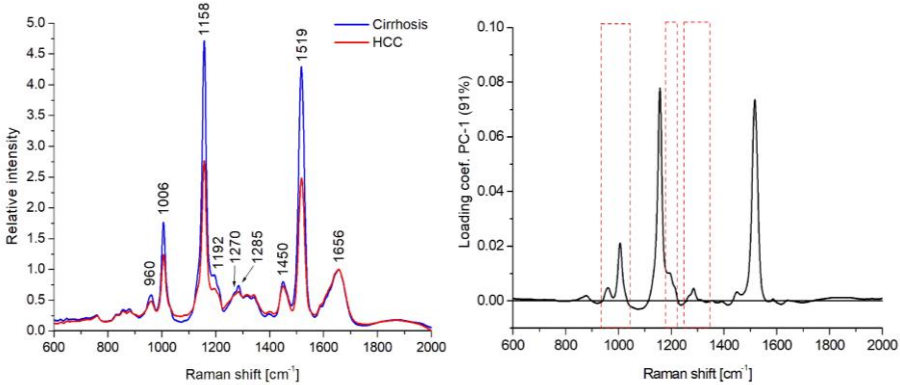

Figure 2: Average Raman spectra of the blood plasma of patients with hepatocellular carcinoma (red, n = 20) and liver cirrhosis (blue, n = 11). Spectra are normalized on the intensity of the amide I band (1656 cm^{-1}) (left). Loadings plot for PC-1 (right). The regions marked with red boxes were used in the final PCA-LDA model.

3.3 Electronic circular dichroism

There are three bands in the ECD spectra of blood plasma (Figure 3, left), one positive with a maximum at 192 nm (π–π* transitions of the peptide bond in proteins) and two partially overlapping negative bands at 209 and 222 nm (π–π* and n–π* transitions of the peptide bond in proteins, respectively)[11]. With ECD being a technique of chiroptical spectroscopy, the overall shape of the spectra is strongly affected by the spatial structure of the analysed molecules. In the case of blood plasma, the spectral profile corresponds to proteins with a predominant α-helical conformation, which is probably due to the high content of human serum albumin, the structure of which is mainly α-helical. There is an apparent decrease in the intensity of all bands in the average spectrum of HCC patients compared to cirrhosis, which suggests possible pathologically induced changes of protein levels and/or conformations. Loading of PC-1, describing 87% of the total variability, matches the profile of the spectrum and; thus, captures the overall intensity changes. Interestingly, the shape of the PC-2 loading curve (Figure 3, right), describing 10% of the total variability, approximately corresponds to the spectral profile of β-sheet proteins[11], confirming the changes in the relative amounts of α-helical and β-sheet proteins.

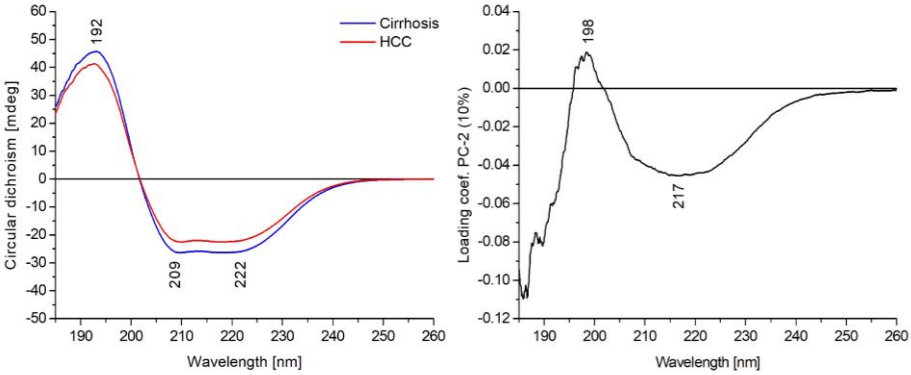

Figure 3: Average ECD spectra of the blood plasma of patients with hepatocellular carcinoma (red, n = 20) and liver cirrhosis (blue, n = 11) (left). Loadings plot for PC-2 (right).

3.4 Statistical evaluation

Data sets generated by the three spectroscopic techniques were subjected to PCA-LDA, combining the methods and initially using the first six PCs for each method. As PCs generated by the PCA capture most of the variability between all spectra but not necessarily between the two studied groups of samples, the PCs used for the final LDA classification were optimized using the standard canonical discriminant coefficients, which indicate the significance of the selected variable for the differentiation of the samples. For FT-IR spectroscopy, PC-1, PC-3 and PC-4 were used in the model, describing mostly the changes in the amide I and amide II regions. All six PCs generated from the selected regions of the Raman spectra were beneficial for the accuracy of the resulting model. In the case of ECD, the best classification of the samples was achieved using only PC-2 and PC-3. The low significance of PC-1 for the differentiation of the samples suggests that the changes in the overall intensity of the ECD spectra are not a sufficient indicator of the disease.

The resulting PCA-LDA model was able to distinguish between the analysed samples with the overall accuracy of 90%. From the total number of 33 samples, only one sample of cirrhosis and two samples of HCC were misclassified (Table 1).

Table 1: Confusion matrix for the cross-validated PCA-LDA model.

from \ to	Cirrhosis	HCC	Total	Correct
Cirrhosis	10	1	11	91%
HCC	2	18	20	90%
Total	12	19	31	90%

To estimate the contribution of each technique, individual sub-models were created using the same PCs as the previous combined model. The overall accuracies were

as follows: 77% for FT-IR spectroscopy, 84% for Raman spectroscopy and 65% for ECD (Table 2). The results show that our unique approach combining different analytical methods is beneficial and even the ECD data, which on their own do not allow for a very accurate classification, possibly provide supplementary information to the Raman and FT-IR measurements.

Table 2: Accuracy of the cross-validated PCA-LDA models for individual spectroscopic methods and their combination.

Method	Principal components	PCA-LDA accuracy
FT-IR	PC-1, PC-3, PC-4	77%
RAMAN	PC-1–6	84%
ECD	PC-2, PC-3	65%
ECD, FT-IR, RAMAN	all of the above	90%

4 Conclusion

We have successfully developed a method for the differentiation of patients diagnosed with HCC from cirrhotic patients based on vibrational and chiroptical spectroscopic data and their statistical processing using PCA-LDA. The average spectra of the two studied groups of patients, together with PC loadings curves generated by PCA, indicate that the most significant changes within the spectra may be attributed to proteins and possible alterations of their conformation associated with the disease. This phenomenon was detected by each spectroscopic technique. The optimization of the process resulted in a combined model with 90% accuracy. It may be noted that also the accuracy of all individual models, especially that one generated from the Raman spectra (84%), is relatively high compared to the currently employed screening methods[7, 8]. As the relevance of the presented approach depends primarily on its ability to detect early stages of the disease, the current promising results should be further verified on larger sample sets containing a high number of early stages of HCC.

5 References

1. BRAY, F., et al. Global cancer statistics 2018: GLOBOCAN estimates of incidence and mortality worldwide for 36 cancers in 185 countries. 2018, vol. 68, no. 6, p. 394-424.
2. BRUIX, J., REIG, M., SHERMAN, M. Evidence-Based Diagnosis, Staging, and Treatment of Patients With Hepatocellular Carcinoma. *Gastroenterology*, 2016, vol. 150, no. 4, p. 835-853.
3. GALLE, P. R., et al. EASL Clinical Practice Guidelines: Management of hepatocellular carcinoma. *Journal of Hepatology*, 2018, vol. 69, no. 1, p. 182-236.
4. ZAMOR, P. J., DELEMOS, A. S., RUSSO, M. W. Viral hepatitis and hepatocellular carcinoma: etiology and management. *Journal of gastrointestinal oncology*, 2017, vol. 8, no. 2, p. 229-242.

5. MATSUSHITA, H., TAKAKI, A. Alcohol and hepatocellular carcinoma. *BMJ open gastroenterology*, 2019, vol. 6, no. 1, p. e000260.
6. ALEXANDER, M., et al. Risks and clinical predictors of cirrhosis and hepatocellular carcinoma diagnoses in adults with diagnosed NAFLD: real-world study of 18 million patients in four European cohorts. *BMC Medicine*, 2019, vol. 17, no. 1, p. 95.
7. SINGAL, A., et al. Meta-analysis: surveillance with ultrasound for early-stage hepatocellular carcinoma in patients with cirrhosis. *Alimentary pharmacology & therapeutics*, 2009, vol. 30, no. 1, p. 37-47.
8. CRISTEA, C. G., et al. Considerations regarding current diagnosis and prognosis of hepatocellular carcinoma. *Journal of medicine and life*, 2015, vol. 8, no. 2, p. 120-128.
9. LASCH, P., KNEIPP, J. *Biomedical Vibrational Spectroscopy*. Hoboken, New Jersey: John Wiley & Sons Inc., 2008. ISBN: 978-0-470-22945-3.
10. BARTH, A. Infrared spectroscopy of proteins. *Biochimica et Biophysica Acta (BBA) - Bioenergetics*, 2007, vol. 1767, no. 9, p. 1073-1101.
11. BEROVA, N., et al. *Comprehensive Chiroptical Spectroscopy: Applications in Stereochemical Analysis of Synthetic Compounds, Natural Products, and Biomolecules*. Hoboken, New Jersey: John Wiley & Sons Inc., 2012. ISBN: 978-1-118-01292-5.
12. LLOVET, J. M., BRÚ, C., BRUIX, J. Prognosis of hepatocellular carcinoma: the BCLC staging classification. *Seminars in Liver Disease*, 1999, vol. 19, no. 3, p. 329-38.
13. TATARKOVIC, M., et al. The minimizing of fluorescence background in Raman optical activity and Raman spectra of human blood plasma. *Analytical and Bioanalytical Chemistry*, 2015, vol. 407, no. 5, p. 1335-1342.
14. NABERS, A., et al. An infrared sensor analysing label-free the secondary structure of the Abeta peptide in presence of complex fluids. *Journal of Biophotonics*, 2016, vol. 9, no. 3, p. 224-34.
15. WITHNALL, R., et al. Raman spectra of carotenoids in natural products. *Spectrochimica Acta Part A: Molecular and Biomolecular Spectroscopy*, 2003, vol. 59, no. 10, p. 2207-2212.
16. RYGULA, A., et al. Raman spectroscopy of proteins: a review. *Journal of Raman spectroscopy*, 2013, vol. 44, no. 8, p. 1061-1076.
17. HABARTOVÁ, L., et al. Chiroptical spectroscopy and metabolomics for blood-based sensing of pancreatic cancer. *Chirality*, 2018, vol. 30, no. 5, p. 581-591.

This work has been supported by Ministry of Health of the Czech Republic, grant nr. NV19-08-00525 and Specific University Research MSMT (21-SVV/2020).

The Influence of Alkaline Activator Type on the Carbonatation Process of the Alkali-activated Blast Furnace Slag

Petr Hrubý
Vlastimil Bílek, Lukáš Kalina, František Šoukal, Libor Topolář, Richard Dvořák

Brno University of Technology, Faculty of Chemistry, Institute of material science

Purkyňova 464/118, Brno-Královo Pole, 612 00
xchrubyp@fch.vut.cz

Carbonatation represents one of the potential degradation mechanisms of the construction materials. the negative impact of the carbonatation are mainly accompanied by the decrease of the pH of the pore solution under the certain value (9–10) and the formation of reaction products (various types of carbonates or bicarbonates). the progress of the carbonatation is significantly dependent on the experimental conditions like the partial pressure of CO_2 or the humidity. the various types of alkaline activators (sodium hydroxide, sodium carbonate and sodium water glass) in 6 % Na_2O dosages were used in this study for the preparation of the alkali-activated blast furnace slag samples for further carbonatation testing when exposed to various environments – exterior, interior, CO_2 chamber and water. the progress of carbonatation was evaluated with a meaning of carbonatation depth determination using the phenolphthalein technique and optical analysis method. the impact of the carbonatation on the mechanical properties was assessed by the compressive and flexural strength measure-

ments. No rapid deterioration of the mechanical properties was observed in case of the sodium hydroxide alkaline activation process. However, a noticeable changes were found for the sodium water glass activated systems especially in terms of exterior and interior storage.
Keywords: Alkali-activated blast furnace slag, carbonatation, carbonatation depth, degradation

Characterization of Bacterial Strains Obtained in Evolutionary Engineering

Vendula Chatrná
Stanislav Obruča, Ivana Nováčková

Brno University of Technology, Faculty of Chemistry,
Institute of Food Science and Biotechnology

Purkyňova 464/118, 612 00 Brno, Czech Republic
Vendula.Chatrna@vut.cz

Evolutionary engineering is a valuable tool for improving properties of microorganisms on phenotype level without a need of a deeper knowledge of genetic characteristics. the bacteria's cell generation time is 0.5 hour, compared to the humans 20 years. It is therefore advisable to study evolutionary engineering on bacteria, as in a relatively short time we can see chances in the phenotype. the application of stress factors under laboratory conditions leads to an unexpected augmentation of bacteria performance in the stressful environment. the criterion chosen in this work to evaluate the success of an adaptation to a specific stress was the amount of polyhydroxyalkanoates (PHAs) generated by wild and adapted strains, moreover, the activities of selected were analyzed to get insight into stress adaptation mechanisms.

Two bacterial strains, *Cupriavidus necator* H16 (CCM 3726) and *Halomonas halophila* (CCM 3662), were chosen for the evolutionary experiments. There strains are producers of PHAs which are biopolyesters stored in cells as energy storage materials by various microorganisms. It is a fully biodegradable and biocompatible family of polymers with interesting physicochemical properties. Copper cation (Cu^{2+}) and sodium chloride (NaCl) were chosen

as the selective pressure for *C. necator* H16; acetic acid (AA) and levulinic acid (LA) for *H. halophila*. the adapted strains were analyzed in regular intervals during long-time evolutionary experiments. A growth potential of the bacteria, together with a yield of PHAs from the biomass by the means of gas chromatography with flame ionization detector (GC-FID) and polymer physicochemical properties (molecular masses and polydispersities) by the means of size exclusion chromatography with multi-angle light scattering (SEC-MALS) were determined. the adapted strains were also exposed to selected stress factors and the amount of viable cells was evaluated by spectral flow cytometry (FC). Metabolic characterization was provided by a determination of specific enzyme activities of enzymes involved in selected cycles. Biomass and PHA production of both wild and adapted *H. halophila* strains cultivated in lignocelluloses hydrolysates were determined. the successful adaptation of adapted strain *H. halophila* to LA in the LA environment was confirmed. This strain was able to produced almost 70% more PHAs than the wild-type strain of this bacteria in the LA environment from the lignocelluloses waste. It was also concluded that *C. necator* H16 successfully adapted to Cu^{2+}.

Keywords: *Evolutionary engineering, polyhydroxyalkanoates, selective pressure, adaptation, bacteria.*

Assessment of potential heavy metal pollution of road dust in arid urban area

Petr Chrást
Jan Chalabala, Václav Pecina, Martin Brtnický, David Juřička, Jindřich Kynický, Michaela Vašinová Galiová

Brno University of Technology, Faculty of Chemistry, Institute of chemistry and technology of environmental protection

Purkyňova 464/118, Brno – Královo Pole, 61200 Brno
petr.chrast@vut.cz

In urbanized areas, heavy metal contamination represents a major issue in terms of environmental quality and health risks related to chronic exposition. Traffic routes are one of major sources of heavy metals in dust, which can be easily transported into environment through wind or rainfall. the main constituents of road dust are industrial ashes, seasonal products of chemical treatment of road surfaces and abrasive emissions from roads and vehicles. Up to 75% of road dust consists of particles smaller than 50 μm. These dust particles adsorb higher contents of heavy metals due to their high specific surface and are most readily transported into surrounding environment. Road dust samples discussed in scope of this study originate from roads in Ulaanbaatar, Mongolia as a city with high degree of air pollution originating from extensive coal burning and industry. After sampling, drying and sieving, the samples were processed into three grain size fractions (<45 μm, 45–63 μm, 63–125 μm). Aqua regia leachates of the samples were obtained using microwave digestion system and analysed using inductively coupled plasma mass spectrometry (ICP-MS) to

obtain content of As, Cd, Cr, Cu, Ni, and Pb. Initial results after analysis of the grain size fraction 45–63 μm do not indicate significant elevation in obtained heavy metal contents compared to published data on road dust in other parts of the world. Obtained contents are utilized for visualization of content profile changes between city centre and adjacent environs. the second part of this study focuses on statistics and correlation between individual heavy metals for further differentiation of heavy metal mobility between individual grain size fractions.

Keywords: *environmental chemistry, inductively coupled plasma, mass spectrometry, road dust, Mongolia, urban pollution, air pollution*

Surface Treatment of Cementitious Systems by Silicates

Valeriia Iliushchenko
Lukáš Kalina, Petr Hrubý, František Šoukal, Tomáš Opravil

Brno University of Technology, Faculty of Chemistry, Institute of Material Chemistry

Purkyňova 464/118, 612 00, Brno, Czech Republic
xciliushchenko@vutbr.cz

The efficiency of the silicate-based surface treatment agents, other words sealers, has been widely investigated over the past decades. the surface treatment utilization protects the cementitious system against the penetration of undesirable substances. Another purpose of sealers application is to reduce the risk of deterioration of cement structures that leads to increasing their durability. Nevertheless, understanding of the several aspects concerning the silicate-based sealers is not entirely clear. This study deals with the action mechanism of selected silicates such as potassium, sodium, lithium silicates and colloidal silica with the cementitious surface. Effectiveness of used sealers in terms of water absorption, hydration mechanism, same as the effect on the microstructure of the cement substrate was studied and evaluated with the contribution of following techniques – rheometry, mercury porosimetry, isothermal calorimetry, Xray diffractometry and scanning electron microscopy. Silicatebased treatment agents were assessed on two sets of specimens; fresh cement pastes (at the age of 1 hour) and on the hydrated ones (24 hrs.), respectively.

As result, certain effectiveness of the used sealers was verified. Film-forming sealers have shown higher effectiveness in

case of their usage on the hydrated cementitious surfaces (24 hrs.). Thus, the dependence of sealers efficiency on the substrate hydration progress was confirmed.

Keywords: *Concrete sealers, treatment agents, calcium silicate hydrate, microstructure*

Study of the influence of water coefficient on porosity and mechanical properties of high-performance concrete

Martin Janča, Pavel Šiler, Martin Alexa*
BRNO UNIVERSITY OF TECHNOLOGY FACULTY OF CHEMISTRY
Purkyňova 464/118, 612 00 Brno, Czech Republic
xcjancam@fch.vut.cz

1 Introduction

1.1. High-performance concrete

Advances in knowledge and understanding of concrete at the microstructure level have led to the creation of another new generation of high-quality concrete[1]. These types represent only a small part of the total world production, but they are still very important materials. High-performance concrete in a given region is always limited by economic conditions in order to be able to compete with conventional concrete. High-quality concretes include materials with excellent compressive strength, excellent durability or environmental resistance[2].

The art of technologists is thus to find the best mixture of raw materials to achieve the lowest water-cement ratio, which has a large influence on the properties of concrete. It is necessary to maintain a water coefficient so that high-quality concrete can be laid, compacted and transported as easily as conventional concrete[3].

1.2. Microstructure of concrete

For improvement of concrete microstructure it is important to manage many of its parameters (homogeneity enhancement, porosity reduction, excellent hydration). To achieve these properties, it is necessary to secure high binder content, low water-binder ratio, high dosage of superplasticizers, excellent mix design and proper curing[4].

Adding fine mineral admixtures like silica fume, metakaolin, fly ash etc., can enhance the physical properties of high-performance concrete. Benefit of these fine mineral admixtures is in the partical shape and composition. Spherical shaped admixtures enhance the rheological properties which positively influence treatment of concrete. And the finess of the particles plays a role in the filler effect. This effect helps to fill the space in concrete and improve its durability[5]. In addition fine mineral admixtures may contain some form of amorphous silica, which reacts and forms secondary calcium-silica-hydrates (C-S-H gel) in the presence of water and calcium hydroxide, similarly to products which are formed during hydration of Portland cement. This pozzolanic reaction has positive impact on the porosity of concrete and consumption of portlandit[6].

1.3. Water-to-cement ratio vs. porosity

Porosity is crucial for the mechanical properties of concrete. There is quite key relationship between water-cement ratio and porosity of concrete. Piasta[7] pointed out that

shrinkage and the water absorption of hardened paste were decreased with low w/c ratio. During hydration of clinker phases a chemical contraction occurs (approximately 8 to 10 %) than the sum of the volumes of water and cement. It leads to the formation of micro-cracks that weaken concrete[8]. A very important step during the preparation of concrete is mixing of fresh concrete. It is necessary to avoid any inhomogeneity but also to reduce capture of air during mixing[9]. Captured air can be considered as a microstructural inhomogeneity. Superplasticizers are not only necessary for reduce water-cement ratio but also for dispersion of cement particles in fresh concrete[10].

2 Experimental

1.4. Materials and methods

Silica fume RW-Füller Q1 from company AMG Silicon was used. It contains mostly amorphous silica (SiO2) and the amount of crystalline quartz is under 0.5 % according to the product list. Portland white cement Aalborg White was used. This cement is characteristic for its white colour, low content of alkali, high sulphate resistance and low chromate content. Particle size distribution of silica fume and Aalborg cement measured by laser diffraction analyzer (HELOS KR Sympatec) are shown in Figure 1 and Figure 2. Normalized washed silica sands of fraction PG I, PG II and PG III were used. These sands meet the requirements of the standardized method ČSN EN 196–1. Water cement ratios varying from 0.22 to 0.30 were used for the preparation of testing samples with dimensions 40 × 40 × 160 mm. Mixing was carried out according to the valid standard 196–1. Prior mixing Superplasticizer MasterGlenium ACE 446 was mixed with water and then added to the mixture. Afterwards mixing followed the requirements of standardized method ČSN EN 196–1.

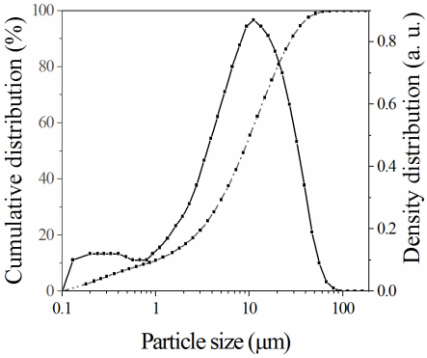

Figure 1. The particle size of Aalborg cement

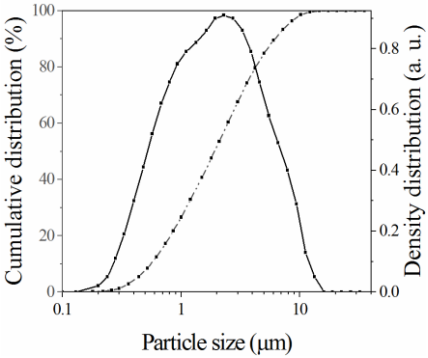

Figure 2. The particle size white silica fume

Table 1. Particle size distribution

Sample (μm)	D50 (μm)	D90 (μm)	D99 (μm)	Modus (μm)
Aalborg cement	8.76	28.40	51.56	11.16
Silica fume	1.92	6.21	10.88	2.29

Particle size measurement in Table 1 shows that modus of silica fume is five times smaller than Aalborg cement. This is very important for filler effect behavior. Top cuts (D99) are 51.56 μm for Aalborg cement beside 10.88 μm for silica fume.

Table 2. Sample compositions

Sample	0.3	0.28	0.26	0.24	0.22
Aalborg cement [g]	1200	1200	1200	1200	1200
Silica fume [g]	400	400	400	400	400
PG I [g]	2310	2310	2310	2310	2310
PG II [g]	643	643	643	643	643
PG III [g]	1667	1667	1667	1667	1667
H_2O [g]	360	336	312	288	264
w/c	0.3	0.28	0.26	0.24	0.22
Plasticizer [g]	48	48	48	48	48

Compositions of prepared mixtures are shown in Table 2. Those marked with small letter w were stored in water. Processability of the mixture was tested. Hägermann-flow table for the flow test of mortar was used. Firstly filled slump cone was removed and spread of the mortar was measured. Then second measurement was applied after fifteen strokes. Spread values are shown in Figure 3.

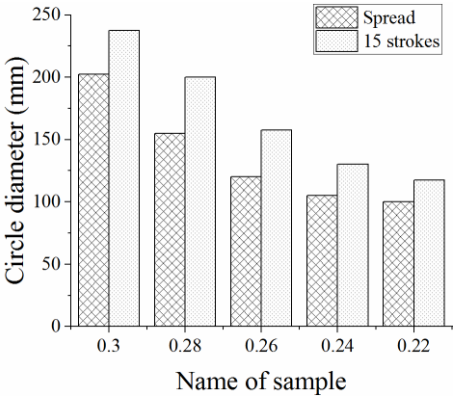

Figure 3. Hägermann-flow table test

Special specimen with the same dimensions as the samples for mechanical properties was prepared for the porosity evaluation. This specimen was cut up to at least 10 pieces. Pores in revealed pores in inner volume of sample were filled and coloured by white Aalborg Portland cement and the photographed. Photographs were subjected to image analysis.

1.5. Results and discussion

Mechanical properties were tested on three 40 × 40 × 160 mm testing specimens for every sample and after defined days of storage. Flexural and compressive strength were tested after 1, 7 and 28 days. Data were acquired by DESTTEST, BETONSYSTEM. Mixtures marked with small letter a were stored in the air. Both types were stored under the same temperature 25 °C.

Average values of flexural strength are shown in Figure 4 and Figure 5. Testing specimens stored in the water showed higher values of flexural strength than those stored on air. Sample 0.26w shows decrease of flexural strength after 7 and 28 days, whereas sample 0.26a follows the trend of increasing strength against decreasing water cement ratio. Similar connection between porosity and w/c ratios presented Benouis in his work[11].

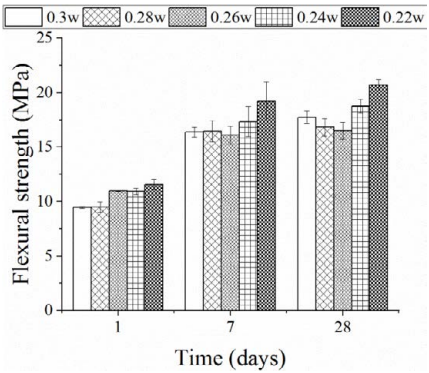

Figure 4. Flexural strength water storing

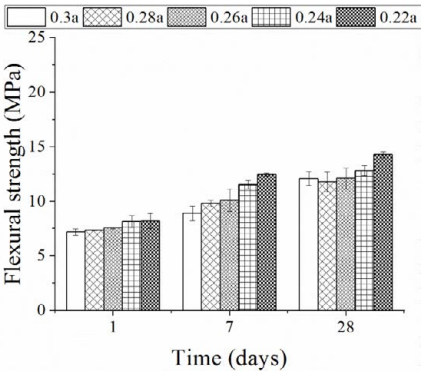

Figure 5. Flexural strength air storing

Average compressive strength values are shown in Figure 6 and Figure 7. Testing specimens stored on air follow the trend of increasing compressive strength with decreasing w/c ratio. On the other hand, sample 0.3w and 0.28w show highest values of strength after 28 days of storage. As we can see, there must be another factor which plays key role in resulting flexural and compressive strength than w/c ratio. These results have led us to assess the porosity of the material, which can play a key role in the resulting strengths.

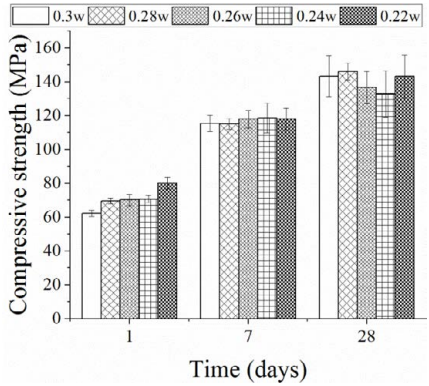

Figure 6. Compressive strength water storing

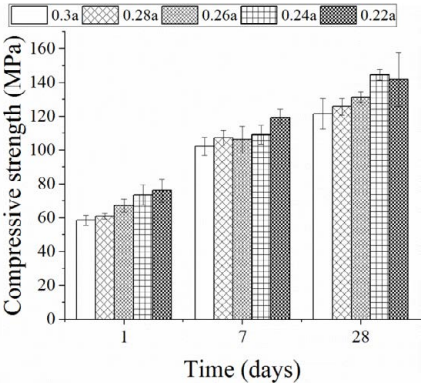

Figure 7. Compressive strength air storing

For clarification of decreasing the compressive and flexural strength in the samples the porosity for each sample was determined. Average values of porosity calculated as percent of inner surface are shown in Figure 8. Figure 9 – Figure 11 show the procedure of analysis.

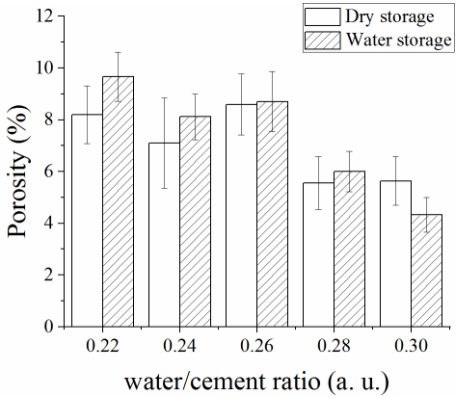

Figure 8. Porosity values

Porosity values show that porosity is decreasing with higher w/c ratios which correspondence to workability test by flow table test. Li in his work presents similar results although different w/c ratios in this paper were used[12].

When comparing mechanical properties with porosity results we can say that lowest porosity exceed in mixtures with highest w/c ratios. On the other hand, water in mixtures with high w/c ratio weakens the cement matrix. Sample 0.26w shows lowest flexural and compressive strength. Two important factors must be underlined, that sample 0.26w has w/c ratio low enough to lost benefit of the workability contribution and still high enough to get positive contribution of low w/c ratio which can be seen for example in Nematollahzade work[3].

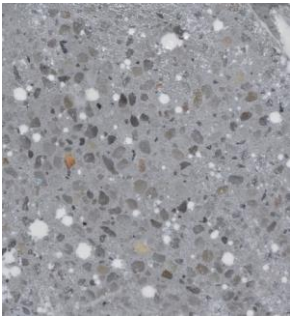

Figure 9. Sample 0.3w photo

Figure 10. Sample 0.3w 8 bit

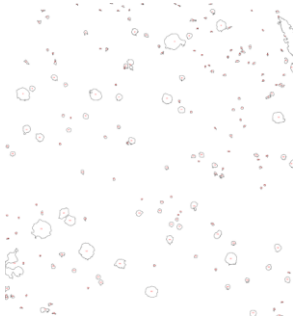

Figure 11. Sample 0.3w result

Another suitable approach that could ensure an improvement of mechanical properties, the vacuum mixing. For comparison, a blend with a w/c ratio of 0.26 between conventional and vacuum mixing was selected.

By using vacuum mixing, higher compressive and flexural strengths were achieved. Vacuum stirring was carried out for 5 minutes at − 90 kPa vacuum. Compressive strength increased by approximately 20 % (Figure 13). Sample of vacuum mixing also undergo

photo analysis for porosity determination. Values of porosity are shown in Figure 12 and correspond to better mechanical properties. Decreasing of porosity is approximately around 80 %.

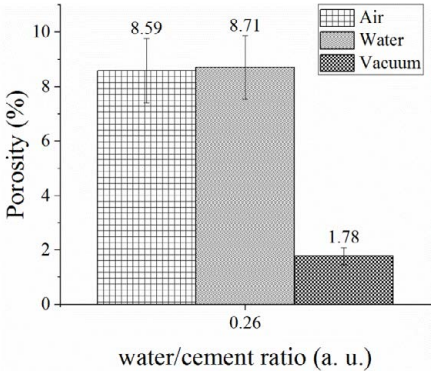

Figure 12. Porosity values of samples 0.26

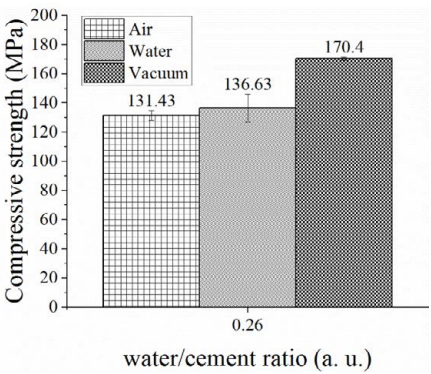

Figure 13. Compressive strength of samples 0.26

4 Conclusion

Values of the porosity results showed that porosity is increasing with decrease of w/c ratio under the value 0.26. Similarly as other researchers the results suggested that compressive strength is higher for lower w/c ratio[13]. On the other hand workability deteriorates as the w/c ratio decreases. Water stored samples exhibit very similar compressive strength within the deviation range. Air stored samples showed a trend with increasing compressive strength along with decreasing the w/c ratio. However, this trend is highly questionable given the magnitude of the deviations. To compare the effect of porosity on concrete, a mixture with a w/c ratio of 0.26 was prepared by vacuum mixing. These result showed that vacuum mixing decrease the porosity of sample while improving mechanical properties.

5 References

1. Derousseau M A, Kasprzyk J R and Srubar W V 2018 Computational design optimization of concrete mixtures: A review. *Cement and Concrete Research* **109** 42-53.
2. Aïtcin P C 2005 Vysokohodnotný beton (Praha: Pro Českou komoru autorizovaných inženýrů a techniků činných ve výstavbě).
3. Nematollahzade M, Tajadini A, Afshoon I and Aslani F 2020 Influence of different curing conditions and water to cement ratio on properties of self-compacting concretes. *Construction and Building Materials* **237**.
4. Mishra O and Singh S P 2019 An overview of microstructural and material properties of ultra-high-performance concrete. *Journal of Sustainable Cement-Based Materials* **8**(2), 97-143.

5. Noaman A, Karim R and Islam N 2019 Comparative study of pozzolanic and filler effect of rice husk ash on the mechanical properties and microstructure of brick aggregate concrete. *Heliyon* **5**(6).
6. Sohail M G, Wang B, Jain A, Kahraman R, Ozerkan N G, Gencturk B, Dawood M and Belarbi A 2018 Advancements in Concrete Mix Designs: High-Performance and Ultrahigh-Performance Concretes from 1970 to 2016. *Journal of Materials in Civil Engineering* **30**(3).
7. Piasta W, Zarzycki B, Afshoon I and Aslani F 2017 The effect of cement paste volume and w/c ratio on shrinkage strain, water absorption and compressive strength of high performance concrete *Construction and Building Materials* **140**, 395-402.
8. Ramezanianpour A M and Hooton R D 2014 A study on hydration, compressive strength, and porosity of Portland-limestone cement mixes containing SCMs. *Cement and Concrete Composites* **51**, 1-13.
9. Zdeb T 2019 Effect of vacuum mixing and curing conditions on mechanical properties and porosity of reactive powder concretes. *Construction and Building Materials*, **209**, 326-339.
10. Sathyan D and Anand K B 2019 Influence of superplasticizer family on the durability characteristics of fly ash incorporated cement concrete. *Construction and Building Materials*, **204**, 864-874.
11. Benouis A, and Grini A 2011 Estimation of Concrete's Porosity by Ultrasounds. *Physics Procedia*, **21**, 53-58.
12. Li L, Zhang H, Guo X, Zhou X, Lu L, Chen M and Cheng X 2019 Pore structure evolution and strength development of hardened cement paste with super low water-to-cement ratios. *Construction and Building Materials*, **227**.
13. Gowri T V, Sravana P and Rao P S 2016 On the Relationship between Compressive Strength and Water Binder Ratio of High Volumes of Slag Concrete. *Int. J. Appl. Eng. Res,* **11**, 1436-1442.

Acknowledgement (This outcome has been achieved with the financial support by the project: GA19-16646S "The elimination of the negative impact of zinc in Portland cement by accelerating concrete admixtures", with financial support from the Czech science foundation.

This work was supported by the project of specific research: FCH-S-20-6340 with the financial support of Brno University of Technology.

This work was supported by the project of specific research: FAST/FCH-J-20-6393 with the financial support of Brno University of Technology.).

Microwave-Assisted Preparation of Organo-Lead Halide Perovskite structures for electronics

Jan Jancik, Anna Jancik Prochazkova, Markus Clark Scharber, Alexander Kovalenko, Jiří Másilko, Niyazi Serdar Sariciftci, Martin Weiter, and Jozef Krajcovic

Brno University of technology

Purkyňova 464/118, 612 00 Brno, Czech Republic
xcjancik@fch.vut.cz

Organo-lead halide perovskites are promising materials for the development of solar cells, solid-state lasers, light emitting diodes (LEDs), photodetectors, etc. Perovskites can easily be deposited from their precursor solutions into a thin film by solution-based processes [1]. Nevertheless, the prepared films possess defects which cause non-radiative recombination, current-voltage hysteresis and rapid degradation due to the low stability of the resulting devices [1].The efficiency of the functional devices descends dramatically when amorphous materials are implemented instead of highly crystalline ones. Therefore, it is challenging to optimize and up-scale the production of large-sized single crystals of perovskite materials. Here, we describe a novel and original approach to MAPbBr3, FAPbBr3, MAPbI2 and FAPbI2 lead halide perovskite single crystals preparation which consists in applying microwave radiation during the crystallization [1]. the facile microwave assisted method of preparation is highly reproducible, fully automated and in addition, it can be applied for various different perovskite

structures. Simultaneously, this eco-friendly method is expected to be easily up-scalable because of its versatility and low energy consumption. We believe that this method will make preparation of single crystals, nanosystems, 2D systems and the final functional devices fabrication (like solar cells, LEDs, photodetectors, i. e.) more convenient and efficient.

The work was supported by the FCH-S-20-6340

[1] Jan Jancik, Anna Jancik Prochazkova, Markus Clark Scharber, Alexander Kovalenko, Jiří Másilko, Niyazi Serdar Sariciftci, Martin Weiter, and Jozef Krajcovic, Crystal Growth & Design 2020 20 (3), 1388 – 1393, DOI: 10.1021/acs.cgd.9b01670

Keywords: *microwave, organo-lead halide perovskite, single crystal*

Relaxation Behaviour of Hydrogel Materials Using Classical Rheology Methods

Martin Kadlec
Jiří Smilek, Miloslav Pekař

Brno University of Technology, Faculty of Chemistry, Institute of Physical and Applied Chemistry

Purkyňova 464/118, 612 00 Brno, Czech Republic
Martin.Kadlec@vut.cz

Proposed paper investigates relaxation behaviour of hydrogel materials using classical rheology methods as a part of the complex rheological characterization of these systems. Specifically, creep and recovery tests as well as three interval thixotropy tests were studied in this paper.

Extensive optimization of these tests was carried out in order to find ideal measurement settings, which for creep tests consist in proper values of applied stress, temperature and duration of loading and relaxation step. the essential variables for three interval thixotropy tests are frequency of oscillation, temperature and applied strain as well as duration for each step. the optimization procedure was performed using 1 wt. % physically crosslinked agarose hydrogel and the tuned tests were applied besides other different concentrations of agarose hydrogel also to hyaluronic acid based hydrogels formed due to interactions between negatively charged polyelectrolyte groups with positively charged surfactants and to polyvinyl alcohol gels chemically crosslinked via borax. These samples were selected to cover a variety of hydro-

gels with mutually different crosslinking principle.
Both experiments confirmed, the agarose gel proved to have the best ability to recover after deformation of all studied samples. Moreover, increasing agarose concentration and decrease in duration of deformation step led to better sample regeneration. on the other hand, the hyaluronic acid based hydrogel reported the worst relaxation properties. Although these results were comparable from both experiments, the percentage structural regeneration from each test was different. Hence, the complex relaxation characteristics cannot be defined using one of the mentioned tests alone and both the creep and the three interval thixotropy tests are highly beneficial in case of study of hydrogel materials' relaxation behaviour.
Obtained results from this paper may lead to more precise description of deformation and relaxation characteristics, which are frequently occurring during treatment as well as application of hydrogel materials.

Keywords: *Rheology, creep tests, three interval thixotropy tests, hydrogels*

Simple multi-analyte LC-MS method for the determination of food additives in soft drinks and alcoholic beverages

Ing. Aliaksandra Kharoshka
Ing. Aleš Krmela, Ph.D., Dr. Ing. Věra Schulzová

University of Chemistry and Technology Prague, Faculty of Food and Biochemical Technology, Department of Food Analysis and Nutrition

Technická 3, 166 28, Prague
kharosha@vscht.cz

Usage of food additives in the food industry is a common manufacturing practice. Due to potential negative biological effects in some population groups suffering from specific health disorders, toxicological evaluations are done for each substance to be used as a food additive. To ensure the safety of the consumer, every additive has its own maximum level limits for various commodities. for the confirmation of the compliance with these limits, reliable and fast analytical methods are being developed. for this purpose, a rapid LC-MS method was developed for the simultaneous determination of different classes of synthetic food additives. the method is capable of nine food colourants, seven sweeteners, two preservatives, and two purine alkaloids determination. Ultra-high performance liquid chromatography with the reverse phase column separation was coupled to mass spectrometry with a single quadrupole mass analyzer. the developed method was applied to the analysis of 76 beverages, including 14 soft drinks, 19 energy drinks, 23 liquors, 14 spirits, and 6 ciders. In addition,

the concentrations quantified conformed to the limits prescribed by the EU (Regulation [EC] No. 1333/2008). the designed method is fast and allows parallel determination of substances with different physico-chemical parameters.

Keywords: *food additives, liquid chromatography, mass spectrometry, beverages*

Preparation of metakaolin with high whiteness

Jan Kotrla
Jiří Bojanovský, Tomáš Opravil, Petr Hrubý

Brno Univerzity of Technology, Faculty of Chemistry,
Institute of Materials Chemistry

Purkyňova 118, 612 00 Brno, Czech Republic
xckotrla@fch.vut.cz

The term kaolin is used to describe white clays whose main mineral is kaolinite Al2Si2O5(OH)4. Kaolinite is formed by the decomposition of various of feldspars and therefore is usually doped with other minerals (quartz, sulphur, feldspars, micas and iron and titanium oxides). the quality of the clays and over all kaolin is measured in function of iron content, because this element gives the red-brown colour to this type of minerals.

This paper summarizes the various possibilities of kaolin bleaching by firing. Kaolin of 20 grams dosage was fired at 1 100 °C for 2 hours. Several types of reducing agents (spar, specially ground quartz (SGQ), alumina and a mixture of graphite and sodium chloride) were used during firing with a goal to reduce the present iron 3+ to less colouring state of Fe2+ thus increase the whiteness of kaolin. It was found that the best effect on increasing the whiteness of kaolin has the firing of the raw material itself. Reducing agents were added in weight rations of 1, 3 and 5 % and have been able to partially increase the whiteness in some cases, but this is an increase of units of percent.

Subsequently, the reduction mixture was selected and used for firing in a sintering furnace. the whiteness of kaolin obtained in sin-

tering furnace was not sufficient. the low efficiency of the sintering furnace was mainly due to unsuitable furnace setting.

Keywords: *bleaching clay, kaolin, sintering furnace, reducing agent*

Thermophilic Bacterium *Schlegelella thermodepolymerans* DSM 15344 as a Producer of Polyhydroxyalkanoates

Xenie Kouřilová, Jana Musilová, Karel Sedlář, Kristína Bednárová
Iva Pernicová, Stanislav Obruča

Brno University of Technology, Faculty of Chemistry, Institute of Food Science and Biotechnology

Purkyňova 464/118, Brno 612 00, Czech Republic
xckourilovax@fch.vut.cz

Thermophilic microorganisms grow and thrive even at temperatures that are inhibitory or even lethal to most microorganisms. for a long time, thermophiles have been considered a unique source of thermostable substances, especially enzymes. However, in the last few years, thermophilic microorganisms have also been considered as production cultures for other substances, e.g. polyhydroxyalkanoates. Higher culture temperatures make it possible to achieve a higher reaction rate, a higher solubility of most chemicals or a reduction in the sterility requirements of the process.

Polyhydroxyalkanoates (PHAs) are biodegradable and biocompatible polyesters that are produced and accumulated by bacteria as intracellular granules. These biopolymers have similar properties to some synthetic plastics but are not harmful to the environment. for that reason, they could be a suitable alternative. Unfortunately, their production cost is still high. Therefore, approaches are being sought to produce PHAs cheaper. One of the possibilities is

the use of the aforementioned thermophilic microorganisms.
One of the representatives of thermophilic microorganisms is the gram-negative bacterium *Schlegelella thermodepolymerans* DSM 15344. This strain was isolated from activated sludge and is unique in its ability to degrade a copolymer containing 3-hydroxybutyrate and 3-mercaptopropionate. the process of PHA degradation was described. Therefore, we began to investigate its biotechnological potential. Our bioinformatic analysis of available draft genomes revealed, that *S. thermodepolymerans* possess *phbCAB* operon and, therefore, might be a producer of PHAs. Production conditions were tested at various temperatures, carbon substrates and precursors suitable for the synthesis of polymers with modified properties. *S. thermodepolymerans* is able to utilize xylose very well, surprisningly, it even prefers xylose over other saccharides and harbors unique operon containing genes encoding for enzymes involved in xylose metabolism. Since xylose is present in numerous lignocellulosic materials, we cultured the bacterium also on model hydrolysates and we also evaluated its sensitivity to microbial inhibitors present in lignocellulose hydrolysates. According to our results, *S. thermodepolymerans* appears to be a very promising producer of PHAs.

Funding: This study was supported by Brno University of Technology intra-university junior project FCH/FEKT-J-20-6399.

Keywords: *Schlegelella thermodepolymerans, thermophiles, polyhydroxyalkanoates, biopolymers*

Development of a method for simultaneous determination of various esters of MCPD and glycidol in palm fat by supercritical fluid chromatography

Tomáš Kouřimský
Vojtěch Hrbek, Klára Navrátilová, Jana Hajšlová

University of Chemistry and Technology,
Prague Faculty of Food and Biochemical Technology,
Department of Food Analysis and Nutrition

Technická 5 166 28 Prague 6, Czech Republic
kourimst@vscht.cz

Fatty acid esters of 2- and 3- monochloropropanediol (2- and 3-MCPD) together with glycidyl fatty acids esters belong to a group of process-induced chemical contaminants, formed in high temperature environments mainly during industrial food processing. They most commonly occur in refined vegetable oils, especially in palm fat. Most potent precursors of MCPD esters are partial esters of glycerol, such as diacylglycerols (DAG). the other major variable is a chlorine source; which was mainly considered to be naturally present inorganic chlorine. However, recent studies, including that by Nestlé Research Centre, indicate the possibility of certain lipophilic organochlorine substances to participate in MCPDs formation.

With regards to the documented toxicity of free MCPD and glycidol, which are effectively released by enzymatic hydrolysis in gastrointestinal tract, and considering the occurrence of these

contaminants in food supply, the Directorate-General for Health and Food Safety (DG SANTE) proposed in 2019 maximum limits for several food commodities. Hence, the requirements for adequate analytical methods and better elucidation of their formation pathways are constantly increasing.

The aim of this study was to develop and optimise a method enabling a rapid, simultaneous determination of various intact esters of MCPD and glycidol in palm fat, with the use of supercritical fluid chromatography coupled with mass spectrometry (SFC-MS) and the possibility to use ion mobility (IM) to separate 2- and 3-isomers of MCPD esters was tested too. Contrary to a routine GC-MS method which determines total MCPD esters after hydrolysis, this way, the pattern of individual species can be characterized.

The SFC-MS method effectively separates and detects 9 esters of MCPD and 7 esters of glycidol in concentration range between 0,1 and 12,5 mg/kg. However, additional modifications are required to meet the recovery and repeatability at 125 µg/kg required by legislation. Separation of the 2- and 3-MCPD isomers by IM has not yet been achieved under the conditions tested so far. As a part of this presentation, critical comparison of SFC-MS and reversed phase LC-MS, the alternative analytical strategy, will be provided.

Keywords: *palm fat, 3-MCPD esters, glycidyl esters, SFC-MS, ion mobility*

Tuning Solid State Polymorph Emission of Sterically Hindered Push-Pull Substituted Stilbenes

Matouš Kratochvíl
Karel Pauk, Stanislav Luňák Jr., Aneta Marková, Aleš Imramovský, Martin Vala, Martin Weiter

Brno University of Technology, Faculty of Chemistry, Materials Research Centre

Purkyňova 118, 612 00 Brno, Czech Republic
Matous.Kratochvil@vut.cz

Organic luminophors exhibiting far red or near infrared (FR/NIR 650–900 nm) emission are highly interesting in the fields of bio-imaging and organic light emitting diodes (OLEDs) fabrication. the low photoluminescence quantum yields (PLQY) of these low band-gap compounds makes useful emitters scarce. A molecule of structure DPA-DPS-DCV (DPA = diphenylamino, DPS = 2,5-diphenyl-stylbene, DCV = dicyanovinylene) is presented. the shifts of absorption and fluorescence maxima in solvents of varying polarity is bathochromic, as is expected in DPA-stilbene-EWG based molecules (EWG = electron withdrawing group). the molecule forms various crystal polymorphs of emission differing in both wavelength and PLQY. First shows moderate monomer-like red emission (5 %, 672 nm), while the second one exhibits more intense and red-shifted (32 %, 733 nm) emission ascribed to the excimer fluorescence. Investigation into tuning these polymorphs brought about a third polymorph with hypsochormic shift

(610 nm). the possibility of transition between these polymorphs is studied.

Keywords: *Solid state emission, infrared emission, crystal polymorphs, emission tuning*

Monitoring of Pharmaceuticals in Scottish Rivers Using Passive Sampling Devices

Pavlína Landová
Ludmila Mravcová, Lydia Niemi, Stuart Gibb

Brno University of Technology, Faculty of Chemistry,
Institute of Chemistry and Technology
of Environmental Protection

Purkyňova 464/118, Brno 612 00, Czech Republic
xclandova@fch.vut.cz

Constantly increasing consumption of pharmaceuticals along with the low capacity of wastewater treatment plants for the effective elimination of these compounds from water is inevitably leading to the emissions of pharmaceuticals into the environment. the presence of such compounds in waters can have various adverse effects on non-target organisms.

Grab sampling technique is usually used for the evaluation of pharmaceutical presence in the water. Although this technique is the easiest and simplest to do it comes with a few shortcomings. It brings only information about pharmaceuticals concentrations at the time of sampling. If the grab sampling frequency is not sufficient it is hard to make any assumptions about the average concentrations of pharmaceuticals in the given area. Average concentrations can be under- or over-estimated by grab sampling. the alternative to the grab sampling is to use passive sampling devices that are placed into the sampled medium (e. g. river) for the extended period of time in which they are continuously sampling.

In our work, we used the combination of passive sampling along with grab sampling technique to evaluate the pharmaceutical contamination of two Scottish rivers, river Dee, and river Thurso. Selected target compounds were: ibuprofen, diclofenac, trimethoprim, clarithromycin, fluoxetine, carbamazepine, paracetamol, and 17α-ethynylestradiol. for passive sampling, POCIS (polar organic chemical integrative sampler) was constructed and calibrated in the laboratory before the field deployment. Grab water samples were processed by the solid-phase extraction and analyzed along with the extracted samples from POCIS by the LC-MS/MS technique. Both sampling techniques proved the presence of pharmaceuticals in river Thurso and Dee. Concentrations were in the units of ng/L with ibuprofen and diclofenac be the most abundant compounds. the overall frequency of the detection of pharmaceuticals was higher when using POCIS.
This work was financially supported by the project FCH-S-20-6446.

Keywords: *POCIS, pharmaceuticals*

Numerical Simulation of Heterogenous Catalytic Reactions

Martin Mačák
Petr Vyroubal, Jiří Maxa

Brno University of Technology, Department of Electrical and Electronic Technology

Technická 3058/10, 616 00 Brno, Czech Republic
xmacak00@vutbr.cz

The catalytic hydrogenation of liquid nitrobenzene is one of the most important chemical processes in the synthesis of aniline, which is a very important compound in the plastics industry. This process, usually occurring in slurry or gas lift reactors, can be generally described as a gas-liquid-solid system, in which a liquid phase acts as a continuous phase, in which reacting gas and catalyst particles are dispersed. Even though this technology is established, the process is usually only studied experimentally, which makes it difficult to study internal phenomena in the reactor. the use of numerical simulations in this area is not very widespread and usually, the simulations only focus on the reaction kinetics and the effects of hydrodynamics are often neglected.

In this work a custom 3D numerical model describing a multiphase reacting flow, which coupled the continuum flow with the Lagrangian discrete particle method, was implemented into Ansys Fluent software. the model was used to investigate the catalytic hydrogenation of liquid nitrobenzene in an injection site of a gas lift reactor. As the complete reaction mechanism is very complicated, a simplified version was used. In the first step, nitrobenzene reacts with hydrogen gas, which produces aniline and water. Then, ani-

line can react with hydrogen to produce cyclohexylamine, which is a side product. To obtain a good quality of the product, it is necessary to maintain the temperature of the mixture in a defined range as for higher temperatures, the side reaction will overtake the main reaction. the results obtained from simulations can help with identifying the effects of the flow on the particle catalysts distribution, heat transport and in result, on the overall reaction mechanism. the presented model can be used to improve the design of existing reactors and increase the production and the quality of the product.

Keywords: *multiphase flow, particle tracking, heterogenous catalysis, Ansys Fluent*

Wet Pre-treatment Methods in Macroelements Recovery from Fly Ash Combined with Acid Leaching

Michal Marko
Tomáš Opravil, František Šoukal, Jaromír Pořízka

Brno University of Technology,
Faculty of Chemistry, Institute of Materials Chemistry

Purkyňova 118, 612 00 Brno, Czech Republic
xcmarkom@fch.vut.cz

Fly ash (FA), as a mass-produced secondary material (coal combustion product) since the middle of the last century, reached up to 30–40 % to be recycled and reused. One of the most auspicious applications of FA in the following decades possibly appears to be a raw material base – the source of macro- and microelements.
This paper summarizes wet types of FA pre-treating techniques to obtain the maximum leachability of macro- elements, such as Al, Fe and Ti in the process of acid leaching. FA pre-treatment or chemical activation is the single key to increase the efficiency of separated elements.
In this research, the wet experiment was based on FA pre-leaching in hydrochloric acid solution (1–5 wt. %). Both high-temperature (HTFA) and fluidized-bed fly and bottom ash (FFA. FBA) were the aims of the study. In the case of FBA and FFA, this reaction led to lower the total alkaline content, esp. reactive calcium oxide, as a result of flue gas desulphurization. the lower free lime content brings a positive effect, while the leachability of Al and Fe increased 2–4 times. Secondary, the grain surface after deposition

in HCl solution changed by the meaning of the creation of new pores, as observed via SEM. Based on experimental data, taking into account the economic ratio and the increase in performance, the use of dilute (1 wt. %) HCl in a molar excess of 30 % to free CaO with a deposition time of 10–30 min at room temperature and constant stirring appears to be the most suitable conditions. on the other hand, in the case of HTFA samples which contain only a small amount of total alkaline content, it is much more advantageous to use more concentrated solutions so that the glass-covered surface of the particles is disturbed and the extraction medium can penetrate the resulting defects and dissolve selected elements.

To conclude, it can be evaluated that the extraction efficiency in the case of FFA and FBA increased 2–4 times, thus achieving a total leachability of up to 85 % of iron and more than 50 % of aluminum in a single-phase extraction into sulfuric acid at room temperature. In the two-stage extraction, the leachability reached up to 95 % Fe and 92 % Al.

Keywords: *fly ash, fly ash utilization, macroelements recovery, acid leaching*

OECT as a Device for Material Characterization: The Role of Parasitic Series Resistance

Aneta Marková, Stanislav Stříteský, Martin Weiter, Martin Vala

Brno University of Technology, Faculty of Chemistry, Institute of Physical and Applied Chemistry
Purkyňova 464/118, 612 00 Brno, CZ
xcmarkovaa@fch.vut.cz

1 Introduction

With regard to new applications in a field of bioelectronics, there is a growing interest in new materials. These materials are then mostly based on newly synthesized organic molecules. In the field of bioelectronics, attention is focused on organic semiconductor polymers. Their basic properties allow their use in organic thin-film transistors (OTFT). One of these OTFT transistors is an organic electrochemical transistor[1].

OECT is a three electrodes device composed of the source, drain and gate electrode. The gate electrode is immersed in an electrolyte. The electrolyte is then in direct contact with the active channel. The active channel is in tight contact between the source and the drain electrode[2]. The OECT requires that the material, that forms the active channel, have the ability to efficiently transport both electronic and ionic charges as the device relies on ionic-electronic volumetric interaction (on the ion-to-electron transduction capability)[3].

Usually, the material for OECT is based on the organic semiconducting polymer, which is doped by insulating counter ion. In OECT, the material undergoes electrochemical redox reactions, where the ions from the electrolyte migrate in or out of the bulk of organic semiconductors to compensate the electronic charges on counter ions. The electronic charges on semiconducting polymer are then injected or extracted by a source or drain electrodes. One of the most studied stable biocompatible organic semiconductor is a *p*-type conjugated polymer poly(3,4-ethylene dioxythiophene) doped with poly(styrene sulfonate) (PEDOT:PSS)[4].

As the OECT is based on the transduction of small-applied voltage on the gate electrode into large changes in the drain current, the transfer curve is measured. These curves describe the changes in output current. One of the characteristic parameters of OECT is a transconductance, g_m. Transconductance is define as the first derivative of the transfer curve and describes the efficiency of transduction. Bernard et al. developed model which describes the transconductance as a function of device geometry, material parameters (charge-carrier mobility, μ, and volumetric capacitance, C^*), and applied voltage. The transconductance is described with respect to geometry by equation 1, where V_T is the threshold voltage, and V_G is a voltage applied to gate electrode. W is a width of active channel, L defines the channel length, it is a distance between source and drain

electrode, and *d* defines the channel thickness, it is a thickness of the organic semiconductor film[2].

$$g_{\mathrm{m}} = \frac{W}{L} d\mu C^{*} \left(V_{\mathrm{Th}} - V_{\mathrm{G}} \right) \tag{1.}$$

Already in 2017 Inal et al. based on this equation showed a way to characterize and compare conductive polymer materials. They used product of μC^{*} as a material-system figure of merit to benchmark ten previously published organic mixed conductor material[5]. However, this seems to apply only to long-channel OECT, or to less conductive materials with low volumetric capacitance. In a case of highly conductive channel, Kaphle et al. showed that contact resistance plays a significant role, and Bernard's model of OECT should be extended for contact resistance[6]. In 2018, Donahue et al. used the correction of the measured transconductance values with respect to the series resistance to calculate the transconductance of the vertical OECT, and expressed this transconductance as intrinsic transconductance[7]. To calculate this value, she used the model for the organic field-effect transistor (OFET) system derived by Antoniadis and Chou in 1987, which is described by equation 2.

$$g_{\mathrm{mi}} = \frac{g_{\mathrm{m}}^{0}}{1 - R_{\mathrm{SD}} g_{\mathrm{d}} \left(1 + R_{\mathrm{S}} g_{\mathrm{m}}^{0} \right)} \tag{2.}$$

where g_{d} is the drain conductance ($g_{\mathrm{d}} = \partial I_{\mathrm{D}} / \partial V_{\mathrm{D}}$), and g_{m}^{0} is

$$g_{\mathrm{m}}^{0} = \frac{g_{\mathrm{m}}}{1 - R_{\mathrm{S}} g_{\mathrm{m}}} \tag{3.}$$

with g_{m} representing the measured transconductance ($g_{\mathrm{m}} = \partial I_{\mathrm{D}} / \partial V_{\mathrm{G}}$), R_{SD} represents the parasitic source-drain resistance independent of the voltage bias, and R_{S} is the parasitic series resistance at the source side[8].

The aim of this work was to prepare OECT with different *Wd*/*L* and study the effect of electrodes conductivity on the resulting transconductance. Change of *Wd*/*L* leads to different conductivity of channel. As the equation 2 describes mainly the OFET system, its used in OECT needs to be more verify. The effect of parasitic series resistance limits the effect of applied voltage on the channel and then the output current.

2 Experimental

Commercial ultra-flat Quartz coated glass slides were bought from Ossila Ltd. (Sheffield, UK). To deposit golden electrodes, the source-drain deposition shadow mask with a variable channel length (25, 50, 75, 100 and 150 μm) and constant channel width (5 mm) was used. From Kurt J. Lesker Company (Munich, DE), the golden pellets evaporation material was bought. Sodium hydroxide, sodium chloride, and isopropyl alcohol were bought from PENTA (Chrudim, CZ). Aqueous suspension of commercially available PEDOT:PSS ink (Heraeus CleviosTM P JET HC V2) was used. Ethylene glycol (EG) was purchased from Sigma Aldrich (St. Louis, MO, USA) and Sylgard 184 poly(dimethylsiloxane) (PDMS) was purchased from DowsilTM (Alphen aan den Rijn, NL). The gold wire with a diameter (484 ± 7) μm and length (1.0 ± 0.1) cm was used as a gate electrode.

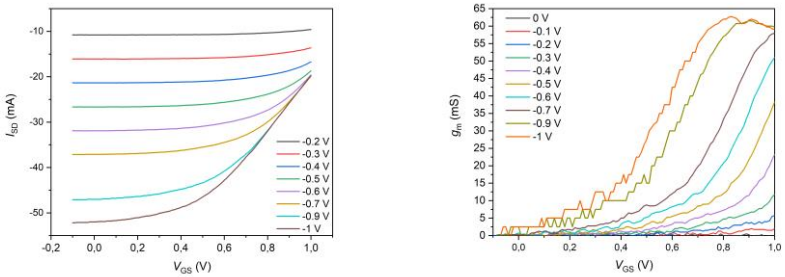

Figure 1: Left: Transfer characteristics for different set-up voltage between source and drain electrodes. Right: The dependence of the calculated transconductance on the applied voltage at the gate electrode. The curves are for different set-up voltage between source and drain electrodes.

Ultra-flat Quartz coated glass slides were used as substrates. The substrates were cleaned in an ultrasound batch (each step 10 minutes). First, the substrates were cleaned with sodium hydroxide (2%), then with distilled water, and isopropyl alcohol (IPA). After cleaning, the substrates were dried at 100 °C. A physical vapor deposition technique was used to prepared golden electrodes (source, drain) with a thickness of 200 nm. Water suspensions of PEDOT:PSS were stirred with a magnetic bar (500 rpm) for 2 hours and filtered through cellulose filter (RC 0.45 μm). PEDOT:PSS films were deposited on substrates by spin-coating. Samples consisted of 1, 2, 4, and 6 layers of PEDOT:PSS were prepared to achieved samples with differing *Wd*/*L*. Every layer was dried at 150 °C (5 minutes) before next layer was deposit. After deposition of last layer, prepared films were dried at 150 °C (15 minutes). The excess of PEDOT:PSS outside of the channel was removed. Then, the films were treated with ethylene glycol (EG) for 15 minutes. After that, the excess of EG was washed with distilled water and IPA. Films were dried again at 150 °C for 15 minutes. Films' thickness was measured by a DektakXT profilometer (BRUKER, USA) and the electrical resistivity of the channel was measured by a multimeter (Keithley 2100). On the end, PDMS (Sylgard 184) frames were attached to the substrates.

To measure output and transient I-V characteristics, the home-builds LabVIEW software and high current measuring apparatus, constructed from galvanic shield voltage source Statron 3253.1 (VSD), Metex MT-3850 (ammeter), National instruments Ni 9263 (VGS) and Ni 9219 (voltmeter) were used.

3 Results and discussion

In order to study the effect of series resistance, OECTs with different PEDOT:PSS layer thicknesses, *d*, and different channel lengths, *L*, were prepared. Every prepared OECT had the same electrodes system with channel width 5 mm and was measured with the same set-up. The thicknesses of the prepared PEDOT:PSS layers were 36, 65, 161, and 275 nm. For every PEDOT:PSS thickness, OECTs with channel lengths 25, 50, 75, 100, and 150 μm were prepared. As an electrolyte, sodium chloride with conductivity 20 mS/cm

was used. To characterize the OECT, the transfer characteristics were measured (Figure 1 Left) and the values of transconductance were calculated for different set-up voltage between the source (S) and drain (D) electrode. The dependence of transconductance on the voltage between gate (G) and drain electrode is shown in Figure 1 Right.

The calculated transconductance, g_m, values were plotted as a function of *Wd/L* in Figure 2. According to the hypothesis (Equation 1), the transconductance should increase linearly with increasing *Wd/L*. However, as can be seen in the Figure 2 (red squares), with increasing *Wd/L* the deviation from linearity increases and the dependence of the transconductance on *Wd/L* bends. That implies, as already mentioned above, that the value of the transconductance can be influenced by the conductivity of the electrode system, i.e. by its electrical resistance, or by other resistors connected in series.

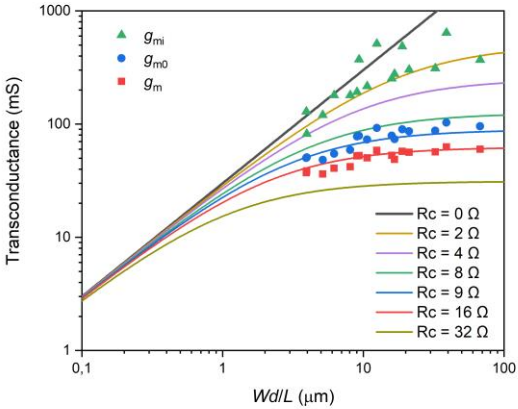

Figure 2: The transconductance as a function of Wd/L. The lines represents calculated theoretical dependences for given contact resistance, R_c, g_m is measured peak transconductance, g_{m0} is a transconductance corrected for source resistance, and g_{mi} is a transconductance corrected for source-drain resistance.

To determine the influence of the contact resistance on the voltage across the sample, a model dependence of the effective voltage on the *Wd/L* ratio was constructed. The effective voltage on the channel can be easily calculated based on the voltage divider and Kirhoff's laws. It follows that the effective voltage on the channel is given by $R_{ch}/(R_{ch} + R_c)$, where R_{ch} is the resistance of the channel, and R_c is the resistance of the electrode system. This dependence is plotted in Figure 3. It can be seen that the dependence of the effective voltage is sigmoidal. This means that due to the more or less manifested voltage divider, there is a certain decrease in the effective voltage on the channel. The effective voltage is lower than the applied voltage, and thus the obtained value of the transconductance is significantly affected. This decrease in the effective voltage will be more noticeable the smaller the electrical resistance of the channel with respect to the electrical resistance of the contacts, i.e. the larger the *Wd/L* ratio is. The curves of the same color (solid and dashed line), for the one channel conductivity, clearly determine the areas for which the influence of the contact resistance can be neglected and for which, on the contrary, the

given OECT layout is unsuitable. Dashed lines represent the contact resistance of 1000 Ω, solid lines represent contact resistance of 1 Ω. Different color of lines represents the different channel conductivity that means the organic semiconducting material has a different conductivity. In addition, it can be observed that this dependence also applies if we have the same electrode system, e.g. contact resistance 1000 Ω, but different channel conductivity.

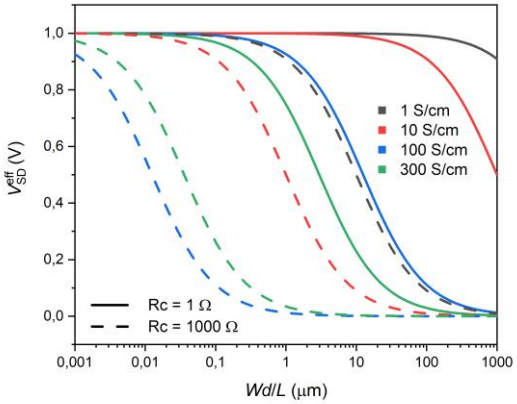

Figure 3: The effective voltage on the channel as a function of Wd/L. Different colors represents different conductivity of the channel (different conductivity of organic semiconductor); dashed and solid lines represent different contact resistance.

Furthermore, a modeled dependence of the percentage decrease of the output current on the parasitic resistance was compiled. From figure 4 it can be seen that with increasing *Wd/L*, the dependence shifts to lower values of parasitic resistance. In the case of different channel conductivity, while maintaining the same *Wd/L* ratio, there is a shift to lower values of parasitic resistance with increasing channel conductivity. As in the previous case, it is possible to see when the maximum effective current is reached, and thus when the parasitic resistance can be neglected and when not. Based on these dependences, we can determine the appropriate *Wd/L* parameters and the appropriate conductivity of the organic semiconductor to prepare the OECT sensor for a particular application.

Figure 2 showed that the dependence of transconductance on *Wd/L* decline from the expected linearity with increasing *Wd/L* ratio. Figure 3 and Figure 4 showed that the deviation from this linearity can be explained by the reduction of the effective voltage on the channel due to the parasitic resistance. Also, it was shown that the effective voltage is proportional to $R_{ch}/(R_{ch} + R_c)$, that means the parasitic resistance is equal to sum of contact resistance and other elements connected in series. Based on the above-mentioned model of Antoniadis and Chou (Equation 2) the expected transconductance value for chosen contact resistances were calculated (solid lines in Figure 2). It can be seen that the value relatively well represents the trends of the measured data. The corrected values for measured transconductance were also calculated. First we calculated g_{m0}, which corrected

values for source resistance and plot the dependence. It can be seen that the deviation from linearity decrease but still some other resistance is included. So, the intrinsic transconductance for measured values based on the Equation 2 were calculated. These values were plot as a dependence on *Wd/L* also into the Figure 2 (green triangles). The intrinsic transconductance values are corrected for source-drain resistance. As we can see from the Figure 2, the still small deviation from linearity suggests that some additional resistance involved in the series contributes to the resulting transconductance, which was not included in the calculation of intrinsic transconductance, e.g. ammeter. The effect of contact and series resistance will be more significant with increasing ratio of *Wd/L* (devices with a short channel).

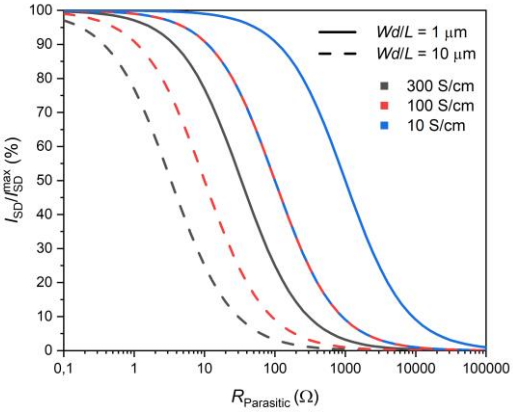

Figure 4: The modeled dependence of the percentage decrease of the output current on the parasitic resistance. Different colors represents different conductivity of the channel (different conductivity of organic semiconductor); dashed and solid lines represent different ratio of Wd/L.

4 Conclusion

This study deals with the effect of contact and series resistance on the transconductance of OECT. The dependence of transconductance on ratio of *Wd/L* shows decline from expected linearity. The modeled dependencies presented in this article showed the effect of contact series resistance. The significant decrease of effective voltage is observed mainly for short-channel devices (with high ratio of *Wd/L*). It was shown that the voltage drop can be described by the division of voltage on resistors in series according to this formula: $R_{ch}/(R_{ch} + R_c)$. The modeled dependencies provide the description for development of OECT with maximum transconductance, and hence sensitivity. In addition, it can be derived when the parasitic resistance can be neglected and when not.

5 References

1. LIAO, Caizhi and Feng YAN. Organic Semiconductors in Organic Thin-Film Transistor-Based Chemical and Biological Sensors. Polymer Reviews. 2013, 53(3), 352-406. DOI: 10.1080/15583724.2013.808665. ISSN 1558-3724.
2. RIVNAY, Jonathan, Sahika INAL, Alberto SALLEO, Róisín M. OWENS, Magnus BERGGREN and George G. MALLIARAS. Organic electrochemical transistors. Nature Reviews Materials. 2018, 3(2), 1-11. DOI: 10.1038/natrevmats.2017.86. ISSN 2058-8437
3. D'ANGELO, Pasquale, Giuseppe TARABELLA, Agostino ROMEO, et al. PEDOT:PSS Morphostructure and Ion-To-Electron Transduction and Amplification Mechanisms in Organic Electrochemical Transistors. Materials. 2019, 12(1), 1-13. DOI: 10.3390/ma12010009. ISSN 1996-1944.
4. CENDRA, Camila, Alexander GIOVANNITTI, Achilleas SAVVA, Vishak VENKATRAMAN, Iain MCCULLOCH, Alberto SALLEO, Sahika INAL a Jonathan RIVNAY. Role of the Anion on the Transport and Structure of Organic Mixed Conductors. Advanced Functional Materials. 2019, 29(5), 1-11. DOI: 10.1002/adfm.201807034. ISSN 1616301X.
5. INAL, Sahika, George G. MALLIARAS and Jonathan RIVNAY. Benchmarking organic mixed conductors for transistors. Nature Communications. 2017, 8(1). DOI: 10.1038/s41467-017-01812-w. ISSN 2041-1723.
6. KAPHLE, Vikash, Shiyi LIU, Akram AL-SHADEEDI, Chang-Min KEUM and Björn LÜSSEM. Contact Resistance Effects in Highly Doped Organic Electrochemical Transistors. Advanced Materials. 2016, 28(39), 8766-8770. DOI: 10.1002/adma.201602125. ISSN 09359648.
7. DONAHUE, Mary J., Adam WILLIAMSON, Xenofon STRAKOSAS, Jacob T. FRIEDLEIN, Robert R. MCLEOD, Helena GLESKOVA and George G. MALLIARAS. High-Performance Vertical Organic Electrochemical Transistors. Advanced Materials. 2018, 30(5). DOI: 10.1002/adma.201705031. ISSN 09359648.
8. CHOU, S.Y. and D.A. ANTONIADIS. Relationship between measured and intrinsic transconductances of FET's. IEEE Transactions on Electron Devices. 1987, 34(2), 448-450. DOI: 10.1109/T-ED.1987.22942. ISSN 0018-9383.

Acknowledgement (This research was supported by the Faculty of Chemistry at BUT under Project no. FCH-S-20-6307 and by the Czech Science Foundation Project no. 17-24707S.).

Visualization of a Ge Structure Using Fluorescent Nanoparticles

Kateřina Marková
Filip Mravec, Miloslav Pekař

Brno University of Technology, Faculty of Chemistry,
Institute of Physical and Applied Chemistry

Purkyňova 464/118, 61200 Brno, Czech rep.
Katerina.Markova@vut.cz

This contribution describes the visualization of the hydrogel structure using the fluorescence lifetime imaging microscopy (FLIM) and subsequent modifications using other software. This method, in conjunction with fluorescent nanoparticles, allows to visualize the exact structure of hydrogels. It is also possible to define the pore size. Only the average value of pore size was mentioned in the articles published so far, but this often does not correspond to the actual structure of hydrogels.

The work is focused on the imaging of selected hydrogels using FLIM analysis and subsequent modification in the specialized software. the simplest way is to use nanoparticles with a specific diameter, where one FLIM image is created for each particle size. Thanks to the z-scan and the selected program, there is possible to convert these images into a 3D structure. Unfortunately, it is not possible to measure exactly the pore size by this measurement, so it has no informative value, but only allows visualization of the actual structure of the hydrogel. for a more accurate analysis, nanoparticles of different sizes and colours were selected, which could be used in one experiment at a time. It could be possible to track sites of varying pore sizes within a single experiment thanks to them.

Aqueous solution of agarose was chosen as the physically cross-linked type of hydrogel and fluorescent-labeled gold nanoparticles with diameters ranging from 10 to 100 nm were used as fluorescent probes.

Keywords: *fluorescence microscopy, nanoparticles, hydrogel, FLIM, 3D image, structure*

Plasticized poly(3-hydroxybutyrate)/poly(D,L-lactide) blends filled with tricalcium phosphate for FDM 3D printing and their biological properties

Veronika Melčová
Kateřina Chaloupková, Radek Přikryl, Lucy Vojtová and Michala Rampichová

Brno University of Technology, Faculty of Chemistry, Institute of Materials Chemistry

Purkyňova 464/118, 612 00 Brno, Czech Republic
xcmelcova@fch.vutbr.cz

Additive manufacturing or 3D printing is a production technology capable of producing nearly any desired shape including complex porous structures. Thanks to this, it is often exploited for the manufacturing of scaffolds for tissue engineering, a modern approach of regenerative medicine. In this work, we have successfully prepared plasticized poly(3-hydroxybutyrate)/polylactide 70/30 blends modified with bioceramic tricalcium phosphate (13 wt%) and used them for Fused Deposition Modeling 3D printing. Two commercial plasticizers, Citroflex B6 (*n*-Butyryl tri-*n*-hexyl citrate) and Syncroflex 3114 (oligomeric adipate ester), in the amount of 12 wt% were used. the materials were firstly subjected to printing parameters optimization, afterwards printability, thermal and mechanical testing and as well as series of biological tests *in vitro* were conducted. Citroflex plasticizer was proven to be effective in enhancing the processability and mechanical properties of studied biopolymer blend, however the biocompatibility of samples

with this citrate-based plasticizer was rather poor. on the other hand, Syncroflex materials showed better warping properties than commercial grade PLA filament and moreover the results of biological tests revealed its potential to be used for stem cell-seeded scaffolds for regenerative medicine of bones.

Využití smíšených tkáňových kultur ve výzkumu biodistribuce nanočástic

Bc. Pavlína Michaláková
vedoucí práce: Ing. Denisa Lizoňová

Vysoká škola chemicko-technologická v Praze, Fakulta chemicko-inženýrská, Ústav chemického inženýrství.
Technická 5, Dejvice, 166 28 Praha 6, Česká republika
michalap@vscht.cz

1 Úvod

I přes značný pokrok na poli onkologické léčby zde přetrvává velké riziko mnoha nežádoucích účinků a zhoršení kvality života pacientů. To je z velké míry zapříčiněno současně užívanými cytostatiky. Signifikantní procento z nich totiž není schopno léčivo doručit pouze k nádorovým buňkám[1]. Tím dochází také k omezení terapeutické použitelnosti této léčby. Jelikož dochází k nadměrné expozici zdravých tkání, nejsou mnohdy intravenózně podaná cytostatika dopravena k nádorovým buňkám v efektivních koncentracích. K maximalizaci účinnosti léčby a minimalizaci nežádoucích účinků by mohlo dojít užitím transportních nosičů – nanočástic – které by léčivo doručily pouze na cílené místo (nádor)[2, 3]. Jejich užití sebou přináší mnoho výhod, přičemž největší z nich je možnost použití velkého množství léčiva, či případně proléčiva, které se uvolní až v nádoru. Problémem této léčby ovšem zatím zůstává, že jsou nanočástice ve velké míře vychytávány buňkami imunitního systému – makrofágy – v procesu zvaném fagocytóza (*Obrázek 1*). Při něm dochází k rozpoznání nanočástic a jiných cizorodých látek imunitními buňkami, jejich pohlcení a následné akumulaci v játrech a slezině[4]. To vede ke snížení doby cirkulace v krevním řečišti a tím pádem také ke snížení pravděpodobnosti úspěšného dopravení nanočástic do nádoru.

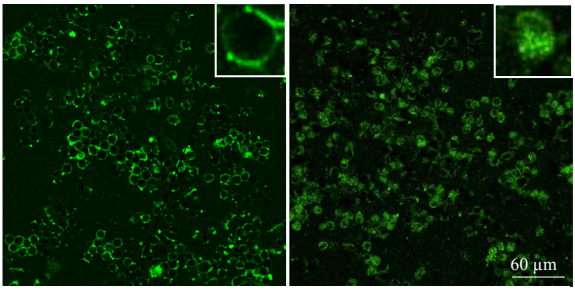

Obrázek 1: Proces fagocytózy fluorescenčně značených nanočástic makrofágy v čase. Vlevo: začátek procesu, kdy je lokalizace nanočástic na povrchu buněk versus vpravo: pokročilé stadium fagocytózy, kdy jsou nanočástice lokalizovány uvnitř buněk.

Tento nežádoucí proces může být minimalizován například modifikací nanočástic polymerem poly(*N*-(2-hydroxypropyl) methakrylamidem) (pHPMA)[5], který snižuje adsorpci krevních proteinů na nanočástice (opsonizace) a tím zabraňuje jejich rozpoznání imunitními buňkami.

V této práci byly studovány interakce nanočástic s nádorovými a imunitními buňkami pomocí průtokové cytometrie a fluorescenční mikroskopie. Kolorektální karcinom je dlouhodobě jednou z nejčastějších diagnóz rakoviny a to nejen v České republice[6]. V této práci byly jako zástupce nádorových buněk použity právě buňky kolorektálního karcinomu.

Nejprve byly připraveny křemičité nanočástice, které byly následně modifikovány polymerem pHPMA. Rozeznání nádorových buněk bylo v případě této práce dosaženo na základě interakce protilátka-antigen (*Obrázek 2*), kdy byly nanočástice modifikovány monoklonální protilátkou IgG M75 [7]. Tato protilátka je specifická pro karbonickou anhydrázu IX (CA IX), jež je preexprimována na pevných hypoxických nádorech (například na nádorech kolorektálního karcinomu) a ve zdravých tkáních se vyskytuje velmi vzácně[8]. V experimentech s fluorescenčním mikroskopem byly použity smíšené buněčné kultury, aby mohlo být ověřeno, zda je možné specifickou adhezi na nádorové buňky a fagocytózu makrofágů detekovat také simultánně, tedy v kompetitivním prostředí a případně posoudit, zda některý z těchto procesů převažuje.

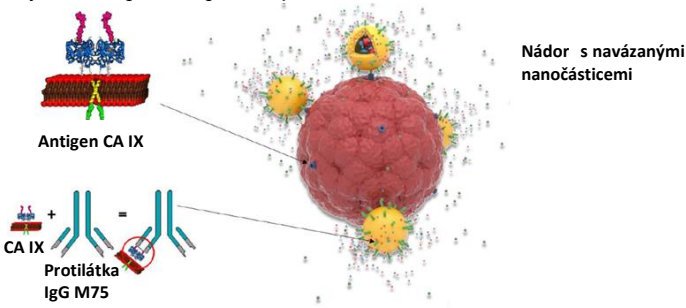

Obrázek 2: Ilustrace aktivního cílení nanočástic na základě vazby protilátka-antigen.

2 Experimentální část

2.1 Příprava a charakterizace nanočástic

Fluorescenčně značené křemičité nanočástice, byly syntetizovány a modifikovány způsobem popsaným dříve[5]. Nanočástice byly nejprve modifikovány polymerem pHPMA (SiO_2-pHPMA) a dále protilátkou IgG M75 (SiO_2-pHPMA-M75). K ověření, zda protilátka IgG M75 váže antigen, byl proveden imunotest. Tento experiment byl proveden na polystyrénové 96-jamkové destičce se speciálně upravenými jamkami s antigenem (PG-MBP, epitop=část antigenu rozeznávaná IgG M75) a kontrolou (MBP). Do prvního řádku byly přidány suspenze nanočástic a v následujících řádcích byla koncentrace částic vždy dvakrát snížena. Po 1h inkubace byly jamky promyty fosfátovým pufrem (PBS).

Nanočástice modifikované monoklonální protilátkou IgG M75 měly zůstat přichyceny k povrchu destičky, zatímco nanočástice modifikované pouze polymerem pHPMA měly být odmyty PBS (*Obrázek 3*). Fluorescence byla analyzována pomocí fluorescenční čtečky Tecan Infinite M200.

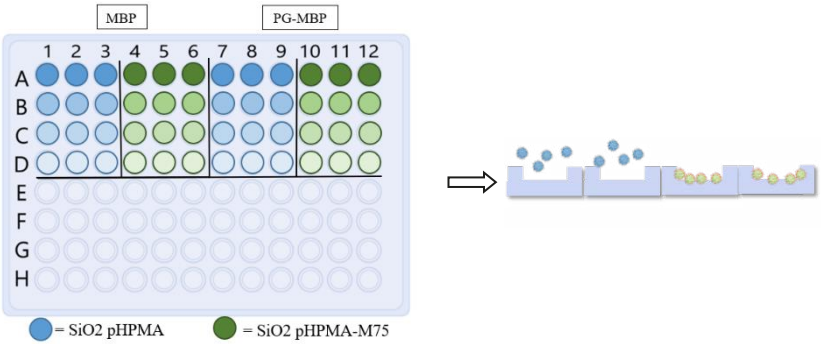

Obrázek 3: Schéma 96-jamkové destičky při provádění imunotestu. Částice bez protilátky (modře) jsou odmyty, zatímco částice s protilátkou (zeleně) jsou naadherovány k povrchu destičky.

2.2 Průtoková cytometrie

Pro experimenty s buňkami byly použity 2 typy buněčných linií – nádorové buňky HT-29, které exprimují CA IX a imunitní buňky J774A.1 (=makrofágy, neexprimují CA IX). Buňky byly sklizeny, spočítány pomocí hemocytometru a v množství 220 000 buněk napipetovány do zkumavek. Po zcentrifugování buněk a jejich promytí 0,5 ml PBS k nim byly přidáno 0,8 mg nanočástic. Po určité době inkubace byly vzorky promyty PBS a přefiltrovány do zkumavek pro průtokovou cytometrii. Experimenty byly prováděny s konstantním množstvím nanočástic a studovaly závislost procesů fagocytózy a specifické adheze v čase. Při měření pomocí průtokové cytometrie byla měřena fluorescence jednotlivých buněk (nanočástice byly značeny fluoresceinem, λ_{ex}=488 nm, λ_{em}=516 nm).

2.3 Fluorescenční mikroskopie

Ke studování, jak se budou vázat částice na imunitní a nádorové buňky v kompetitivním prostředí bylo využito fluorescenční mikroskopie. Pro tyto experimenty byly připraveny smíšené buněčné kultury imunitních buněk J774A.1 a nádorových buněk HT-29. Oba typy buněčných linií byly společně zaočkovány do 24-jamkové destičky v celkovém množství 50 000 buněk na jamku (do jedné jamky bylo tedy zaočkováno 25 000 HT-29 a 25 000 J774A.1 buněk). Po 48 hodinách inkubace, kdy se množství buněk v jamkách mělo zvýšit na 200 000 (doba dělení buněk je zhruba 24 hodin), byly přidány nanočástice. Pro označení imunitních buněk ve smíšených kulturách HT-29 a J774A.1 byly použity mikročástice pHrodo™ Red Zymosan Bioparticles™ (pHrodo™), které jsou fluorescenční jen po pohlcení imunitními buňkami.

3 Výsledky a diskuse

3.1 Příprava a charakterizace nanočástic

Částice byly charakterizovány pomocí dynamického rozptylu světla (DLS) a transmisního elektronového mikroskopu (TEM). Měření pomocí DLS bylo provedeno v kyvetách s PBS bezprostředně po přípravě a modifikaci nanočástic. Jejich velikost byla 160 nm. *Obrázek 4* ukazuje distribuci velikosti připravených nanočástic podle objemu a jejich TEM snímek.

Schopnost protilátky IgG M75 vázat antigen byla ověřena imunotestem. Δ Fluorescence je rozdíl mezi signálem získaným z jamek modifikovaných antigenem PG-MBP a signálem z jamek pouze s kontrolním proteinem MBP. V případě nanočástic SiO_2-pHPMA je výsledný signál negativní, což může být důsledkem nepřesného pipetování, či vyšší afinity těchto nanočástic ke kontrolnímu proteinu než k antigenu.

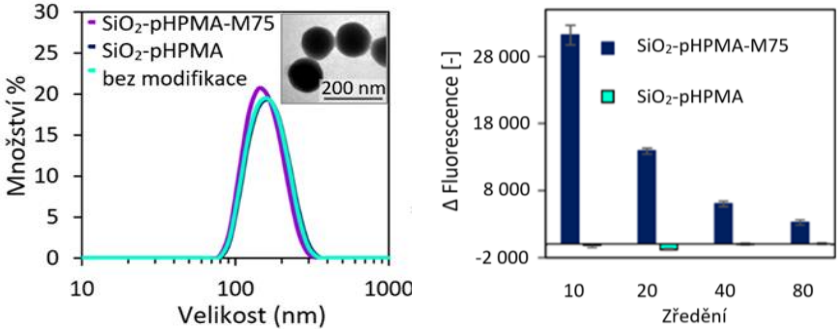

Obrázek 4: Vlevo: distribuce velikosti nanočástic a jejich TEM snímek. Vpravo: Výsledky imunotestu. Protilátka IgG M75 je schopna vázat antigen.

3.2 Průtoková cytometrie

Experiment ke zjištění časové závislosti procesů fagocytózy nanočástic makrofágy a interakcí protilátka-antigen byl proveden s nanočásticemi o koncentraci 40 μg/ml a s 220 000 buňkami. Výsledky z průtokového cytometru jsou vyobrazeny na *Obrázek 5*. Pro účely farmakokinetického modelu bude využita rychlost těchto procesů. Na vodorovné ose je znázorněno množství fluorescence jednotlivých buněk. Na svislé ose je četnostní hustota, která udává, jak velké množství buněk se s danou fluorescencí nachází ve vzorku. S rostoucím časem se na grafech fluorescence buněk zvyšuje, protože je na ně navázáno větší množství fluorescenčních nanočástic.

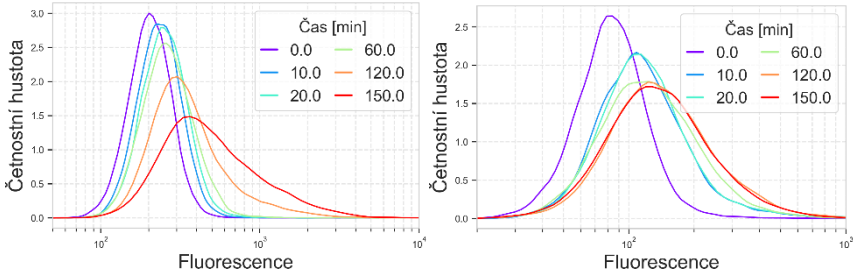

Obrázek 5: Výsledky z průtokové cytometrie s nanočásticemi s protilátkou a imunitními buňkami J774A.1 (vlevo) či nádorovými buňkami HT-29 (vpravo).

3.3 Fluorescenční mikroskopie

Pomocí fluorescenční mikroskopie byly získány snímky smíšených buněčných kultur imunitních a nádorových buněk. Imunitní buňky J774A.1 byly nejprve označeny mikročásticemi pHrodo™, které jsou fluorescenční jen po pohlcení imunitními buňkami (*Obrázek* ***6***). Díky lokalizaci fluorescence bylo určeno, že imunitní buňky rostou jednotlivě (červená), zatímco nádorové buňky HT-29 (nejsou fluorescenční) rostou při sobě a tvoří ostrůvky.

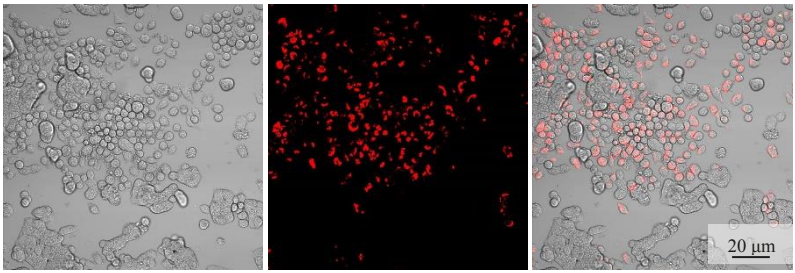

Obrázek 6: Smíšená buněčná kultura po označení mikročásticemi pHrodo™ po 2 hodinách inkubace. Vlevo: transmisní snímek, uprostřed: fluorescenční snímek, vpravo: proložený snímek.

Poté byly se smíšenými kulturami provedeny také experimenty se syntetizovanými nanočásticemi bez protilátky (SiO_2-pHPMA) a s protilátkou (SiO_2-pHPMA-M75). Na snímku *Obrázek* **7** můžeme vidět, že nanočástice bez protilátky (SiO_2-pHPMA) se na nádorové buňky HT-29 nevážou. Na snímku *Obrázek 8* můžeme naopak pozorovat jak se částice s protilátkou (SiO_2-pHPMA-M75) zachytávají na membráně nádorových buněk HT-29 (díky výskytu CA IX), zatímco v případě imunitních buněk J774A.1 jsou nanočástice díky fagocytóze lokalizovány uvnitř buněk. Nanočástice SiO_2-pHPMA-M75 se za experimentálních podmínek vážou více na nádorové buňky HT-29 (*Obrázek 8*, vpravo). Na

snímku *Obrázek 8* vlevo je interakce nanočástic s imunitními buňkami o něco menší než na snímku vpravo, což může být zapříčiněno nasycením těchto buněk mikročásticemi pHrodo™.

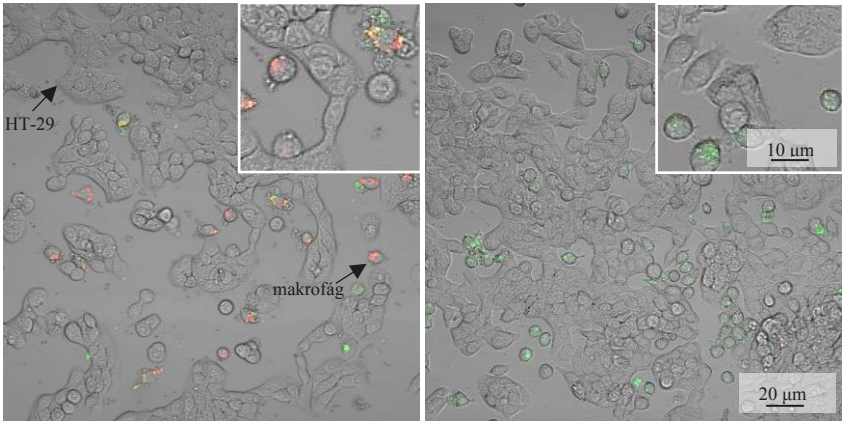

Obrázek 7: Snímky smíšených buněčných kultur z fluorescenční mikroskopie s nanočásticemi bez protilátky (SiO_2-pHPMA) (zelená, nanočástice se nevážou na nádorové buňky HT-29). Vlevo: s mikročásticemi pHrodo™ uvnitř imunitních buněk (červená). Vpravo: bez mikročástic pHrodo™.

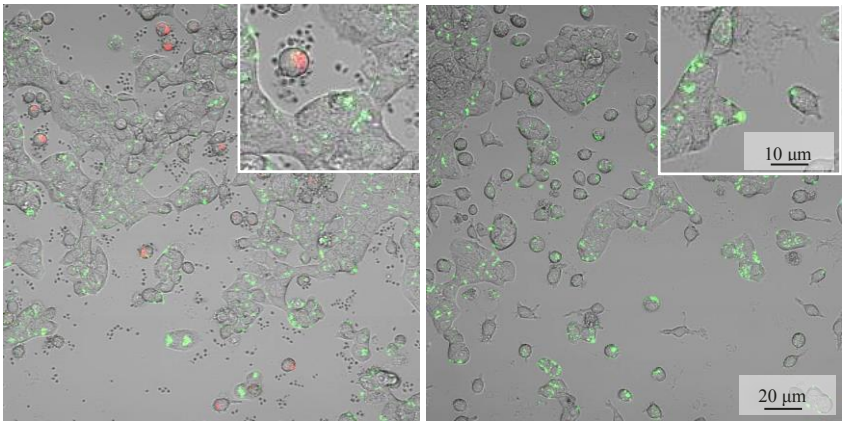

Obrázek 8: Snímky smíšených buněčných kultur z fluorescenční mikroskopie s nanočásticemi s protilátkou (SiO_2-pHPMA-M75). Vlevo: s mikročásticemi pHrodo™ uvnitř imunitních buněk (červená). Vpravo: bez mikročástic pHrodo™. Nanočástice s protilátkou se ve větší míře vážou na nádorové buňky a jsou navázány na jejich membráně. Na snímku vlevo je interakce nanočástic s imunitními buňkami o něco menší než na snímku vpravo, což může být zapříčiněno přesycením těchto buněk mikročásticemi pHrodo™.

4 Závěr

Křemičité nanočástice byly modifikovány polymerem pHPMA a monoklonální protilátkou IgG M75 a následně charakterizovány. Schopnost protilátky IgG M75 vázat antigen byla potvrzena imunotestem a velikost nanočástic byla změřena dynamickým rozptylem světla (d=160 nm). Fluorescenční mikroskopie v kombinaci s průtokovou cytometrií byla použita za účelem pochopení procesů fagocytózy nanočástic makrofágy (buněčná linie imunitních buněk J774A.1) a specifických interakcí protilátka-antigen (buněčná linie kolorektálního karcinomu – HT-29). Pomocí průtokové cytometrie byl zkoumán vliv různých inkubačních časů nanočástic s buňkami a byly získány kvantitativní data pro sestavení farmakokinetického modelu (není v této práci zobrazen). K ověření, zda je možné výše zmíněné procesy detekovat také simultánně, byly provedeny experimenty se smíšenými buněčnými kulturami linií buněk J774A.1 a HT-29, kdy byly imunitní buňky J774A.1 označeny mikročásticemi pHrodo™. Tyto experimenty byly vyhodnoceny pomocí fluorescenční mikroskopie. Potvrdilo se, že se nanočástice s protilátkou IgG M75 vážou na nádorové buňky HT-29 i ve smíšené kultuře a jsou na těchto buňkách detekovány ve větším množství, v porovnání s buňkami imunitními. Toho je dosaženo díky použití polymeru pHPMA („zneviditelnění" částic) a protilátek IgG M75 (aktivní cílení).

Poděkování
Mé poděkování patří zejména Ing. Denise Lizoňové za její odbornou pomoc a vedení práce. Dále Ing. Ivaně Křížové a Ing. Jiřímu Kolářovi za vyhodnocení experimentů pomocí průtokové cytometrie. Ráda bych poděkovala také prof. Františkovi Štěpánkovi, Ph.D.za jeho cenné poznatky.

5 Literatura

1. Vasir, J. K.; Labhasetwar, V., Targeted Drug Delivery in Cancer Therapy. *Technology in Cancer Research & Treatment* **2005,** *4* (4), 363-374.
2. Kumari, P.; Ghosh, B.; Biswas, S., Nanocarriers for cancer-targeted drug delivery. *J Drug Target* **2016,** *24* (3), 179-91.
3. Malam, Y.; Loizidou, M.; Seifalian, A. M., Liposomes and nanoparticles: nanosized vehicles for drug delivery in cancer. *Trends Pharmacol Sci* **2009,** *30* (11), 592-9.
4. Owens, D. E., 3rd; Peppas, N. A., Opsonization, biodistribution, and pharmacokinetics of polymeric nanoparticles. *Int J Pharm* **2006,** *307* (1), 93-102.
5. Lizoňová, D.; Majerská, M.; Král, V.; Pechar, M.; Pola, R.; Kovář, M.; Štěpánek, F., Antibody-pHPMA functionalised fluorescent silica nanoparticles for colorectal carcinoma targeting. *RSC Advances* **2018,** *8* (39), 21679-21689.
6. Douaiher, J.; Ravipati, A.; Grams, B.; Chowdhury, S.; Alatise, O.; Are, C., Colorectal cancer-global burden, trends, and geographical variations. *J Surg Oncol* **2017,** *115* (5), 619-630.
7. Závada, J.; Závadová, Z.; Pastorek, J.; Biesová, Z.; Ježek, J.; Velek, J., Human tumour-associated cell adhesion protein MN/CA IX: identification of M75 epitope and of the region mediating cell adhesion. *British Journal of Cancer* **2000,** *82* (11), 1808-1813.
8. Král, V.; Mader, P.; Collard, R.; Fábry, M.; Horejsí, M.; Rezácová, P.; Kozísek, M.; Závada, J.; Sedlácek, J.; Rulísek, L.; Brynda, J., Stabilization of antibody structure upon association to a human carbonic anhydrase IX epitope studied by X-ray crystallography, microcalorimetry, and molecular dynamics simulations. *Proteins* **2008,** *71* (3), 1275-87.

Monitoring of Gadolinium Anomaly in Soil, Grapevine and Wine Samples from the Czech Republic

Frederika Mišíková
Anna Krejčová, Jan Patočka

The University of Pardubice, Faculty of Chemical Technology, Institute of Environmental and Chemical Engineering
Studentská 573, CZ–532 10 Pardubice, Czech Republic
frederika.misikova@student.upce.cz

1 Introduction

Rare earth elements (REEs) are a common part of all components of the environment in small quantities[1,2,3,4]. They are used in many areas, such as medicine, agriculture and industry[1,4,5,6,7]. The use of REEs is growing mainly due to their use in new technologies[1,3,7,8] (e.g. computers, smartphones, and permanent magnets)[8]. Their consumption grows by about 6% per year[8]. REEs are becoming indispensable for the transition to a low-carbon economy (electric cars, photovoltaic panels, wind turbines, etc.)[8]. Increased use of REEs is also associated with expanding mining, which can lead to fundamental changes in their natural distribution worldwide and especially in the composition of their chemical forms [1,2,7,8]. Anthropogenic REEs are usually in a more bioavailable and more soluble form than naturally occurring REEs[1,8]. Exposure to REEs may pose a health risk through workplaces and the environment[2,7,9]. They are dangerous to human health because they cause serious health issues such as nephrogenic systemic fibrosis and severe damage to nephrological systems, dysfunctional neurological disorder, oxidative stress, male sterility, etc.[6]. Recently, REEs have been considered emerging contaminants for these reasons[1,2,3,4,6].

Waste from mining and the use of REEs in industrial, agricultural and medicinal technologies affect the environment[1,2,7]. Several studies have shown that REE concentrations have recently increased in various components of the environment (e.g. soil, sediment, wastewater and surface water)[8]. Subsequently, they are bioaccumulated in living organisms (e.g. algae and bivalves)[8], and then they can enter the food chain and have a dangerous effect on human health in this way[2].

Gadolinium (Gd) is one of these emerging contaminants[4]. Naturally, it can only be found in mixed minerals together with other REEs[10]. It is used in many different technologies (e.g. in compact discs, computer memories or in the cores of nuclear reactors), various industries (e.g. iron and steel industry, petroleum industry), and also in medicine (contrast agents)[4,5,9]. Gd together with other REEs are released into the environment through widespread use of phosphate fertilisers of Chinese origin[2,3,4,11].

Anthropogenic sources of Gd are also farm animal feed, to which REEs are added as growth stimulators[4,12].

Currently, gadolinium-based contrast agents (GdCAs) are commonly used in magnetic resonance imaging (MRI) in clinical diagnostics and biomedical research[4,5]. GdCAs are stable complexes with various organic ligands[5]. Stabilisation of the Gd^{3+} ion in the complex is necessary due to its high toxicity in hydrated form[5,13]. The release of the Gd^{3+} from the complex is possible through transmetalation with other ions in the body[14]. GdCAs are not inert drugs and can cause serious and life-threatening conditions, including side effects of acute non-renal (e.g. anaphylactic reaction), acute renal (e.g. contrast-induced nephropathy) or delayed (e.g. nephrogenic systemic fibrosis) and injection site problems (e.g. local necrosis)[15]. Side effects may occur in patients with impaired renal function[15]. No information is currently available on the long-term toxic effects of GdCAs in healthy patients without renal impairment[16] as Gd complexes are easily filtered by the kidneys[17]. Their biological half-life is approximately 1.5 to 2 hours in patients with normal renal function[15]. Due to their high stability in the human body, GdCAs are excreted unmetabolised, especially in the urine, into hospital wastewater within a few hours after application[4,5].

Gd enters the environment in many different places[9]. Particularly it is the disposal of household equipment[9] and Gd emissions in hospitals with MRI services[5]. Anthropogenic Gd gradually accumulates in soil and water (surface and wastewater) and causes an increase in concentration compared to the natural content of Gd and concentrations of other REEs[4,5,9]. This phenomenon is called the gadolinium anomaly[4,5]. The fate of anthropogenic Gd in the environment is determined by the properties of Gd compounds and the environment itself. Specific environmental conditions determine whether Gd compounds are immobilised (e.g. on soil particles or sediments), mobilised (i.e. soluble)[18] or bioaccumulated in organisms and can enter the food chain[2]. The potential risk to human health can be assessed by monitoring the concentration of REEs in daily foods (vegetables, grains, meat)[2].

The calculation of the gadolinium anomaly begins with determining the REEs concentrations[19]. Normalisation of the amount of REEs is usually performed with respect to the reference geological standard, e.g. NASC (North American Shale Composite)[19] or the more commonly used PAAS (post-Archean Australian Shale)[5,13]. These standards represent the average composition of REEs in the upper layer of the earth's crust[19]. The calculation of the gadolinium anomaly is based on the ratio of the real normalised concentration Gd and Gd concentration corresponding to the natural background obtained by interpolating the normalised concentrations of two neighbouring REEs (Sm and Tb)[19] according to the equation (1)[5]:

$$Gd_{anom} = Gd_{N\text{-}total} / Gd_{N\text{-}geo} = Gd_{N\text{-}total} / (0.33 \times Sm_N + 0.67 \times Tb_N) \quad (1)$$

where Gd_{anom} is a positive gadolinium anomaly, $Gd_{N\text{-}total}$ and $Gd_{N\text{-}geo}$ are normalised concentrations of total and geogenic Gd, and Sm_N and Tb_N are normalised concentrations of Sm and Tb[5,19]. The anthropogenic concentration of Gd (Gd_{ant}) is calculated by the equation (2)[19]:

$$Gd_{ant} = Gd_{total} - Gd_{geo} \quad (2)$$

where Gd_{total} is the total content of Gd and Gd_{geo} is the content of geogenic Gd[19]. Subsequently, a graph of normalised concentrations of all REEs is created where it is possible to observe an increase in the normalised Gd concentration in the case of a positive gadolinium anomaly[19].

The aim of this study is to monitor the content of anthropogenic Gd in various samples originating from vineyards (soil, leaves and berries of the grapevine, and wine) in the Czech Republic (Bohemia and Moravia).

2 Experimental

2.1 Samples and preparation

Four types of samples were selected for the purposes of this work, namely vineyard soil, leaves and berries of grapevine, and wine. Samples were taken from the wine-growing regions of Moravia (BEN, IVI, KOS, MEL) and Bohemia (HAN, KOC), from three wine-growing sub-regions (velkopavlovická, mikulovská and mělnická), from three wine-growing villages (Hustopeče, Pouzdřany and Kutná Hora). Sampling took place at six wineries. The comparative sample (KRE) was taken in the private garden of a University of Pardubice employee. Table 1 summarises the list of samples, their origin and describes the individual fertilisation of soils and spraying of grapevine leaves.

Table 1: List of samples, their origin and description

Sample	Village (region)	Variety	Soil fertilisation	Spraying grapevines
BEN	Pouzdřany (M)	RS, MP	organic, industrial	fungicides, herbicide, fertiliser
HAN	Kutná Hora (B)	Pa, SZ, Dr, RM	organic	fungicides, fertiliser
IVI	Hustopeče (M)	RR, RS, Fr, RM	industrial	fungicides
KOC	Kutná Hora (B)	De, RB	organic, green	fungicides, herbal extracts
KOS	Hustopeče (M)	RR, Fr	organic, industrial	fungicides, fertiliser
MEL	Hustopeče (M)	RR, Fr, RM	without fertilisation	fungicides
KRE	Pardubice (B)	unknown	organic	fungicides

De - Děvín, Dr - Dornfelder, Fr - Blaufränkisch, MP - Blauer Portugieser, Pa - Pálava, RB - Pinot Blanc, RM - Pinot Noir, RR - Riesling, RS - Pinot Gris, SZ - Silvaner; M - Moravia, B - Bohemia

Sampling took place in two stages. The first stage took place in the autumn of 2019, when samples of vineyard soil and grapevines (leaves, berries) were taken. The second stage took place in the winter of 2019/2020 when young wines of the year 2019 were sampled. The wines were made from varieties selected in the first phase and were taken in PE bottles (100 ml per sample). Soil sampling (500 g per sample) was performed from two depths (0 to 30 cm, 30 to 60 cm), each at opposite ends of a row of one variety. Samples of leaves, blade and petiole (approx. 5 to 7 pieces per sample) and samples of berries (1 to 2 bunches of grapes per sample) were taken above the soil collection point. All samples were stored in PE bags. A total of 70 soil samples, 35 leaf samples, 35 berry samples and 15 wine samples were collected. Soil samples were dried at room temperature with air and stored in PE bags. Leaf samples were dried in paper bags in a laboratory oven UM 400 (Memmert, Germany) at 60 °C for 48 hours. The dried soil and leaf samples were stored in a dark place at room temperature. Samples of berries and wines were stored in a freezer at −18 °C.

All samples were prepared for analysis in duplicate. The dried soil samples were homogenised and sieved on a sieving apparatus AS 200 (Retsch GmbH, Germeny) using a 2 mm sieve. Particles larger than 2 mm were removed. The extraction with dilute nitric acid (2 M) according to the legislation of the Czech Republic was used for sieved soil samples[20]. An exact sample weighing about 10 g was inserted into a 250 ml PE closable bottle, 100 ml of 2 M HNO_3 was added, shaken by hand and left for 16 hours at room temperature. Then it was extracted for 60 minutes on a rotary shaker RSR 01 (Labio, Czech Republic). The suspension was filtered into a dry 100 ml PE closable bottle. Samples were diluted 100-fold with ultra-pure water prior to analysis.

The dried leaf samples (blade and petiole) were crushed first by hand and then in a mortar. The crushed leaves were sieved with a fine tea sieve. The obtained powder was transferred to a resealable PE bag and homogenised. Samples of stemless berries were transferred to Petri dishes and lyophilised in a lyophiliser L4-110 (Gregor Instruments, Czech Republic) at 0.015 hPa and −110 °C for 22 hours. After drying, the berries were crushed in a mortar and homogenised. They were stored in PE bags. Microwave decomposition of leaf and berry samples and reference material were performed in DAC-100S digestion vessels with the Multi Tube system using the Speedwave XPERT Microwave Digestion System (Berghof GmbH, Germany). About 0.1 g of sample was weighed and 2.5 ml of sub-boiled HNO_3 (65%) was added to the insert. To the Teflon digestion vessels, 20 ml of 65% HNO_3 and three 10 ml inserts with sample and digestion reagent were added. The cooled digested sample was transferred to a 25 ml volumetric flask and then stored in 50 ml PE sealable bottles. Leaf and berry samples were not further diluted for analysis.

Wine samples were thawed and tempered to room temperature before analysis. For analysis, the samples were diluted ten times with ultra-pure water.

2.2 Reference materials and spikes

The validity of the analytical results was verified using certified reference materials (CRMs) GBW 10052 Green Tea, GBW 07603 Bush Twigs and Leaves (GBW, China) and BCR 679 White Cabbage Powder (IRMM, Belgium). CRMs were mineralised and treated in the same manner as grapevine samples. Enriched samples (spikes) were also used.

2.3 Reagents and standards

All the reagents used were of analytical-reagent grade. Distilled water was further purified using the Ultra Clear GP TWF UV UF TM ultra-pure water preparation equipment (Evoqua Water Technologies, Germany). HNO_3 (65%) (Lach-Ner, Czech Republic) was distilled in sub-boiling distillation equipment BSB-939-IR (Berghof GmbH, Germany).

For instrument calibration and sample spiking, the commercially available multi-elemental stock standard solution M008 (Analytika, Czech Republic) containing 100 mg L^{-1} of elements "A" (Ce, La, Nd, Pr) and 20 mg L^{-1} of elements "B" (Dy, Er, Eu, Gd, Ho, Lu, Sm, Tb, Tm, Y, Yb) and single-element standard solution 1.000 ± 0.002 g L^{-1} of In (SCP Science, Canada) were used. Ethanol (96%) (Lach-Ner, Czech Republic) was used for calibration solutions for wine sample analysis.

For analysis of all types of samples, the multi-element standards containing 10, 5, 1, 0.5, 0.1, 0.05, 0.01 μg L^{-1} of elements "A" and 2, 1, 0.2, 0.1, 0.02, 0.01, 0.002 μg L^{-1} of elements "B" were used. Sub-boiled 65% HNO_3 was added to the calibration solutions and blanks with a final concentration of 100 μl per 10 ml of solution for stabilization. For the wine samples analysis, calibration solutions were prepared with the addition of 96% ethanol with a final content of 0.15 ml per 10 ml. Each of the blanks, standards, spikes and samples contained an internal standard In in the final concentration of 1 μg L^{-1} (leaf, berries, wine) and 5 μg L^{-1} (soil). Ultra-pure water was used to prepare all solutions.

2.4 Instrumentation

Elemental analysis of the samples, standards, spikes and CRMs was performed using the ICP orthogonal acceleration time-of-flight mass spectrometer (ICP-oa-TOFMS) OptiMass 9500 (GBC, Australia) equipped with a concentric nebuliser coupled with a temperature controlled cyclonic spray chamber. The operating conditions of analysis were as follows: plasma power 1 200 W; plasma, auxiliary and nebuliser gas flow rates were 12, 0.55 and 0.91 L min^{-1}, and multiplier gain 2700 V. The external calibration with the internal standard In was used for quantification. Five-second data acquisition time and three replicates were used for measurement. Selected unwanted ranges of m/z were excluded from detection using the device "smart gate". Working isotopes (^{89}Y, ^{139}La, ^{140}Ce, ^{141}Pr, ^{146}Nd, ^{147}Sm, ^{153}Eu, ^{158}Gd, ^{159}Tb, ^{163}Dy, ^{165}Ho, ^{166}Er, ^{169}Tm, ^{173}Yb, ^{175}Lu) were selected with regard to possible isobaric overlaps of interfering ions with the same mass. The selection of isotopes was done using a mass spectrum of samples and the spectral library of ICP-oa-TOFMS.

3 Results and discussion

The aim of this work was to monitor the content of anthropogenic Gd and the presence of gadolinium anomaly in samples from vineyards from the Czech Republic. A significant part of the work was design of experiment, i.e. suitable analytical procedures for sampling, preparation and the analysis of samples (soil, leaves and berries of grapevine, and wine). The sample set represented a large and diverse group. The preparation of each sample type for analysis and the ICP-MS analysis itself had to be optimised.

3.1 Validation and analytical performance

Before processing the samples, it was necessary to verify the reliability of the methods prepared for the analysis of soil, leaves and berries of grapevine, and wine. The ICP-MS technique requires more attention during operation, so it is necessary to include elements of quality control (recalibration, control samples) more often. The methods were validated using CRMs. Long-term repeatability and recovery of analyses were also monitored. Instrumental detection limits and detection limits of individual methods were determined.

The results of analyses of the CRMs were compared with the values given in the certificates. The experimentally found values matched the certified values declared by the

manufacturer. The recoveries for REEs were found from 80 to 119 %. Furthermore, standard addition method was used to assess the reliability of the method. The verification was performed for soil samples (KOS RR 1. OD 30-60, MEL RM 2. OD 30-60), for leaf samples (HAN RM 2. OD, KOS RR 2. OD) and wine samples (HAN RM, IVI RR). The recoveries ranged from 80 to 120 %.

Long-term repeatability and recovery of ICP-MS analyses were verified by analysis of calibration standards. The recovery of the analyses results was expressed as the ratio of the found and theoretical concentration and ranged between 80 to 119 %. Long-term repeatability expressed as relative standard deviations (RSD) was from 0.4 to 12 %.

Instrumental limits of detection (0.1 to 2.4 ng L-1) and limits of detection and determinability of procedures for all sample types were determined. The method used was sufficiently reliable and sensitive for the determination of the selected elements in selected types of samples.

3.2 Gadolinium anomaly

The gadolinium anomaly was observed in samples of soils, leaves and berries of the grapevine, as well as in wine. The observed REE contents were normalised to the PAAS geological standard[21] and the Gd content of natural origin was determined using equations (1) and (2). Table 2 summarises the gadolinium anomaly for soil, leaf, berry and wine samples for individual samples.

The mean gadolinium anomaly was 1.75 for soil samples, which is slightly higher than the 1.5 threshold[22] and these values differ to a statistically significant extent (p-value 0.000 0). In a study by Bendakovská et al., a gadolinium anomaly of 3.1 to 3.4 was found for surface waters[5]. Bendakovská determined the gadolinium anomaly for water (3.31) and sediment (2.30) of Matiční Lake in Pardubice[23]. Our values are lower than those reported by Bendakovská in both works. Intervals of gadolinium anomaly values for other sample types were wide. They ranged for leaf samples from 3.07 to 21.5, for berry samples from 3.80 to 19.1, and for wine samples from 5.01 to 23.5.

Differences in the gadolinium anomaly were found in the grapevine plant in the area of Kutná Hora and in Moravia (p-value 0.000 0). No statistically significant differences were found for these localities in the gadolinium anomaly for soil (p-value 0.355 0), berries (p-value 0.095 7) or wine (p-value 0.709 5). It can be assumed that the amount of Gd stored in the plant depends on the accepted chemical form of Gd.

Figure 1 shows graphs of normalised REE concentrations in all samples for soils, leaves, berries, and wine. It is possible to observe an increase in Gd concentration compared to other REEs. This phenomenon is due to the presence of anthropogenic Gd in all types of samples.

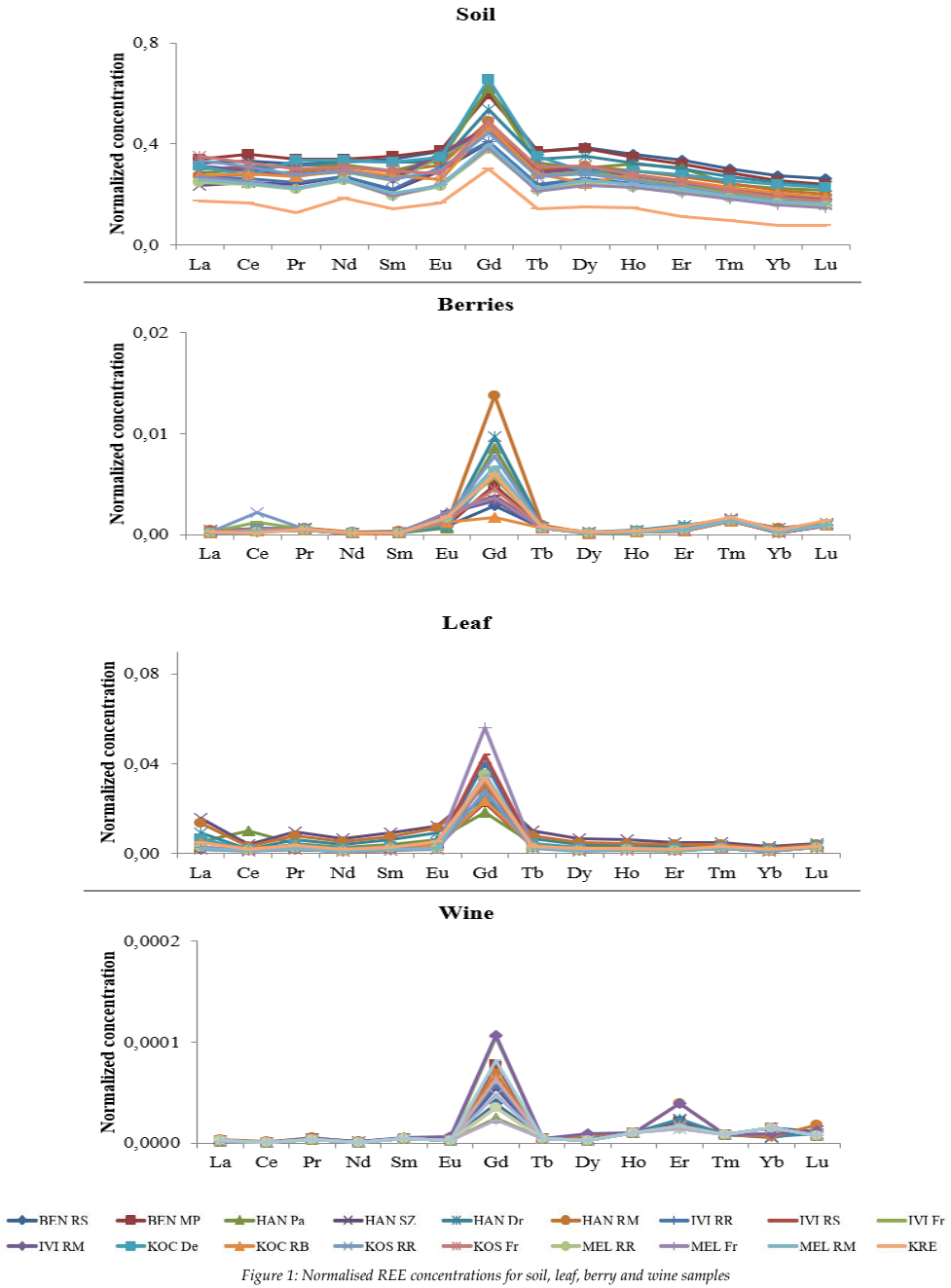

Figure 1: Normalised REE concentrations for soil, leaf, berry and wine samples

Table 2: Gadolinium anomaly values for soil, leaf, berry and wine samples

Sample	Gadolinium anomaly			
	Soil	Leaf	Berries	Wine
BEN RS	1.70	13.6	6.15	8.83
BEN MP	1.63	8.08	10.6	17.5
HAN Pa	1.97	4.32	17.6	5.46
HAN SZ	1.79	3.07	10.7	12.1
HAN Dr	1.60	3.92	17.8	15.0
HAN RM	1.66	3.87	19.1	15.4
IVI RR	1.75	16.3	7.1	13.1
IVI RS	1.65	20.0	8.7	7.83
IVI Fr	1.71	14.2	10.5	23.5
IVI RM	1.65	13.2	6.86	22.3
KOC De	1.90	6.11	13.2	
KOC RB	1.68	7.11	3.80	
KOS RR	1.67	13.9	14.6	10.8
KOS Fr	1.60	14.9	9.26	14.2
MEL RR	1.81	13.9	13.6	7.88
MEL Fr	1.86	21.5	7.55	5.01
MEL RM	1.82	14.9	14.2	18.2
KRE	2.13	11.1	11.0	

4 Conclusion

In the study, the gadolinium anomaly as indicator of the presence of anthropogenic gadolinium was observed for 70 soil samples, 35 leaf samples, 35 berry samples and 15 wine samples from Bohemia and Moravia from the Czech Republic. 15 REEs (Ce, Dy, Er, Eu, Gd, Ho, La, Lu, Nd, Pr, Sm, Tb, Tm, Y, Yb) were monitored. The average value of the gadolinium anomaly of all soil samples was 1.75, which is a slightly higher value compared to the threshold value of 1.5 reported in the literature. The obtained data were compared with available studies from the Czech Republic. The values of gadolinium anomaly we found for soil samples from various places in the Czech Republic are lower than the values found for surface waters and sediment in the East Bohemian region. The gadolinium anomaly values ranged for leaf samples from 3.07 to 21.5, for berry samples from 3.80 to 19.1, and for wine samples from 5.01 to 23.5.

5 References

1. GONZÁLEZ, Verónica, Davide A.L. VIGNATI, Marie-Noelle PONS, Emmanuelle MONTARGES-PELLETIER, Clément BOJIC and Laure GIAMBERINI. Lanthanide ecotoxicity: First attempt to measure environmental risk for aquatic organisms. *Environmental Pollution* [online]. 2015, 199, 139-147 [2020-11-09]. ISSN 02697491. Available from: DOI: 10.1016/j.envpol.2015.01.020
2. LI, Xiaofei, Zhibiao CHEN, Zhiqiang CHEN and Yonghe ZHANG. A human health risk assessment of rare earth elements in soil and vegetables from a mining area in Fujian Province, Southeast China. *Chemosphere* [online]. 2013, 93(6), 1240-1246 [2020-11-09]. ISSN 00456535. Available from: DOI: 10.1016/j.chemosphere.2013.06.085

3. RUÍZ-HERRERA, León F., Lenin SÁNCHEZ-CALDERÓN, Luis HERRERA-ESTRELLA and José LÓPEZ-BUCIO. Rare earth elements lanthanum and gadolinium induce phosphate-deficiency responses in Arabidopsis thaliana seedlings. *Plant and Soil* [online]. 2012, 353(1-2), 231-247 [2020-11-09]. ISSN 0032-079X. Available from: DOI: 10.1007/s11104-011-1026-1
4. SAATZ, Jessica, Doris VETTERLEIN, Jürgen MATTUSCH, Matthias OTTO and Birgit DAUS. The influence of gadolinium and yttrium on biomass production and nutrient balance of maize plants. *Environmental Pollution* [online]. 2015, 204, 32-38 [2020-11-09]. ISSN 02697491. Available from: DOI: 10.1016/j.envpol.2015.03.052
5. BENDAKOVSKÁ, Lenka, Anna KREJČOVÁ, Tomáš ČERNOHORSKÝ and Jana ZELENKOVÁ. Development of ICP-MS and ICP-OES methods for determination of gadolinium in samples related to hospital waste water treatment. *Chemical Papers* [online]. 2016, 70(9) [2020-11-09]. ISSN 1336-9075. Available from: DOI: 10.1515/chempap-2016-0057
6. GWENZI, Willis, Lynda MANGORI, Concilia DANHA, Nhamo CHAUKURA, Nothando DUNJANA and Edmond SANGANYADO. Sources, behaviour, and environmental and human health risks of high-technology rare earth elements as emerging contaminants. *Science of The Total Environment* [online]. 2018, 636, 299-313 [2020-11-09]. ISSN 00489697. Available from: DOI: 10.1016/j.scitotenv.2018.04.235
7. WEI, Binggan, Yonghua LI, Hairong LI, Jiangping YU, Bixiong YE and Tao LIANG. Rare earth elements in human hair from a mining area of China. *Ecotoxicology and Environmental Safety* [online]. 2013, 96, 118-123 [2020-11-09]. ISSN 01476513. Available from: DOI: 10.1016/j.ecoenv.2013.05.031
8. LERAT-HARDY, Antoine, Alexandra COYNEL, Lionel DUTRUCH, et al. Rare Earth Element fluxes over 15 years into a major European Estuary (Garonne-Gironde, SW France): Hospital effluents as a source of increasing gadolinium anomalies. *Science of The Total Environment* [online]. 2019, 656, 409-420 [2020-11-09]. ISSN 00489697. Available from: DOI: 10.1016/j.scitotenv.2018.11.343
9. ZARE-DORABEI, R., P. NOROUZI and M.R. GANJALI. Design of a novel optical sensor for determination of trace gadolinium. *Journal of Hazardous Materials* [online]. 2009, 171(1-3), 601-605 [2020-11-09]. ISSN 03043894. Available from: DOI: 10.1016/j.jhazmat.2009.06.044
10. GREENWOOD, N. N. a Alan EARNSHAW. *Chemie prvků*. Praha: Informatorium, 1993, Volume 2. ISBN 80-85427-38-9.
11. PANG, Xin, Decheng LI and An PENG. Application of Rare-earth Elements in the Agriculture of China and its Environmental Behavior in Soil. *Journal of Soils and Sediments* [online]. 2001, 1(124), 143-148 [2020-11-09]. Available from: DOI: 10.1065/espr2001.05.065
12. MIGASZEWSKI, Zdzisław M. and Agnieszka GAŁUSZKA. The Characteristics, Occurrence, and Geochemical Behavior of Rare Earth Elements in the Environment: A Review. *Critical Reviews in Environmental Science and Technology* [online]. 2014, 45(5), 429-471 [2020-11-09]. ISSN 1064-3389. Available from: DOI: 10.1080/10643389.2013.866622
13. BAU, Michael and Peter DULSKI. Anthropogenic origin of positive gadolinium anomalies in river waters. *Earth and Planetary Science Letters* [online]. 1996, 143(1-4), 245-255 [2020-11-09]. ISSN 0012821X. Available from: DOI: 10.1016/0012-821X(96)00127-6

14. SHERRY, A. Dean, Peter CARAVAN and Robert E. LENKINSKI. Primer on gadolinium chemistry. *Journal of Magnetic Resonance Imaging* [online]. 2009, 30(6), 1240-1248 [2020-11-09]. ISSN 10531807. Available from: DOI: 10.1002/jmri.21966
15. BELLIN, Marie-France and Aart J. VAN DER MOLEN. Extracellular gadolinium-based contrast media: An overview. *European Journal of Radiology* [online]. 2008, 66(2), 160-167 [2020-11-09]. ISSN 0720048X. Available from: DOI: 10.1016/j.ejrad.2008.01.023
16. GRÄFE, J.L., F.E. MCNEILL, S.H. BYUN, D.R. CHETTLE and M.D. NOSEWORTHY. The feasibility of in vivo detection of gadolinium by prompt gamma neutron activation analysis following gadolinium-based contrast-enhanced MRI. *Applied Radiation and Isotopes* [online]. 2011, 69(1), 105-111 [2020-11-09]. ISSN 09698043. Available from: DOI: 10.1016/j.apradiso.2010.07.023
17. XIAO, Yu-Dong, Ramchandra PAUDEL, Jun LIU, Cong MA, Zi-Shu ZHANG and Shun-Ke ZHOU. MRI contrast agents: Classification and application (Review). *International Journal of Molecular Medicine* [online]. 2016, 38(5), 1319-1326 [2020-11-09]. ISSN 1107-3756. Available from: DOI: 10.3892/ijmm.2016.2744
18. MENAHEM, Adi, Ishai DROR and Brian BERKOWITZ. Transport of gadolinium- and arsenic-based pharmaceuticals in saturated soil under various redox conditions. *Chemosphere* [online]. 2016, 144, 713-720 [2020-11-09]. ISSN 00456535. Available from: DOI: 10.1016/j.chemosphere.2015.09.044
19. RABIET, M., F. BRISSAUD, J.L. SEIDEL, S. PISTRE and F. ELBAZ-POULICHET. Positive gadolinium anomalies in wastewater treatment plant effluents and aquatic environment in the Hérault watershed (South France). *Chemosphere* [online]. 2009, 75(8), 1057-1064 [2020-11-09]. ISSN 00456535. Available from: DOI: 10.1016/j.chemosphere.2009.01.036
20. ZBÍRAL, Jiří. *Analýza půd II: Jednotné pracovní postupy*. Brno: ÚKZÚZ, 1996.
21. PIPER, David Z. and Michael BAU. Normalized Rare Earth Elements in Water, Sediments, and Wine: Identifying Sources and Environmental Redox Conditions. *American Journal of Analytical Chemistry* [online]. 2013, 04(10), 69-83 [2020-11-09]. ISSN 2156-8251. Available from: DOI: 10.4236/ajac.2013.410A1009
22. BAU, Michael, Andrea KNAPPE and Peter DULSKI. Anthropogenic gadolinium as a micropollutant in river waters in Pennsylvania and in Lake Erie, northeastern United States. *Geochemistry* [online]. 2006, 66(2), 143-152 [2020-11-09]. ISSN 00092819. Available from: DOI: 10.1016/j.chemer.2006.01.002
23. BENDAKOVSKÁ, Lenka. *Gadolinium based contrast agents in the aquatic environment and the possibilities of their removal*. Pardubice, 2019. Disertační práce. Univerzita Pardubice, Fakulta chemicko-technologická. Vedoucí práce doc. Ing. Anna Krejčová, Ph.D.

Olive Oil Authenticity: Detection of Soft-Deodorized Oils in Extra-Virgin Olive Oils Using Metabolomic Approach

Klára Navrátilová
Vojtěch Hrbek, Kamila Hůrková, Jana Hajšlová

University of Chemistry and Technology, Prague,
Faculty of Food and Biochemical Technology, Department of Food Analysis and Nutrition

Technická 3, 166 28 Prague 6, Czech Republic
klara1.navratilova@vscht.cz

Extra-virgin olive oil represents a popular food commodity not only due to its sensory quality but also for its health-promoting effects. However, high-price with continuously increasing demand for high-quality olive oil makes it vulnerable for economically motivated fraudulent practices. This study has been focused on extra-virgin olive oil adulteration with soft-deodorized olive oils, which is recently one of the most serious olive oil authenticity issues.

Metabolomic fingerprinting (non-target screening) has been chosen as a promising strategy to discriminate between samples of extra-virgin olive oils and soft-deodorized olive oils and their mixtures. Polar (methanol-water) extracts of olive oils were investigated using ultra-high performance liquid chromatography coupled to high-resolution mass spectrometry (UHPLC-QTOF-HRMS) and subsequent chemometric evaluation of generated data was performed to construct classification models and identify marker compounds. the results showed, that deodorization process,

although performed under 'soft' conditions compared to 'classic' high temperature deodorization, induced some oxidation, and ten tentatively identified markers were mainly oxidized fatty acid derivatives.

To lower the detection limits and to investigate the possibility to target these markers with low-resolution instruments in control laboratories, all the samples were analyzed also by UHPLC-QqQ-MS/MS. Two compounds, methyl ricinoleate and unspecified oxidized derivative of oleic acid, were selected as the best markers enabling recognition of undeclared soft-deodorized olive oil addition.

Keywords: *extra-virgin olive oils, authenticity, soft-deodorization, metabolomic fingerprinting, UHPLC-HRMS*

Acknowledgement: This work was supported by METROFOOD-CZ research infrastructure project (MEYS Grant No: LM2018100) including access to its facilities and financial support was also from specific university research (MSMT No 21-SVV/2020).

Assessment of air pollution in the Czech Republic by emerging chlorinated contaminants

Ondřej Pařízek
Jakub Tomáško, Jana Pulkrabová

University of Chemistry and technology Prague,
Faculty of food and biochemical technology,
Department of food and nutrition analysis

Technická 5, 166 28, Prague 6, Czech Republic
parizekn@vscht.cz

Polychlorinated naphthalenes (PCNs), polychlorinated biphenyls (PCBs) and short-chain chlorinated paraffins (SCCPs) are listed as persistent organic pollutants (POPs) on the Stockholm convention. They can be found in various environmental compartments, including atmosphere. Air pollution might be a significant source of human exposure to these contaminants. SCCPs are suspected of having adverse effects on human health and are classified as possibly carcinogenic to humans. PCBs and PCNs are suspected of being hepatotoxic and several of the congeners exhibit dioxin-like toxicity. PCBs are considered probable human carcinogens. the aim of this study was (i) to implement the analytical procedure for the simultaneous isolation of SCCPs, 11 congeners of PCNs and 8 congeners of PCBs from filters of high volume samplers used for air sampling and (ii) to apply the newly validated method within the pilot study assessing the air pollution in two regions of the Czech Republic, the locality Litvínov (area polluted by industry) and the locality České Budějovice (reference area). Extraction of target compounds was carried out in the Soxhlet apparatus (hexane: dichlormethane, 1:1, *v*/*v*) and followed by purification on

the silica column (analytes eluted by hexane:dichlormethane, 3:1, *v*/*v*). PCNs and PCBs were then analyzed simultaneously by gas chromatography – tandem mass spectrometry in electron ionisation (GC-EI-MS/MS) and CPs were analyzed by gas chromatography – high-resolution mass spectrometry in negative chemical ionization (GC-NCI-HRMS). Limits of quantification (LOQs) were determined as 10 pg/filter (SCCPs), 0,005–0,05 pg/filter (individual PCNs) and 0,01 pg/filter (PCBs). Firstly the method was validated for both SCCPs and PCNs, recoveries determined from spiked samples ranged from 86 % to 102 % (SCCPs) and from 79 % to 120 % (PCNs). Repeatabilities were 9 % and 5–16 % for SCCPs and PCNs, respectively. Within the pilot survey, the successfully validated analytical procedure was applied to a set of 50 samples of high-volume air sampling filters collected from two localities of the Czech Republic (České Budějovice, Litvínov) at various seasons. Comparing the concentrations of aromatic pollutants air in České Budějovice was more contaminated by more than 60 % than in Litvínov. the average concentration in the air of České Budějovice was 0,013 pg/m³ for sum of detected PCNs (tri-penta congeners) and 2 pg/m³ for the sum of all indicator PCBs. However, opposite trends were found in SCCPs, in which twice as high concentrations were measured in the air from Litvínov, compared to the air from České Budějovice. the average concentration of SCCPs in the Litvínov was 119 pg/m³.

Keywords: *persistent organic pollutants, gas chromatography, ambient air*

Contamination of Urban Soils by Cd: An Example of a Coal Mining City (Shariin Gol, Mongolia)

Václav Pecina
Renata Komendová
David Juřička
Martin Brtnický

Brno University of Technology, Faculty of Chemistry, Institute of Chemistry and Technology of Environmental Protection

Purkyňova 118, 612 00 Brno, Czech Republic
xcpecina@fch.vut.cz

Cadmium is considered worldwide as one of the most common and at the same time the most dangerous pollutants from the group of heavy metals. the most common ways in which Cd can enter the environment anthropogenically include mining, coal burning, smelting or transport. Therefore, especially coal mining cities can be severely contaminated and need special attention. the aim of this study was to evaluate the pollution of urban soils (0–10 cm) by Cd in an important coal mining Mongolian city Shariin Gol using the Single Pollution Index (PI) and the Dutch Soil Guidelines target value for Cd as a background. PI values ranged from 1.10 to 2.38 with an average value of 1.82, which represents low pollution. Although the pollution of topsoil in Shariin Gol is low, it locally achieves moderate pollution (PI value is between 2 and 3). Due to the fact that mining heaps around the city have higher Cd contents (PI > 2.0), it can be expected that due to wind and wa-

ter erosion there will be continuous contamination of urban soils by transport of cadmium-contaminated material in future years, which can be further increased by active and intensive mining activities and transport. Based on the results, it can be concluded that although there is a theoretically very significant risk of pollution by Cd, the real pollution of the topsoil by this element is currently low and therefore does not pose a risk to human health and local ecosystems.

Keywords: *urban soils, heavy metals, mining, coal, Single Pollution Index*

Fast Centrifugal Partitioning Chromatography (FCPC) – Innovative Method for Separation of Biologically Active Compounds from *Cannabis*

Petra Peukertová, František Beneš, Marie Fenclová, Zuzana Bínová, Matěj Malý, Jana Hajšlová

University of Chemistry and Technology Prague,
Faculty of Food and Biochemical Technology,
Department of Food Analysis and Nutrition

Technická 5, 166 28, Prague 6, Czech Republic
peukertp@vscht.cz

Plants of the genus *Cannabis sativa* L. are unique producers of phytocannabinoids and many other bioactive compounds. In the recent decade, products based on non-psychotropic phytocannabinoid, cannabidiol (CBD), have become very popular as they are believed to provide several health benefits (e.g. antioxidant, anti-inflammatory, and analgetic effects). However, the isolation of pure CBD, free of psychotropic Δ^9-tetrahydrocannabinol (Δ^9-THC), and its precursor Δ^9-tetrahydrocannabinolic acid (Δ^9-THCA-A) which are always present, in at least small amounts, in *Cannabis* plants together with many other phytocannabinoids, is not an easy task.
In this study, we investigated the potential of Fast Centrifugal Partitioning Chromatography (FCPC), a hydrostatic version of countercurrent chromatography, to separate CBD and its precursor, cannabidiolic acid (CBDA) from other common components of hemp extract obtained by supercritical fluid extraction.

In the first phase, we experimentally determined partition coefficients (K_D) and calculated separation factors (α) for 17 phytocannabinoids in altogether 46 model immiscible solvent mixtures, UHPLC-HRMS technique was used for the analysis of individual phases. the following solvent systems were identified as the most suitable: (i) heptane:ethyl acetate:ethanol:water (3:1:3:1, *v:v:v:v*) and (ii) hexane:ethyl acetate:methanol:water (9:1:9:1, *v:v:v:v*). Both systems enabled the separation of CBD/CBDA from Δ^9-THC-like compounds and differ in their separation efficiency within individual groups of substances, which may be further of interest, depending on the specific application.

Keywords: *Fast Centrifugal Partitioning Chromatography, bioactive compounds, phytocannabinoids, UHPLC-HRMS*

The Influence of Non-canonical Structures on the P53 Isoforms Binding to DNA

Otília Porubiaková[1,2]
Natália Bohálová[2,3], *Václav Brázda*[1,2]

[1]*Brno University of Technology, Faculty of Chemistry, Purkyňova 118, 612 00 Brno, Czech Republic*
[2]*The Czech Academy of Science, Institute of Biophysics, Královopolská 135, 612 65Brno, Czech Republic*
[3]*Masaryk University, Faculty of Science, Department of Experimental Biology, Kamenice 5, 625 00 Brno, Czech Republic*

xcporubiakova@vutbr.cz

1 Introduction

Protein p53, as the most studied tumour suppressor protein, play crucial role in basic biological processes [1] by controlling the expression of target genes either by activation or inhibition of p53-responsive promoters [2, 3]. P53 isoforms are clinically relevant. It has been observed that these isoforms are differentially expressed in normal and tumour tissue [5].

The *TP53* gene is located on the human chromosome 17p13.1. By multiple promotors, alternative splicing and the internal ribosome entry site, this gene is able to create 12 different isoforms of p53 protein [4, 5]. Expression of the isoforms is regulated by alternative promoter usage and alternative splicing. The α isoform retains all the exons including exons 10 and 11, which translate the hinge and the oligomerization domain of p53. By transcription of exon 9β or the exon 9γ, created by alternative splicing, translation led to the β and γ isoforms of p53 protein. In both cases, mentioned exons have stop codons, causing C-terminal truncation of varying lengths [5].

P53 protein occupies a tetrameric conformation of four identical subunits and acts as a transcription factor [6, 7]. This protein consists of 6 domains: the two transactivation domains (TAD I and TAD II), the proline rich-domain (PRD), the DNA-binding domain (DBD or core domain), the hinge domain (HD), the oligomerization domain (OD) and the carboxy-terminal regulatory domain (CTD) [8]. We are interested in the C-terminal domain (CTD) which controls the structure and function of the entire protein [9]. The CDT recognizes and binds to damaged DNA by non-specific DNA-binding site [10, 11].

The main function of p53 protein is sequence specific binding to DNA sequence motif, composed of two decamer 1/2 -sites that can be separated by up to 13 bases. It has been observed that canonical consensus sequences are a limiting factor in the organization and number of target genes within the p53 transcriptional network. However, p53 can function also from noncanonical sequences comprising only a decamer ½-site or ¾-site, what was observed from experiments using yeast and human cell systems [12].

2 Material and methods

2.1 Preparation of plasmids

Vectors containing coding sequences of p53 isoforms were prepared by Gateway cloning system [13]. pAG414GALccdB-HA destination vector containing inducible GAL promoter and pAG415GPDccdB-HA destination vector with the constitutive GPD promoter were used. cDNA of p53 isoforms in destination vectors was isolated from *E. coli* STBL3 strain by commercial plasmid isolation kit.

2.2 Yeast strain and luciferase assay

The chosen p53 REs were cloned following Delitto Perfetto method to *Saccharomyces cerevisiae* haploid strain yLFM-ICORE (MATα leu2-3, 112 trp1-1 his3-11,15 can1-100; ura3-1; ade2::RE::pCyc1::LUC1) [14]. yLFM isogenic derivates were transformed with pAG414GAL-empty/pAG415GPD-empty as control and pAG414GAL-p53/pAG415GPD-p53 as vector for the expression of protein of interest, as described [15]. Purified transformed colonies were incubated in 120 µl of selective media containing no, medium and high percentage of galactose to induce p53 expression. Luciferase reporter assay was performed as described [12].

2.3 Statistical analysis

Data of transactivation assay were plotted as fold of luciferase induction over empty vector, with were cells that do not contain a p53 expression plasmid and were cultured under the same conditions. Mean and standards deviation of at least three biological replicates are presented. Statistical significance was evaluated using Student's t-test.

3 Results and discussion

Saccharomyces cerevisiae haploid strain yLFM-ICORE was used for deriving a panel of isogenic reporter strain.

In experiments we investigated the influence of predicted cruciform forming structures to p53 binding affinity. We cloned the chosen p53 RE sequences into yeast isogenic *S. cerevisiae* strain at chosen chromosomal location upstream of the luciferase reporter gene to measure the transactivation potential of p53 isoforms with various theoretical p53 binding affinity (ΔlogKd) and energy required for cruciform rank evaluated by Palindrome analyser [16] (*Table 1.*). The energy required for destabilization of cruciform structure is presented in ΔG column and CF rank column represent inverted repeat signature.

Table 1: Sequences and characterization of cloned p53 target sequences[17]

	Sequence		ΔlogKd	ΔG	CF rank
XA	AAACATGCCC	GGGCATGCCC	0,80	-10,48	7-0-0
TT	GGGCATGTCT	GGGCATGCCC	0,80	-18,01	9-2-1
XG	GGGCATGCCC	AAACATGCCC	0,18	-17,75	7-6-0
GCG	GGGCATGCCC	GGGCATGCCC	0,18	-16,91	10-0-1
XT	TTTCATGCCC	CGGGCATGCC	0,32	-10,00	7-0-0
WC	GGGCACGCCC	GGCATGCCC	0,32	-16,82	10-0-1
CFNO	CATGATGTGA	TCACATGATG	2.69	-17,32	10-0-0

We analysed p53-dependent transactivation activity (TA) on the luciferase reporter gene placed in specific chromatin context in yeast. P53 target sequences were cloned upstream of the luciferase gene at the ADE2 locus.

We measured transactivation potential by luciferase assay after 24 hours in the inducing media, where transcription of the p53 protein was under control of GAL1 promoter. Expression was controlled by presence of galactose in the media. We used media without galactose, with 0,008% and 0,032% of galactose which led to basal, moderate or high levels of expression (*Figure 1.*).

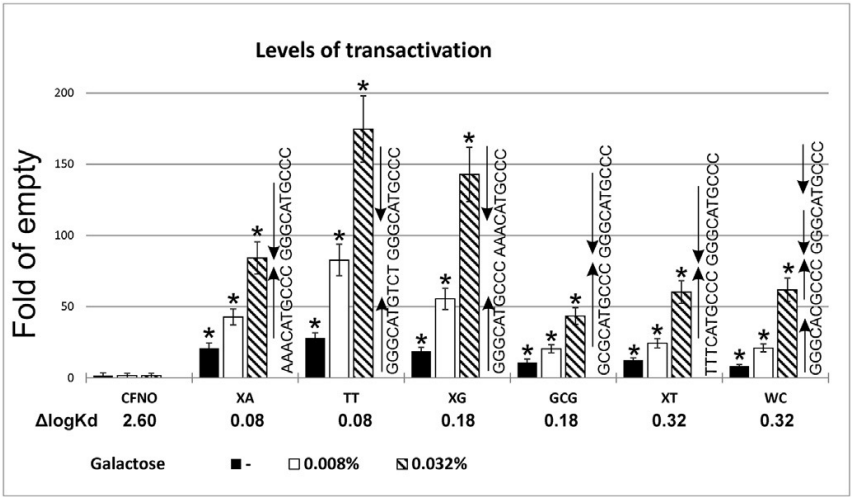

Figure 1. p53-dependant transactivation potential in modified yeast strains. P53 protein was expressed under an inducible GAL1 promoter in three different containing of galactose in the media. Graph plot represents average fold over empty vector. The significant differences are depicted by asterisk [17].

Yeast strain containing the CFNO sequence, which cannot form the cruciform structure, did not show any significant change in transactivation. We observed the significantly higher responsiveness to p53 level with constructs XA, TT and XG in comparison to other strains. It is possible to see difference in TA between XA and TT

construct despite of identical predicted binding affinity and surprisingly, higher transactivation signal for XG construct with lower predicted binding affinity (mainly for 0,032% of galactose in the inducing media).

After that we made decision to use for following experiments constructs XA and TT with the same predicted binding affinity for analysing transactivation activity of p53 protein isoforms which differ with modifications in C-terminal domain. To control level of expression, the TA was measured in media without galactose and with containing of 0,2% and 2% galactose for following higher responsiveness than in previous experiment.

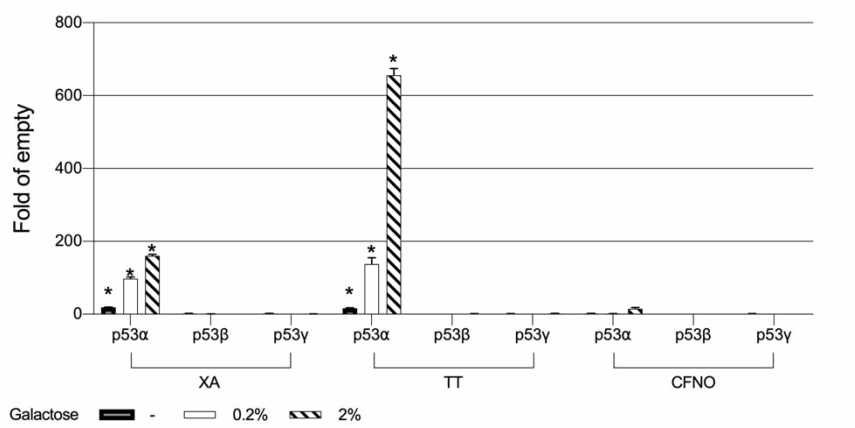

Figure 2. p53-dependent transactivation potential in yeast isogenic system. All used p53 isoforms express under inducible GAL1 promoter. The graph plot shows average fold of induction over empty vector. Here are presented the results with three levels of p53 induction measured after 24 hours of induction. The significant induction of p53 dependent transactivation (p<0,05) is indicated by asterisk.

P53α protein induced transactivation more in TT strain than in XA strain, what supported previous experiment. It was also observed, that increasing the amount of galactose in the media led to a proportional increase of transactivation of p53α isoform. This trend did not apply for isoforms p53β and p53γ, that were not able to transactivate the reporter.

Similarly, the transactivation potential of constitutively expressed p53 (GPD promoter) was significantly higher for the p53α isoform compared to the p53β and p53γ isoforms, which were not able to transactivate the reporter (*Figure 3*).

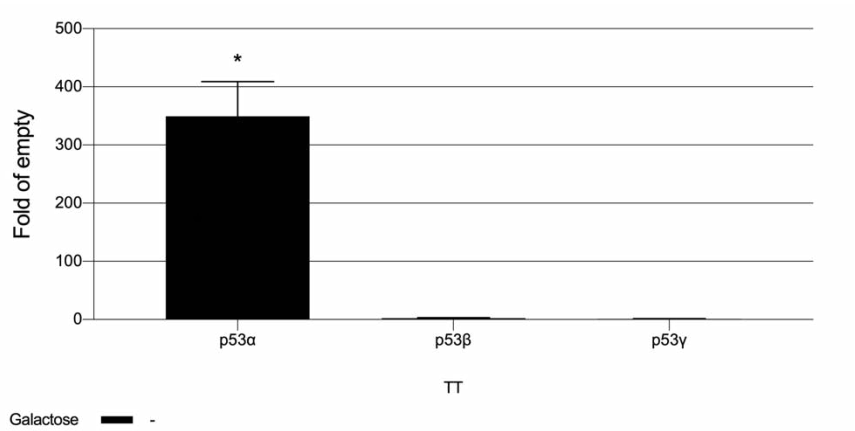

Figure 3. p53-dependant transactivation potential in yeast isogenic system. Isoforms expressed under constitutive GPD promoter were used. On the graph, fold of induction over empty vector is shown. Transactivation potential after 24 hours of induction and in media without any content of galactose was measured. The significant induction of p53 dependent transactivation ($p<0,05$) is indicated by asterisk.

To elucidate the role of inverted repeats on the transcriptional activity of p53 isoforms, we tested three yeast isogenic strains containing XA, TT and CFNO construct. All strains were co-transformed so that the activity of p53α expressed alone or combined with the other p53 isoforms could be assessed in the various reporter strains. P53α was expressed under the constitutive GPD promoter while p53β and p53γ isoforms were expressed under the *GAL1* promoter at basal, moderate and high expression (*Figure 4.*). In the media without galactose, expression of p53 isoforms is approximately same, because only p53α is expressing constitutively. With addition of galactose to the media transactivation potential was changing. Significant decreasing of transactivation potential was found for co-expressed p53β and p53γ isoforms. However, placing the potential cruciform structure upstream of the p53 RE led to changes in apparent functional interaction between co-expressed p53 isoforms.

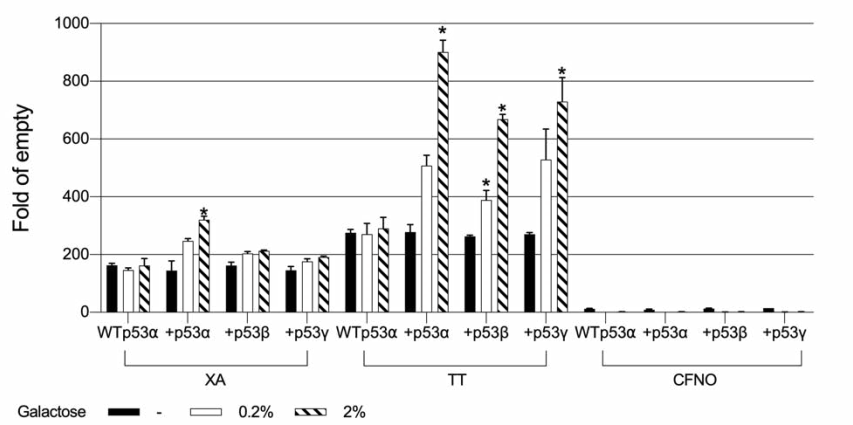

Figure 4. Influence of inducible expressed p53 isoforms on transactivation potential of constitutively expressed FLp53α. The histogram contains results of luciferase assay after 24 hours incubation on media without and with 0,2% and 2% of galactose. For measuring of transactivation activity three isogenic yeast systems were used. The significant induction of p53 dependent transactivation (p<0,05) is indicated by asterisk.

4 Discussion

Protein p53 is transcription factor that recognizes cruciform structures. These structures are important for determinants for protein-DNA binding [18].

Recently the interactions between p53 and cruciform structures has been demonstrated [17]. However, the role of these structures in regulation transcription by p53 isoforms have not been evaluated. We analysed sequences with high propensity to form cruciform structures positioned upstream of active p53 RE using yeast reporter systems.

After cloning seven designed structures, we found, that two strains considered as best predicted targets for p53 binding affinity (based on ΔKd) behave differently. Surprisingly, the strain (XG) with lower predicted binding affinity showed. Higher responsiveness as XA strain. These results suggest that p53-dependent transactivation is determined not only by the target sequence but also by local DNA structure.

For analysing of p53α, p53β and p53γ isoforms we used strains with cloned TT and XA structure. in both strains we were able to detect the expression of the reporter gene after FLp53α induction with different amount of galactose in the media. Compared to FLp53α, isoforms p53β and p53γ are modified in oligomerization domain of the protein and are not able to transactivate reporter gene alone. On the other hand, the combination of these isoforms with FLp53α caused significant decreasing of transactivation potential in both used strains.

DNA structure is an important determinant for binding of proteins [18, 19]. Cruciform structures are critically involved to initiation of replication and regulation of gene expression in different tissues. It was determined that binding of the protein will prefer to bind to DNA with prefer specific structural architecture of DNA. Natural p53 target sequences in their cruciform conformation stabilized by the DNA supercoiling may be one of the favourite elements for the effective p53-DNA binding [20]. Both the p53 target

sequence and the topological conditions thus play an important role in the p53-DNA recognition, with possible implications in the p53-controlled regulatory network. Therefore, it appears that p53 isoforms composition could be a selective determinant in p53 transactivation specificity. However, intensity of the p53 binding to p53 binding site is dependent also on the particular p53 target sequence.

5 References

1. LANE, D. P. p53, guardian of the genome. *Nature*. July 1992. Vol. 358, no. 6381, p. 15–16. DOI 10.1038/358015a0.

2. QIAN, Hua, WANG, Ting, NAUMOVSKI, Louie, LOPEZ, Charles D and BRACHMANN, Rainer K. Groups of p53 target genes involved in specific p53 downstream effects cluster into different classes of DNA binding sites. *Oncogene*. November 2002. Vol. 21, no. 51, p. 7901–7911. DOI 10.1038/sj.onc.1205974.

3. LEVINE, Arnold J. p53, the Cellular Gatekeeper for Growth and Division. *Cell*. February 1997. Vol. 88, no. 3, p. 323–331. DOI 10.1016/S0092-8674(00)81871-1.

4. KHOURY, M. P. and BOURDON, J.-C. p53 Isoforms: An Intracellular Microprocessor? *Genes & Cancer*. 1 April 2011. Vol. 2, no. 4, p. 453–465. DOI 10.1177/1947601911408893.

5. KHOURY, M. P. and BOURDON, J.-C. The Isoforms of the p53 Protein. *Cold Spring Harbor Perspectives in Biology*. 1 March 2010. Vol. 2, no. 3, p. a000927–a000927. DOI 10.1101/cshperspect.a000927.

6. VOUSDEN, Karen H. and LANE, David P. p53 in health and disease. *Nature Reviews Molecular Cell Biology*. April 2007. Vol. 8, no. 4, p. 275–283. DOI 10.1038/nrm2147.

7. JEFFREY, P., GORINA, S. and PAVLETICH, N. Crystal structure of the tetramerization domain of the p53 tumor suppressor at 1.7 angstroms. *Science*. 10 March 1995. Vol. 267, no. 5203, p. 1498–1502. DOI 10.1126/science.7878469.

8. KIM, SeJin and AN, Seong Soo A. Role of p53 isoforms and aggregations in cancer: *Medicine*. June 2016. Vol. 95, no. 26, p. e3993. DOI 10.1097/MD.0000000000003993.

9. CHILLEMI, Giovanni, KEHRLOESSER, Sebastian, BERNASSOLA, Francesca, DESIDERI, Alessandro, DÖTSCH, Volker, LEVINE, Arnold J. and MELINO, Gerry. Structural Evolution and Dynamics of the p53 Proteins. *Cold Spring Harbor Perspectives in Medicine*. April 2017. Vol. 7, no. 4, p. a028308. DOI 10.1101/cshperspect.a028308.

10. VIELER, Maximilian and SANYAL, Suparna. p53 Isoforms and Their Implications in Cancer. *Cancers*. 25 August 2018. Vol. 10, no. 9, p. 288. DOI 10.3390/cancers10090288.

11. JOERGER, Andreas C. and FERSHT, Alan R. Structural Biology of the Tumor Suppressor p53. *Annual Review of Biochemistry*. June 2008. Vol. 77, no. 1, p. 557–582. DOI 10.1146/annurev.biochem.77.060806.091238.

12. JORDAN, Jennifer J., MENENDEZ, Daniel, INGA, Alberto, NOURREDINE, Maher, BELL, Douglas and RESNICK, Michael A. Noncanonical DNA Motifs as Transactivation

Targets by Wild Type and Mutant p53. COHEN-FIX, Orna (ed.), *PLoS Genetics*. 27 June 2008. Vol. 4, no. 6, p. e1000104. DOI 10.1371/journal.pgen.1000104.

13. *User guide: Gateway Technology with Clonase II - A universal technology to clone DNA sequences for functional analysis and expression in multiple systems* [online]. 2012. Life technologies corporation. Available from: tools.thermofisher.com/content/sfs/manuals/gateway_clonaseii_man.pdf

14. LION, Mattia, RAIMONDI, Ivan, DONATI, Stefano, JOUSSON, Olivier, CIRIBILLI, Yari and INGA, Alberto. Evolution of p53 Transactivation Specificity through the Lens of a Yeast-Based Functional Assay. ROEMER, Klaus (ed.), *PLOS ONE*. 10 February 2015. Vol. 10, no. 2, p. e0116177. DOI 10.1371/journal.pone.0116177.

15. PORUBIAKOVÁ, Otília, BOHÁLOVÁ, Natália, INGA, Alberto, VADOVIČOVÁ, Natália, COUFAL, Jan, FOJTA, Miroslav and BRÁZDA, Václav.

16. BRÁZDA, Václav, KOLOMAZNÍK, Jan, LÝSEK, Jiří, HÁRONÍKOVÁ, Lucia, COUFAL, Jan and ŠŤASTNÝ, Jiří. Palindrome analyser – A new web-based server for predicting and evaluating inverted repeats in nucleotide sequences. *Biochemical and Biophysical Research Communications*. September 2016. Vol. 478, no. 4, p. 1739–1745. DOI 10.1016/j.bbrc.2016.09.015.

17. BRÁZDA, Václav, ČECHOVÁ, Jana, BATTISTIN, Michele, COUFAL, Jan, JAGELSKÁ, Eva B., RAIMONDI, Ivan and INGA, Alberto. The structure formed by inverted repeats in p53 response elements determines the transactivation activity of p53 protein. *Biochemical and Biophysical Research Communications*. January 2017. Vol. 483, no. 1, p. 516–521. DOI 10.1016/j.bbrc.2016.12.113.

18. BRÁZDA, Václav, LAISTER, Rob C, JAGELSKÁ, Eva B and ARROWSMITH, Cheryl. Cruciform structures are a common DNA feature important for regulating biological processes. *BMC Molecular Biology*. 2011. Vol. 12, no. 1, p. 33. DOI 10.1186/1471-2199-12-33.

19. BRÁZDA, Václav, HÁRONÍKOVÁ, Lucia, LIAO, Jack and FOJTA, Miroslav. DNA and RNA Quadruplex-Binding Proteins. *International Journal of Molecular Sciences*. 29 September 2014. Vol. 15, no. 10, p. 17493–17517. DOI 10.3390/ijms151017493.

20. JAGELSKÁ, Eva B., PIVOŇKOVÁ, Hana, FOJTA, Miroslav and BRÁZDA, Václav. The potential of the cruciform structure formation as an important factor influencing p53 sequence-specific binding to natural DNA targets. *Biochemical and Biophysical Research Communications*. January 2010. Vol. 391, no. 3, p. 1409–1414. DOI 10.1016/j.bbrc.2009.12.076.

Novel method for isolation of PHB from bacterial biomass

Aneta Pospíšilová,
Radek Přikryl, Ivana Nováčková

Brno University of Technology, Faculty of Chemistry

Purkyňova 188, 612 00 Brno
pospisilova-a@seznam.cz

Polyhydroxybutyrate (PHB) serves as an alternative to conventional plastics for a variety of applications. To find large-scale use, its production must be profitable, sustainable and environmentally friendly, while meeting challenging quality demands. We have developed an isolation method employing salts of fatty acids that is more economical and greener than comparable methods with other surfactants. Concentrated *Cupriavidus necator* biomass suspension is digested using small amount of sodium salts of fatty acids. After the reaction, the polymer is separated by centrifugation. the method offers several advantages over other surfactant-based methods. Other surfactants are produced from petrochemical or primary agricultural raw materials by complex multi-step processes. the sodium salts of fatty acids, on the other hand, can be obtained by a one-step reaction using a secondary feedstock (waste cooking oil). After use of other surfactants, hard-to-manage wastewater is obtained. In our method, the wastewater can be processed via simple precipitation with small amount of acid to reduce content of organic carbon, which simplifies wastewater treatment. the precipitate contains mainly fatty acids and other biomolecules and was found to be readily metabolized by the PHB-producing bacteria. Therefore, it can be

utilized in the process as co-substrate for biomass production. Furthermore, this method provides high quality PHB (purity 96%, M_w = 389 000) in high yields (99%). We used the polymer for a real-world application (3D printing) to demonstrate its applicability for material development.

Effects of microplastics to aquatic environment

Ing. Petra Procházková

Brno University of Technology, Faculty of Chemistry,
Institute of Chemistry and Technology
of Environmental Protection

Purkyňova 464/118, Brno 612 00, Czech republic
Petra.Prochazkova1@vut.cz

Plastics with their pervasive distribution are gradually becoming a global threat to the environment. Plastic items undergo slow degradation and fragmentation to smaller particles called microplastics. This is done by various factors in the environment such as sunshine, abrasion, interaction with living organisms. Microplastics can be defined as solid synthetic particles or polymer matrices with regular or irregular shape and with a size in the range of 1 μm to 5 mm. These particles are insoluble in water.

Waste water treatment plants and applications of sewage sludge are main entrance pathways of microplastics into the ecosystem. Also, the transmission of particles from their original storage (landfill, construction zone) to the environment occurs by the action of wind. Microplastics are transported different ways after entering the ecosystem. Transport routes can be divided into aquatic, terrestrial and atmospheric. Thus, the invasion of microplastic particles occurs across all ecosystems at different trophic levels.

Ecotoxicological studies of microplastics are focused to two types of compounds – to polymers and their additives and then to chemical compounds sorbed on plastic particles from the environment (metals, PCB). These compounds can be toxic, muta-

genic or endocrine disruptors. Some of these compounds may be released again either in the environment or in bodies of living organisms. These days, we deal with influence of PHB microparticles to aquatic organism *Daphnia magna* via acute and reproductive ecotoxicity tests.

Keywords: *microplastics, ecotoxicity tests, PHB*

New possibilities in the analysis of modified trichothecenes type A in oats: immunoaffinity purification and enzymatic hydrolysis

Nela Průšová, Zbyněk Džuman, Jana Hajšlová, Milena Stránská-Zachariášová

University of Chemistry and Technology Prague,
Faculty of Food and Biochemical Technology,
Department of Food Analysis and Nutrition

Technicka 3, 166 28 Prague 6, Czech Republic
Nela.Prusova@vscht.cz

In the recent years, growing attention has been paid to modified / 'masked' mycotoxins, i.e. mycotoxin conjugates which are formed during (i) plant detoxification processes, or (ii) specific food technologies. In addition to glycosides of the most well-known trichothecene deoxynivalenol (DON), the presence of mono- / oligoglycosides of other trichothecenes, e.g. HT-2 / T-2 toxins (HT-2 / T-2), has also been published so far. the presence of these modified mycotoxins in a human diet has become an issue of health concern, which is underlined also by Scientific opinion issued by European Food Safety Authority in 2017. Whereas analytical standards for mycotoxin glycosides (except DON-3-glucoside) are not available, effective strategies for their isolation and detection are of major importance. In our study, we focused on the quantification of free and modified HT-2 and T-2 in oat samples for which these contaminants are characteristic. Both direct analysis of free HT-2 / T-2, as well as indirect analysis of HT-2 after the enzymatic

hydrolysis, were utilized (the glucosidase from *Aspergillus niger* used in our work was shown to effectively cleave the glycosidic bond in HT-2 glycosides only). Altogether, 52 oat samples were processed by using our previously developed purification and pre-concentration based on the immunoaffinity chromatography cross-reacting with the HT-2 / T-2 glycosides (*Prusova et al., 2019*). the enzymatic hydrolysis was performed for the aliquot of the pre-concentrated extract. Analytical determination of both free mycotoxins, as well as their modified forms (both before and after hydrolysis), was realized by ultra-high performance liquid chromatography coupled to high resolution tandem mass spectrometry (U-HPLC-HRMS/MS). Free T-2 was quantified in all 52 samples and its monoglucoside was present in 43 samples. In the case of HT-2, free form as well as its monoglucoside was present in 48 samples, and HT-2-diglucoside was detected in 29 samples. the percentage of HT-2 originally present in the form of glycosides from the total HT-2 content ranged from 0.1% to 56%.

Keywords: *U-HPLC-HRMS/MS, modified mycotoxins, oats, immunoaffinity columns, enzymatic method*

Acknowledgements: This work was supported by the Ministry of Education, Youth and Sports (project No 8E18B045) and by Specific university research (grant No A2_FPBT_2020_061).

Reference: Prusova, N. et al. New possibilities in effective isolation of modified type A trichothecenes: survey of suitability of commercially available immunoaffinity columns. 9th International Symposium on Recent Advances in Food Analysis; Prague, Czech Republic; 5.–8. 11. 2019.

Study of the Influence of Selected Compounds on Stability of Beer Foam

Lenka Punčochářová

Brno University of Technology, Faculty of Chemistry,
Department of Food Chemistry and Biotechnologies

Purkyňova 118, 612 00 Brno, Czech Republic
xcpuncocharoval@fch.vut.cz

Beer foam as an important aspect in evaluating the beer quality is one of the qualitative parameter during beer consumption. Czech consumers prefer thick, creamy and long lasting beer foam. Beer contains various amounts of constituents that may positively or negatively influence the beer foam stability. Whereas proteins, iso-α-acids, phenolic compounds, some metal ions and polysaccharides increase formation and the stability of beer foam, e.g., lipids have the opposite effect. In this research, the relation between selected parameters (proteins, phenolic substances and bitter substances) and the beer foam stability was studied in various types of Czech beer (lager beers, lager beers originated from microbreweries and lager beers with different original gravity) and comparison of eventual differences within studied groups of Czech beer. the beer foam stability was determined by the NIBEM-T method, total protein content (PC) was determined using Hartree-Lowry method, total phenolic content (TPC) was determined according to the Folin-Ciocalteu's method. Bitter substances were determined by standard European Brewery Convention method (EBC 9.8) as bitterness of beer. Differences between tested groups of beer were evaluated by ANOVA with $\alpha = 0.005$. Within the groups of Czech beers, no statistically significant dif-

ferences were found in the stability of beer foam determined by the NIBEM method ($p = 0.3150$). A statistically significant difference was observed in total protein content between lager beers with different original gravity and other two groups of lager beers ($p = 0.0004$). All three studied groups differed statistically in total phenolic content and bitterness ($p < 0.0001$). Correlation analysis of chemical composition factors with the beer foam stability was performed. the results showed weak positive correlation between total protein content ($r = 0.40$) and beer foam stability (NIBEM 30) and very similar trend was observed for total phenolic content ($r = 0.34$). Bitterness reported slightly stronger positive correlation ($r = 0.46$). the results of this study did not indicate significant influence of the selected parameters on the stability of beer foam.

Keywords: *beer foam stability, proteins, phenolic substances, bitter substances*

Analysis of the Mixing Process Performance in Mixtures for Direct Tablet Compression Using Segregation Test

Simona Römerová
Adam Karaba, Petr Zámostný

University of Chemistry and Technology Prague, Faculty of Chemical Technology,
Department of Organic Technology
Technická 5, 166 28, Praha 6, Czech Republic
Simona.Romerova@vscht.cz

1 Introduction

Tablets are nowadays the most common solid dosage form. Mostly it is because of their easy preparation, good stability, and patient compliance. The preferred preparation process is direct tablet compression. It can provide high performance at relatively low costs. The blend for direct compression does not undergo extensive process steps (like creation of interactive mixtures during wet granulation) so high levels of homogeneity and low segregation tendencies are a necessity.

One of the main steps in a direct tablet compression process is mixing. Mixing itself can be described as a displacement of particles (molecules, crystals, etc.) relatively to each other, until the maximum level of disorder (completely random arrangement of particles) is achieved.[1-2]

During the mixing process the arrangement of particles in the blend develops with time spent in the mixer. At the beginning of the process, there is a separated (segregated) blend (Figure 1 a)). Already mixed blends can be divided into two groups: 'perfect' mixtures (Figure 1 b)), offering point uniformity, and 'random' mixtures (Figure 1 c)), where the probability of finding one type of particle at any point in the blend is equal to its proportion in it.[1]

The opposite process to mixing is segregation. During mixing, the processes of mixing and segregation always take place at the same time. The extent of segregation depends on the properties of each individual mixture. The resulting state, after the mixing is complete, is actually achieved by reaching a steady state between mixing and segregation.[3] Generally, segregation occurs when particles with different properties, such as particle size, shape or density, tends to stay in specific zones of the system (equipment, process, etc.) with higher probability. This prevents the formation of the random mixture.[3-4] Another causes of segregation could be external influences, such as air flow or vibration, which are able to set the particles in motion.[4]

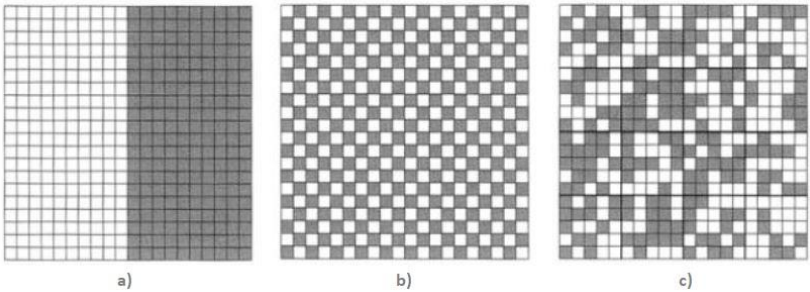

Figure 1: Mixture types (for binary particulate solids): a) perfectly segregated mixture, b) 'perfect' mixture, c) 'random' mixture.[5]

Knowing whether the mixture is prone to segregation is useful already at the beginning of the development of certain product or process. Based on these information it is possible to adjust the mixture or the whole process to minimize the segregation extent and to assure its proper performance.[4]

2 Experimental

Model mixtures with composition simulating the ones which are commonly used for direct tablet compression were prepared using different formulation processes. Each mixture was then submitted to the segregation test.

2.1 Materials

For this study a model drug (active ingredient, API), which formulation into direct compression mixtures is known to be challenging, was chosen. It comes with a variety of particle sizes and morphologies, which can greatly influence the mixing process. More specifically, in the centre of attention was API batch U800. It was mixed with excipients to create the resulting formulation. Excipients used were microcrystalline cellulose, pregelatinized corn starch, crospovidone, magnesium stearate, anhydrous colloidal silica, and yellow iron oxide. All materials were kindly provided by Zentiva, k.s., Czech Republic. Characterization of all the materials was done with the static light scattering system (Mastersizer 2000 and 3000, Malvern Instruments, UK) and with the scanning electron microscope (FE MIRA II LMU, Tescan, Czech Republic). Figure 2 illustrates morphology differences between the drug and the main excipient. All obtained characteristics for the API and most important excipients are listed in Table 1.

Table 1: Particle size and morphology of the used materials.

API batch	Particle morphology	D(10) (µm)	D(50) (µm)	D(90) (µm)
active ingredient (U800)	columnar/equant	3.1	15.2	68.5
microcrystalline cellulose	irregular equant/columnar	29.5	113.2	228.7
pregelatinized corn starch	equant	50.9	106.8	190.2
crospovidone	irregular equant	44.2	130.0	297.3

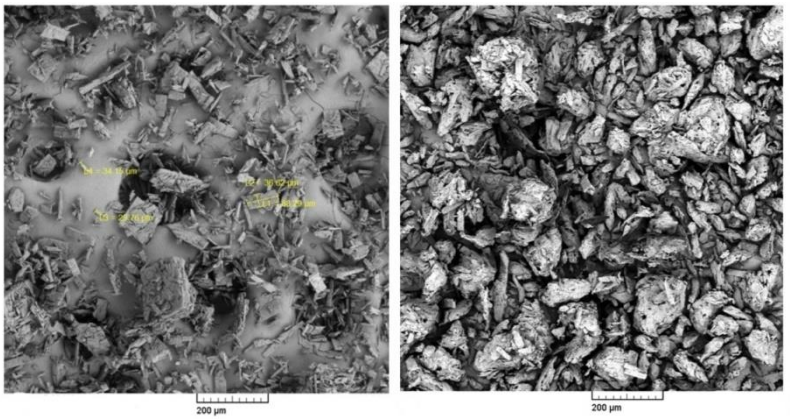

Figure 2: SEM images. Left – API, 250x mag., right – microcrystalline cellulose, 200x mag.

2.2 Blend composition and preparation

All materials were mixed together so the blend would have composition alike one of those for the low API content (5 mg/450 mg tablet) directly compacted tablets. Each prepared mixture weighed 45 g, so it sufficiently fills the segregation test equipment. Two alternative methods of blend preparation were used.

The multi-step mixing consisted of weighing smaller parts of final blend, then subjecting each one of them to sieving (AS 200, Retsch, Germany, with 710 µm sieve). After sieving, those partial blends were mixed at 55 rpm using TURBULA® T2F, Willi A. Bachhofen AG, Switzerland. Particular weights and other parameters of the multi-step mixing process are summarized in Table 2.

In contrast with the multi-step process, simple mixing without any sieve treatment was the second method of blend preparation. The first three blends from the multi-step process (Table 2) created the initial one for this case. Without any previous sieving, it was mixed for 20 minutes. Afterwards the rest of the materials were added and the whole blend was mixed for another 5 minutes. Mixing speed was also set at 55 rpm.

Table 2: Partial blends composition and mixing parameters for the multi-step mixing process.

Step	Component	Weight (g)	Mixing time (min)
1	active ingredient (U800)	2.500	20
	microcrystalline cellulose	10.000	
	anhydrous colloidal silica	0.500	
2	blend from step 1	13.000	20
	microcrystalline cellulose	10.000	
	pregelatinized corn starch	6.375	
3	blend from step 2	29.375	20
	microcrystalline cellulose	12.648	
	crospovidone	1.403	
	yellow iron oxide	0.035	
4	blend from step 3	43.460	5
	magnesium stearate	0.893	

anhydrous colloidal silica	0.648

2.3 Segregation test

The segregation test equipment was based on the utility model no. 22553[6]. It consisted of two glass tubes (elements) provided with a clutch on its bottom, regulating the movement of the material inside (Figure 3).

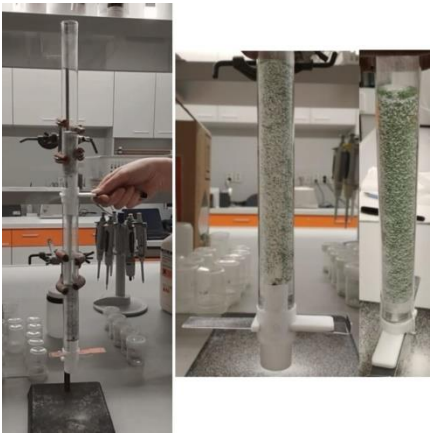

Figure 3: Segregation test equipment. Left – whole apparatus during test, right – clutch regulating the material movement – details[6].

During the test, the two tubes were placed on top of each other and the prepared blend was placed into the closed top element of experimental setting carefully, so the initial level of homogeneity after mixing has been preserved. After the upper tube was fully loaded and placed above the other one, the clutch was opened to allow the powder to flow between the elements. Once the cycle was complete, the positions of the tubes were switched, and the test proceeded into the next cycle. During predetermined cycles (usually 1st, 5th, 10th and 15th), five samples were taken to represent the composition of the mixture over the entire height of the element. This was done by opening the clutch of the upper element above a sampling container instead of the connected bottom element.

For each mixture analysis of drug content in the taken samples was done using liquid chromatography (HPLC Prominence LC 20 with PDA detector, Shimadzu, Japan).

3 Results and discussion

Two mixtures of the same composition prepared for model drug U800 through different mixing processes described in Section 2.2 were subjected to the segregation test to evaluate their segregation tendencies. For each sampled cycle of the segregation test, the dependencies of the normalized drug content on the position (height) in the column were plotted. Then a linear regression was applied to the data to acquire the values of slopes of

the lines, *K*. The *K* values were thereafter plotted against the number of performed segregation test cycles (Figure 4) to determine the value of the segregation coefficient, *KK*, by regression analysis.

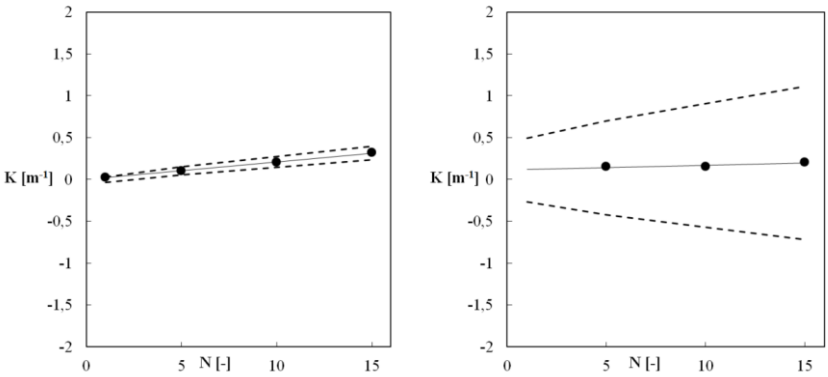

Figure 4: K values against the number of segregation cycles for batch U800 after the simple mixing (left) and the multi-step process (right). ●, experimental data; □, linear regression for determining the segregation coefficient (KK); --, confidence band.

The segregation coefficient describes the tendency of a mixture to segregate. Its negative values indicate that the API tends to collect at the bottom of the column (e.g. percolation segregation), while the positive values means that API moves to the upper part (e.g. fluidized segregation). The absolute value of the segregation coefficient then describes the extent of this segregation.

The segregation coefficient values for blends with the tested drug batch are 0.0212 ± 0.0008 m^{-1}number of $cycles^{-1}$ for the simple mixing and 0.0056 ± 0.0028 m^{-1}number of $cycles^{-1}$ for the multi-step preparation process (Figure 5).

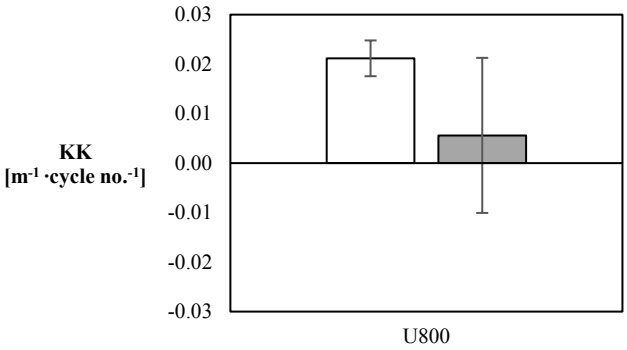

Figure 5: Measured segregation coefficients comparison. White – simple mixing, grey – multi-step preparation process.

The multi-step preparation leads to decrease in segregation extent, which is quite significant. That can be probably related to tested API batch morphology (Figure 2). The small, needle-like particles when mixed more thoroughly are prone to adhesion on the surface of the bigger excipient particles. However, during the simple mixing process they are not given enough energy to adhere on excipients. It leads to fluidization and collection of the active ingredient on the top of the mixture column. Fluidization is also a case for the particles with columnar shape. They are too big to adhere on excipients, but small enough to stay afloat longer during the powder flow, than the rest of the blend, so the fluidization segregation manifests with them, too.

For this batch the multi-step preparation process is very well justified. Segregation tendencies are effectively minimized throughout this more complicated and time-demanding process.

4 Conclusions

A simple segregation test can be a useful source of information on the true necessity of the mixing process steps in directly compressed tablets manufacturing, especially when there is a variation in the drug particle size and morphology. In this case the particle characteristics of the used batch do not simply correspond with used excipients, so the multi-step mixing process is necessary to achieve resulting tablets with sufficient content uniformity. On the contrary, the mixing process could probably be simplified, if an API with particle size close to the excipients is used, or when the amount of drug particles with different size and morphology would be different than the one presented here.

5 References

1. Hickey, A. J., *Pharmaceutical Process Engineering*. Taylor & Francis: 2001.
2. Poux, M.; Fayolle, P.; Bertrand, J.; Bridoux, D.; Bousquet, J., Powder mixing: Some practical rules applied to agitated systems. *Powder Technology* **1991,** *68* (3), 213-234.
3. Williams, J. C., The mixing of dry powders. *Powder Technology* **1968,** *2* (1), 13-20.
4. Baxter, T.; Prescott, J., Process Development, Optimization, and Scale-up: Powder Handling and Segregation Concerns. In *Developing Solid Oral Dosage Forms*, 2009; pp 637-665.
5. Jezerská, L. Získávání a zpracování pevných lékových forem. Disertační práce, VŠCHT Praha, 2008.
6. Zámostný, P.; Patera, J.; Hušková, P. Zařízení pro stanovení sklonu směsi partikulárních látek k segregaci. užitný vzor CZ 22553. 2011.

Acknowledgements: This work was supported from the grant of Specific university research (MSMT No 21SVV/2020) – grant No A2_FCHT_2020_010.

The authenticity of Poppy Seeds: How to Detect the Undeclared Hydrothermal Treatment?

Kateřina Šebelová
Monika Benešová, Lucie Chytilová, Vladimír Kocourek, Jana Hajšlová,

University of Chemistry and Technology in Prague,
Faculty of Food and Biochemical Technology,
Department of Food Analysis and Nutrition

Technická 5, 166 28 Prague 6, Czech Republic
sebelovk@vscht.cz

The adulteration of quality food poppy seeds by cheap waste seeds from pharmaceutical varieties has become a frequent practice in recent years. the pharmaceutical varieties of *Papaver somniferum* L. are characterized by high opium alkaloids content in poppy straw and, consequently, the poppy seeds surface is often fairly contaminated during latex collection. for that reason, such seeds cannot be used for human consumption, moreover, their sensorial quality is rather poor. In any case, the high content of opium alkaloids and their pattern may indicate fraud as the food poppy varieties registered in the Czech Republic never exceed the national legislative maximum limit of 25 mg/kg of morphine alkaloids in seeds. However, counterfeiters have found a way how to reduce the amount of opium alkaloids on the seeds surface. They use a process dedicated to poppy seeds "stabilization" during which are seeds exposed to high temperature and hot steam. the process is mentioned in the European Commission Recommenda-

tion 2014/662 / EU on good practices to prevent and to reduce the presence of opium alkaloids in poppy seeds and poppy seed products. Although significant seeds decontamination occurs in this way, the use of this process has to be declared on the label, which is not often the case.

This study is devoted to methods suitable for distinguishing thermostabilized poppy seeds from untreated seeds. the first method chosen was a metabolomic analysis using ultra-performance liquid chromatography with high-resolution tandem mass spectrometric detection (U-HPLC–HRMS/MS). A chemometric model capable of distinguishing thermostabilized seeds from untreated seeds and correctly classifying 100 % of samples was created. Furthermore, characteristic markers were identified. In addition, it was possible to distinguish mixtures of thermostabilized and untreated seeds mixed in different ratios. As a cheap and rapid alternative, a new method based on the Fourier-transform infrared spectroscopy (FTIR) was developed for the measurement of lipase activity in seeds. While the growing signal of the carboxylic group of successively released free fatty acid can be observed in native seed (34–163 % after 24 hours), thermostabilized samples showed no change in acid value. It was further observed, that neither the variety nor the years of harvest had a significant effect on the lipase activity. However, the possible effect of the origin of seeds was observed.

Acknowledgement: This work was supported by the OPPC (CZ.2.16/3.1.00/21537 and CZ.2.16/3.1.00/24503), NPU I LO1601, METROFOOD-CZ (MEYS Grant No: LM2018100), and by National Agency for Agriculture Research (Project no. NAZV-QK1720263).

Inorganic Thermal insulation material for masonry elements

Martin Sedlačík
Tomáš Opravil

Brno University of Technology,
Faculty of Chemistry,
Institute of Materials Chemistry
Purkyňova 464/118, 612 00, Brno, Czech Republic
xcsedlacik@vutbr.cz

With the increasing focus on energy balance of buildings and simplifying of the building construction process, hollow clay bricks with cavities filled with thermal insulating material, are finding increasing popularity in the recent years. However, all of the commercially available products use either organic insulators or a combination of inorganic material with an organic binder for this purpose. In this work, foam glass was used as an insulating filler for hollow clay bricks as a more environmentally friendly substitute of common insulators with the aim to increase longevity, recyclability and fire resistance compared to the commercially available filled masonry blocks.

Foam glass was prepared from waste packaging glass and limestone via powder sintering method. Influence of foaming agent content, water content, glass cullet particle size, foaming temperature and holding time on bulk density, pore size and morphology of foam glass samples was investigated. Possibilities of using foam glass to produce purely inorganic filled hollow clay bricks without any additional binders, by direct foaming of glass in the cavity of the brick, were investigated. Different approaches

to manufacturing thermal insulating masonry blocks by foaming of glass inside fired hollow bricks were investigated. Lastly, we successfully prepared hollow bricks filled with foam glass by direct foaming of glass in the cavity of an unfired brick using firing regime similar to that of typical masonry ceramics. Prepared foam glass showed good adhesion to the ceramic body and low bulk density.

Keywords: *Thermal insulating materials, foam glass, masonry elements*

Mixotrophic growth and increased salinity – possible tools for increasing the PHB production in cyanobacteria?

Zuzana Šedrlová
Eva Slaninová, Petr Sedláček, Ines Fritz, Stanislav Obruča.

1 Brno University of Technology, Faculty of Chemistry, Institute of Food Chemistry and Biotechnology

Purkyňova 118, 612 00 Brno, Czech Republic
Zuzana.Sedrlova@vut.cz

Polyhydroxyalkanoates (PHA) are microbial biopolymers which occur in the cell as intracellular granules and serve as a carbon and energy source. PHA have comparable physicochemical properties as some petrochemical plastics, furthermore, they are completely biodegradable. Nevertheless, PHA production is financially demanding. To reduce the price many waste products are used as input material for heterotrophic bacteria. To promote PHA production frequently it is necessary to apply some stress factors – temperature, salt, lack of nutrients, etc. the most important heterotrophic PHA producers are *Cupriavidus necator* H16 and *Halomonas halophila*.

Cyanobacteria are ecologically important prokaryotic gram-negative organisms capable of oxygenic photosynthesis. They also synthesize many secondary metabolites such as glycogen, carotenoids, but importantly also the PHA. the PHA production by cyanobacteria is time demanding and not effective enough, but the big advantage is the fact they do not require any organic substrate because cyanobacteria can fix CO_2. for PHA cyanobacterial pro-

duction only the water, some minerals, light and CO_2 are required. In this work, we employed cyanobacterial strains *Synechocystis* PCC 6803 and *Synechocystis* CCALA 192. In our study firstly we investigated the effect of NaCl in media on PHA production. Secondly, we looked into mixotrophic growth of cyanobacteria with several compounds such as acetate, propionate, glucose or their combinations. We tested the ability to produce PHB and copolymers. In the third case, we investigated the viability of PHA poor and rich cultures exposed to various stress factors to investigate the involvement of PHA in the stress response of cyanobacteria.

Funding: This study was partly funded by the project GA19 – 19-29651L of the Czech Science Foundation (GACR) and partly funded by the Austrian Science Fund (FWF), project I 4082-B25. This work was supported by Brno Ph.D. Talent – Funded by the Brno City Municipality.

Keywords: *cyanobacteria, PHA, heterotrophic, salinity*

An isolation of a protein from a wheat bran

Zuzana Slavíková
Jaromír Pořízka, Pavel Diviš

Brno University of Technology, Faculty of Chemistry,
Institute of Food Science and Biotechnology

Purkyňova 464/118, 612 00, Brno, Czech Republic
zuzana.slavikova@vut.cz

The wheat bran is an outer layer of a wheat kernel and a by-product of flour production. Annual worldwide production of the wheat bran is about 150 million tons, but only about 60 % of this amount is utilized, especially for food supplementation. Wheat bran is rich in dietary fiber, minerals, vitamins or phenolic compounds, which could be prevention of many diseases (colon cancer, cardiovascular diseases). Proteins are also valuable component of the wheat bran (about 16 wt. %). They positively influence dough properties and bread quality, which is the reason why their extraction could be profitable.

The model experiment of protein extraction from wheat bran was held in five steps. First, wheat bran proteins were released from the matrix by water (1:20), which pH was adjusted to 11 by 1M NaOH, and shaken for 30 min (100 rpm). Then the suspension was centrifuged (8000 rcf, 15 min) and the supernatant was collected. the value of the pH of the supernatant was adjusted to 4 by 1M H_2SO_4. the solution was shaken to support the precipitation of proteins and then centrifuged again. Finally, sedimented material was lyophilized, weight and amount of proteins in the material was verify by Hartree-Lowry method.

Optimalization steps of extraction were divided into 3 categories: a pre-treatment of the wheat bran, a modification of the extraction process and a modification of the precipitation. Every step was implemented to the model extraction individually. the defatting (1:3 hexane, 30, 45 and 60 °C) and the grounding of wheat brans were parts of the pre-treatment. Different extraction times (1, 2, 3 h), the temperature (30, 45 and 60 °C), the ratio of bran and extract water (1:15, 1:30) and repeated extraction (2´, 3´) are the optimalization steps of the extraction process. the modification of the temperature (-4, 4 °C) and the pH (3, 5) was the optimalization of the precipitation of proteins. After evaluation of individual steps, a combination of several steps was also realized.
With the combination of optimalization steps 81,4 ± 0,7 mg/g of material was gained and it contains over 90 % of pure proteins. the most of it was proved as digestible during the GIT simulation experiment. the most abundant amino acids are arginine and glutamic acid. According to total amino acid content, the extracted material could be considered a potential vegan food supplement.

Keywords: *Wheat bran, protein, protein extraction.*

Utilization of recycled brick waste for growing the agricultural plants

Ing. Barbora Šmírová
doc. Ing. Tomáš Opravil, Ph.D.

Brno University of Technology, Faculty of Chemistry, Institute of Materials Chemistry

Purkyňova 464/118, 612 00 Brno, Czech Republic
Barbora.smirova@vut.cz

Brick recyclate, as same as brick, excel with very high porosity. for this reason this work deals with possible implementation of plant growth aids (fertilizers) on the inside surface of such highly porous material. This work studies possibilities of preparation of brick recyclate with the content of components supporting plant growth and what is maximum amount of supporting substances, that later will be released back into surrounding enviroment (soil), is possible to incorporate into the brick recyclate. Brick recyclate is a material that can bind water in the soil and nourish cultivated plants at the same time. Brick recyclate was saturated with commercial NPK fertilizer and laboratory prepared fertilizer based on NPK. Such prepared brick recyclate was used for growth experiment on agricultural plants (tomatoes, corn). Prepared brick recyclate was subjected to x-ray diffraction, thermogravimetry and differential thermal analysis, scanning electron microscopy and energy dispersive spectroscopy analysis. Amount of available plant nutrients have been determined by ultraviolet-visible spectroscopy and inductively coupled plasma optical emission spectrometry. Subsequently, the growth course, germination and yields of selected crops were monitored. It was verified that the material

based on recycled brick enriched with nutrients improves the distribution of nutrients in the soil and positively affects the germination, growth and yields of tested crops.

Klíčová slova: *brick production, brick recyclate, sorption capatity, soil, fertilizer, nutrients for plants, agricultural plants*

Characterization of SiO_2 Nanofluid by High Resolution Ultrasonic Spectroscopy

Sarka Sovova,
Miloslav Pekar

Brno University of Technology, Faculty of Chemistry,
Institute of Physical and Applied Chemistry

Purkynova 464/118, 612 00 Brno, Czech Republic
xcsovova@fch.vut.cz

Lately, interesting properties of nanoparticles have attracted the attention of many researchers. Silicon dioxide, also called silica nanoparticles, is inorganic material widely used in biomedical fields, especially due to their biocompatibility, stability, high surface area, controllable shape, size and surface charge. High-Resolution Ultrasonic Spectroscopy is a novel non-invasive, non-destructive real-time method for characterization of molecular and micro-structural transformation in solutions or dispersions. the advantage of this technique is that the sample does not need to be transparent because the ultrasonic waves propagate through most materials. As the ultrasound wave propagate through the sample, it evaluates intermolecular forces in the sample by repetitive compression and decompression during propagation in the sample. As the sound wave causes compression and decompression of the sample, it loses part of energy. This energy loss causes lowering of sound wave amplitude. It gives the information about structural changes, ligand binding to macromolecules, association and other chemical changes of the sample. In

this work, LUDOX® colloidal silica (TM-40, HS-40, SM) water suspension of different particle size (22, 12, 7 nm) and concentration range (0–30, resp. 40 wt%) was studied by High-Resolution Ultrasonic Spectroscopy and DSA 5000 M Density and Sound Velocity Meter. Also, their interactions with representative proteins were investigated. the effect of temperature, 25 and 37 °C, on nanoparticles properties was studied.

Keywords: *Silicon dioxide, LUDOX®, High-Resolution Ultrasonic Spectroscopy, density*

Determination of biogenic amines in Swiss and Dutch type cheeses

Michal Sýkora
Eva Vítová, Agnieszka Pluta-Kubica

Brno University of Technology, Faculty of Chemistry,
Institute of Food chemistry and biotechnology

Purkyňova 464/118, Brno 612 00
xcsykoram@gmail.com

HPLC is well-established technique in the analysis of food biogenic amines, usually performed for qualitative analysis. This project presents an elaboration of several Edam and Emmental type cheeses to quantify biogenic amines that are typical in the dairy products and an evaluation of suitability of this technique to detect adulteration of dairy products. Compounds representing main biogenic amines of the dairy products were investigated: 2-phenylethylamine, cadaverine, histamine, putrescine, spermidine, spermine, tryptamine, tyramine. Amongst analyzed cheese were found significant differences in the content of cadaverine, histamine, putrescine, and tyramine. the sample from German manufacturer showed an increase of cadaverine and putrescine by a factor of 8 and 10 respectively, yet the lowest total content of biogenic amines. the Edam samples review uncovered comparable content of cadaverine, 2-phenylethylamine, spermine and spermidine from all the polish producers. Significant differences were found within all the samples, which endorses the possibility to establish an adulteration pursuit model.

Keywords: *Biogenic Amines, second keyword: Cheese*

Study of Liposomes Membrane Properties by Fluorescence Spectroscopy

Jana Szabová
Filip Mravec

Brno University of Technology, Faculty of Chemistry,
Institute of Physical and Applied Chemistry

Purkyňova 464/118, 612 00, Brno, Czech Republic
Jana.Szabova@vut.cz

Liposomes are biocompatible and biodegradable vesicles composed from lipids with size range from nm to μm. They are considered as a safe drug delivery system for hydrophobic or hydrophilic drugs. Hydrophobic drugs are stored in the liposomes membrane (hydrocarbons tails) and hydrophilic in the cavity of vesicles (water). Leakage of encapsulated or incorporated drugs from liposomes is influenced by membrane properties. To prevent this leakage, it is important to understand membrane fluidity (viscosity) and its phase behaviour. It is also necessary to found out how some components of phospholipid bilayer influence these properties. Fluorescence spectroscopy is a very useful and sensitive tool for this problematic. Laurdan is an amphiphilic probe located in the outer part of the membrane and it reacts to the fluidity of the membrane. Anisotropy of Diphenylhexatriene examines the microviscosity of the inner part of the bilayer. Both probes carry complex information about membrane properties.

Keywords: *Liposomes, Dynamic Light Scattering, Electrophoretic Light Scattering, Fluorescence Spectroscopy, Laurdan, Diphenylhexatriene.*

Contamination of Vegetable Oils by Mineral Oils and Polycyclic Aromatic Hydrocarbons: A Czech Market Survey

Jakub Tomáško
Veronika Vondrášková, Jana Pulkrabová

University of Chemistry and Technology Prague,
Faculty of Food and Biochemical Technology,
Department of Food Analysis and Nutrition

Technická 5, 166 28 Prague 6, Czech Republic
Jakub.Tomasko@vscht.cz

Mineral oils are a crude oil fraction consisting of a complex mixture of saturated hydrocarbons (MOSH) and aromatic hydrocarbons (MOAH). MOSH might pose as tumour promoters and MOAH may be mutagenic to humans, and it is therefore important to monitor their occurrence in food.

In this study, a method for the determination of MOSH/MOAH in vegetable oils using comprehensive gas chromatography coupled with time-of-flight mass spectrometry (GCxGC-TOFMS) was developed. A solid phase extraction technique with a silver modified (0.3 % *w*/*w*) silica gel as a stationary phase and a mixture of hexane:dichloromethane (3:1, *v*/*v*) as a mobile phase was used for the isolation of MOSH/MOAH from vegetable oil samples. the instrumental analysis was carried out employing 6890N GC system (Agilent Technologies, USA) coupled with Pegasus 4D (LECO Corporation, USA).

The method was validated on a sunflower oil on three different concentration levels (n=6 for each level; 25, 100 and 250 mg/kg)

spiked by mineral oil standard mixture (Type A and B for EN 14039 and ISO 16703, Sigma-Aldrich, USA). the quantification was performed using a standard addition method. the mean recoveries varied from 84 to 92 % and the repeatabilities (expressed as relative standard deviations, RSDs) varied from 7 to 19 %.

The MOSH/MOAH were determined in vegetable oils from the Czech market (n=29; rapeseed oils, n=10; sunflower oils, n=10; olive oils, n=7; blended oils, n=2). the concentrations ranged from <10 to 88 mg/kg (MOSH, which were determined above limit of quantification (LOQ) of 10 mg/kg in 10 out of 29 oils) and <0.7 to 1.9 mg/kg (MOAH, which were determined above LOQ of 0.7 mg/kg in 7 out of 29 oils). the rapeseed oils were the most frequently contaminated (6 out of 10 contained either MOSH or MOAH above LOQs). Another contaminants determined in the vegetable oils were 12 polycyclic aromatic hydrocarbons (PAHs), which are produced by pyrosynthesis from organic matter and some of them are carcinogenic. They were isolated from the lipids by gel permeation chromatography (GPC) using Bio Beads S-X3 (Bio-Rad Laboratories, USA) as a stationary phase and chloroform as a mobile phase. An ultra-high performance liquid chromatography with fluorescence detection (1290 Infinity II, Agilent Technologies, USA) was employed for the PAHs analysis. the concentrations ranged from 4 to 36 μg/kg (sum of 12 PAHs; all oils contained at least 9 out of 12 monitored PAHs above their LOQs). There was no observed correlation between MOSH/MOAH and PAHs contamination levels.

Acknowledgement: Grant of Specific university research No A1_FPBT_2020_002, METROFOOD-CZ (MEYS Grant No: LM2018100) are greatly acknowledged.

The Effect of Freezing Rate on Properties of PVA Hydrogels Prepared by Cyclic Freezing/Thawing

Monika Trudičová
Jan Zahrádka, Petr Sedláček, Miloslav Pekař

Brno University of Technology, Faculty of Chemistry,
Institute of Physical and Applied Chemistry

Purkyňova 118, 612 00 Brno, Czech Republic
xctrudicova@fch.vut.cz

Hydrogels are hydrophilic, three-dimensional networks that can absorb large amount of water or biological fluids, and thus have the potential to be used as prime candidates for biosensors, drug delivery systems, and carriers or matrices for cells in tissue engineering. Optical, mechanical, and transport properties of hydrogels are crucial for their potential applications. One of the widely used polymers for preparation of hydrogels for biomedical applications is polyvinyl alcohol (PVA). PVA hydrogels can be formed via physical crosslinking (e.g. by cyclic freezing/thawing of aqueous PVA solutions) or with a chemical cross linker (e.g. glutaraldehyd). Physically crosslinked PVA hydrogels are more suitable candidates for biomedical applications because they do not contain residues of potentially hazardous substances (e.g. crosslinkers and others). Properties of a physically crosslinked PVA hydrogel can be influenced by the concentration of PVA and by the temperature of freezing that defines the freezing rate.

This work therefore focuses on the study of changes in the optical and mechanical properties caused by the modification of

the preparation process of PVA hydrogels. the microstructure was also observed and the connection between the change in optical and mechanical properties and the change in structure were evaluated. Hydrogels in this work were prepared via cyclic freezing/thawing under different cryogenic conditions (liquid nitrogen, two different laboratory freezers and ice bath) and with different concentrations of polyvinyl alcohol (2.5 to 15 wt. %).
Rheology was the main technique to study the mechanical properties of the hydrogels. Optical properties were studied only visually because of the insufficient transparency of some samples. the microstructure of selected samples was observed by scanning electron microscopy after freeze-drying. Results showed that the concentration of polyvinyl alcohol in the hydrogel partially changes the properties of the resulting hydrogel. However, the rate of freezing has the major effect on the properties.

Keywords: *hydrogel, polyvinyl alcohol, rheology, scanning electron microscopy*

The Effect of Substitution and Aromatic Ring Condensation on the Optical Properties of Alloxazine: a Theoretical Study

Jan Truksa
Denisa Cagardová, Martin Michalík, Jan Richtár, Jozef Krajčovič, Martin Weiter, Vladimír Lukeš

Brno University of Technology, Faculty of Chemistry, Institute of Physical and Applied Chemistry
Purkyňova 464/118, 612 00 Brno, Czech Republic
xctruksa@vutbr.cz

1 Introduction

Organic molecules known as flavins, which are derived from alloxazine (**AL**), and isoalloxazine (benzo[g]pteridine, see Fig. 1), have recently gained considerable attention due to their efficient light absorption and luminescence properties[1,2]. These molecules are widely present in biological systems. Perhaps the most common is vitamin B2, riboflavin, which is a part of *e.g.* the skin and nervous system[3] and enzymatic reactions such as phototropism and phototaxis[4]. Other isoalloxazine (i**AL**) derivatives are cofactors of DNA photolyase[4]. Riboflavin has also been successfully used to treat infectious keratitis as a photoantimicrobial agent, due to its ability to generate singlet oxygen after illumination with blue visible light5.

Due to their biocompatibility and intriguing spectroscopic properties, alloxazine-based molecules are candidates for use in biosensorics and semiconductor applications, such as photovoltaics[6].

Therefore, we have decided to present a theoretical analysis of the influence of different substituents, ranging from small groups of atoms to large conjugated moieties, on the optical properties of flavins. Even if some of the presented molecules are not possible to synthesize, they can still provide an insight into the limits of alloxazine modification. So, the smallest system in this study is the native Alloxazine molecule, while the largest is a condensed Corenene derivative (**Cor**). Similarly, the $-NH_2$ and $-NO_2$ groups are used to investigate the influence of a strong electron donor or acceptor. The Lumichrome derivative has been chosen to provide a group without a significant effect on the electron density. Various heterocyclic structures have also been considered. The molecules considered in this study are shown in Fig. 1. The effect of adding linear fused rings, such as Naphthalene or Pentacene will be the object of a different study.

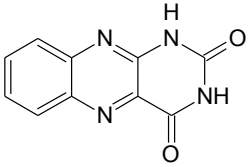

Alloxazine (**AL**)

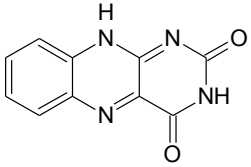

isoAlloxazine (i**AL**)

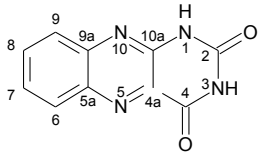

AL

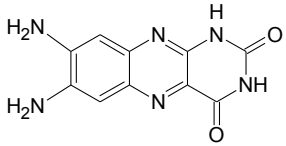

NH

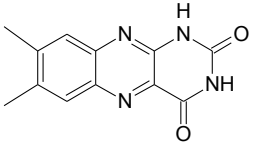

CH (Lumichrome)

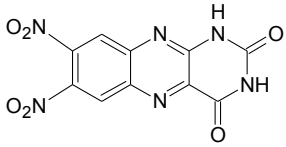

NO

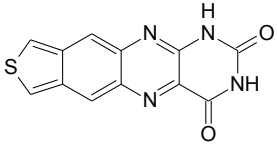

Th

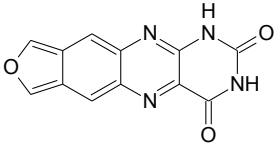

Fu

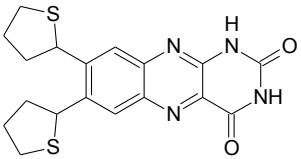

2Th

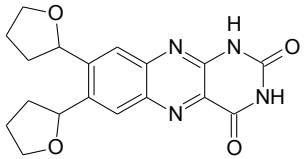

2Fu

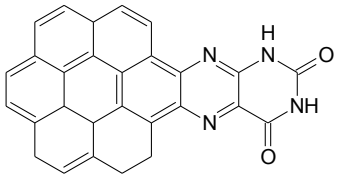

Cor

Figure 1: The structures of molecules, considered in this study. Note the special atom numbering in Alloxazine

To describe the spectroscopic properties of the studied molecules, the energies of their frontier molecular orbitals – the highest occupied (HOMO), and lowest unoccupied (LUMO) molecular orbitals. The most important descriptor will be their energy difference, denoted here as HOMO/LUMO Gap, or simply Gap. This is because the magnitude of the Gap corresponds to the energy needed to excite an electron to the LUMO orbital.

Both isomeric forms of alloxazine have been considered, since the isomerization had been shown to have a significant effect on absorption spectra. For instance, the isoAlloxazine molecule has an absorption maximum at 440 nm, compared to 380 nm for the Alloxazine. Furthermore, isoAlloxazine exhibits an order-of-magnitude greater fluorescence quantum yield[7].

The aim of this contribution is to present the spectroscopic effects of flavin modification with various moieties, and to explore trends in modification e.g. with electron donor and acceptor groups, heterocycles and fused aromatic groups.

2 Experimental

The Gaussian 09 program package was used for performing the quantum-chemical calculations[8]. The optimal geometries of studied molecules were calculated by the DFT method with the B3LYP (Becke's three parameter Lee–Yang–Parr) functional[9] without any constraints (energy cut-off of 10^{-5} kJ mol^{-1}, final RMS energy gradient under 0.01 kJ mol^{-1} A^{-1}). If multiple conformations with respect to the spatial orientations were possible, the ones with minimal steric repulsions and most intramolecular hydrogen bonds were considered. The 6-31+G* basis set of atomic orbitals was applied[10]. In pursuance of optimized B3LYP geometries, the vertical singlet transition energies and oscillator strengths between the initial and final electronic states were computed by time dependent (TD)-DFT method[11]. For the sake of simplicity, the molecules were modelled in the gas phase.

3 Results and Discussion

The orbitals, taking part in the dominant absorption band of each molecule are shown in Table 1. Their respective energy gaps, the wavelengths λ of the strongest predicted absorptions and corresponding oscillator strengths, denoted by *f*, are shown in Table 2. For the simple **AL**, **NH**, **CH** and **NO** molecules, the strongest transitions correspond to HOMO − 1/LUMO transitions in the Alloxazine form, and HOMO/LUMO transitions in the isoAlloxazine form.

Since the energy difference of LUMO and a lower occupied orbital is greater than the Gap, it makes sense that only light with a higher energy – therefore lower λ – would be able to excite the electron. This explains why the spectrum of Alloxazine is blue shifted with respect to isoAlloxazine. The strongest absorptions typically correspond to HOMO/LUMO transitions.

The case of the heterocyclic compounds is slightly more complicated. The oxygen-containing molecules **Fu**, i**Fu**, **2Fu**, i**2Fu** all have the strongest transitions between the HOMO − 1/LUMO orbitals. Indeed, the dominant absorption bands of these molecules are all the same, except for i**Fu**.

Table 1: The orbitals, participating in the strongest absorptions

Molecule	Dom. transition	Molecule	Dom. transition
AL	HOMO − 1/LUMO	**iAL**	HOMO/LUMO
NH	HOMO − 1/LUMO	**iNH**	HOMO/LUMO
CH	HOMO − 1/LUMO	**iCH**	HOMO/LUMO
NO	HOMO − 1/LUMO	**iNO**	HOMO/LUMO
Th	HOMO − 1/LUMO	**iTh**	HOMO − 1/LUMO
2Th	HOMO/LUMO	**i2Th**	HOMO/LUMO
Fu	HOMO − 1/LUMO	**iFu**	HOMO − 1/LUMO
2Fu	HOMO − 1/LUMO	**i2Fu**	HOMO − 1/LUMO
Cor	HOMO/LUMO + 1	**iCor**	HOMO − 1/LUMO

Table 2: The frontier MO energy differences, strongest excitation wavelengths and oscillator strengths of the studied molecules

Molecule	Gap (eV)	λ (nm)	*f*	Molecule	Gap (eV)	λ (nm)	*f*
AL	4.418	313	0.16	i**AL**	3.459	404	0.17
NH	3.939	354	0.24	i**NH**	3.104	436	0.30
CH	4.297	322	0.22	i**CH**	3.373	413	0.20
NO	4.214	364	0.11	i**NO**	3.437	412	0.16
Th	3.771	367	0.24	i**Th**	3.559	394	0.51
2Th	3.259	443	0.26	i**2Th**	2.826	522	0.23
Fu	3.942	357	0.13	i**Fu**	3.242	413	0.36
2Fu	4.103	344	0.32	i**2Fu**	3.878	357	0.47
Cor	3.813	367	0.23	i**Cor**	2.945	482	0.29

Inspecting Table 1, the HOMO − 1/LUMO Gap for i**Fu** is around 0.5 eV smaller than for **Fu**, which explains the absorption band difference.

The dominant transition in the sulfur-containing molecules **Th** and i**Th** has the HOMO − 1/LUMO character, and their absorption band difference is quite small. On the other hand, both the **2Th** and the i**2Th** molecules have a dominant HOMO/LUMO transition, and the absorption bands are therefore red shifted with respect to **Th**/i**Th**.

Finally, the Cor and iCor molecules have a dominant HOMO/LUMO + 1 transition, and a HOMO − 1/LUMO transition, respectively. The energy level differences of these orbitals explain the different absorption bands.

With regards to donor or acceptor group substitution, it appears to have a serious influence, as evidenced by the **NH**, **CH**, and **NO** molecules. Apparently, the presence of strong electron-donating or -accepting substituents lowers the energy gap, and therefore moves the absorption band to higher wavelengths. Heterocyclic electron-donating moieties, and the large conjugated aromate Coronene, have a similar effect, of comparable magnitude. However, except for iCor, the effect of substitution seems smaller in the

isoAlloxazine form. This may be explained by a lack of double bond the middle ring of the alloxazine moiety (see Fig. 1), which leads to weaker conjugation across the molecule.

While the oscillator strength of the dominant absorption in isoAlloxazine form is generally higher than in the Alloxazine form, there certainly does not seem to be a conclusive trend across all molecules. Heterocyclic derivatives have higher values of *f* than the other molecules. Table 3 shows other absorption maxima of the studied molecules. Clearly, it is possible to synthesize red light absorbing flavins by modifying the Alloxazine moiety with heterocycles.

Table 3: Other absorption maxima of the studied molecules

Molecule	λ (nm)	*f*	Molecule	λ (nm)	*f*
AL	358	0.06	i**AL**	319	0.12
NH	389	0.13	i**NH**	347	0.17
CH	366	0.06	i**CH**	327	0.16
NO	331	0.10	i**NO**	330	0.11
Th	601	0.02	i**Th**	569	0.01
2Th	357	0.26	i**2Th**	354	0.15
Fu	619	0.02	i**Fu**	577	0.01
2Fu	449	0.26	i**2Fu**	527	0.24
Cor	449	0.17	i**Cor**	517	0.04

4 Conclusion

In this study on the modification of (iso)Alloxazine molecules, the theoretical possibility of tuning the absorption properties was demonstrated. It was shown that, especially by substituting heterocycles, it is possible to cover a significant range of the visible light spectrum, up to around 600 nm. Since conjugated molecules generally have a smaller Gap, it should theoretically be possible to drive the absorption peaks even farther to the red-light range by adding a larger system of fused heterocycles to the flavin moiety. The substitution of strong electron donor and acceptor groups. The blue shift of Alloxazine molecules with respect to their isomers was explained by analyzing the computed absorption spectra and noting that different MOs take part in the excitations.

5 References

1. MARIAN, Christel M., Setsuko NAKAGAWA, Vidisha RAI-CONSTAPEL, Bora KARASULU and Walter THIEL. *Photophysics of Flavin Derivatives Absorbing in the Blue-Green Region: Thioflavins As Potential Cofactors of Photoswitches*. *The Journal of Physical Chemistry B* [online]. 2014, **118**(7), 1743-1753 [cit. 2020-11-09]. ISSN 1520-6106. Available in: doi:10.1021/jp4098233
2. KORMÁNYOS, Attila, Mohammad S. HOSSAIN, Ghazaleh GHADIMKHANI, et al. *Flavin Derivatives with Tailored Redox Properties: Synthesis, Characterization, and*

Electrochemical Behavior. *Chemistry - A European Journal* [online]. 2016, **22**(27), 9209-9217 [cit. 2020-11-09]. ISSN 09476539. Dostupné z: doi:10.1002/chem.201600207

3. Butler, BF and Topham RW. *Comparison of changes in the uptake and mucosal processing of iron in riboflavin-deficient rats*. Biochem Mol Biol Int. 1993; 30(1): 53-61
4. AI, Yue-Jie, Feng ZHANG, Shu-Feng CHEN, Yi LUO and Wei-Hai FANG. *Importance of the Intramolecular Hydrogen Bond on the Photochemistry of Anionic Hydroquinone (FADH −) in DNA Photolyase. The Journal of Physical Chemistry Letters* [online]. 2010, 1(4), 743-747 [cit. 2020-11-09]. ISSN 1948-7185. Available in: doi:10.1021/jz900434z
5. SAID, Dalia G., Mohamed S. ELALFY, Zisis GATZIOUFAS, et al. *Collagen Cross-Linking with Photoactivated Riboflavin (PACK-CXL) for the Treatment of Advanced Infectious Keratitis with Corneal Melting*. *Ophthalmology* [online]. 2014, 121(7), 1377-1382 [cit. 2020-11-09]. ISSN 01616420. Available in: doi:10.1016/j.ophtha.2014.01.011
6. IRIMIA-VLADU, Mihai, Pavel A. TROSHIN, Melanie REISINGER, et al. *Edible Electronics: Biocompatible and Biodegradable Materials for Organic Field-Effect Transistors*. *Advanced Functional Materials* [online]. 2010, 20(23), 4017-4017 [cit. 2020-11-09]. ISSN 1616301X. Available in: doi:10.1002/adfm.201090104
7. SIKORSKA, Ewa, Igor V. KHMELINSKII, David R. WORRALL, Jacek KOPUT and Marek SIKORSKI. *Spectroscopy and Photophysics of Iso- and Alloxazines: Experimental and Theoretical Study. Journal of Fluorescence* [online]. 2004, 14(1), 57-64 [cit. 2020-11-09]. ISSN 1053-0509. Available in: doi:10.1023/B:JOFL.0000014660.59105.31
8. Frisch, M.J., G.W. Trucks, H.B. Schlegel, G.E. Scuseria, M.A. Robb, J.R. Cheeseman, et.al. *Gaussian09 Revision D.01*, Gaussian Inc. Wallingford CT (2013)
9. Lee, C, W Yang and RG Parr. *Development of the Colle-Salvetti correlation-energy formula into a functional of the electron density. Phys Rev B*. 1988; 37(2): 785–789 [cit. 2020-11-09]. Available in: https://doi.org/10.1103/PhysRevB.37.785
10. HARIHARAN, P. C. and J. A. POPLE. *The influence of polarization functions on molecular orbital hydrogenation energies. Theoretica Chimica Acta* [online]. 1973, 28(3), 213-222 [cit. 2020-11-09]. ISSN 0040-5744. Available in: doi:10.1007/BF00533485
11. FURCHE, Filipp and Reinhart AHLRICHS. *Adiabatic time-dependent density functional methods for excited state properties. The Journal of Chemical Physics* [online]. 2002, 117(16), 7433-7447 [cit. 2020-11-09]. ISSN 0021-9606. Available in: doi:10.1063/1.1508368

The work has been supported by Slovak Research and Development Agency (APVV-15-0053) and VEGA 1/0504/20. V.L. thanks to Ministry of Education, Science, Research and Sport of the Slovak Republic for funding within the scheme "Excellent research teams". We are grateful to the HPC centre at the Slovak University of Technology in Bratislava, which is a part of the Slovak Infrastructure of High Performance Computing (SIVVP project, ITMS code 26230120002, funded by the European region development funds, ERDF) for the computational time and resources made available. The research was supported by Czech Science Foundation project 17-24707 S. J.T. thanks to the internal grant FCH-S-20-6340 of the Brno University of Technology. Computational resources were supplied by the project "e-Infrastruktura CZ" (e-INFRA LM2018140) provided within the program Projects of Large Research, Development and Innovations Infrastructures.

Occurrence of chlorinated paraffins in human blood serum and problems of their quantification

Denisa Turnerová
Jakub Tomáško, Jana Pulkrabová

University of Chemistry and Technology,
Prague Faculty of Food and Biochemical Technology,
Department of Food Analysis and Nutrition

Technická 5, 166 28 Praha 6, Czech Republic
turnerod@vscht.cz

Short chain chlorinated paraffins (SCCPs) and medium chain chlorinated paraffins (MCCPs) are a group of several thousand compounds of similar chemical structure. SCCPs have been classified as persistent organic pollutants. Dietary intake is considered to be the main source of exposure to SCCPs and MCCPs but another road of exposure could be inhalation. SCCPs and MCCPs have been identified in fish, vegetable oil, seeds and ither food commodities.

The aim of the study was to validate the method for the determination of SCCPs and MCCPs in human blood serum. the triple liquid-liquid extraction procedure employing extraction mixture n-hexan:diethylether (9:1, v/v) followed by purification on the SPE florisil column was applied. Final identification/quantitation of SCCPs and MCCPs were performed using gas chromatography coupled with high resolution mass spectrometry operated in negative chemical ionization.

The method validation was performed at 3 concentration levels 3000, 15000 and 35000 ng/g lipid weight (lw). Recoveries of SC-

CPs and MCCPs ranged from 98 to 130 % and from 80 to 113 %, respectively. Repeatabilities of both groups of CPs were in the range 8–20%. the successfully validated analytical method was used for analysis of 274 human blood serum samples collected in two sampling periods (142 samples in spring and 132 samples in autumn) in three regions of the Czech Republic (Prague, Ostrava and České Budějovice.). These samples were obtained from police officers participating in the project „Healthy Aging in Industrial Environment". Concentrations of SCCPs in the serum samples in both the 1st round and the 2nd round range between <100–3019 ng/g lw (median 464 ng/g lw) and <100–2748 ng/g lw (median 120 ng/g lw), respectively.

The quantification of MCCPs in some human serum samples was a challenging task. In 38 serum samples collected within the 1st sampling period an amount of MCCPs was below limit of quantification. for 41 serum samples the response of MCCPs was out of a calibration curve and thus could not be quantified. Just in 63 serum samples the concentration of MCCPs could be calculated. These samples were divided into two groups based on the chlorine content and the results of samples from group 1 were several times higher than in 2nd group. This problem with MCCPs specific congener identification and quantitation could be caused by different congeners C_{16} and C_{17} profile in samples and standards. the solution would be the application of well characterizes standards which are unfortunately not currently commercially available.

Can high-resolution mass spectrometry (HRMS) –based metabolomics be used for a varietal classification of wines?

Leos Uttl
Vaclav Kadlec, Zbynek Dzuman, Mona Ehlers, Carsten Fauhl-Hassek, Jana Hajslova

University of Chemistry and Technology,
Faculty of Food and Biochemical Technology,
Department of Food Analysis and Nutrition

Technicka 5, 166 28 Prague 6, Czech Republic
uttll@vscht.cz

Wine is one of the most popular alcoholic beverages in many countries worldwide. However, due to its great financial value and relatively large amount produced, it is also one of the most common commodities which are subject to fraud and mislabelling. Several wine attributes can be adulterated including geographic origin, harvest year, variety from which it was prepared etc. Therefore, in the last few years, there has been growing interest in developing analytical methods for wine authentication. While analytical methods for the identification of wine by geographical origin exist and are implemented in official control, a sufficiently reliable strategy for authentication of wine variety is still missing.

Considering the complexity of wine matrix, metabolomic fingerprinting in combination with sample direct injection (without prior extraction), was selected as a suitable tool to address this challenging task. As an analytical platform, U-HPLC-Q-Orbitrap instrument (Q-Exactive Plus) was used. In total, 61 authentic samples

of three different wine varieties (obtained in cooperation with German Federal Institute for Risk Assessment, Berlin) were analyzed within our study. the generated data, after automated data mining and alignment, were processed by principal component analysis (PCA) and then by partial least squares discriminant analysis (PLS-DA). Statistically significant variables important for the grape variety classification were chosen according to their VIP (variable importance in projection) score. the resulting statistical models were validated and assessed according to their R2 (cum) and Q2 (cum) parameters. the most promising model enabled successful classification of 96 % of wine samples. In addition, tentative identification of the variable with highest VIP score (3-O-Caffeoylquinic acid, $C_{16}H_{18}O_9$, also possible: 4-O-, 5-O-) was performed. Our results indicate that the metabolic fingerprinting of wine samples might be used as an effective tool for variety authentication.

Keywords: *wine, authentication, metabolomics, mass spectrometry*

Acknowledgement: This work was supported by specific university research (MSMT No 21-SVV/2020) and METROFOOD-CZ research infrastructure project (MEYS Grant No: LM2018100) including access to its facilities.

Utilization of Mica Separated from Washed Kaolin

Ing. Josef Vaculík
doc. Ing. Tomáš Opravil, Ph.D.

Brno University of Technology,
Faculty of Chemistry,
Institute of Materials Chemistry

Purkyňova 464, 612 00 Brno Medlánky, Czech republic
xcvaculikj@vutbr.cz

This paper aims to laboratory test the possibilities of utilization mica separate, which arises during the process of floating kaolin as a by-product together with sand, which is not widely used today. Mica and sand are then separated by flotation or vibration. the mica separate thus formed was subjected to analysis. XRD and heating microscopy methods were used for analysis. XRD analysis detected multiple phases, such as quartz, kaolinite, muscovite and couple of feldspar (orthoclase, albite). Subsequently, experiments with mica separation as a filler in composites based on epoxy resins were set up and performed. Furthermore, the separate was tested as a part of plasters and visual building elements. Last but not least, the separate was mixed into the ceramic, which was then subjected to firing in the selected mode and XRD analysis was also performed on fired samples with ceramic. This paper provides a comprehensive overview of the above-mentioned possibilities of using mica separation, which is based on a sufficient amount of experimental data.

Keywords: *mica, muscovite, floating kaolin, mica separate, ceramic, composites, plasters*

Antidepressants and Anxiolytics in the Environment

Petra Venská[1], Martina Repková

Brno University of Technology, Faculty of Chemistry, Department of Chemistry and Technology of Environmental Protection

Purkyňova 464/118, 612 00 Brno, Czech Republic
1xcvenska@vutbr.cz

Antidepressant and anxiolytics are groups of psychoactive pharmaceuticals that represent a serious environmental risk when released to the water streams. Increased consumption of antidepressants and anxiolytics leads to the potential effect on non-target organisms such as changes in food and reproductive behaviour, socialisation or boldness. These changes can lead to reduced survival chances in aquatic organisms as well as some birds or mammals.

Growing consumption of these pharmaceuticals is a world-wide problem since effects on non-target animal were observed all around the world – in fresh and marine water. In the Czech Republic, antidepressants rank high on the list of most commonly prescribed drugs and in our environment behaviour-changing concentrations of anxiolytics were already detected. Our wastewater treatment plants (WWTP) are not constructed to effectively remove these substances from waster. Small streams and its organisms are more endangered because there is not so much dilution in the effluent from the WWTP. Also, small villages tend to use alternative wastewater management systems and – for example – root zone wastewater treatment plants seem to have no removal

efficiency. So far, there are only a limited number of economically meaningful solutions to eliminate antidepressants from water.

Keywords: *Antidepressants, Anxiolytics, Advanced Oxidation Processes, Psychoactive pharmaceuticals*

Use of a pilot scrubber separation device for specific pollutant in the air

Jaroslav Vlasák
Tomáš Svěrák, Ondřej Krištof, Josef Kalivoda, Petr Horvát

Brno University of Technology, Faculty of Chemistry,
Institute of Materials Science

Purkyňova 464/118, 612 00 Brno, Czech Republic
xcvlasakj@fch.vut.cz

Industrial gas cleaning, also called scrubber, is a basic chemical engineering issue that aims to capture gaseous components from a mixture of gases. Various physicochemical processes and biological processes are part of this issue, and one of these processes is absorption. If we talk about the process in which chemical reactions take place, we are talking about chemisorption. In general, we can separate any gaseous substance in a scrubber. This work is mainly focused on industrial waste gases. These are mainly carbon dioxide and ammonia gases. the choice of these two gases is due to current worldwide research, which proves that they are one of the most difficult gases for the atmosphere, so this work deals mainly with the problem of these gases. the economics of the operation of such a separation device also play an extremely important role, which is why our device is designed to be able to operate even in smaller companies. the goal is to find a scrubber separation device that will have perfect efficiency at the lowest possible acquisition cost. All this can be achieved with the right combination of separation liquids and a suitable design of the entire scrubbber device.

Keywords: *gas scrubber, liquid, gas, carbon dioxide, sodium hydroxide, absorption, chemisorption, ammonia,*

Police Officer Exposure to Polycyclic Aromatic Hydrocarbons in Three Locations of the Czech Republic

Veronika Vondrášková
Ondřej Pařízek
Kateřina Urbancová
Jana Pulkrabová

University of Chemistry and Technology, Prague, Faculty of Food and Biochemical Technology, Department of Food Analysis and Nutrition

Technická 3, 166 28 Prague, Czech Republic
Veronika.Vondraskova@vscht.cz

Polycyclic aromatic hydrocarbons (PAHs) are ubiquitous environmental contaminants which are formed during incomplete combustion of organic matter. the carcinogenic potential of some metabolites created in exposed organisms during metabolic processes can pose a risk to human health. the major metabolites excreted into urine are monohydroxylated PAHs (OH-PAHs) which are typically considered as biomarkers of human exposure. the aim of this study was to analyse 11 OH-PAHs in urine samples using ultra-high performance liquid chromatography coupled with tandem mass spectrometry (UHPLC-MS/MS). the urine samples were collected from Czech police officers within the HAIE project (Healthy Aging in Industrial Environment) in 2 sampling periods (*spring*, less air polluted season and *autumn*, more air polluted season). A total of 277 urine samples were collected from police officers in 3 different cities of the Czech Republic (Ceske Bude-

jovice, Prague and Ostrava). the most abundant analytes in all measured samples were naphthalene-2-ol and phenanthrene-1-ol. the analytes chrysene-6-ol and benzo[*a*]pyren-3-ol were not detected in any samples. In the 1st sampling round (*spring*) the median concentration of sum 9 OH-PAHs in the urine samples decreased in the order of: Ostrava > Ceske Budejovice > Prague (5.84 > 5.14 > 4.43 μg/g creatinine). In the 2nd sampling round (*autumn*) the median concentration of sum 9 OH-PAHs in the urine samples decreased in the order of: Ostrava > Prague > Ceske Budejovice (7.37 > 6.05 > 5.22 μg/g creatinine). In both sampling periods the highest concentrations of the 9 OH-PAHs were found in urine samples from Ostrava. In all studied locations the concentrations measured in urine samples collected in the spring were lower compared to the concentrations measured in urine samples collected in the autumn. However, a statistically significant difference (α=0.05) in the concentrations between sampling periods was observed only for samples from Ostrava. Within the HAIE project the analysis of 24 PAHs in the air from personal air samples was also performed. No significant correlation was found between concentration of PAHs in the air and their metabolites (OH-PAHs) in urine from exposed police officers. the authors would like to thank the Institute of Experimental Medicine AS CR in Prague and the University of Ostrava for providing the samples.

Keywords: *ultra-high performance liquid chromatography with tandem mass spectrometry, monohydroxylated PAHs, urine*

Utilization of Grape Seed Lignin in Polyhydroxyalkanoate Blends

Pavel Vostrejš [1, 2*]
Adriana Kovalcik [1]

[1]Brno University of Technology, Faculty of Chemistry, Institute of Food Science and Biotechnology

Purkynova 118, 612 00 Brno, Czech Republic,

[2]Brno University of Technology, Faculty of Chemistry, Institute of Physical and Applied Chemistry

Purkynova 118, 612 00 Brno, Czech Republic
Pavel.Vostrejs@vut.cz

Lignin is one of the most widespread biopolymers in the world. It is a complex polyphenol compound with a branched three-dimensional structure. This structure is formed by aromatic monolignols derived from hydroxycinnamyl alcohol. Nowadays, lignin is mostly obtained as a by-product in the pulp and paper industry. Lignin is most often used as a waste fuel. Laboratory lignin can be isolated by various technics, including the most common methods such as Kraft, sulfite, soda or organosolv process. the fundamental effect on lignin properties has the presence of sulfur in the structure. Sulfur compounds arise through Kraft and sulfite processes. Lignin obtained from the sulfite process is soluble in water, Kraft lignin only in alkaline solutions. the main advantage of organosolv and soda lignin is that they are sulfur-free. However, both are insoluble in water.

Lignin due to its bio-origin, aliphatic-aromatic composition and high abundancy possess theoretically a wide range of applica-

tions. Attention is mostly focused on the copolymerization and blending of lignin with various kinds of polymers, such as polyurethanes, phenol-formaldehyde and epoxy resins, polyesters and others.

In our research, we used lignin isolated from grape seeds that are waste products in the wine industry. Lignin was isolated by soda process and showed a high antioxidant activity thanks to its phenolic structure. Our work summarizes the effect of lignin addition on the properties of polyhydroxyalkanoate films. Principally, grape seeds lignin was mixed with crystalline poly(3-hydroxybutyrate) and amorphous polyhydroxyalkanoate via solution casting. the PHA/lignin films showed improved mechanical, thermal and gas barrier properties. the further advantage of these films was high antioxidant efficiency. All prepared samples proved their compostability comparable with a paper standard. Moreover, the obtained biomass after composting enhanced the plant growing.

Acknowledgement: This work was funded through the Internal Brno University of Technology project FCH-S-20-6316

Keywords: *lignin, grape seeds, polyhydroxyalkanoates, films, composting, physico-mechanical properties*

Transport Properties of Biopolymeric Hydrogels

David Vyroubal, Martina Klučáková

Brno University of Technology, Faculty of Chemistry, Materials Research Centre, Purkyňova 118/464, 612 00 Brno, Czech Republic
David.Vyroubal@vut.cz

1 Introduction

Hydrogels are in three-dimensional network structure which are generated through crosslinking from polymer materials. In addition to its high water content, it also has a strong water absorption ability[1]. Hydrogels have a wide range of applications, especially in medical and pharmaceutical areas[2]. Hydrogels are used for their similarity to biological tissues and for other unique characteristics. They are often used for drug delivery systems in medicine[3,4,5]. Their advantages are reduced side effects, prolonged drug action and low frequency with which drugs need to be administered[6,7]. Hydrogels contain a large amount of water so one of the main problems is that they are not capable of solubilizing hydrophobic compounds. This incompatibility between hydrophobic solutes and hydrogels can be solved by the incorporation of some hydrophobic domains into the hydrogel structure[5]. Biocompatibility of hydrogel is still provided by aqueous internal phase and hydrophilic network of the hydrogel. Hydrophobic domains then enable solubilization of hydrophobic compounds in the structure of the hydrogel. Hydrogels with the hydrophobic domains can be prepared by the interactions between biopolymer-like electrolytes with oppositely charged surfactant ions[8,9]. In this work, sodium form of hyaluronan and cationized dextran were used as polyelectrolytes. As oppositely charged surfactants sodium dodecyl sulfate (SDS) and Septonex were used. Hyaluronan and dextran are both naturally occurring carbohydrate-based biopolymers. Dextran is bacterial-derived polysaccharide made up from α-1,6-linked D-glucopyranose residues, appearance and frequency of α-1,2; α-1,3 and α-1,4-linked side chains depend on the production process or the production organism[10]. Hyaluronan is a linear polysaccharide formed by alternating units of β-1,3 and β-1,4-linked glucuronic acid and N-acetylglucosamine[11]. Hyaluronan and dextran are both biocompatible, biodegradable, non-toxic, high water soluble and offer high content of functional groups which are usable for cross-linking[12].

In this work, two different ways of diffusion were studied. The first way of study was the release of dyestuff from hydrogels based on dextran and hyaluronan into different solutions. The second way of study was the incorporation of dye into these hydrogels. Study is focused to evaluate the potential of hydrogels for use in the development of drug-delivery systems. For this use it is necessary to describe them in

terms of their diffusivity and permeability in different solutes. Atto 488 was chosen as a model of hydrophilic diffusion probe and Nile red was chosen as a model of hydrophobic diffusion probe. The aim of this work is to describe capacity and capability of hydrogel to: (1) absorb dyes by the diffusion from their solutions into prepared hydrogel; (2) release incorporated dyes by the diffusion from prepared hydrogel into different solutions. Diffusion coefficients and structural parameters of these hydrogels were studied to assess the potential for use in the development of drug-carrier systems.

2 Materials and methods

In this study, cationized dextran and sodium form of hyaluronan were used as polyelectrolytes. Sodium form of hyaluronan was purchased from Contipro (Czech Republic) and used in two different molecular weights as 340 kDa (LMW) and 1 540 kDa (HMW). Carbethoxypendecinium bromide (Septonex, Czech Pharmacopoeia quality) was purchased from GBNchem Company (Czech Republic) and used as surfactant for hyaluronan. Cationized dextran, more precisely diethylaminoethyl-dextran hydrochloride (DEAED) purchased from Sigma-Aldrich (Czech Republic) was used in molecular weight 500 kDa. Sodium dodecyl sulfate (SDS, ≥98.5 %) was obtained from Sigma-Aldrich (Czech Republic) and used as surfactant for dextran. Dyes Atto 488 and Nile red were both purchased from Sigma-Aldrich (Czech Republic).

All stock solutions were prepared in 0.15M NaCl solution using purified water (PureLab ELGA system). Salt solution was used because preliminary experiments showed that a non-zero ionic strength on the aqueous medium is important for obtaining gel-like materials[13,14]. Samples of hydrogels was prepared by mixing surfactant and polyelectrolyte stock solutions in a 1:1 volume ratio. The concentrations of initial stock solutions of polyelectrolytes and surfactants are given in ***Table 1***.

Table 1: Concentrations of initial stock solutions used to prepare hydrogels

Hydrogel	Polyelectrolyte	Concentration of polyelectrolyte (% w/v)	Surfactant	Concentration of surfactant (mM)
D-I	Cationized dextran	4	SDS	400
D-II	Cationized dextran	4	SDS	100
H-I	HMW hyaluronan	2	Septonex	200
H-II	HMW hyaluronan	2	Septonex	100
L-I	LMW hyaluronan	2	Septonex	200
L-II	LMW hyaluronan	2	Septonex	100

For study of release incorporated dye from hydrogel into solution, Nile red was dissolved in the surfactant stock solution and then incorporated into the hydrogel during its preparation when mixing with polyelectrolyte stock solution. Nile red was used in ten different initial concentrations which are given in ***Table 2***. Hydrogels with incorporated dye were equilibrated for 24 hours after preparation and then separated from the liquid residue. One set of hydrogels was always left with the original supernatant which was formed during the preparation of hydrogel). Hydrogels separated from liquid were

weighted and covered by 5 cm^3 of 0.15M NaCl solution or surfactant with a concentration equal to half of the initial one.

For study of absorption of dye from solution into hydrogel, Atto 488 was dissolved in Septonex (200mM for H-I, L-I and 100mM for H-II, L-II) or physiological saline (0.15M NaCl). Nile red was dissolved in Septonex (200mM for H-I, L-I and 100mM for H-II, L-II) and in SDS (400mM for D-I and 100mM for D-II). Dyes were used in ten different initial concentrations listed in ***Table 2***. After preparation, hydrogels were equilibrated (24 h) and separated from the liquid residue. Hydrogels were then covered by 5 cm^3 of Septonex, SDS or NaCl solution with dissolved dye.

The concentration of dyes in solutions above the hydrogels in both methods (release/absorption) was monitored by means of UV/VIS spectrometry (Hitachi U-3900). The data were used for the determination of dye release or absorption in hydrogels[15,16] distribution coefficients[16,17] and their diffusivity[15–18].

Table 2: Initial concentrations of dyes used for diffusion experiments

Index	Concentration of dye for release from hydrogel experiments (μM)	Concentration of dye in solution for absorption experiments (μM)
a	2	0.1
b	3	0.3
c	4	0.5
d	5	0.7
e	6	0.8
f	7	0.9
g	8	1
h	9	3
i	10	5
j	15	7

3 Results and discussion

In this study, several different approaches for the investigation of transport of model dyes from and into hydrogels were applied. Interactions of polyelectrolytes with oppositely charged surfactant ions can result in the dissolution of hydrophobic compounds in micelle-like nanocontainers formed by these surfactants.

3.1 Diffusion from solution into hydrogel

Dyes were prepared in various solutions. Atto 488 was prepared as its water solution in 0.15M NaCl for both types of hydrogels and in 100mM and 200mM Septonex for hyaluronan-based hydrogels. Nile red was prepared as its solution in 100mM and 400mM SDS for measurements in dextran-based hydrogels and in 100mM and 200mM Septonex for hyaluronan-based hydrogels. Concentrations of both used surfactants

Septonex and SDS were much higher than its critical micellar concentration (CMC). Critical micellar concentration of Septonex is around ~0.8mM[19,20,21] and CMC of SDS is around ~8mM[19,22,23]. Due to high concentrations of stock solutions above CMC, dyes should be completely distributed in the micelles of both surfactants. On the contrary, Atto 488 was dissolved in 0.15M water solution of NaCl and therefore we assumed that it diffused into hydrogels in the form of simple (partially dissolved) molecules. The theoretical ratio of charges between surfactant (SDS, Septonex) and polyelectrolyte (cationized dextran, hyaluronan) are ~1 for D-II; ~2 for H-II and L-II; and ~4 for D-I, H-I, L-I. We assumed that a part of surfactant can be exhausted for the formation of hydrogel networks. In the case of D-II, H-II and L-II, the large amount of surfactant is consumed for cross-linking of hydrogel and the content of surfactant in pores is low. In contrast for hydrogels D-I, H-I and L-I, this part is relatively small, therefore the pore structure in hydrogel contains solution with surfactant micelles. Therefore, differences between used hydrogels based on chemically identical raw materials were probably connected with the use of different concentrations of surfactants on cross-linking, which means different ratios between functional groups in biopolymers and surfactant ions. If we take account of these differences in the dextran-based hydrogels, we can assume the faster diffusion into hydrogel D-II with low theoretical ratio of charges. However, the results of the diffusion coefficients for hyaluronan-based hydrogels are opposite. Diffusion into hyaluronan-based hydrogels with higher theoretical ratio of charges (H-I, L-I) is faster. The probable theory for hyaluronan-based hydrogels is that higher excess of Septonex surfactant non-consumed for cross-linking actively participates in the diffusion and binds dye into its micelles. The examples of kinetic data are shown in ***Figure 1***. We can see that the amount of dye diffused into more cross-linked hyaluronan-based hydrogel H-I is higher than in less cross-linked H-II. On the other hand, the amount of dye diffused into less cross-linked dextran-based hydrogel D-II is higher than in more cross-linked D-I. The dye content in hydrogels increased strongly mainly in first days.

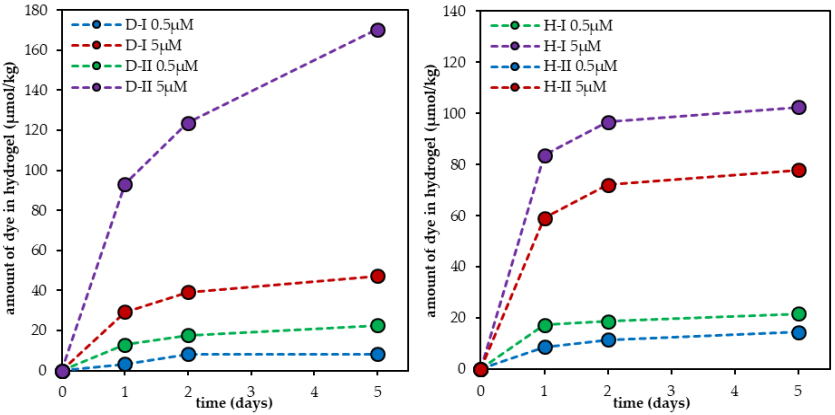

Figure 1: The amount of dyes diffused into hydrogels in the dependence on time: Dextran-based hydrogels with Nile red (left) and hyaluronan-based hydrogels with Atto 488 (right)

The examples of the diffusive flux in the dependence on initial dye concentration for dextran-based hydrogels are shown in ***Figure 2***. The rate of diffusion was strongly influenced by initial concentration of dye solution used as the source of diffusion particles. We can see that the diffusive flux is much higher in D-II hydrogels with lower theoretical ratio of charges (~1). A summary of all diffusion coefficients obtained is then shown in ***Table 3***.

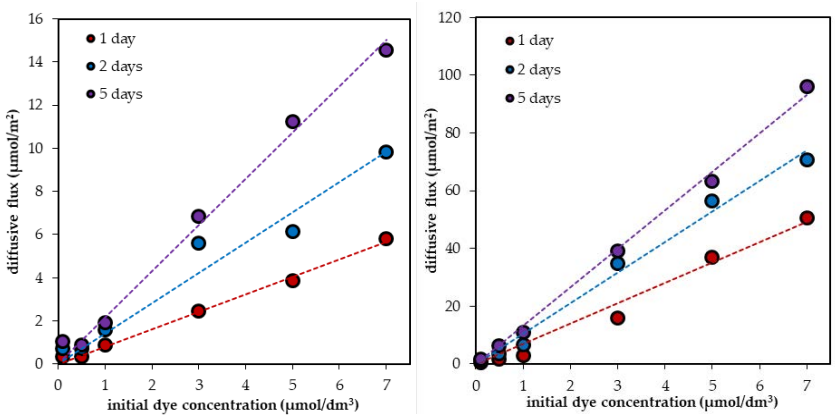

Figure 2: Examples of the diffusive flux from solution into hydrogel in the dependence on initial dye concentration for hydrogels D-I (left) and D-II (right) with Atto 488

The values of effective diffusion coefficients listed in ***Table 3***. were based on mathematical model developed by Klučáková et al.[17]. This model was developed for the diffusion couple with phase interface. In this work, the couple is comprised by the hydrogel (acceptor part) and the solution of dye above hydrogel (donor part). Both parts are placed in cylindrical vessel.

Table 3: Effective diffusion coefficients of dyes in hydrogels for diffusion from solution into hydrogel

	Diffusion coefficients (m²/s)			
Hydrogel	**Nile red in SDS**	**Nile red in Septonex**	**Atto 488 in Septonex**	**Atto 488 in NaCl solution**
D-I	4.22×10^{-10}	nd	nd	1.55×10^{-10}
D-II	4.63×10^{-10}	nd	nd	3.92×10^{-10}
H-I	nd	7.86×10^{-10}	5.93×10^{-10}	1.21×10^{-9}
H-II	nd	7.40×10^{-10}	5.69×10^{-10}	4.14×10^{-10}
L-I	nd	5.53×10^{-10}	4.78×10^{-10}	7.17×10^{-10}
L-II	nd	4.28×10^{-10}	4.28×10^{-10}	5.26×10^{-10}

The diffusion coefficient of Nile red in water is 3.3×10^{-10} m²/s [24]. Results published by Zhang et al. showed that the diffusion coefficient of Atto 488 in water is 4.0×10^{-10} m²/s [23,24]. We can see that diffusion coefficients of Atto 488 and Nile red in water are lower (except D-I and D-II hydrogels with Atto 488 in NaCl solution) in comparison with our obtained results of diffusion coefficients in hydrogels. If we compare our measured diffusion coefficients of dyes in hydrogels with their diffusion coefficients in aqueous solution, then the coefficients in hydrogels have higher values and the diffusion of dyes in hydrogels is faster than in aqueous medium. Thus, higher diffusion coefficients of the dyes in the hydrogels may support the theory that free micelles of surfactants non-consumed for cross-linking located in the pores of hydrogel could accelerate diffusion.

3.2 Diffusion from hydrogel into solution

In release experiments, the Nile red was incorporated into the hydrogel structure during hydrogel preparation. Nile red was used in ten different initial concentrations listed in ***Table 2***. Therefore, one type of hydrogel had ten different concentrations of NR. As was expected only a small part of initial dye concentration was incorporated into hydrogels during their preparation, higher part of dye remained in the surfactant (supernatant) solution. The content of NR in hydrogels based on the same polyelectrolyte was higher for the hydrogels prepared using less concentrated surfactant, specifically in hydrogels D-II, H-II and L-II. As already mentioned, differences between hydrogels based on identical materials probably depends on the use of different initial concentrations of surfactants and thus resulting in different ratios between functional groups in biopolymers and surfactant ions.

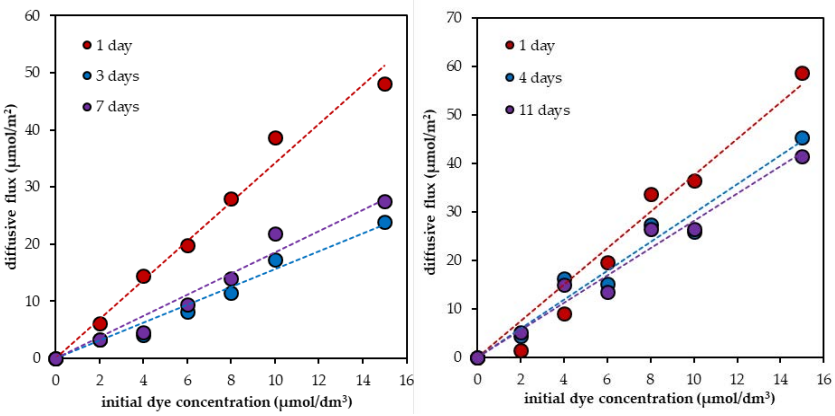

Figure 3: Examples of the diffusive flux from hydrogel into SDS solution in the dependence on initial dye concentration for hydrogels D-I (left) and D-II (right) with Nile red

In ***Figure 3***, we can see the examples of the diffusive flux in the dependence on initial dye concentration for dextran-based hydrogels. The values of diffusion coefficients

determined from diffusive flux seemed to be independent on the content of initial concentration of Nile red in the studied systems in the used concentration range. We can see that the diffusive flux is higher in D-II hydrogels with lower theoretical ratio of charges (~1). A summary of all diffusion coefficients determined is then shown in ***The*** experiment of releasing the probe from the hydrogel structure into solution shows that the diffusion coefficients are influenced by many factors as well as in the case of diffusion from solution into hydrogel. The dye in these gels may be in the form of nanocontainers similar to micelles that are incorporated in a „pearl necklace structure", or in the form of more mobile free micelles or their aggregates. Diffusion coefficients of dye upon diffusion out of the hydrogel structure increase with increasing molecular weight of the polyelectrolytes and with the charge ratio between surfactant and biopolymer. Nile red in hydrogels with more concentrated surfactant is probably released in the form of free micelles and also depends on the size of these micelles in relation to the type of surfactant.

Table 4.

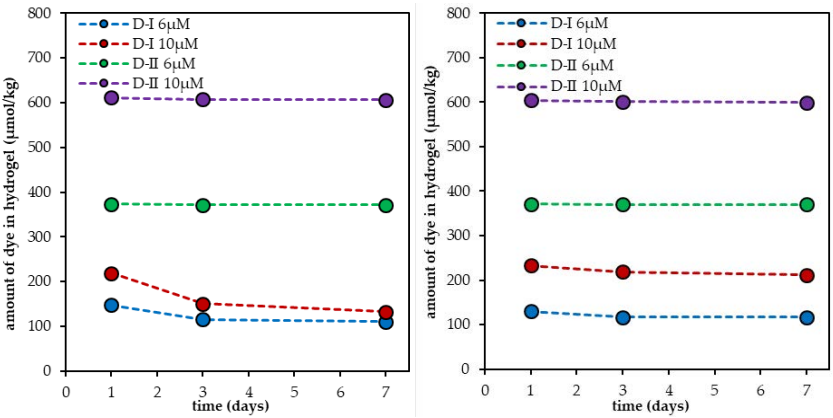

Figure 4: The amount of dyes diffused from hydrogels into solution in the dependence on time: (1) Diffusion from dextran-based hydrogel into SDS solution (left); (2) Diffusion from dextran-based hydrogel into NaCl solution (right)

The diffusion coefficients obtained during the release experiments of dye from hydrogel are in an order of 10^{-11} whereas in the case of diffusion experiments from the solution into the hydrogel, the diffusion coefficients are in an order of 10^{-10}. The greatest difference in diffusion coefficients of release and absorption of dye experiments is

probably caused by interactions between the dye and the hydrogel. If we take the diffusion of the dye from solution into the hydrogel, the interactions between the dye and the hydrogel only begin. We can say that the front of the diffusion is constantly coming into the clean hydrogel (without probe) and the probe is just starting to interact, so it will move faster than it is with the release of dye from the gel. If the dye is already incorporated in the hydrogel structure, the front of the diffusion is practically at the interface of the gel and the solution, thus the dye must additionally break bonds with the hydrogel and subsequently travel through the hydrogel which already contain the dye. The biggest difference is probably due to whether the dye begins to interact with the hydrogel or is already contained in the hydrogel. Another interesting fact is that the diffusion coefficients of the probe released from hydrogel into solution do not differ between different solutions (surfactant/NaCl solution). Release diffusion coefficients are almost identical for both the surfactant and the NaCl solution, and the environment into which the probe diffuses does not matter (see for example ***Figure 4***). In contrary, for diffusion from solution into hydrogel, the individual diffusion coefficients vary considerably depending on the type of solution. If we compare the individual diffusion coefficients depending on the used initial concentration of the surfactant for crosslinking, we find that when the dye release from hydrogel into solution, the diffusion coefficients are always higher for more crosslinked hydrogels (D-I, H-I, L-I). This also applies to hyaluronan hydrogels when the dye diffuses from solution into a hydrogel. For dextran hydrogels, the diffusion coefficients for absorption of dye from solution into hydrogel are opposite. The experiment of releasing the probe from the hydrogel structure into solution shows that the diffusion coefficients are influenced by many factors as well as in the case of diffusion from solution into hydrogel. The dye in these gels may be in the form of nanocontainers similar to micelles that are incorporated in a „pearl necklace structure", or in the form of more mobile free micelles or their aggregates. Diffusion coefficients of dye upon diffusion out of the hydrogel structure increase with increasing molecular weight of the polyelectrolytes and with the charge ratio between surfactant and biopolymer. Nile red in hydrogels with more concentrated surfactant is probably released in the form of free micelles and also depends on the size of these micelles in relation to the type of surfactant.

Table 4: Effective diffusion coefficients of Nile red in hydrogels for diffusion from hydrogel into solution

	Diffusion coefficients (m^2/s)	
Hydrogel	**Release form hydrogel into surfactant**	**Release from hydrogel into NaCl solution**
D-I	6.95×10^{-11}	6.95×10^{-11}
D-II	1.21×10^{-11}	1.26×10^{-11}
H-I	4.72×10^{-11}	4.57×10^{-11}
H-II	1.35×10^{-11}	1.18×10^{-11}
L-I	6.38×10^{-11}	6.97×10^{-11}
L-II	3.29×10^{-11}	3.39×10^{-11}

4 Conclusion

In this work, two different approaches of the diffusion of dyes in hydrogels based on a combination of polyelectrolyte and opposite charged surfactant were studied. Hydrogels were based on the combination of sodium form of hyaluronan with Septonex as surfactant and cationized dextran with sodium dodecyl sulfate as surfactant. The diffusion of dyes from or into hydrogels is influenced by several factors. Dyes presented in micelle-like nanocontainers can be in different forms such as mobile free micelles and micelle aggregates or immobilized into „pearl necklace structure". One of the factors is amount of surfactant non-consumed for cross-linking located in the pores of hydrogel. Another of the possible factors is difference in branching between linear hyaluronan and non-linear dextran.

5 References

1. KAITH, B.S. and Kiran KUMAR. In vacuum synthesis of psyllium and acrylic acid based hydrogels for selective water absorption from different oil–water emulsions. Desalination. 2008, 229(1-3), 331-341. ISSN 00119164.
2. FAN, Lihong, Huan YANG, Jing YANG, Min PENG and Jin HU. Preparation and characterization of chitosan/gelatin/PVA hydrogel for wound dressings. Carbohydrate Polymers. 2016, 146, 427-434. ISSN 01448617.
3. HURLER, Julia, Ole Aleksander BERG, Merete SKAR, Anne Hilde CONRADI, Pål Jarle JOHNSEN and Nataša ŠKALKO-BASNET. Improved Burns Therapy: Liposomes-in-Hydrogel Delivery System for Mupirocin. Journal of Pharmaceutical Sciences. 2012, 101(10), 3906-3915. ISSN 00223549.
4. LU, Changhai, Roshan B. YOGANATHAN, Michael KOCIOLEK and Christine ALLEN. Hydrogel Containing Silica Shell Cross-Linked Micelles for Ocular Drug Delivery. Journal of Pharmaceutical Sciences. 2013, 102(2), 627-637. ISSN 00223549.
5. PEKAŘ, Miloslav. Hydrogels with Micellar Hydrophobic (Nano)Domains. Frontiers in Materials. 2015, 1. ISSN 2296-8016.
6. HUYNH, Cong Truc, Minh Khanh NGUYEN and Doo Sung LEE. Injectable Block Copolymer Hydrogels: Achievements and Future Challenges for Biomedical Applications. Macromolecules. 2011, 44(17), 6629-6636. ISSN 0024-9297.
7. SHI, Wenping, Yanwen JI, Xinge ZHANG, Shujun SHU and Zhongming WU. Characterization of pH- and Thermosensitive Hydrogel as a Vehicle for Controlled Protein Delivery. Journal of Pharmaceutical Sciences. 2011, 100(3), 886-895. ISSN 00223549.
8. LI, Dongcui and Norman J. WAGNER. Universal Binding Behavior for Ionic Alkyl Surfactants with Oppositely Charged Polyelectrolytes. Journal of the American Chemical Society. 2013, 135(46), 17547-17555. ISSN 0002-7863.
9. PICULELL, Lennart. Understanding and Exploiting the Phase Behavior of Mixtures of Oppositely Charged Polymers and Surfactants in Water. Langmuir. 2013, 29(33), 10313-10329. ISSN 0743-7463.
10. VETTORI, Mary Helen P B, Kate C BLANCO, Mariana CORTEZI, Cristian J B LIMA and Jonas CONTIERO. Dextran: effect of process parameters on production,

purification and molecular weight and recent applications. 2012, 2012(31), 171-186. ISSN 16780493.
11. ZHANG, Wei, Xin JIN, Heng LI, Run-run ZHANG and Cheng-wei WU. Injectable and body temperature sensitive hydrogels based on chitosan and hyaluronic acid for pH sensitive drug release. Carbohydrate Polymers. 2018, 186, 82-90. ISSN 01448617.
12. OH, Jung Kwon, Ray DRUMRIGHT, Daniel J. SIEGWART and Krzysztof MATYJASZEWSKI. The development of microgels/nanogels for drug delivery applications. Progress in Polymer Science. 2008, 33(4), 448-477. ISSN 00796700.
13. KROUSKÁ, J., M. PEKAŘ, M. KLUČÁKOVÁ, B. ŠARAC and M. BEŠTER-ROGAČ. Study of interactions between hyaluronan and cationic surfactants by means of calorimetry, turbidimetry, potentiometry and conductometry. Carbohydrate Polymers. 2017, 157, 1837-1843. ISSN 01448617.
14. VENEROVÁ, Tereza and Miloslav PEKAŘ. Rheological properties of gels formed by physical interactions between hyaluronan and cationic surfactants. Carbohydrate Polymers. 2017, 170, 176-181. ISSN 01448617.
15. KALINA, Michal, Martina KLUČÁKOVÁ and Petr SEDLÁČEK. Utilization of fractional extraction for characterization of the interactions between humic acids and metals. Geoderma. 2013, 207-208, 92-98. ISSN 00167061.
16. KLUČÁKOVÁ, Martina. Complexation of Metal Ions with Solid Humic Acids, Humic Colloidal Solutions, and Humic Hydrogel. Environmental Engineering Science. 2014, 31(11), 612-620. ISSN 1092-8758.
17. KLUČÁKOVÁ, Martina and Miloslav PEKAŘ. Transport of copper(II) ions in humic gel—New results from diffusion couple. Colloids and Surfaces A: Physicochemical and Engineering Aspects. 2009, 349(1-3), 96-101. ISSN 09277757.
18. SMILEK, Jiří, Petr SEDLÁČEK, Michal KALINA and Martina KLUČÁKOVÁ. On the role of humic acids' carboxyl groups in the binding of charged organic compounds. Chemosphere. 2015, 138, 503-510. ISSN 00456535.
19. DUTKIEWICZ, E., and A. JAKUBOWSKA. Effect of electrolytes on the physicochemical behaviour of sodium dodecyl sulphate micelles. 2002, 280(11), 1009-1014. ISSN 0303-402X.
20. KARGEROVÁ, A. and M. PEKAŘ. Ultrasonic study of hyaluronan interactions with Septonex—A pharmaceutical cationic surfactant. Carbohydrate Polymers. 2019, 204, 17-23. ISSN 01448617.
21. FISCHER, J. and P. JANDERA. Chromatographic behaviour in reversed-phase high-performance liquid chromatography with micellar and submicellar mobile phases: effects of the organic modifier. Journal of Chromatography B: Biomedical Sciences and Applications. 1996, 681(1), 3-19. ISSN 03784347.
22. UMLONG, I.M. and K. ISMAIL. Micellization behaviour of sodium dodecyl sulfate in different electrolyte media. Colloids and Surfaces A: Physicochemical and Engineering Aspects. 2007, 299(1-3), 8-14. ISSN 09277757.
23. ZHANG, Xuzhu, Andrzej PONIEWIERSKI, Aldona JELIŃSKA, Anna ZAGOŻDŻON, Agnieszka WISNIEWSKA, Sen HOU and Robert HOŁYST. Determination of equilibrium and rate constants for complex formation by fluorescence correlation spectroscopy supplemented by dynamic light scattering and Taylor dispersion analysis. Soft Matter. 2016, 12(39), 8186-8194. ISSN 1744-683X.
24. ZHANG, Li-Xiang, Xiao-Hong CAO, Wei-Peng CAI and Yao-Qun LI. Observations of the Effect of Confined Space on Fluorescence and Diffusion Properties of

Molecules in Single Conical Nanopore Channels. Journal of Fluorescence. 2011, 21(5), 1865-1870. ISSN 1053-0509.

Acknowledgement

This work was supported by the Czech Science Foundation, project No. 16-12477S and by the project LO1211 from National Programme for Sustainability I (Ministry of Education, Youth and Sports, Czech Republic).

Preparation of Mg-Ti Based Bulk Materials via Powder Metalurgy

Martin Žilinský

Brno University of Technology, Faculty of Chemistry
Institute of Material Chemistry, Purkyňova 464, 612 00
Brno-Medlánky
xczilinsky@vutbr.cz

The aim of this thesis is preparation and characterization of bulk magnesium–Titanium based materials. In the first theoretical part properties of base materials and the complexity of preparation alloy from these metals is discussed. Second part is focused on powder metallurgy and its applicability on Mg–Ti system. In another part particle composites are described.

The experimental part of this thesis was the preparation of bulk Mg–Ti materials from metal powders. for sample preparation conventional methods of powder metallurgy and spark plasma sintering was employed. Furthermore a characterisation of these materials was done. Microstructure was observed. Present phases were found using X-ray diffraction analysis. Amounts of these phases were determined using a scanning electron microscope with energy–dispersive spectrometry and using X-ray fluorescence. Furthermore hardness was measured and bending test with evaluation was done. Significant difference in results of sample preparation using conventional methods of powder metallurgy and spark plasma sintering was observed.


VYSOKÉ UČENÍ
TECHNICKÉ
V BRNĚ
FAKULTA
CHEMICKÁ